Wolfgang Jud, BSc.

Enzymatic phosphorylation using acid phosphatases: Overcoming limitations

MASTER'S THESIS

to achieve the university degree of

Master of Science

Master's degree programme: Chemistry

submitted to

Graz University of Technology

Supervisor

O.Univ.-Prof. Dr.phil. Kurt Faber

Department of Chemistry
University of Graz

Organic and Bioorganic Chemistry
Heinrichstraße 28/II

Graz, March 2016

AFFIDAVIT

I declare that I have authored this thesis independently, that I have not used other than the declared sources/resources, and that I have explicitly indicated all material which has been quoted either literally or by content from the sources used. The text document uploaded to TUGRAZonline is identical to the present master's thesis.

15.3.2016	Wolfgang Huk
Date	Signature

Abstract

Biocatalytic methods for introducing phosphate groups into organic molecules employ either ATP-dependent kinases, which naturally form phosphate esters, or phosphatases, phosphate ester hydrolyzing proteins, which can also be operated in the reverse direction and transfer a phosphate moiety from a suitable donor to an acceptor alcohol. In the recent past, the latter class of enzymes has received much attention, since in contrast to using kinases, the need for cofactor recycling is obviated and the substrate spectrum is considerably broader. In this context mostly pyrophosphate (PP_i) has been employed as the phosphate donor, since it is cheap and easy to prepare. However, PP_i exhibits chelating effects towards divalent metal ions, rendering it an unfavorable donor with metal-dependent phosphatases and additionally at least one equivalent of phosphate is produced as by-product, which is often undesired, not only from an academic point of view. Other high-energy donors, such as p-nitrophenyl phosphate or phosphocreatine, are also accepted by many phosphatases, as has been reported in earlier publications. The aim of the current investigations was probing a variety of (non-)natural organic donors in transphosphorylation reactions with metal-dependent and metal-independent phosphatases. Furthermore, during the course of practical work, two methods for suppressing enzyme-catalyzed product hydrolysis over time, a common issue of transphosphorylation reactions involving phosphatases, have been developed. These involve tight pH control and proper choice of enzyme concentration.

Zusammenfassung

Biokatalytische Methoden, um organische Moleküle mit Phosphatgruppen zu erstellen, bedienen sich entweder ATP-abhängiger Kinasen, die auch in der Natur Phosphorsäureester bilden, oder Phosphatasen, Proteine, die Phosphorsäureester hydrolysieren und auch in umgekehrter Richtung betrieben werden können, um eine Phosphatgruppe von einem passenden Donor auf einen Akzeptoralkohol zu übertragen. In jüngster Vergangenheit wurde der letzteren Enzymklasse viel Beachtung geschenkt, da im Gegensatz zum Einsatz von Kinasen das Recycling des Cofaktors überflüssig und das Substratspektrum breiter ist. In diesem Zusammenhang wurde meist Pyrophosphat (PP_i) als Phosphatdonor eingesetzt, da es billig und leicht darzustellen ist. Allerdings zeigt PP_i Chelateigenschaften gegenüber divalenten Metallionen, was es zu einem ungünstigen Donor für metallabhängige Phosphatasen macht, und darüber hinaus wird mindestens ein Äquivalent Phosphat als Nebenprodukt erhalten, was nicht nur von einem akademischen Standpunkt aus betrachtet oft unvorteilhaft ist. Andere energiereiche Donorsubstanzen, wie etwa *p*-Nitrophenylphosphat oder Phosphokreatin, werden ebenso von vielen Phosphatasen akzeptiert, wie es in älteren Veröffentlichungen ausgeführt wurde. Das Ziel der gegenwärtigen Forschung war es, eine Vielzahl (nicht) natürlicher organischer Donorsubstanzen in Transphosphorylierungsreaktionen mit metallabhängigen und metallunabhängigen Phosphatasen zu testen. Weiterhin wurden im Zuge der praktischen Arbeit zwei Methoden entwickelt, die enzymkatalysierte Hydrolyse des Produkts im Laufe der Zeit, die ein häufiges Problem von Transphosphorylierungsreaktionen mit Phosphatasen darstellt, zu unterdrücken. Diese umfassen eine strenge Kontrolle des pH-Wertes und die genaue Wahl der Enzymkonzentration.

Contents

1 Introduction and Theoretical Background

Phosphate anhydrides and esters play an essential role in Nature and are distributed across the entire living world [1]. They are involved in a multitude of cellular processes including secretion, phototransduction and cell proliferation regulating signal-transduction pathways [2], glycolysis, gluconeogenesis, fatty acid metabolism, nucleotide biosynthesis, the Calvin cycle and the pentose phosphate pathway [3]. Phosphoryl groups form the backbone of DNA and RNA (Figure 1) and phosphates prevail the main source of biochemical energy in the form of adenosine triphosphate (ATP), phosphoenolpyruvate (PEP) and creatine phosphate (CP) [1, 4] for example, which all have low $\Delta G''°$ values for hydrolysis (see Section 1.3). Phospholipids, which are ubiquitous in all biological membranes, and also cofactors such as thiamine pyrophosphate (TPP) [3] and nicotinamide adenine dinucleotide phosphate (NADPH/NADP$^+$) [5] add to the list of significant phosphate ester containing compounds in biochemistry. Kinases (EC 2.7.1.X–2.7.4.X) [6], like hexokinase [7] or glycerol kinase [8], and phosphorylases (EC 2.4.X.X, glycosyltransferases, and 2.7.7.X, nucleotidyltransferases) [6], like sucrose phosphorylase [9] or glycogen phosphorylase [10], form P−O bonds in Nature, however many more types of enzymes exist, which deal with phosphorylated compounds [11]. Among them are phosphatases, a large and diverse group of enzymes, which hydrolyze phosphate esters and/or anhydrides and belong to several classes, for instance EC 3.1.3.X (phosphoric monoester hydrolases) and EC 3.6.X.X (acting on acid anhydrides) [6]. As will be described in more detail in the following sections, these enzymes cannot only transfer phosphate groups to water, but also to a broad range of acceptor alcohols, when suitable high-energy donors are employed. The identification and characterization of such donors with various phosphatases was a main target of the investigations in Section 2.
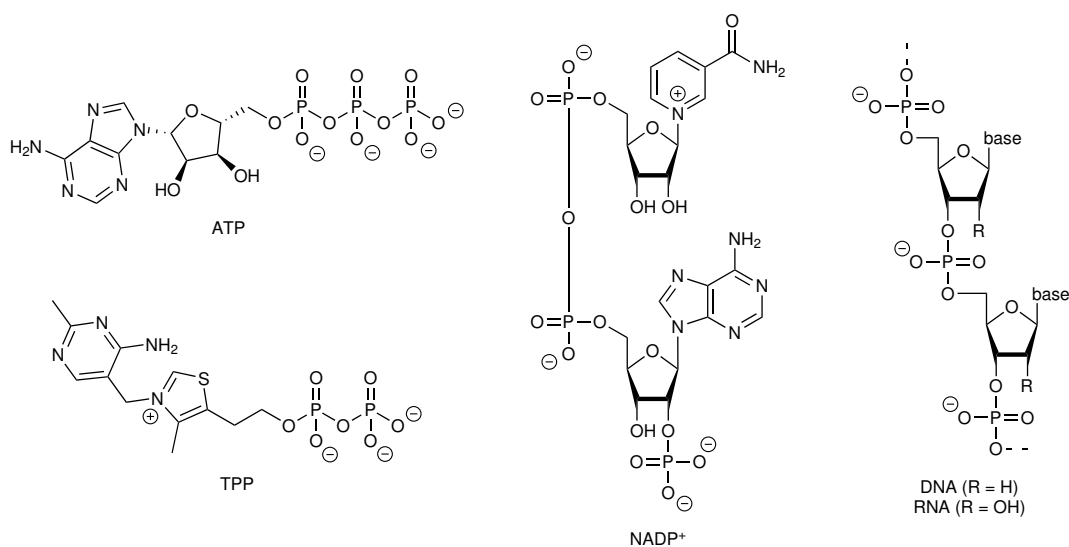
Figure 1: Examples of important phosphorylated compounds in Nature

4

1.1 Phosphate Esters in Nature, Organic Chemistry and Medicinal Chemistry

1.1.1 Natural Role of Phosphate Esters

Several reasons exist why Nature selected phosphates: They are ionized at physiological pH [12], which makes them stay within cells. At the same time, negative charges are important for the "packaging" of nucleic acids and binding of cofactors to enzymes [1]. Phosphate diesters further represent an ideal choice for linking nucleic acids, since their negative charge distribution and ionization energies are more favorable compared to alternatives like citric acid or silicic acid in preventing attacks by nucleophiles, rendering DNA very stable. Still, nucleic acid cleavage can readily be conducted by enzymes, which lift kinetic restrictions and increase reaction rates 10^9 to 10^{12}–fold [1]. As already indicated, in biochemistry a large variety of enzymes, dedicated to hydrolyzing phosphorylated species of many kinds, including ATP (see also Table 1), has evolved and phosphate (P_i) or pyrophosphate (PP_i) have prevailed as the preferred leaving groups of Nature [3].

1.1.2 Applications in Organic Chemistry

Classical organic synthesis in contrast usually depends on less stable/more reactive groups than phosphate dianions, like halides, triflates or tosylates for nucleophilic displacement or elimination reactions. Although in some name reactions phosphoryl groups act as leaving groups, such as in the Appel [13] or the Mitsunobu-reaction [14], in that case phosphine oxides and not phosphates are generated and the driving force of those reactions resides in the oxidation of P(III) to P(V) [15]. In spite of that, some researchers tackled investigations towards phosphate esters being the leaving group, but in hardly any report other species than triesters were the reaction intermediates, presumably because of the lower solubility of mono- and diesters in organic solvents due to their negative charge.

Guijarro et al. [16] for instance reported that trialkyl phosphates, which were prepared from the corresponding alcohols with $POCl_3$ under basic conditions, can be converted into organolithium compounds in a 4,4'-di-tert-butylbiphenyl (DTBB) catalyzed lithiation. They were subsequently reacted in-situ with several electrophiles under Barbier-type reaction conditions. Trisubstituted phosphates, where $R^1=R^2=R^3$ (Figure 2), as well as mixed phosphates ($R^1=R^2\neq R^3$) were assayed and minor amounts ($<10\%$) of pinacol-type products were observed when coupling with carbonyl compounds.
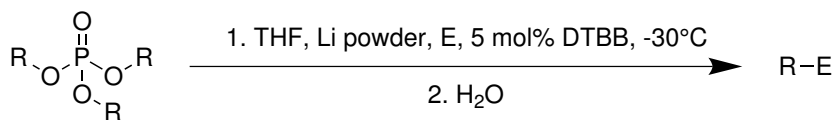
Figure 2: Reaction conditions employed by Guijarro et al. : E = electrophile = Me_3SiCl, $PhMe_2SiCl$, PhCHO, Et_2CO, PhCOEt; R = Et, $CH_2CH=CH_2$, Pr^i, Bu^n, Ph; scheme adapted from Guijarro et al. [16]

A less toxic and and more convenient alternative to the Chugaev elimination for the dehydration of secondary alcohols to yield alkenes was devised by Quast and Dietz [17]: After the formation of a diphenyl phosphate ester by reaction of the alcohol with triphenyl phosphate or diphenyl phosphochloridate in the presence of base in water-miscible, high boiling solvents, such as sulfolane, the intermediates were subjected to thermolysis to furnish alkenes, which were distilled from the mixture (Figure 3). While the exact mechanism of the elimination was not elucidated by the authors, the ratios of the dehydration products obtained from menthol and neomenthol as well as the rearrangement of alkenes by 1,2-shifts indicated the presence of ionic intermediates.
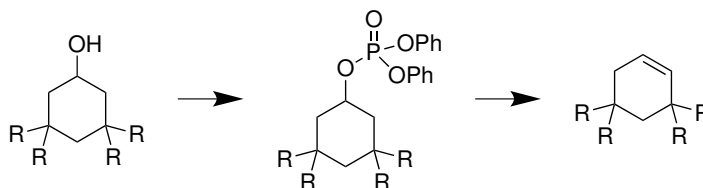
Figure 3: Dehydration of cyclohexanol (R = H) and the tetramethyl (R = Me) derivative via in-situ generated alkyl diphenyl phosphates and thermolysis, as reported by Quast et al. [17]

Finally, Yanagisawa et al. pointed out that allylic phosphates can be substituted with Grignard reagents in the presence of a transition metal [18]. The regioselectivity of the reaction (S_N2 versus S_N2') can be triggered by using appropriate catalysts, as depicted in Figure 4.
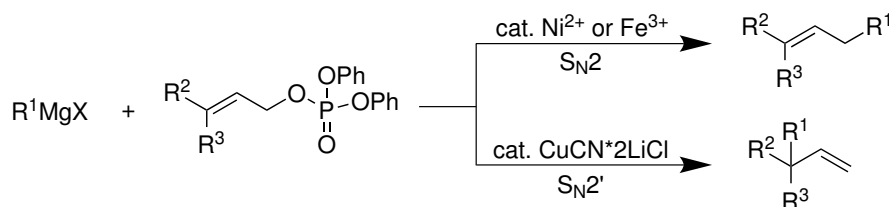
Figure 4: Substitution of allylic phosphates by Grignard reagents, as described by Yanagisawa et al. [18]

Chiral phosphoric acid esters, which act as Brønsted acids, can be used as organocatalysts in a variety of enantioselective transformations [19]. For instance, phosphoric

acid diesters with 1,1'-bi-2-naphthol (BINOL) and derivatives thereof catalyze an enantioselective Mannich reaction, yielding optically active β-amino ketones, as outlined in Figure 5. By choosing aryl or diaryl substituents at the 3,3'-positions (G) of the binaphthyl, enantioselectivity could further be enhanced.
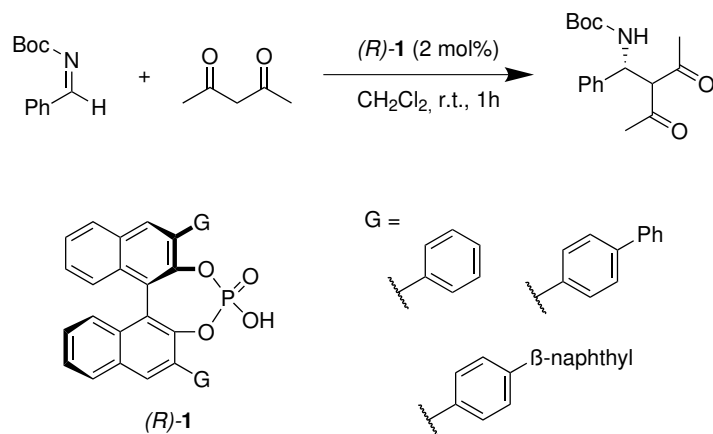
Figure 5: Enantioselective Mannich reaction, catalyzed by BINOL-derived monophosphoric acids [19]

In terms of biocatalysis, dihydroxyacetone phosphate (DHAP) is a very prominent phosphate ester. Enzymes, like fructose 1,6-diphosphate aldolase or fuculose 1-phosphate aldolase belong to group I aldolases and are dependent on DHAP as donor (nucleophile) [20,21]. A multitude of carbohydrates may be stereoselectively synthesized using these enzymes, such as the naturally occurring D-fagomine, an iminosugar, which modulates bacterial adhesion and lowers postprandial blood glucose [22]. Group I aldolases can also be utilized to produce non-natural carbohydrates, which due to structural similarities to natural sugar moieties, inhibit glucosidases, carbohydrate-degrading enzymes, and therefore can mend lysosomal storage disorders and diabetes [23]. Examples of such compounds are the sugar-mimicking pyrrolidine derivatives synthesized by Calveras et al. using fuculose 1-phosphate aldolase, rhamnulose 1-phosphate aldolase and DHAP [24].

Since many aldolases are restricted to their donor [20], several different biocatalytic methods for the (in-situ) generation of the unstable DHAP and other substrates, such as D-glyceraldehyde-3-phosphate (G3P), were established [25]. These are among the most important representatives of phosphorylated intermediates in biocatalysis and will therefore be discussed more thoroughly in Section 1.5.4.

Nucleotides, which are often added to food due to their flavor enhancing properties, are meaningful examples for phosphate esters produced industrially with an annual worldwide production of $16\,000\,\text{t}$ [26]. Among them are inosine 5'-monophosphate (5'-IMP) and guanosine 5'-monophosphate (5'-GMP), which are responsible for the umami

taste [26]. The biological activity of those compounds is dependent on the position of the phosphate group: Inosine 2'-monophosphate and inosine 3'-monophosphate for instance are tasteless [27]. A convenient, regioselective phosphorylation of inosine [28–31] and guanosine [32] can be achieved using (mutated) phosphatases and was conducted by the group of Asano. A more detailed overview on transphosporylation reactions involving phosphatases is given in Section 1.5.3.c.

Further industrial applications of phosphate esters in form of phosphorylated sugars range from glucosamine 6-phosphate as knee pain treatment and food supplement against osteoarthritis to ingredients of cosmetics (moisturizers) and detergents [33].

1.1.3 Applications in Medicinal Chemistry

Drugs are often administered in a masked form, as so-called prodrugs, which are transformed into an active species in the body by a chemical or enzymatic reaction [34]. The motivation behind this usually is the improvement of several properties like absorption, distribution, metabolism & excretion of the compound and, such as in the case of orally administered glycosidase inhibitors, also the relief of unwanted side effects, like gastrointestinal problems [35]. In this context, phosphate may be attached to a free hydroxyl moiety of a drug to increase water solubility until being cleaved off in vivo by alkaline phosphatases for instance that are present in many tissues, such as the intestinal epithelium, the liver and kidney tubules [36]. Prednisolone sodium phosphate, an immunosuppressant for children, is an example for this type of prodrug (Figure 6), which is 30x more water-soluble then prednisolone and in addition has a less unpleasant taste [34]. Other compounds belonging to the same class are fosamprenavir, a HIV protease inhibitor [37], and fosphenytoin, an anti-seizure medication. The phosphate moiety of the latter compound is attached through a hydroxymethyl linker, which upon cleavage of the P−O bond undergoes spontaneous hydrolysis and phenytoin is released [38,39].
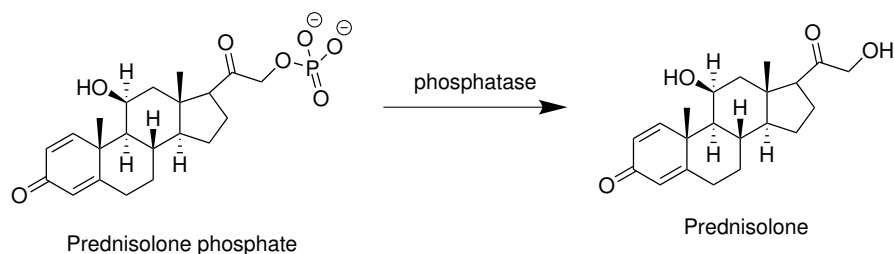
Figure 6: Dephosphorylation of prednisoline phosphate by a phosphatase, adapted from Huttunen et al. [34]

A very smart prodrug concept for amines involving phosphates was described by Nicolau et al. [36]: After hydrolysis of the phosphate ester, the butanamide derivative rapidly lactonizes and thereby releases the active amine moiety of the drug (Figure 7).
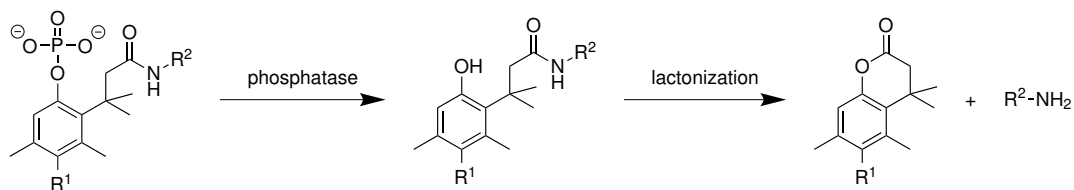
Figure 7: Prodrug system for amines, adapted from Nicolaou et al. [36], R^1 = H or OH

An utterly different strategy has to be pursued, when an "active" drug should carry phosphate groups. In that case hydrophilicity has to be reduced by suitable masking groups to enable diffusion of the compound across the plasma membrane to its site of action. Only within cells, these groups are cleaved off chemically or via endogenous enzymes and the medication stays trapped inside [40]. Some drugs are subsequently phosphorylated even further by kinases, giving rise to the active triphosphorylated form [34].

A very straightforward approach for masking phosphates is the formation of acyloxyalkyl or alkyloxycarbonyloxyalkyl esters (Figure 8). Upon cleavage of one of the carbonate or carboxylate esters by an esterase, a hydroxymethyl intermediate is formed, that quickly decomposes into formaldehyde and a phosphoric acid diester, which is further converted by a phosphodiesterase [41]. Phosphonates can be esterified in a similar fashion, albeit more than one stereoisomer of the final compound is produced.
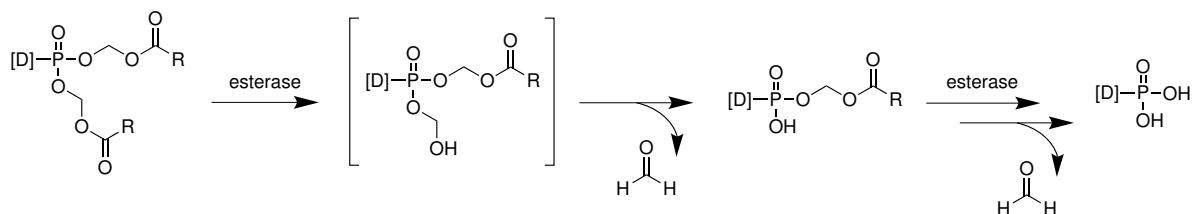
Figure 8: Phosphate/phosphonate groups masked by formation of acyloxyalkyl or alky-loxycarbonyloxyalkyl esters, R = Me, i-Bu, O-i-Pr, [D] = drug, scheme adapted from Hecker et al. [41]

The HepDirect system (Figure 9) for phosphate masking has been devised to specifically target liver cells [34]. Local cytochrome P_{450} monooxygenases mediate an oxidation of the benzylic carbon next to the phosphate/phosphonate ester bond, yielding a hemiketal, which spontaneously undergoes ring opening and β-elimination to give rise to the active drug [42].

9
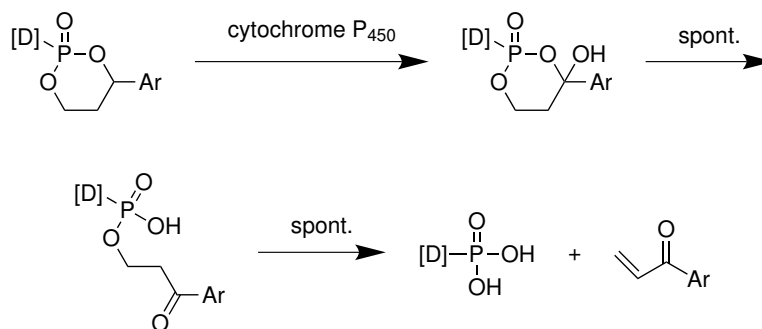
Figure 9: Phosphate/phosphonate groups masked by formation of cyclic 1-aryl-1,3-propanyl esters, [D] = drug, scheme adapted from Erion et al. [42]

1.2 Chemical Routes to Phosphate Monoesters

As phosphate esters encompass many fields of (bio)chemical, industrial and pharmaceutical research, a variety of methods have been developed to access such compounds via traditional synthetic routes. Phosphorus containing starting compounds can either be in oxidation state V or III (the latter are more reactive, but water-sensitive and an oxidation step is required in the end [43]) and comprise phosphoryl chloride, $POCl_3$ [43–47], and phosphorochloridates, $(RO)_2POCl$ [48–50], as well as phosphorus trichloride, PCl_3 [51–53], and chlorophosphines, $(RO)_2PCl/ROPCl_2$ [52]. Halide-free strategies also exist, in which *N*-phosphoryl oxazolidinones [54], phosphorothioates, $(RO)_2POSR$ [55–58], and phosphoro(di)amidites, $ROP(NR_2)_2/(RO)_2PNR_2$ [43,59], are utilized for example. Further, phosphoric acid (esters) can be esterified with an alcohol employing activating agents, such as carbodiimides [43,53].

The following section will predominantly focus on methods applicable to the formation of phosphoric acid monoesters, which typically make use of P(V)–compounds. For a comprehensive list of all known strategies regarding the synthesis of mono-, di- and triesters, the reader is referred to relevant literature and the references cited therein [43,53,58].

1.2.1 Activation of Phosphoric Acid (Esters)

Monoesters of phosphoric acid can be prepared via activation with dicyclohexylcarbodiimide (DCC, Figure 10) similar to carboxyl esters [53], albeit one has to consider that in case of this particular phosphoryl group transfer a different mechanism applies and no pentavalent intermediate is formed. It is also active enough to produce diesters and by far not the only coupling agent that has been characterized in conjunction with phosphoric acid (esters). For instance triesters were obtained from

diesters, when treated with e.g. mesitylenesulfonyl chloride or mesitylenesulfonyl tetra-zolide (MST, Figure 10). The latter has the advantage of producing a weak nucleophile, which is less prone than chloride to attack the newly formed ester [53]. Further examples for the preparation of monophosph(on)ates include CCl_3CN [43], $SOCl_2$ [60], bromotris(dimethylamino)phosphonium hexafluorophosphate (BroP) and N,N,N',N',-bis(tetramethylene)chlorounium tetrafluoroborate (TPyClU) [61].
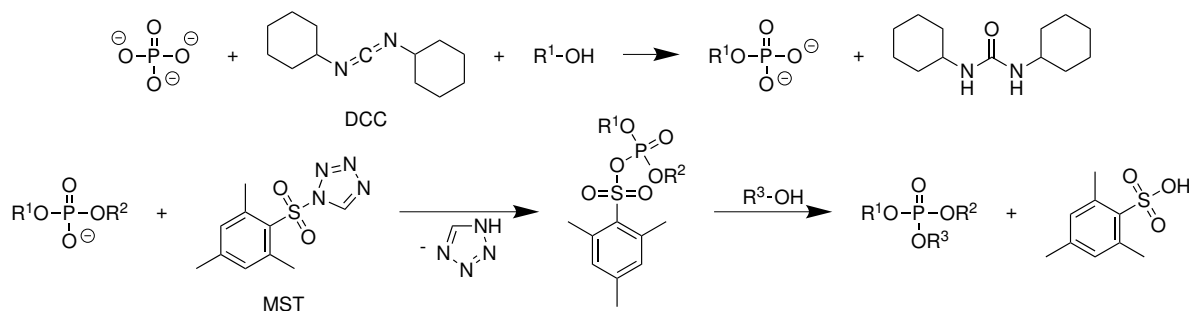
Figure 10: Activation of inorganic phosphate with dicyclohexylcarbodiimide (DCC) and activation of phosphate diesters with mesitylenesulfonyl tetrazolide (MST) [53]

In the last decade attempts have been made to discover further methods for the selective generation of monoesters from activated phosphoric acid and alcohols following the principles of green chemistry. These include the formation of acetyl phosphate intermediates [62], a refined strategy of trichloroacetonitrile activation [63], nucleophilic base catalysis [45] and even utilization of oxorhenium(VII)–species [64]. Articles by Sakakura et al. are recommended to the interested reader.

1.2.2 Phosphoryl chloride

Phosphoryl chloride is among the most widely utilized phosphorylating agents for the generation of mono-, di- and triesters [43] and can even be used industrially. For instance Aitken and coworkers described an upscalable method for the transformation of primary alcohols, applied in 1.8 fold excess with respect to $POCl_3$, into symmetrically substituted phosphoric acid diesters in the presence of Et_3N and subsequent steam hydrolysis [44].

With different reaction conditions and an excess of phosphoryl chloride, monoesters can be obtained (Figure 11) and nucleosides are even regioselectively phosphorylated on the primary hydroxy group: Yoshikawa et al. identified trialkyl phosphates to be accelerators in that reaction and water to inhibit 2'-OH or 3'-OH phosphorylation [46]. Later, Sowa and Ouchi developed an improved method with complete selectivity for the 5'-OH group using $POCl_3$, water and pyridine in a molar ratio of 2:1:2 [47].
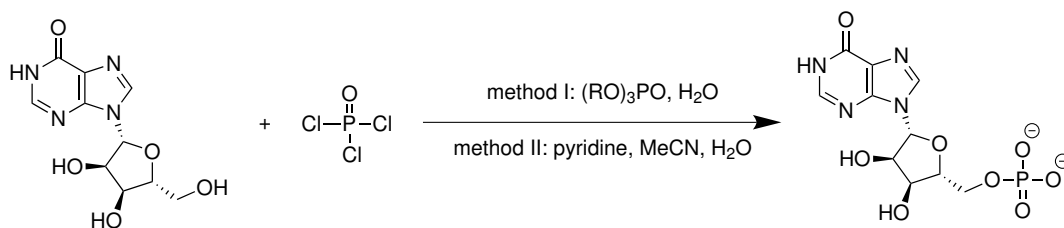
Figure 11: Regioselective phosphorylation of inosine with POCl$_3$ reported by Yoshikawa et al. (method I, [46]) and Sowa and Ouchi (method II, [47])

It is worth pointing out that in neither method depicted in Figure 11 the active phosphorylating agent is POCl$_3$. Rather, adducts (Figure 12) of the acid chloride and trialkyl phosphate (method I) or tetrachloropyrophosphate and pyridinium chloride (method II) were identified.
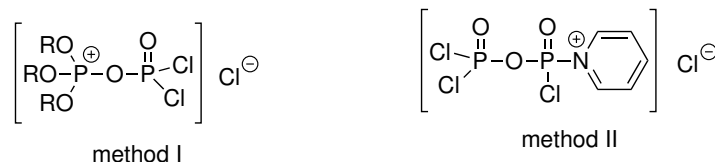
Figure 12: Active phosphorylating agents identified by Yoshikawa et al. (method I, [46]) and Sowa and Ouchi (method II, [47])

1.2.3 Phosphorochloridates

Khawaja and Reese qualified *o*-phenylene phosphorochloridate as a very powerful phosphorylating agent [48]. The mechanism proceeds via the formation of a triester (Figure 13) with an alcohol, R^1−OH, in the presence of Et$_3$N, 2,6-lutidine or pyridine in THF, dioxane, benzene or acetonitrile, followed by hydrolysis with an excess of water and at least one equivalent of base to yield an *o*-hydroxyphenyl phosphate ester, which is oxidatively converted into the monoester R^1−OPO$_3^{2-}$. The last step may be achieved via Br$_2$/H$_2$O [48], which is preferable for acid-labile esters, but limited to saturated alcohols. Olefinic esters can be obtained using HIO$_4$ under acidic conditions. Monoesters, which are acid labile *and* unsaturated can be prepared by oxidation with Pb(OAc)$_4$ in dioxane under alkaline conditions [49]. Primary, tertiary and even sterically demanding alcohols were esterified employing this method, emphasizing the reactivity of *o*-phenylene phosphorochloridate.

Another phosphorochloridate, bearing two 2,2,2-trichloro-1,1-dimethyl substituents (Figure 14), was designed for the selective phosphorylation of the 5'-OH group of nucleoside derivatives. After formation of a triester in pyridine and DMAP, the desired nucleotide is obtained via selective cleavage with cobalt(I)-phthalocyanine [50].
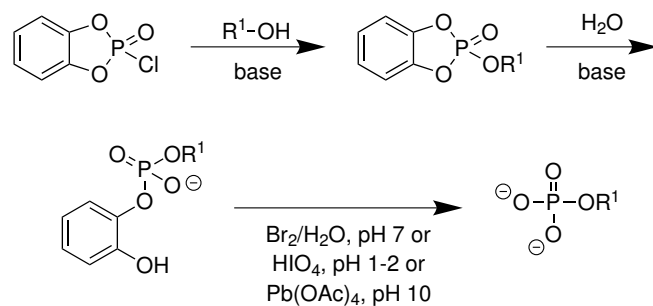
Figure 13: Preparation of phosphoric acid monoesters via *o*-phenylene phosphorochloridate, investigated by Khawaja and Reese [48, 49]
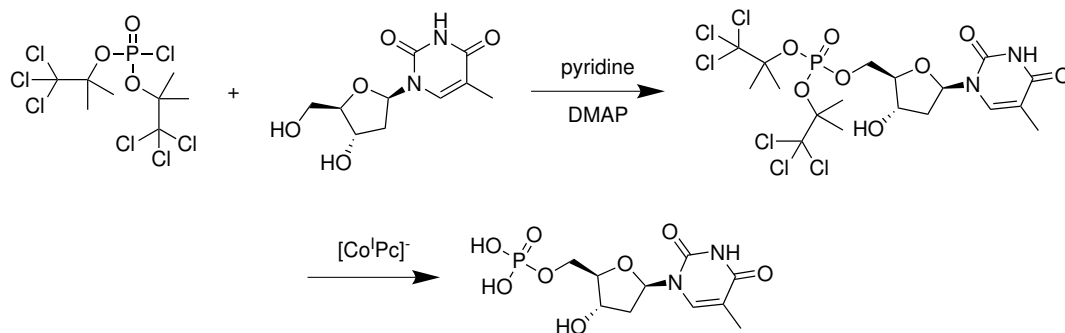
Figure 14: Phosphorylation of the 5'-OH group of thymidine by bis(2,2,2-trichloro-1,1-dimethyl) monochlorophosphate, as described by Kellner et al. [50]

1.2.4 Phosphorothioates

Ohkawa and coworkers investigated the phosphorylating abilities of 2-(methylthio)-4*H*-1,3,2-benzodioxaphosphorine 2-oxide [55, 56], outlined in Figure 15. By heating of the compound in DMF with an amine catalyst and an alcohol, an *O*-alkyl *O*-2-hydroxybenzyl *S*-methyl phosphorothioate is generated, which is reacted with cyclohexylamine to yield a phosphorothioate monoester via an intermediate formation of a carbenium ion. Finally, the methylthio group can easily be removed by iodine oxidation to give a phosphoric acid monoester [57, 58]. Still, the nature of R−OH should not be too complex: If (2'-OH, 3'-OH) unprotected nucleosides are phosphorylated with this method, a mixture of products, including a 2',3'-cyclic phosphate, is obtained [57].

1.2.5 Phosphoric Acid Monoesters as Phosphorylating Agents

Two types of phosphoric acid monoesters are employed as phosphorylating agents. Compounds belonging to the first class bear a good leaving group and readily undergo an ester exchange reaction with alcohols in the presence of base. *p*-Nitrophenyl phosphate (pNPP) [65] and 2-(*N,N*-dimethylamino)-4-nitrophenyl phosphate [58] can be named as representative examples. A general reaction scheme is presented in Figure 16.
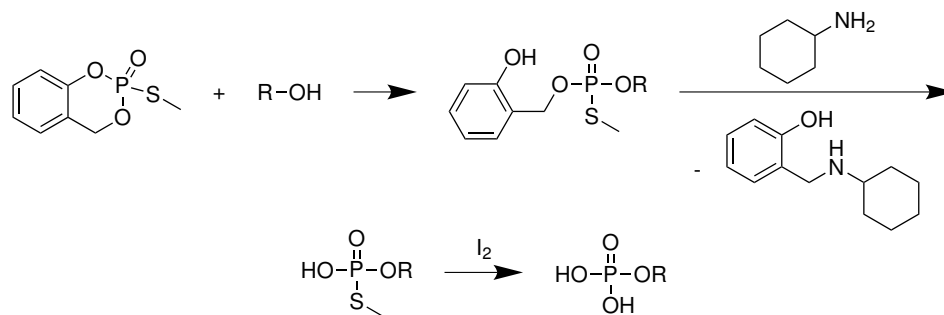
Figure 15: Formation of phosphoric acid monoesters, starting from 2-(methylthio)-4*H*-1,3,2-benzodioxaphosphorine 2-oxide, according to Ohkawa et al. [55–57]
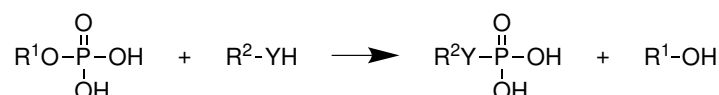
Figure 16: General scheme of an ester exchange reaction; Y = O, S, NH for pNPP and Y = O, S for 2-(*N,N*-dimethylamino)-4-nitrophenyl phosphate

In phosphate monoesters, which can be assigned to the second class, the alkyl group, like 2-cyanoethyl, acts as a blocking group (Figure 17). First, diesters are formed from these substrates with an alcohol via activation by e.g. DCC. Subsequently, the blocking group is removed e.g. under mild alkaline conditions [66].
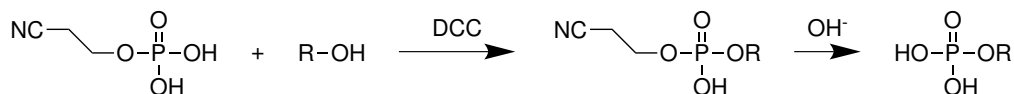
Figure 17: Synthesis of phosphoric acid monoesters utilizing 2-cyanoethyl phosphate, adapted from Tener et al. [66]

Compounds from both of the above mentioned classes have been reported to yield phosphoric acid monoesters [58], however the outcome of the strategies outlined above strongly depends on the reaction conditions and the nature of the substrates. For example if pNPP is employed, polyphosphates are obtained, if a large excess of pydirine is used [65] and among the drawbacks of the 2-cyanoethyl method (anhydrous triethylamine/aq. ammonia) is the formation of bis-phosphates in the synthesis of 5'-phosphates of L-ribonucleosides [58].

1.2.6 P(III)–Compounds

Diethyl phosphorochloridodithioite (Figure 18) is an example of a P(III)–compound employed in the synthesis of monoalkyl phosphates. After reaction with an alcohol under basic conditions, a phosphite is formed, which can be oxidized to the monoester

with I_2/H_2O. Depending on the nature of R−OH, the overall yields range from 39–66 % [67].
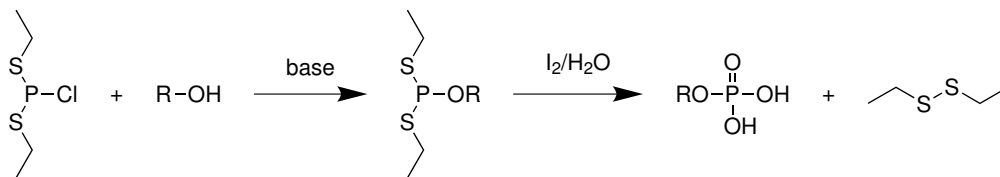
Figure 18: Preparation of phosphoric acid monoesters, starting from diethyl phosphorochloridodithioite, as examined by Takaku et al. [67]

The main application of P(III)–Compounds, however, is the synthesis of di- and triesters of phosphoric acid. To this end, phosphorus trichloride, PCl_3 [51–53], and chlorophosphines, $(RO)_2PCl$ or $ROPCl_2$ [52], as well as phosphoro(di)amidites, $ROP(NR_2)_2$ or $(RO)_2PNR_2$ [43,59], are commonly employed.

1.3 High-Energy Phosphorylated Compounds in Nature

Phosphoryl transfer reactions in biochemisty are determined by thermodynamics. Phosphate donors have a more negative free energy of hydrolysis, $\Delta G'^{\circ}_{hydro}$, than acceptors. Thus, a compound from Table 1 can phosphorylate all other compounds named underneath it [68]. For instance, the phosphoamide phosphocreatine is capable of converting ADP to ATP in the presence of a suitable enzyme [69].

Table 1: $\Delta G'^{\circ}_{hydro}$ values for common metabolites [68], structures in Figure 19

metabolite	$\Delta G'^{\circ}_{hydro}$ [kJ mol^{-1}]	
phosphoenolpyruvate (PEP)	-62	
carbamoyl phosphate (CP)	-51	
1,3-bisphosphoglycerate	-49	
acetyl phosphate (AcP)	-43	
phosphocreatine (PC)	-43	high-energy compounds
pyrophosphate (PP$_i$)	-33	
phosphoarginine	-32	
ATP $\longrightarrow$ AMP + P$_i$	-32	
acetyl CoA	-32	
ATP $\longrightarrow$ ADP + P$_i$	-30	
glucose 1-phosphate	-21	
glucose 6-phosphate	-14	low-energy compounds
glycerol 3-phosphate	-9	
AMP $\longrightarrow$ adenosine + P$_i$	-14	
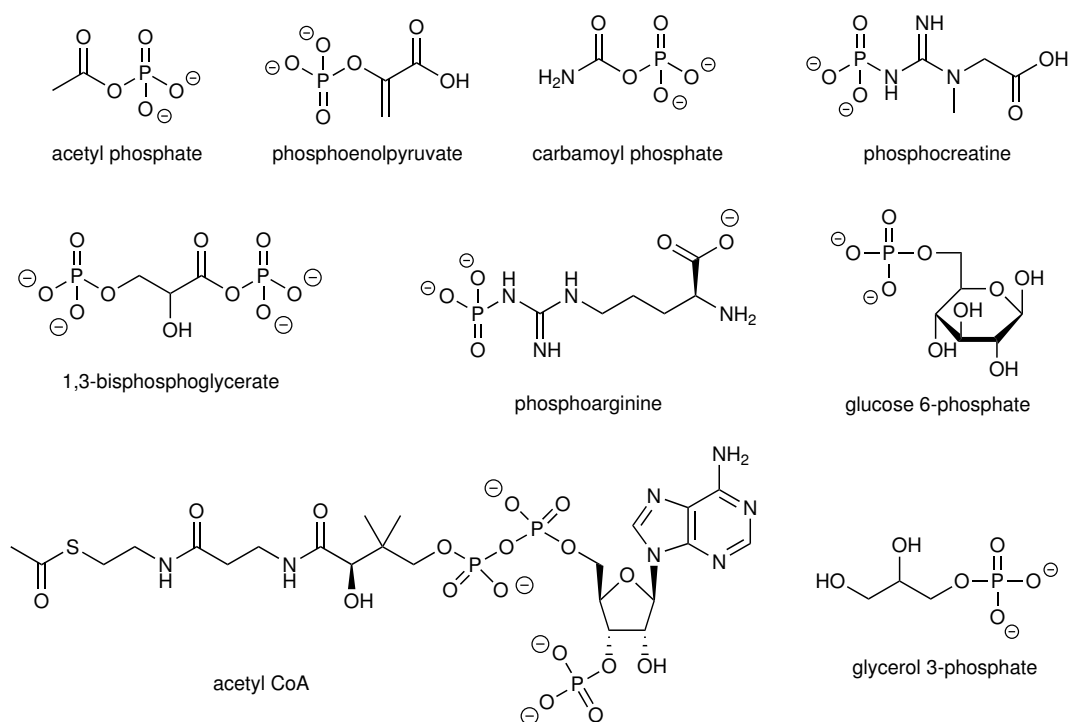
Figure 19: Examples of common metabolites

The "energy currency" of Nature, *adenosine triphosphate* (ATP), can also be found in the list. A main concept in biology is the activation of a low-energy compound via phosphorylation, which enables it to undergo further transformations. Kinases catalyzing this process are typically ATP-dependent [70]. Although phosphate ester formation is thermodynamically uphill, the hydrolysis of the high-energy $P-O$ bond of ATP releases quantities of energy large enough to render the overall phosphoryl transfer process thermodynamically favorable. Low-energy phosphorylating agents from Table 1 on the other hand can only function as such, if the transfer reaction is coupled to a thermodynamically more favored reaction [3].

Phosphoenolpyruvate (PEP) is on top of Table 1. It is generated from 2-phosphoglycerate by an enolase in glycolysis and subsequently its phosphate moiety is transferred onto ADP by pyruvate kinase. The highly negative free energy of hydrolysis can be attributed to the tautomerisation of PEP into the keto form, once the phosphate ester is hydrolyzed. In gluconeogenesis, PEP is formed via a different pathway in the mitochondria [3]:

$$\text{pyruvate} + CO_2 + \text{ATP} + H_2O \xrightarrow{pyruvate\ carboxylase} \text{oxaloacetate} + \text{ADP} + P_i + 2\,H^+$$

$$\text{oxaloacetate} + \text{GTP} \xrightarrow{phosphoenolpyruvate\ carboxylase} \text{PEP} + \text{GDP} + CO_2$$
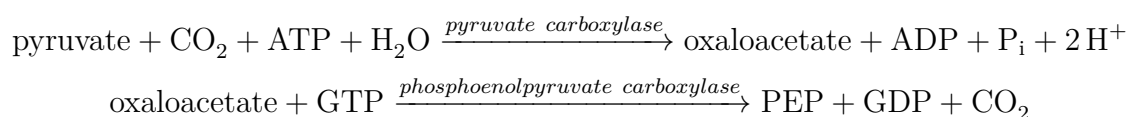
PEP also occurs in the photorespiration regulating C_4 pathway of tropical plants, where it is converted to oxaloacetate, which carries CO_2 from mesophyll cells, that are in

16

contact with air, to bundle-sheath cells, where photosynthesis takes place. The overall reaction of the pathway can be summarized as follows [3]:

$$CO_2(\text{mesophyll cell}) + ATP + H_2O \longrightarrow CO_2(\text{bundle}-\text{sheath cell}) + AMP + 2P_i + H^+$$

Finally, PEP also plays a role in the synthesis of the aromatic amino acids phenylalanine, tyrosine and tryptophan, where it is condensed with erythrose 4-phosphate in the initial step. Later in the same pathway, another molecule of PEP is reacted with shikimate 3-phosphate to give a 5-enolpyruvyl intermediate that decomposes into chorismate [3].

The second compound in Table 1, *carbamoyl phosphate* (CP) with its high-energy anhydride bond, is formed e.g. in the beginning of the urea cycle and also in the de novo synthesis of pyrimidine nucleotides by carbamoyl phosphate synthetase from HCO_3^- and NH_4^+ at the expense of two molecules of ATP (Figure 20) [3]. Notably, in both pathways, CP acts as a carbamoyl group donor and not as a phosphorylating agent.
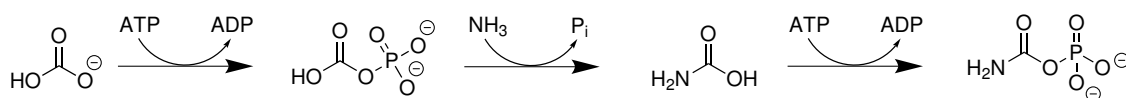
Figure 20: Formation of CP by carbamoyl phosphate synthetase, scheme modified from Stryer [3]

Phosphocreatine (PC) represents a high-energy phosphate group donor in muscles of vertebrates, which can regenerate ATP for a limited amount of time, before metabolism has to take over [3]:

$$\text{creatine phosphate} + ADP + H^+ \xrightleftharpoons{\text{creatine kinase}} ATP + \text{creatine}$$
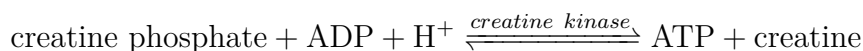
Acetyl phosphate (AcP) is a metabolic intermediate in many anaerobic bacteria and *E. coli*, which typically is formed from acetyl CoA by phosphotransacetylase. It serves in substrate level phosphorylation of ATP during anaerobic growth in a reaction mediated by acetate kinase [71]:

$$\text{acetyl CoA} + P_i \xrightleftharpoons{\text{phosphotransacetylase}} AcP + CoA$$
$$AcP + ADP \xrightleftharpoons{\text{acetate kinase}} \text{acetate} + ATP$$
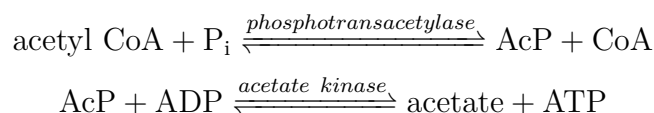
AcP and PEP for example can be chemically synthesized for their application in biocatalytic phosphorylation/ATP regeneration reactions with purified enzymes (see Section 1.4.2). The disodium salt of AcP can readily be formed by acylation of phosphoric
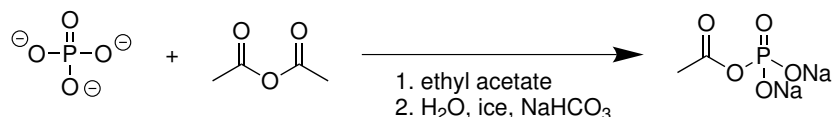
Figure 21: Synthesis of acetyl phosphate (AcP), described by Crans and Whitesides [72]

acid with acetic anhydride in ethyl acetate prior to extraction of AcP into water, extraction of acetic acid from the aqueous layer with ethyl acetate and neutralization of the solution to pH 7 for storage and use, as outlined in Figure 21.

The preparation of PEP in contrast is much more elaborate [73]. Hirschbein and coworkers suggested a synthetic route (Figure 22) starting with bromination of pyruvic acid, formation of the dimethyl ester of PEP with trimethyl phosphite in a Perkow reaction and alkaline hydrolysis of the triester to yield the monopotassium salt.
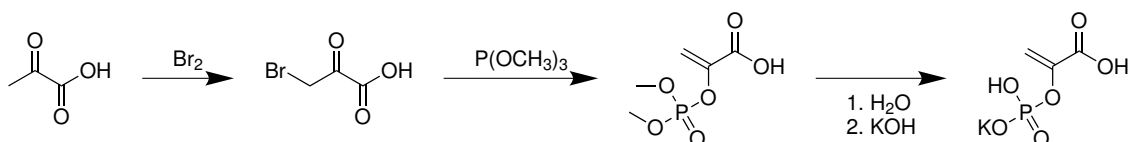
Figure 22: Synthesis of phosphoenolpyruvate (PEP), suggested by Hirschbein et al. [73]

1.4 Kinases

Most of the classical synthetic methods for obtaining phosphate esters described in Section 1.2 make use of very reactive reagents, require precisely tuned reaction conditions to prevent the formation of unwanted side products, and display constraints with respect to the nature of the substrate, which may render them unsuitable for particular problems. Especially the regioselective phosphorylation of polyhydroxy compounds, such as nucleosides, is challenging and, apart from the two methods depicted in Section 1.2.2, typically require multiple protection an deprotection steps [20, 74]. In order to address these issues, several biocatalytic routes have been developed. The following section will cover the advantages and shortcomings of using enzymes belonging to the class of kinases for that task.

1.4.1 General Considerations

Kinases belong to the Enzyme Comission (EC) categories 2.7.1.X–2.7.4.X, transfer a phosphate moiety predominantly from ATP to alcohol, nitrogenous, carboxy or phosphate groups [6] and form esters of lower energy [70]. An example reaction of the 6'-OH

selective phosphorylation of glucose by glucokinase at the expense of ATP is given in Figure 23. Aside from being regiospecific, phosphate transfer reactions employing kinases can also be enantio- [75] and diastereospecific [76].
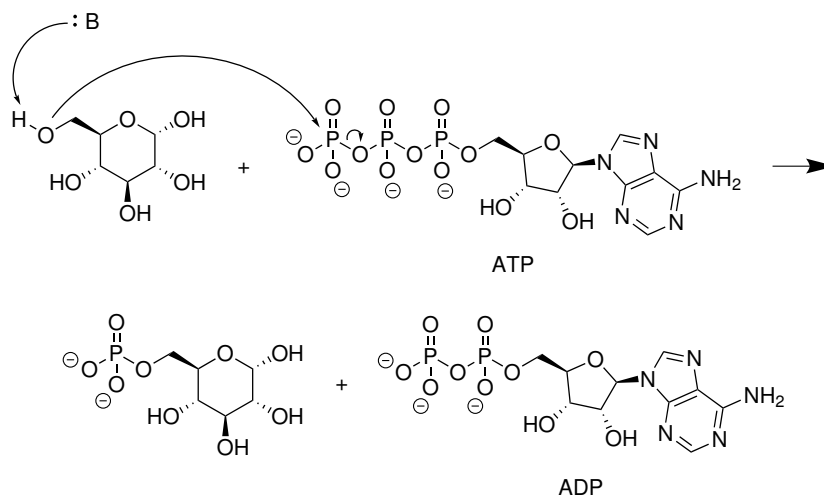
Figure 23: Regioselective phosphorylation of glucose by glucokinase and ATP as the phosphorylating agent [77]

The use of stoichiometric amounts of cofactor is unfavorable, not only economically, but also thermodynamically [68]: High concentrations of ADP can shift the reaction equilibrium towards the substrate side. Consequently, ATP is employed just in catalytic amounts and recycled ideally 10^2–10^6 times [20, 78] by another kinase, which in turn is dependent on a (preferably cheap and stable) phosphorylated donor (Figure 24). This application of cell-free enzymes in the regeneration of ATP has been reported to be more specific and more compatible with other components of enzymatic reactions than chemical methods or protocols employing whole cells [78].
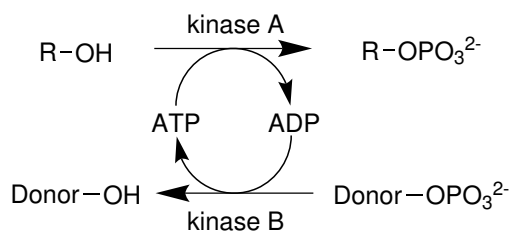
Figure 24: Regeneration of ATP with a second kinase [20]

1.4.2 ATP Recycling Methods

Several high-energy phosphorylated compounds presented in Table 1 in Section 1.3 can be utilized as a phosphorylating agent for ATP regeneration with an appropriate enzyme. Some of the most common systems are presented below.

- PEP/pyruvate kinase: The phosphorylated donor is difficult to prepare (see Section 1.3) and both phosphoenolpyruvate [74] and pyruvate [70] inhibit kinases, but PEP represents a strong phosphorylating agent (see Table 1) and is furthermore very stable (see Section 2.3). Pyruvate kinase in addition has a very low K_M to ADP of only 0.1 mM [79], which makes it the enzyme of choice with low cofactor concentrations.

- AcP/acetate kinase is the most widely used ATP-regeneration system [70]. Acetyl phosphate is easy to prepare (see Section 1.3), but is not as stable as PEP (see Section 2.3) and has a lower phosphorylating potential (see Table 1). Acetate was described to be a weak inhibitor of acetate kinase [70] and AcP was identified to inhibit hexokinase [80]. The K_M of acetate kinase to ADP is 0.4 mM [81].

- Methoxycarbonyl phosphate (MCP)/acetate kinase: The development of this system aimed at the replacement of AcP as phosphorylated donor [79] and has several advantages: The phosphorylating potential of MCP is similar to PEP, but its preparation from phosphate and methyl chloroformate in aqueous solution is significantly less cumbersome (solutions of MCP can be used without further purification). Upon hydrolysis of the P−O bond of MCP, methyl carbonate is released, which rapidly decomposes into methanol and CO_2. A major drawback of this method is the limited half-life of MCP of only 0.3 h at 25 °C and neutral pH.

- Further systems for ATP-regeneration have been summarized by Faber [20] and Whitesides [70] and include carbamoyl phosphate (CP)/carbamyl kinase, polyphosphate (polyP)/polyphosphate kinase as well as phosphocreatine (PC)/kreatine kinase.

1.4.3 Representative Kinases and Applications in Phosphate Ester Formation

Hexokinase (EC 2.7.1.1) catalyzes the regioselective phosphorylation of the primary hydroxy group of hexoses [6]. As an example it was employed by Pollak and coworkers to generate glucose 6-phosphate (G6P), a valuable compound for NAD(P)H cofactor regeneration [82], on a molar scale using the AcP/acetate kinase system for ATP recycling [7]. It is not eminently specific to the type of substrate, since pyranose and furanose analogs of glucose are accepted as well as carbohydrates, in which the secondary OH-moieties are replaced by e.g. fluorine [74]. The latter class of compounds may give rise to new pharmaceuticals, since they represent strong inhibitors of the nonfluorinated type due to the similarity of C−F and C−OH in bond length and polarity, but not in reactivity [83].

The natural substrate of *Glycerol kinase* (EC 2.7.1.30) is glycerol [8], which is enantio- and regioselectively phosphorylated to D-glycerol 1-phosphate, however dihydroxyacetone (DHA) and a wide range of primary alcohols are also accepted [20, 75] and can be

phosphorylated in a stereoselective fashion [84]. Consequently, glycerol kinase has been used by Wong et al. in the synthesis of dihydroxyacetone phosphate (DHAP), which subsequently was converted into fructose 6-phosphate with triosephosphate isomerase and an aldolase [85]. DHAP may however also be generated in a phosphatase-mediated reaction [86], which will be discussed in more detail in Section 1.5.4.

NAD kinase (EC 2.7.1.23) is able to transform NAD^+ into the more expensive $NADP^+$ quantitatively, as pointed out by Walt and coworkers [87]. In the corresponding manuscript, ATP was regenerated employing the AcP/acetate kinase system.

Non-ATP-dependent kinases were found in various Gram-positive bacteria such as *Arthrobacter sp.*, which utilize polyphosphate (polyP) as phosphorylating agent [88]. It is a common belief that polyP was the precursory high-energy compound to ATP, as some kinases can use both donors. In addition, the crystal structure of polyP/ATP glucomannokinase resembles the structure of hexokinase, confirming theories of a common ancestor [89]. *Polyphosphate glucokinase* (PPGK) and *polyP-glucose 6-phosphotransferase* (PGPTase, EC 2.7.1.63) as examples of this class of enzymes catalyze the transfer of a phosphate moiety from polyP to the 6'-OH group of glucose [33].

To summarize, kinases may readily be used in certain phosphorylation tasks, however, since they evolved to synthesize particular compounds in Nature, they only tolerate limited variations regarding their substrate. The next section therefore will introduce phosphatases, which can also be utilized for the formation of phosphate esters, but display a broader substrate spectrum, as they are involved in biochemical degradation. In addition, these enzyme are not dependent on ATP as cofactor.

1.5 Phosphatases

In Nature, the hydrolysis of phosphate esters is catalyzed by phosphatases, a very large and diverse group of enzymes. Some of them are known to fulfill distinct functions: For instance the membrane bound glucose 6-phosphatase (G6Pase), located in the liver and the kidney cortex, plays a critical role in the regulation of blood glucose [90] and the dephosphorylation of protein-tyrosyl residues by protein tyrosine phosphatases (PTPs) represents an important cellular control mechanism [91]. Assigning phosphatases to EC categories is difficult, since most of them have a rather relaxed substrate spectrum and can catalyze the hydrolysis of both phosphate esters (EC 3.1.3.X, phosphoric monoester hydrolases) and acid anhydrides (EC 3.6.X.X: acting on acid anhydrides), such as in pyrophosphate (PP_i) [92]. Consequently, different methods for categorization were developed [93], which may be based on sequence similarity, but also on certain properties

like pH optimum (alkaline versus acid), origin, substrate profile (specific versus non-specific) or substrate size (low versus high mass) [94]. The following section intends to give an overview of prominent phosphatase families and point out representative enzyme examples, which were either already applied in biocatalytic transformations or could be promising candidates, as well as their catalytic mechanism. Further and most importantly, the employment of phosphatases in the synthetic direction in order to generate phosphate esters in the presence of a suitable donor will be covered.

1.5.1 Overview and Examples

Although phosphatases act on $P-O$ bonds in a number of ways, they can be summarized into two main groups: Enzymes, which catalyze a direct nucleophilic attack by water on phosphate esters and enzymes, which form a phosphoenzyme intermediate. Both types can employ metal ions, which lower the activation energy for bond fission [68]. In phosphoenzyme-intermediate-forming phosphatases, metals increase the nucleophilicity of amino acid residues in the active site [93], whereas in the non-intermediate-forming type, they coordinate to non-bridging oxygen atoms of the phosphate ester, rendering phosphorus more electrophilic [77], and furthermore they make the attacking nucleophile (e.g. water) more nucleophilic [93]. The mechanism of both types of phosphatases proceeds through an $S_N 2$-like nucleophilic attack on phosphorus rather than carbon, which has been investigated by Hass et al. in experiments with glucose 6-phosphatase (intermediate-forming) and $H_2^{18}O$ [95] (Figure 25): ^{18}O was found exclusively in the free phosphate (determined by mass spectrometry). Consequently, inversion at the P-atom is observed with phosphatases, which catalyze a direct phosphoryl transfer to water [96, 97], whereas members of the phosphoenzyme-intermediate-forming group perform a double inversion on the phosphorus atom, resulting in a net retention of the configuration [98]. Enzymes can be experimentally classified into one of the two groups, when being exposed to e.g. ^{17}O & ^{18}O-labeled phosphate esters [98].
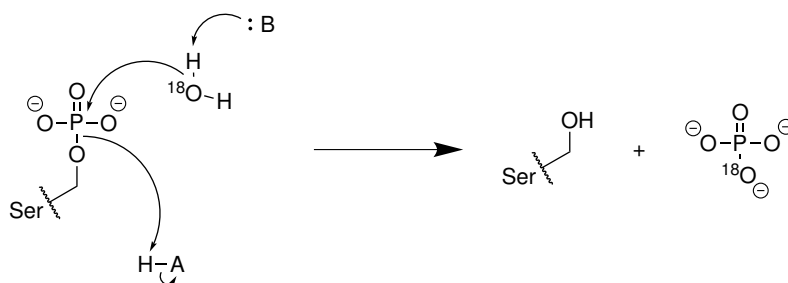
Figure 25: Hydrolysis of the phosphoserine intermediate in glucose 6-phosphatase proceeds via attack on the P-atom [77]

Purple acid phosphatases (PAPs, EC 3.1.3.2 [6]) belong to the non-intermediate-forming group and contain either Fe(III)–Fe(II), Fe(III)–Zn(II) or Fe(III)-Mn(II) centers, which are surrounded by seven invariant amino acids [93]. They hydrolyze phosphoric acid monoesters and amide substrates [99], but their precise catalytic mechanism is still enigmatic: After formation of a pre-catalytic complex and subsequent coordination of the phosphate to at least the divalent metal ion [93], it is either attacked by a bridging hydroxide or by a non-coordinating hydroxide in the second coordination sphere to expel the leaving group. Finally, the bound phosphate is replaced by two water molecules in a poorly understood sequence [99]. Until now, these enzymes have not been employed in the synthetic field yet.

Enzymes constituting the *histidine phosphatase superfamily* do not require metal ion cofactors and form a phosphoenzyme intermediate. Acid phosphatases, as well as some bacterial and fungal phytases (EC 3.1.3.26 [6]) belong to this large class of proteins [100]. During catalysis, a histidine residue in the highly positively charged (hence phosphate ester stabilizing) active site is phosphorylated. The leaving group is protonated via a glutamate or an aspartate residue, as depicted in Figure 26. Following that, the intermediate is attacked by water, unless a competitive acceptor is present. In this case transphosphorylation may occur, which has been demonstrated already in the 1950s by Morton employing an acid phosphatase from prostate gland, phosphocreatine as donor and glucose, glycerol, 1,2-propanediol, dihydroxyacetone and glyceraldehyde as substrates [101].
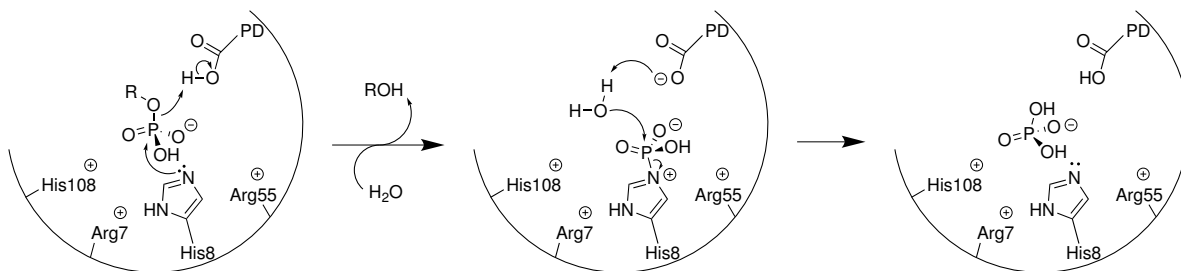
Figure 26: Catalytic mechanism of phosphatases belonging to the histidine superfamily; PD = proton donor (aspartate or glutamate), numbering as in *E. coli* SixA, modified from Rigden [100]

Phytate (*myo*-inositol hexakisphosphate), the major form of phosphorus in plants, is the natural substrate of phytases [102]. Supplementation of these enzymes in animal food obviates the need for inorganic phosphorus supplementation and concomitantly prevents the excretion of non-metabolized dietary phytate, which would cause environmental problems [103]. In the field of biocatalysis, phytase has been employed in the one-pot synthesis of 5-deoxy-5-ethyl-D-xylulose (Figure 27): After phosphorylation of

glycerol by phytase, DL-glycerol 1-phosphate was converted to dihydroxyacetone phosphate (DHAP) by glycerol phosphate oxidase (GPO), which was further condensed with butanal by fructose 1,6-diphosphate aldolase (FruA) after raising the pH. Following the aldol reaction, the pH was lowered again in order to re-enable the activity of phytase, dephosphorylate 5-deoxy-5-ethyl-D-xylulose phosphate and yield the product [104].
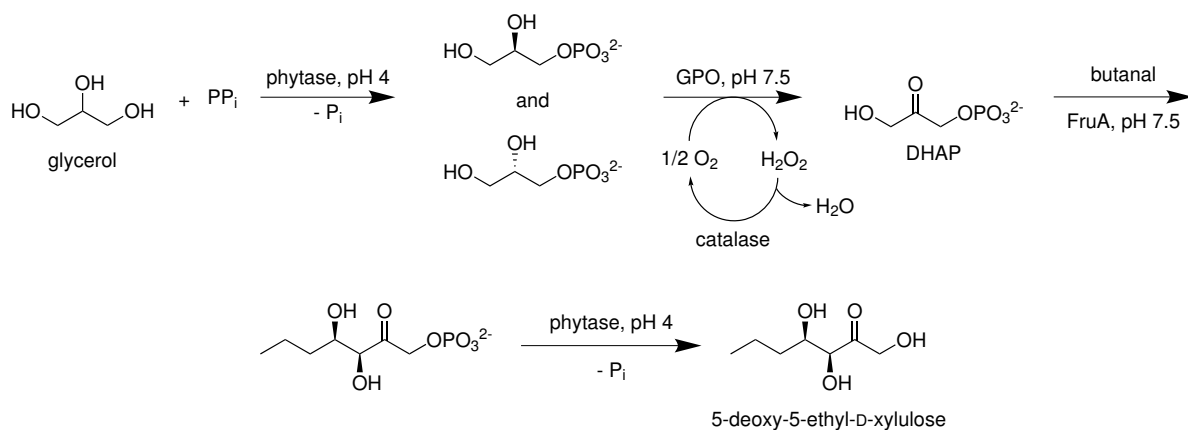
Figure 27: One-pot synthesis of 5-deoxy-5-ethyl-D-xylulose according to Schoevaart et al. [104], DHAP = dihydroxyacetone phosphate, GPO = glycerol phosphate oxidase, FruA = fructose 1,6-diphosphate aldolase

Protein tyrosine phosphatases (PTPs) are metal-independent enzymes, which hydrolyze phosphate esters of tyrosine residues and thereby regulate cellular processes like proliferation, growth and differentiation [105]. They form phosphocysteine intermediates, which can either be attacked by water or an alcohol [106], however the latter has scarcely been investigated. All PTPs possess a "phosphate binding loop", which consists of an arginine residue and main chain nitrogens, which are oriented, so that they can interact with the equatorial O-atoms of the phosphate group [105]. The catalytic mechanism is delineated in Figure 28.
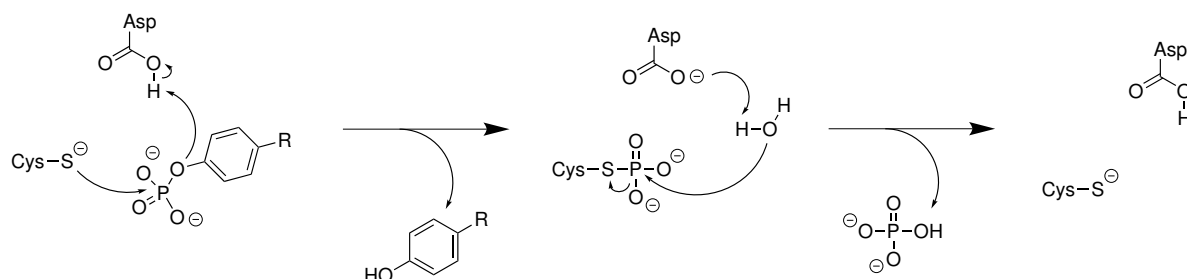
Figure 28: Catalytic mechanism of protein tyrosine phosphatases (PTPs) [105]

The majority of proteins belonging to the *haloacid dehalogenase* (HAD) superfamily are phosphate monoester hydrolases (79 %) and ATPases (phosphoanhydride hydrolases, 20 %) and can be found in all three superkingdoms of life [107] being involved in a

variety of pathways, such as organ formation, as well as in diseases like cancer or neurological disorders [108]. HAD-like phosphatases form a phosphoaspartate intermediate (Figure 29) and at the same time are dependent on Mg^{2+}. The metal aids in positioning the phosphate moiety for an attack of Asp and stabilizes the approximation of the nucleophile to the substrate electrostatically [108]. YniC-Ec [109] as a representative enzyme of this class was investigated in the experimental part (Section 2).
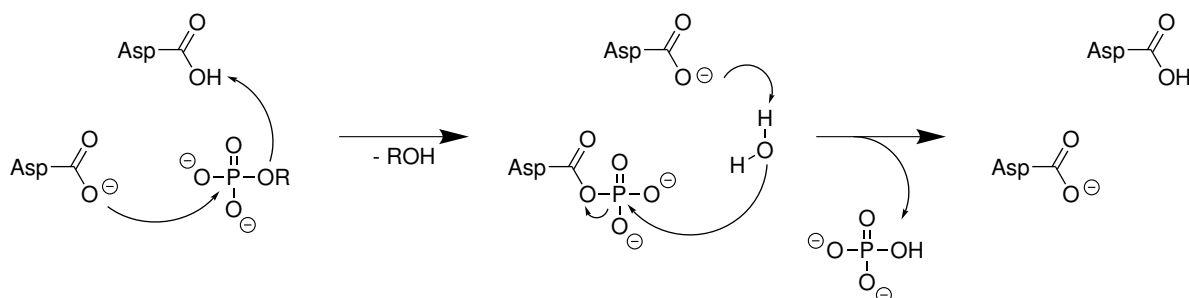
Figure 29: Catalytic mechanism of HAD-like phosphatases [108]

Given their significance, the next two sections will focus on alkaline phosphatases and bacterial non-specific acid phosphatases (NSAPs), which were applied in both the hydrolytic and the synthetic mode in numerous biocatalytic transformations.

1.5.2 Alkaline Phosphatases

Alkaline Phosphatases (APs) are dimeric enzymes with an alkaline pH optimum, which can be found in most organisms [93], typically contain two Zn^{2+} and one Mg^{2+} ion in the active site and hydrolyze both phosphomonoesters and (with low activity) diesters [110]. They accept a broad range of substrates and often form a phosphoserine intermediate, which can be attacked either by water or an alcohol [93]. The transphosphorylation activity of APs has already been investigated in the 1950s [111] and a multitude of transformations utilizing these enzymes in both the hydrolytic and the synthetic direction have been reported since. This section deals with the catalytic mechanism of APs and gives a cursory overview of their application in biocatalysis.

1.5.2.a Catalytic Mechanism

The AP from *E. coli* has been extensively studied in the past decades, which included elucidation of its mechanism. Only the role of Mg^{2+} is not fully understood, although recent studies deliver conclusive evidence of the metal stabilizing the transferred phosphate moiety via a coordinated water molecule in the transition state (TS) rather than acting as a general base catalyst [112]. In addition to the three metal ions in the active site, a

25

conserved Arg residue is present, which is considered to play a role in TS-stabilization as well as substrate binding [93].

A simplified transition state model is given in Figure 30. As summarized by Cleland and Hengge [93], the phosphate ester is hydrogen-bonded to Arg166 and also coordinates to both Zn^{2+} ions. The phosphoenzyme intermediate (E-P) is formed via Ser102 (upon deprotonation and coordination to Zn2), which performs an in-line attack at the phosphorus center, expelling the leaving group with its negative charge being stabilized by Zn1 in the TS. Subsequently, water or an alcohol can coordinate to Zn1, enabling a nucleophilic attack on the phosphoserine intermediate. At a pH < 7, the rate-limiting step is the hydrolysis of E-P, whereas at pH > 7 the ultimate release of phosphate determines the speed of the reaction [93].
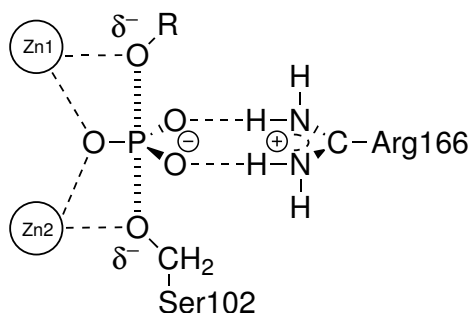
Figure 30: X-ray structure based model of interactions in the TS in an alkaline phosphatase catalyzed reaction, numbering as in *E. coli* AP [93]

PhoK/SPHSX from *Sphingomonas. sp.* strain BSAR-1, employed in Section 2 and described by Bihani et al. [113], has less than 15% sequence identity to *E. coli* AP and is more related to nucleotide phosphodiesterases (NPP), albeit it shows striking preference for action on monoesters. Further differences from the *E. coli* enzyme include Thr as a catalytic residue instead of Ser, the lack of a Mg^{2+} binding pocket, the deletion of Arg, which stabilizes the phosphate in the TS in *E. coli* AP, and the requirement of Zn^{2+} and Ca^{2+} for activity. Nonetheless, the geometry of its active site (bimetallic zinc core, coordinated by His and Asp) and the way the phosphoryl group is oriented during catalysis resemble other APs, suggesting a similar in-line displacement mechanism with a trigonal-bipyramidal TS, as outlined above.

1.5.2.b Dephosphorylation

The employment of alkaline phosphatases in the hydrolytic mode is particularly valuable in synthetic tasks, in which regioselective dephosphorylation is demanded. For instance, the synthesis of 2'-carboxy-D-arabinitol 1-phosphate, an inhibitor of ribulose

1,5-bisphosphate carboxylase, studied by Gutteridge and coworkers, proceeded via formation of 2'-carboxy-D-arabinitol 1,5-bisphosphate, which was exposed to both an alkaline and an acid phosphatase [114]. AP produced a 4:1 mixture of the desired compound and the 5'-phosphate, whereas the acid phosphatase yielded 2'-carboxy-D-arabinitol 1-phosphate almost quantitatively.

Further substrates subjected to dephosphorylation by APs were for example *p*-nitrophenyl phosphate and its phosphorothioate analog [115] as well as naphthyl 1,2-dioxetane phosphates [116]. In addition, ligation of DNA can be prevented by removal of the 5'-phosphate group by an AP, which represents a useful tool in molecular biology [117].

1.5.2.c Transphosphorylation

As already briefly mentioned, the phosphotransferase activity of APs has already been reported several decades ago: In 1958 Morton used APs purified from cow's milk and calf intestinal mucosa in the generation of phosphoric acid monoesters of glucose, fructose, glycerol, 1,2-propanediol, DL-glyceraldehyde and dihydroxyacetone (DHA) with e.g. phosphocreatine (PC) and pyrophosphate (PP_i) as donors [111].

Later, Pradines et al. also employed APs in the phosphorylation of simple alcohols, polyols and diols with PP_i or polyphosphate as donors [118]. High substrate concentrations were chosen to shift the equilibrium and favor transphosphorylation. The same group also described the production of glycerol 1-phosphate with immobilized AP, which was identified to be regio- but not stereoselective [119]. Notably, phosphate as donor at concentrations of 0.4 M–0.8 M and an excess of glycerol (80 % v/v) were employed and good yields (75 g L^{-1}, 41 %) could be obtained.

Gettins and coworkers investigated the phosphorylation of tris(hydroxymethyl)aminomethane (Tris) by AP via ^{31}P-NMR and found the transphosphorylation activity to increase significantly at pH 8 to 10 [120]. This finding matches the observations from Pradines et al. of APs being most active at pH 6 in the hydrolytic and at pH 8.5 in the synthetic mode [118]. Most likely, alkaline conditions are required for the alcohol, whose pKa is lowered likely by a Zn^{2+} ion, to be deprotonated [68].

Further general aspects regarding transphosphorylation, which apply to all kinds of phosphatases, but predominantly have been discussed in literature in conjunction with non-specific acid phosphatases, are given in Section 1.5.3.c.

1.5.3 Bacterial Non-specific Acid Phosphatases

Bacterial non-specific acid phosphatases (NSAPs) are monomeric or oligomeric enzymes with an M_r of 25–30 kDa per subunit, can either be membrane-bound lipoproteins or soluble periplasmic proteins, hydrolyze a wide range of phosphoric acid esters and display an activity maximum at acidic to neutral pH [121]. Based on their amino acid sequence, they can be divided into the three subclasses A, B and C [94].

Class A non-specific acid phosphatases are characterized by the common sequence motif K-X(6)-R-P-X(12,54)-P-S-G-H-X(31,54)-S-R-X(5)-H-X(2)-D [121], which can also be found in vanadate containing haloperoxidases [122], mammalian glucose 6-phosphatases [123] and some lipid phosphatases [124]. Therefore, *apo*-chloroperoxidases, which lack vanadate as prosthetic group, can function as phosphatases [125] and conversely, vanadate-supplemented acid phosphatases have been described to show bromoperoxidase activity [126]. According to sequence, substrate spectrum and susceptibility to inhibition, class A proteins can be further assigned to subgroups A1–A3 [121]. PhoC-Mm from *Morganella morganii* [27,29], PhoN-Sf from *Shigella flexneri* and NSAP-Eb from *Escherichia blattae* [28,127] belong to subclass A1 and can dephosphorylate e.g. 5'- and 3'-nucleoside monophosphates, glucose 6-phosphate and aryl phosphates [121]. The prototype enzyme for subclass A2, PhoN-Se from *Salmonella enterica ser. Typhimurium* LT2, also has a very broad substrate specificity, acts on e.g. nucleoside di- and triphosphates and, in contrast to A1 proteins, hydrolyzes also secondary phosphorylated alcohols [121, 128]. Apy-Sf, an apyrase or ATP diphosphohydrolase from *Shigella flexneri*, is a representative of a subclass A3 NSAP. Despite its different substrate preference, its sequence was found to be highly similar to the phosphatase from *Escherichia blattae* [129].

Class B NSAPs are completely unrelated to class A and identified by the sequence motif F-D-I-D-D-T-V-L-F-S-S-P [121]. AphA-St from *Salmonella enterica ser. Typhimurium* LT2 was the first enzyme of that group being characterized [130]. Phosphatases belonging to NSAPs of class C, which can be found for instance in *Clostridium perfringens* [131], are cell-surface associated and share sequence similarities to class B NSAPs as well as many other families of phosphohydrolases. They all have a common motif that contains four invariant Asp residues, which implies that they belong to the same superfamily, often referred to as "DDDD" [94].

NSAPs form a phosphoenzyme intermediate, however the nature of the catalytic residue and the requirement for metal cofactors vary with different members of the superfamily, as will be elaborated in the following section. Nonetheless, similar to other types of phosphatases, a common feature of several NSAPs aside from catalyzing dephosphorylation reactions, is that they readily transfer a phosphate moiety from a suitable donor

to hydroxy-groups of a multitude of organic molecules, if operated under appropriate reaction conditions. Hence, they have been investigated by different research groups in an attempt to establish alternatives to existing kinase-mediated (trans)phosphorylation reactions, which will be covered in Section 1.5.3.c.

1.5.3.a Catalytic Mechanism

With the aid of X-ray structures of phosphatases from *Salmonella typhimurium* [132] and *Escherichia blattae* [29] as well as mutational analysis [133], the catalytic mechanism of class A phosphatases was elucidated. $N^{\epsilon 2}$ of His197 performs a nucleophilic attack on the substrate phosphoric acid ester or anhydride in an S_N2-type fashion, furnishing a phosphohistidine intermediate, as depicted in Figure 31, which can either be attacked by water (hydrolysis, I) or an alcohol (transphosphorylation, II). $N^{\delta 1}$ of His158 acts as a general acid/base catalyst and activates the water/alcohol for the attack on the phosphohistidine intermediate [133]. Notably, the positive charge on the His197 ring is stabilized by Asp201, which makes the $N^{\epsilon 2}$–P bond formation possible.
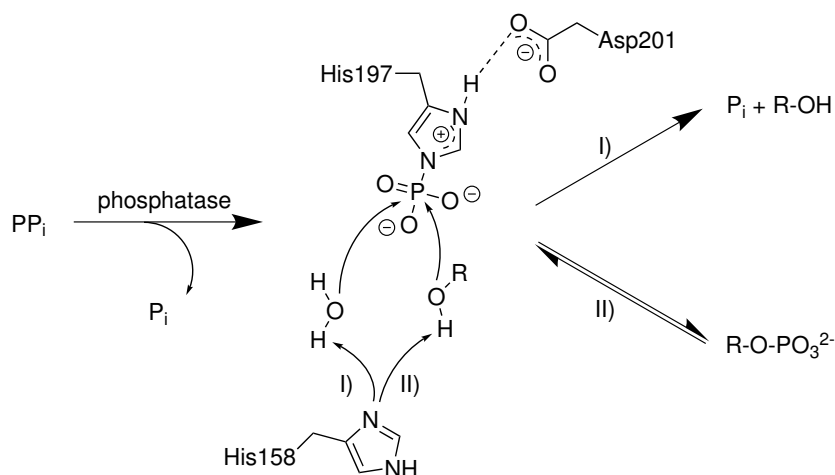
Figure 31: Catalytic mechanism of NSAPs, numbering as in PhoN of *Salmonella typhimurium* [132], the phosphohistidine intermediate can either be hydrolyzed by water (I) or attacked by an alcohol (II) [133, 134]

The class B NSAP AphA-St also belongs to the L2-haloacid dehalogenase superfamily, which accounts for its different catalytic mechanism and its requirement for Mg^{2+}. The structure of its active site is given in Figure 32. As summarized by Makde et al. [135], the nucleophilic Asp46 attacks the P-center of the substrate, giving a phosphoaspartate intermediate. Asp48 acts as the general acid/base catalyst, which donates a proton to the leaving group in the first step and activates water or an alcohol in the subsequent hydrolysis of the phosphoenzyme intermediate.
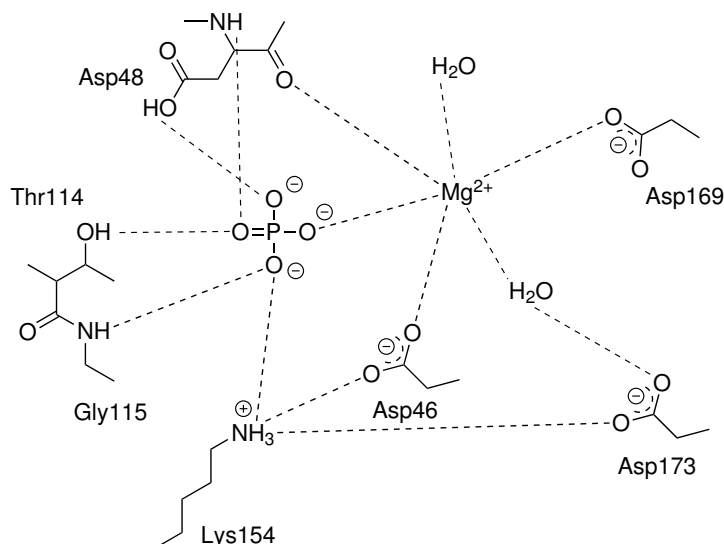
Figure 32: Active site of AphA-St from *Salmonella enterica ser. Typhimurium* LT2 with a bound phosphate, according to Makde et al. [135]

1.5.3.b Dephosphorylation

The production of chiral alcohols is often achieved by lipase-mediated enantioselective hydrolysis of carboxyl esters (kinetic resolution) [20]. Also phosphatases may be used for that task, albeit such reactions have been investigated to a lesser extent so far (Figure 33): For instance, Kimura et al. reported the resolution of D-*allo*-threonine & D-threonine by an acid phosphatase [136]. Similarly, as pointed out by van Herk and coworkers, PhoN-Se hydrolyzed *O*-phospho-DL-threonine to give L-threonine with high enantioselectivity (E > 200) [137]. Surprisingly, the same enzyme, when exposed to *O*-phospho-DL-serine, produced D-serine, but with lower enantiomeric excess. Consequently, random mutagenesis was performed to alleviate the issue and two mutants were obtained (N151D and V78L), which displayed increased selectivity [137].

Even if no enantioselectivity is demanded, employing acid phosphatases can be preferable to chemical methods, for instance when the product of a DHAP-dependent-aldolase-catalyzed C−C bond formation is labile. To this end, acid phosphatases can be employed to give rise to the final chiral polyol product under mild conditions [138].

1.5.3.c Transphosphorylation

As briefly remarked before, employing phosphatases in phosphorylation reactions as an alternative to kinases has significant benefits: There is no requirement for e.g. ATP as cofactor and the substrate specificity is more relaxed due to the occurrence of phosphatases in degradation rather than synthetic pathways. Nonetheless, phosphorylation reactions are thermodynamically disfavored and reversible with phosphatases: Once the
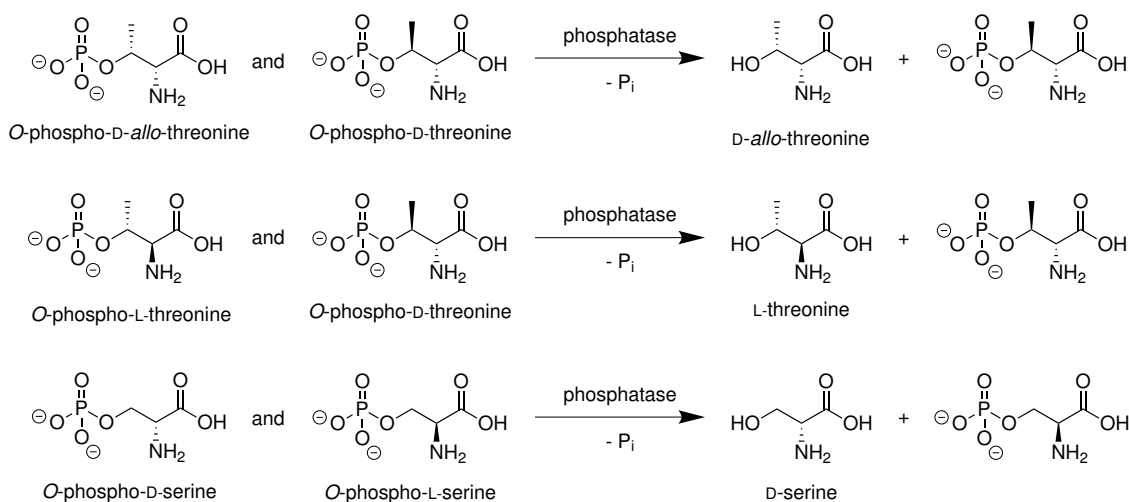
Figure 33: Kinetic resolution with acid phosphatases

donor phosphate is entirely consumed, hydrolysis of the initially formed ester/product by the enzyme begins to dominate. Consequently, the product titer depends on the reaction time and tight kinetic control of the overall process is required. The fate of different species in a typical phosphatase-mediated transphosphorylation reaction with pyrophosphate (PP_i) as donor molecule is given in Figure 34.

Since under transphosphorylation conditions there is always competition between water and the substrate as phosphate acceptor (see Figure 31), the effectiveness of the phosphorylation depends on the K_m for the alcohol [68]. In addition, as often water is used as solvent (c = 55.5 M) in such transformations, a high acceptor concentration is helpful to render the interplay between it and the phosphorylated enzyme more likely.

In spite of the drawbacks, several groups tackled research on phosphorylation reactions involving phosphatases. In this regard, NSAPs were by far the most investigated superfamily, especially in the last two decades, although reports about utilizing acid phosphatases in transphosphorylation reactions already dates back to the 1940s: Axelrod [139] and Appleyard [140] employed acid phosphatases from orange juice or prostate and incubated them with an acceptor alcohol and pNPP or phenolphthalein diphosphate as donors. In these early experiments however, it was not yet proven that the phosphotransferase activity originated from the phosphatase in the enzyme preparations [140].

Subsequently, several other NSAPs and related enzymes were found to exhibit phosphotransferase activity: Bacterial strains like *Salmonella typhimurium* [141] (enzymes AphA-St and PhoN-Se, discussed below) or *E. coli* [142, 143] were identified to express acid phosphatases capable of performing phosphorylation reactions. Substrates for the *E. coli* enzyme, isolated and purified by Brunngraber and Chargaff, included nicotinamide riboside (NR, 3'-OH phosphorylated) and nicotinamide adenine dinucleotide

31
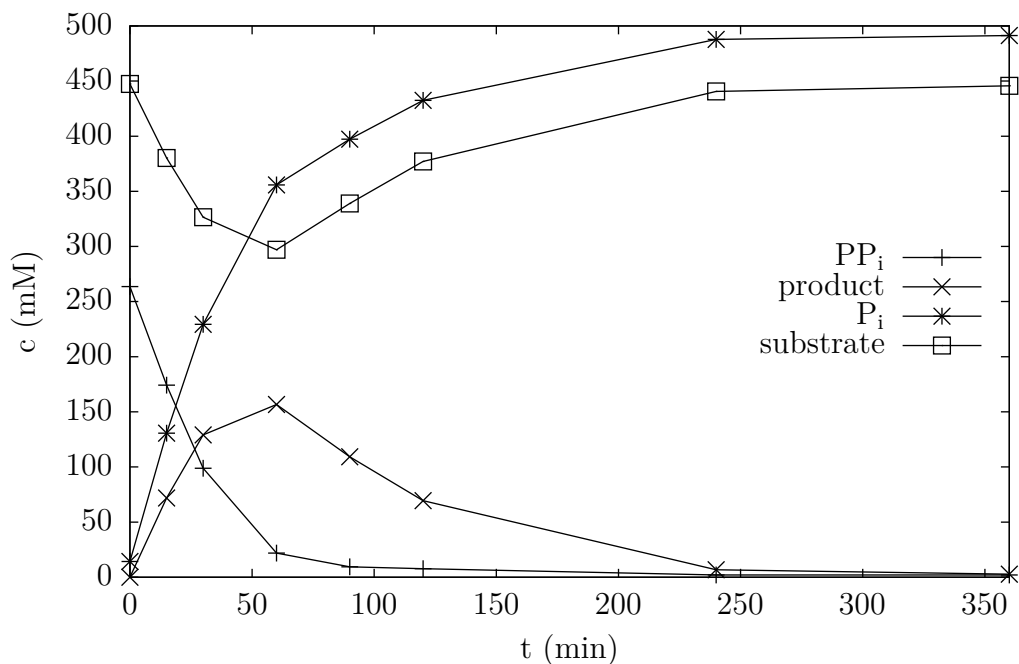
Figure 34: Fate of PP_i (pyrophosphate, donor), P_i (phosphate), substrate (alcohol) and product concentration over time in an NSAP-catalyzed transphosphorylation reaction. The phosphate from PP_i is transferred to the substrate in the beginning (here until $t = 60\,\text{min}$). As soon as the donor concentration falls below a certain threshold, the product is hydrolyzed by the enzyme.

(NAD, OH of adenosine phosphorylated) [142]. Mammalian glucose 6-phosphatase, described by Arion et al., has the same active site as class A NSAPs [123] and accepts pyrophosphate (PP_i), glucose 6-phosphate, carbamoyl phosphate (CP) and other organic phosphates as donors in transphosphorylation reactions [144].

Nucleosides

The large-scale preparation of nucleosides, which display flavor enhancing properties (5'-IMP and 5'-GMP, see Section 1.1), by NSAPs has been of particular interest recently due to drawbacks of traditional methods: For instance the production of inosine 5'-monophosphate (5'-IMP) by guanosine/inosine kinase (GIKase) requires ATP recycling, rendering the whole process more complex [145]. Consequently, the group of Y. Asano developed an alternative method involving class A1 NSAPs from either *Morganella morganii* (PhoC-Mm) [27] or *Escherichia blattae* (NSAP-Eb) [30] using cheap pyrophosphate (PP_i) as donor (Figure 35). PP_i has significant advantages over organic donors, especially in a large-scale environment, since it is easy to prepare [146] and was classified as "generally recognized as safe" (GRAS) by the Food and Drug Administration in the United States [68]. However, it exhibits chelating properties and can bind metal ions

like Ca^{2+}, Mg^{2+} and Fe^{2+}, which is detrimental to the activity of metal-dependent phosphatases (see Section 2.5.1). In addition, at least one equivalent of phosphate by-product is formed, which renders product isolation difficult.
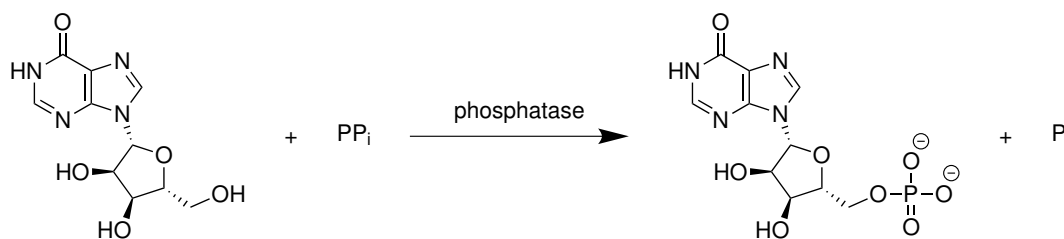
Figure 35: Phosphorylation of inosine with an acid phosphatase and pyrophosphate (PP_i) as donor

The wild-type enzymes from both strains were subjected to either random (PhoC-Mm) [29] or rational site-directed mutagenesis (NSAP-Eb) [28,31] to further increase productivity and minimize product hydrolysis. *E. coli* overproducing the 11-point mutant from NSAP-Eb produced $156\,g\,L^{-1}$ of 5'-IMP with a molar yield of $79\,\%$ in $24\,h$ [28], which is comparable to the results obtained from the 2-point mutant of PhoC-Mm: $101\,g\,L^{-1}$ of 5'-IMP in $88\,\%$ molar yield in $24\,h$ [29].

Another class A1 NSAP, PhoN-Sf from *Shigella flexneri*, immobilized on Immobead 150, was successfully applied in the phosphorylation of inosine in a continuous-flow reactor by Wever and coworkers to yield 5'-IMP on gram scale with PP_i as the donor [147].

Carbohydrates

PhoN-Sf from *Shigella flexneri* and PhoN-Se from *Salmonella enterica ser. Typhimurium* LT2 were also found capable of phosphorylating various carbohydrates including mannose, galactose, allose, α-methyl D-glucopyraniside (MADG) and even disaccharides like sucrose with PP_i as the donor [128]. $100\,mM$ D-Glucose for example were efficiently converted into $60\,mM$ D-glucose 6-phosphate (D-G6P) by PhoN-Sf and $100\,mM$ PP_i (Figure 36). Interestingly, PhoN-Sf displayed strong preference for the D- instead of the L-enantiomer of the sugar and D-G6P, once formed, was hardly hydrolyzed by the enzyme.

As the phosphorylation of D-glucose was found to be very efficient, a three enzyme cascade (acid phosphatase, glucose 6-phosphate dehydrogenase and ketoreductase) was set up by Hartog et al. [148], which featured in-situ generation of D-G6P from glucose and PP_i by PhoN-Sf to facilitate redox cofactor regeneration. The total turnover number for NADPH was reported to be greater than 3000 [148]. Later, the production of D-G6P
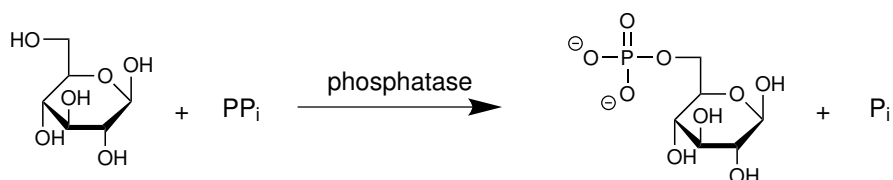
Figure 36: Phosphorylation of D-glucose with an acid phosphatase and pyrophosphate (PP$_i$) as donor

was further enhanced with PhoN-Sf, immobilized on Immobeads and stable for more than ten days, in a fed-batch reactor and in a continuous-flow system [147].

Alcohols

The class A NSAPs PhoN-Sf and PhoN-Se are also capable of phosphorylating polyalcohols, aromatic, cyclic and simple alcohols [128]. Similarly, also the class B NSAP AphA-St exhibits phosphotransferase activity with e.g. aliphatic primary alcohols and pNPP as donor [149]. Notably, glycerol is accepted by PhoN-Sf as substrate and DL-glycerol 1-phosphate is formed (Figure 37) [128], which represents an alternative to utilizing alkaline phosphatases or phytase, as described by Pradines et al. [118,119] and summarized in Section 1.5.2.c. The production of DL-glycerol 1-phosphate by PhoN-Sf was even conducted on a larger scale in a continuous-flow reactor with 500 mM glycerol and 250 mM PP$_i$, yielding 110 mM product at the outlet of the system [147].
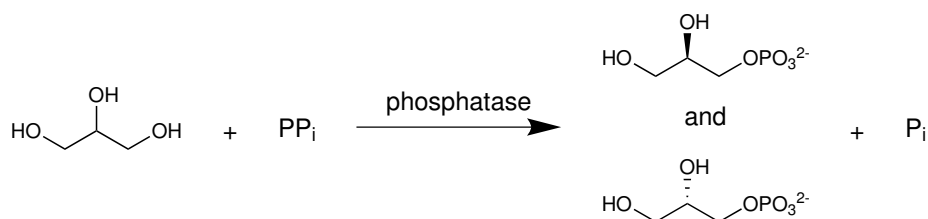
Figure 37: Phosphorylation of glycerol with an acid phosphatase and pyrophosphate (PP$_i$) as donor

1,3-Dihydroxyacetone phosphate (DHAP)

1,3-Dihydroxyacetone phosphate (DHAP), an unstable but mandatory substrate for DHAP-dependent aldolases (see Section 1.1), can also be synthesized by PhoN-Sf and PhoN-Se (Figure 38): van Herk and coworkers demonstrated the formation of 52 mM DHAP by PhoN-Sf from 500 mM dihydroxyacetone (DHA) and 240 mM PP$_i$ in $\sim$100 min [86]. The unfavorable high K$_m$ of PhoN-Se for DHA (3.6 M) was lowered by directed evolution to give a single mutant (V78L), which produced 25 % more DHAP at the maximum [25]. To circumvent the rapid hydrolysis of DHAP by the NSAP, it can be

directly utilized by an aldolase, present in the same reaction vessel, and converted into a carbohydrate [86]. The in-situ phosphorylation of substrates for aldolase-mediated reactions is an important application for various kinds of phosphatases in biocatalysis and therefore some examples will be given in the following section.
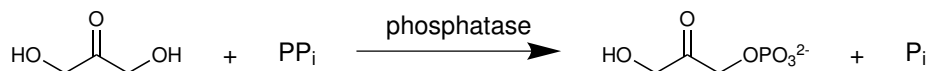
Figure 38: Phosphorylation of dihydroxyacetone (DHA) with an acid phosphatase and pyrophosphate (PP_i) as donor

1.5.4 Cascade Reactions involving Phosphatases

Most multienzyme processes for the production of (non-)natural carbohydrates involve the formation of phosphorylated species, typically dihydroxyacetone phosphate (DHAP) or D-glyceraldehyde 3-phosphate (G3P) [80]. Although kinases can also be used for this task [150], employing phosphatases has the advantage that in cascades they can occupy a bifunctional role: Generation of the substrate for the aldolase and dephosphorylation of the final carbohydrate phosphate [104, 151, 152]. The pathways discussed below are outlined in Figure 39.
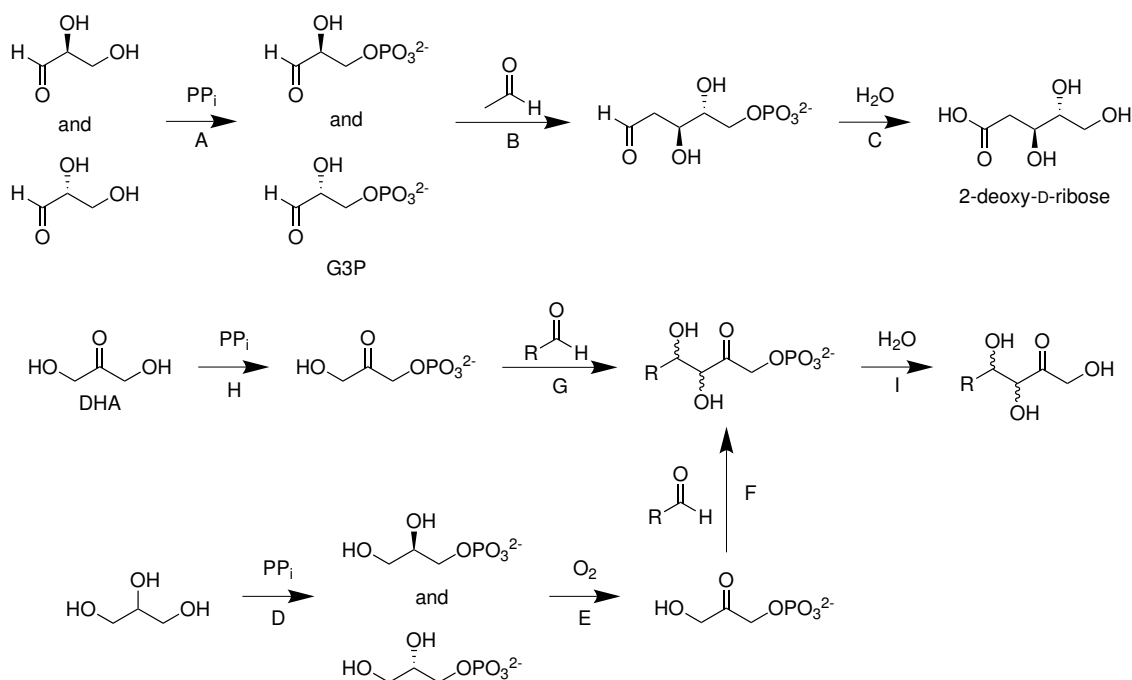
Figure 39: Pathways for the production of carbohydrates discussed in the current section. A/C: acid phosphatase, B: 2-deoxyribose 5-phosphate aldolase (DERA), D/I: phosphatase, E: L-glycerol phosphate oxidase (GPO), catalase, F/G: aldolase, H: acid phosphatase or kinase

35

An example for the route D-E-F-I with phytase acting in steps D and I and fructose 1,6-bisphosphate aldolase (FruA/RAMA) in step F was already described in Section 1.5.1. Babich and coworkers investigated the same pathway, but with PhoN-Sf being employed in steps D and I, which, in contrast to the cascade with phytase, did not require a pH adjustment [152]. Four different aldolases and several aldehydes, including propanal and isobutanal, were tested and to show the usefulness of the cascade, D-fagomine (see Section 1.1) was produced.

The pathway H-G-I has also been reported by van Herk et al.: DHA was phosphorylated by PhoN-Sf with PP_i as donor. After subsequent coupling of DHAP to propanal by RAMA, the product 5,6-dideoxy-D-*threo*-2-hexulose was produced via dephosphorylation by the acid phosphatase [86]. Later, a flow system with immobilized PhoN-Sf and either RAMA or rhamnulose 1-phosphate aldolase (RhuA) was set up, which also followed the H-G-I route. Among the aldehydes tested was *N*-alloc-3-aminopropanal, a precursor in the synthesis of D-fagomine [153].

The V78L mutant of PhoN-Se, which was already mentioned above, was utilized in a cascade following the route A-B-C: 200 mM DL-glyceraldehyde were phosphorylated by the mutant in the presence of 100 mM PP_i and the obtained DL-glyceraldehyde 3-phosphate was coupled to 50 mM acetaldehyde by 2-deoxy-D-ribose 5-phosphate aldolase (DERA) to give 2-deoxy-D-ribose 5-phosphate, which was finally dephosphorylated by the acid phosphatase to yield 5.5 mM of product [25].

1.5.5 Organic Donors and Phosphatases

In publications regarding transphosphorylation reactions with phosphatases, pyrophosphate (PP_i) is the by far most investigated phosphate donor. Nonetheless, as already indicated in prior sections, also organic donors are well accepted by various phosphatases. Among them, *p*-nitrophenyl phosphate (pNPP) is a very prominent example, since pNPP itself as well as the by-product *p*-nitrophenol can be easily tracked spectrophotometrically [154] (see Section 3.1.3). Table 2 lists some publications, in which alternative phosphate donors have been used in transphosphorylation reactions. Still, these are mainly kinetic studies. Interestingly, preparative applications with organic donors have scarcely been reported, in spite of their striking benefits over PP_i: Many of them lack chelating properties and hence permit the employment of metal-dependent phosphatases. At the same time, during the course of the reaction, significantly less phosphate by-product is produced (see Section 2), which simplifies product isolation.

Some organic donors, like AcP or PEP, can readily be utilized as the ultimate phosphate source in transphosphorylation reactions involving two kinases and ATP as a

"phosphate-shuttle" (see Section 1.4 and Figure 24). However, using these donors directly in conjunction with a phosphatase, represents a much simpler setup (Figure 40).

$$R-OH \xrightarrow{\text{phosphatase}} R-OPO_3^{2-}$$

$$\text{AcP} \qquad \text{acetate}$$
$$\text{or} \qquad \text{or}$$
$$\text{PEP} \qquad \text{pyruvate}$$
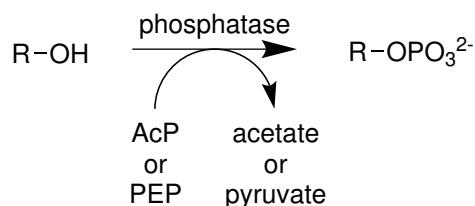
Figure 40: Transphosphorylation with phosphatases and acetyl phosphate (AcP) or phosphoenolpyruvate (PEP) as donors

In spite of that, reports about the ability of the enzymes selected in Section 2.1 to accept organic donor molecules were rare in recent literature: YniC-Ec had been already characterized in hydrolysis of small phosphate donors, including AcP and CP, but not in transphosphorylation [109] and AphA-St was reported to be active in phosphate transfer from pNPP to a broad range of organic alcohols [149], however no attempts have been made to increase the spectrum of organic donor molecules. PhoN-Sf and PhoN-Se both showed significant performance in phosphorylation of numerous alcohols as well as carbohydrates [128] and have been also employed in enzymatic cascades [148,152] as well as in continuous flow reactors in an immobilized form [147,153]. Still, in all cases PP_i was used as the donor. The mutants of NSAP-Eb and PhoC-Mm were both designed for the production of 5'-nucleotides on an industrial scale [28,29], thus again only pyrophosphate was selected as the phosphate source. Also phytase was only described to accept PP_i in the phosphorylation of glycerol [104].

Table 2: Overview of publications discussing organic donors

substrate	donor	enzyme type	reference
glucose, fructose, glycerol	phosphocreatine (PC), phosphoenolpyruvate (PEP), glucose 1-phosphate	Alkaline phosphatase	[155]
glucose, fructose, glycerol, 1,2-propanediol, DL-glyceraldehyde, dihydroxyacetone	PC, phenolphthalein phosphate, phenyl phosphate, adenosine 5-phosphate, β-glycerophosphate, PEP, hexose diphosphate, p-nitrophenyl phosphate (pNPP)	Alkaline phosphatase	[111]
tris(hydroxymethyl)aminomethane (Tris), glycerol	pNPP	Alkaline phosphatase	[120]
Tris, ethanolamine, di- & triethanolamine, dimethylaminoethanol, 3-amino-1-propanol, L-serine, L-serine methyl ester, glycerol, ethylene glycol	pNPP	Alkaline phosphatase	[154]
glucose	adenosine 5'-phosphate, cytidine 5'-phosphate, guanosine triphosphate, mannose 6-phosphate	Alkaline phosphatase	[92]
serine, ethanolamine, propanolamine, butanol, glycerol, L-glucose, Tris	cysteamine S-phosphate, serine O-phosphate, aminoethanol O-phosphate, pNPP	Alkaline phosphatase	[156]

Table 2: Overview of publications discussing organic donors (continued)

substrate	donor	enzyme type	reference
1,2-propanediol, glycerol, DL-glyceraldehyde, dihydroxyacetone, glucose	phenyl phosphate, phosphocreatine (PC), β-glycerophosphate, pNPP	Acid phosphatase	[101]
adenosine, uridine	pNPP, 3'-UMP, 5'-UMP	Acid phosphatase (class B NSAP)	[157]
glycerol	pNPP	Acid phosphatase	[158]
inosine	pNPP, phenylphosphate, carbamoyl phosphate (CP), acetyl phosphate (AcP), ATP, ADP, AMP, glucose 6-phosphate, glucose 1-phosphate	Acid phosphatase (class A NSAP)	[32]
glucose	AcP		[159]
pyridoxine	pNPP, phenyl phosphate, AcP	Acid phosphatase	[160]
ascorbic acid	pNPP, ATP, AcP	Acid phosphatase	[161]
glucose	AcP, CP	Acid phosphatase	[162]

39

2 Results and Discussion

The performance of a broad range of potential organic phosphate donors, which are described in Section 2.2, in transphosphorylation with various phosphatases, introduced in Section 2.1, has been evaluated with the model substrate 1,4-butanediol (14OH), as well as methyl α-D-glucopyranoside (MADG) and 2-hydroxyethyl acrylate (HEA). Best enzyme candidates were selected in preliminary studies with acetyl phosphate (AcP), phosphoenolpyruvate (PEP), carbamoyl phosphate (CP) and phosphocreatine (PC) in comparison with pyrophosphate (PP$_i$). Phosphate transfer reactions were optimized in terms of selected parameters, such as amount of donor and substrate. During the course of these studies, the HAD-like phosphatase YniC-Ec was found to be a special case in terms of transphosphorylation. Thorough investigation of reactions with PEP, where no hydrolysis of the thermodynamically disfavored product 4-hydroxybutyl phosphate occurred due to a drop in pH, led to the observation that keeping the pH within a very narrow range, specific for each enzyme, can be used as a valuable tool to kinetically control transphosphorylation. Below a well-defined pH, hydrolysis is almost entirely switched off while maintaining the transphosphorylation abilities of the phosphatase. This "ideal" pH was found for PiACP, PhoN-Sf, PhoN-Se, Lw and AphA-St and confirmed to be independent of the nature of the donor. Immobilisation of PhoN-Se on various polymer beads bearing oxirane functional groups has been attempted in order to exploit the reversible "automatic shutoff" in phosphate transfer reactions with PEP. Finally, new non-natural donors, which represent also enolphosphates like PEP, were synthesized and tested along with 2,2,2-trifluoroethyl phosphate (TFEP), provided by BASF, in reactions with the best enzyme candidates at the "optimum" pH and 14OH as substrate.

2.1 Biocatalysts

The phosphatases described in Table 3 were selected for transferring a phosphate moiety from various donor substances, listed in Section 2.2, to the model substrate 1,4-butanediol (14OH), as well as methyl α-D-glucopyranoside (MADG) and 2-hydroxyethyl acrylate (HEA).

Table 3: Biocatalysts. AP: alkaline phosphatase, HP: histidine phosphatase superfamily, HAD: haloacid dehalogenase

enzyme	enzyme group	structure of subunit	metal/subunit	active residue	comment
PiACP from *Prevotella intermedia*	class A NSAP	monomer $\sim 30\,\mathrm{kDa}$	none	His	similar sequence to PhoC-Mm-2 [163]
PhoN-Sf from *Shigella flexneri*	class A NSAP	homodimer $\sim 27\,\mathrm{kDa}$	none	His	phosphorylates various carbohydrate substrates, a wide range of simple, aromatic and cyclic alcohols & polyalcohols with PP_i as donor [128]
PhoN-Se from *Salmonella enterica ser. Typhimurium* LT2	class A NSAP	homodimer $\sim 28\,\mathrm{kDa}$	none	His	wide substrate spectrum, similar to PhoN-Sf
PhoC-Mm-2 2-point mutant from *Morganella morganii*	class A NSAP	homotetra- or homohexamer $\sim 25\,\mathrm{kDa}$ per subunit	none	His	engineered for production of phosphorylated nucleosides, like inosine 5'-monophosphate (5'-IMP) [27, 29]
NSAP-Eb-11 11-point mutant from *Escherichia blattae*	class A NSAP	homohexamer $\sim 25\,\mathrm{kDa}$ per subunit	none	His	engineered for production of e.g. 5'-IMP [28, 127]
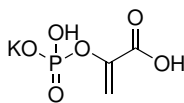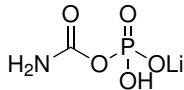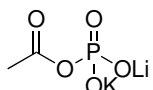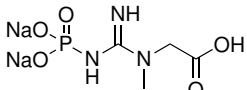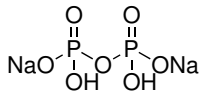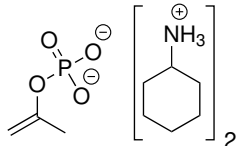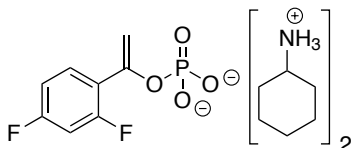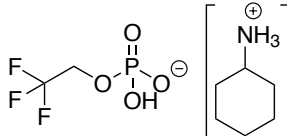
Table 3: Biocatalysts. AP: alkaline phosphatase, HP: histidine phosphatase superfamily, HAD: haloacid dehalogenase (continued)

enzyme	enzyme group	structure of subunit	metal/subunit	active residue	comment
AphA-St from *Salmonella enterica ser. Typhimurium* LT2	class B NSAP	homotetramer $\sim 24\,\mathrm{kDa}$ per subunit	Mg^{2+}	Asp	phosphorylation of mono-, di- and trihydroxy alcohols with pNPP as donor [130,149]
PhoK or **SPHSX** from *Sphingomonas. sp.* Strain BSAR-1	AP	dimer $\sim 60\,\mathrm{kDa}$	$2\ Zn^{2+}$, $1\ Ca^{2+}$	Thr	pH optimum of 9.0 in hydrolysis of pNPP [164]
phytase from *Aspergillus niger* (from BASF)	HP	monomer $\sim 52\,\mathrm{kDa}$ (without glycosylation)	none	His	cleaves the P−O bond of phytate, known to improve the uptake of minerals in various animals [102], transphosphorylation activity hardly described
YniC-Ec from *Escherichia coli*	HAD-like	homodimer $\sim 24\,\mathrm{kDa}$	Zn^{2+}/Mn^{2+}, Co^{2+} or Mg^{2+}	Asp	active in hydrolysis of pNPP, acetyl phosphate & carbamoyl phosphate [109]
Lw phosphatase from *Leptotrichia wadei*			none		similar sequence to PhoC-Mm-2

2.2 Donors for Transphosphorylation

Table 4 sums up all compounds tested for suitability as donors in transphosphorylation with phosphatases from Section 2.1. Most of them are key intermediates in biochemical pathways or derivatives of them and show considerably low $\Delta G'^\circ$ values for hydrolysis [4]. Pyrophosphate (PP$_i$), a cheap inorganic donor, was appended to the list as reference compound, already being well-characterized in conjunction with phosphorylation reactions of various alcohols with PhoN-Se and PhoN-Sf as an example [128, 134].

Table 4: Overview of donors for transphosphorylation

donor	name	M_W [g mol^{-1}]	$\Delta G'^\circ$ [kJ mol^{-1}]
	Phosphoenolpyruvate monopotassium salt (PEP)	206.14	-62
	Lithium carbamoylphosphate dibasic hydrate (CP), anhyd.	152.89	-51
	Lithium potassium acetyl phosphate (AcP)	184.06	-43
	Phosphocreatine disodium salt hydrate (PC), anhyd.	255.08	-43
	Disodium pyrophosphate (PP$_i$)	221.94	-33
	Isopropenyl phosphate (di)cyclohexylammonium salt (IPP)	336.41	
	1-(2,4-difluorophenyl)vinyl phosphate (di)cyclohexylammonium salt (DFPVP)	434.46	
	2,2,2-trifluoroethyl phosphate monocyclohexylammonium salt (TFEP)	279.19	

2.3 Stability of Organic Donors

Since AcP, CP and PC are prone to spontaneous hydrolysis, the half-life of the donors under conditions typical for transphosphorylation has been identified by ^{31}P-NMR to be $\sim 7\,h$ for AcP, which also corresponds to reports by Lipmann and Tuttle [165], $\sim 6\,h$ for CP and $\sim 3\,h$ for PC (Figures 41, 42 and 43). These figures match the expected leaving group ability of acetate with a pKa of ~ 4.8 [166] and creatine with a pKa of ~ 3.4[1]. Carbamate with a pKa of ~ 5.9[1] also serves as a fairly good leaving group due to its further tendency to decompose into ammonia and carbon dioxide. From control reactions in screenings it could be deduced that PEP does not hydrolyze significantly for several days under typical transphosphorylation conditions (pH ~ 4), despite tautomerisation into the keto form occurs upon cleavage of the P$-$O bond. This might be due to the two negative charges at this pH (pKa values of phosphate ~ 2.15, ~ 7.1 and ~ 12.4 [12], pKa of the carboxylic group ~ 4.8), rendering PEP very well shielded against an attack by a nucleophile. Isopropenyl phosphate (IPP) and 1-(2,4-difluorophenyl)vinyl phosphate (DFPVP) were already characterized by Moriguchi et al. at neutral, acidic and basic pH. The half-life was $9\,min$ for IPP at pH 7 ($< 1\,min$ at pH 1) and $516\,min$ for DFPVP at pH 7 ($13\,min$ at pH 1) [167]. Due to the very limited stability of AcP, CP, PC, as well as IPP and DFPVP in particular, the formation of phosphate (P_i) was difficult to be precisely monitored during the course of transphosphorylation reactions. Also the initial concentration of the donors, especially in case of the extremely short-lived IPP could only vaguely be estimated.
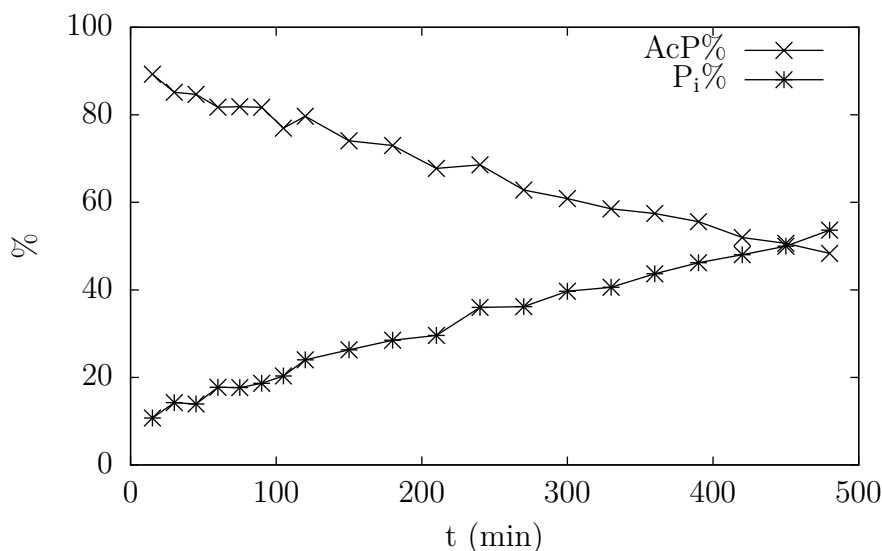
Figure 41: Hydrolysis of $100\,mM$ AcP in presence of $500\,mM$ 14OH, pH 4.2, room temperature, analysis via ^{31}P-NMR

---

[1] Calculated using Advanced Chemistry Development (ACD/Labs) Software V11.02 (© 1994-2015 ACD/Labs), accessed via SciFinder 09/2015
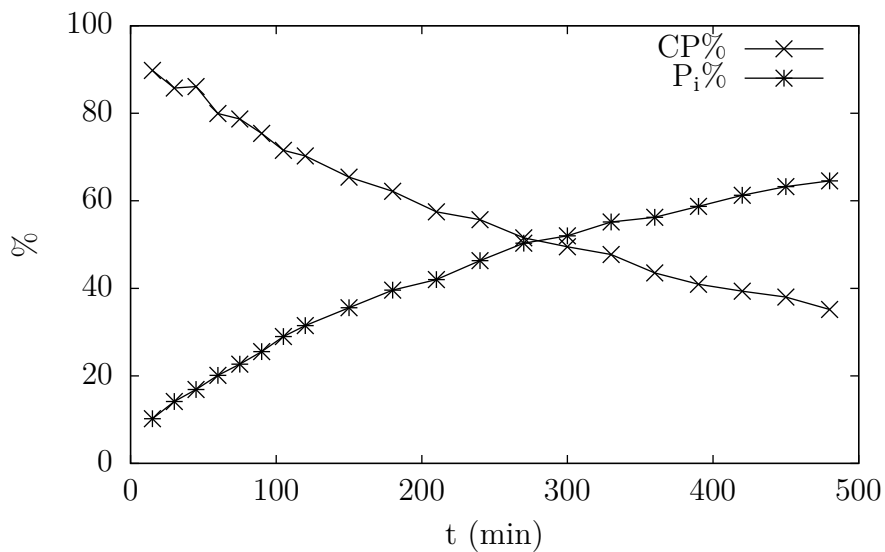
Figure 42: Hydrolysis of 100 mM CP in presence of 500 mM 14OH, pH 4.2, room temperature, analysis via ^{31}P-NMR
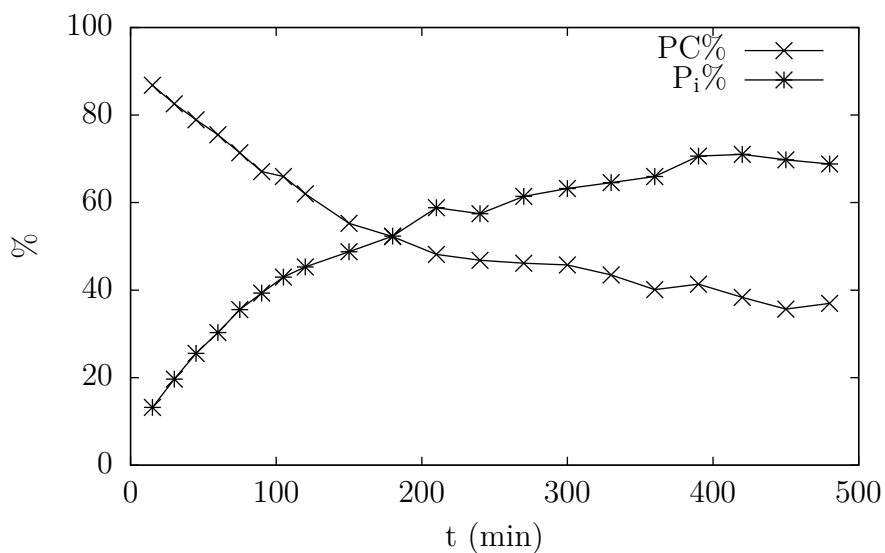
Figure 43: Hydrolysis of 100 mM PC in presence of 500 mM 14OH, pH 4.2, room temperature, analysis via ^{31}P-NMR

2.4 Scope of Parameters in Transphosphorylation

Apart from testing different phosphatases, donors and substrates, during the course of practical work on the project, several modifications to the general setup for transphosphorylation from Section 3.3.2.a were applied as attempts to kinetically control the reaction and obtain higher product levels, which included variations of the following parameters:

- pH (2.9–9.0 depending on the nature of the phosphatase)
- amount of $MgCl_2$ for AphA-St and YniC-Ec (10–100 mM)
- concentration of substrate (100–1000 mM for 14OH)
- concentration of donor (50–1000 mM for various donors)
- amount of enzyme (2.1–42 µM [50–1000 µg mL^{-1}] for YniC-Ec and 0.5–4 U mL^{-1} for all other enzymes)

2.5 Preliminary Studies

Initial assays for each phosphatase with the new donors AcP, PEP, CP and PC were conducted and the product and phosphate levels were compared with the data obtained from reactions with PP$_i$ in Section 2.5.1. Based on these observations, the most promising enzyme candidates were selected for follow-up screenings. Initially, according to the general procedure (Section 3.3.2), 4 U of enzyme (except for 6 U phytase at pH 4.2 and 50 or 200 µg mL^{-1} [only with AcP and PEP] YniC-Ec due to its low A_{spec}), 500 mM 14OH and 100 mM phosphate donor in 1 mL deionized (DI) H$_2$O were employed and the reactions were carried out at pH 4.2 (except for SPHSX, which required an alkaline pH of 9.0 and phytase, which was also assayed at pH 2.5) at 30 °C and 600 rpm shaking with 1 % DMSO as the internal standard (IS). One unit (U) of phosphatase activity is equivalent to the amount of p-nitrophenol (µmol) released within one minute in an assay measuring the dephosphorylation of p-nitrophenyl phosphate (see Section 3.1.3).

2.5.1 Transphosphorylation with PP$_i$ as donor
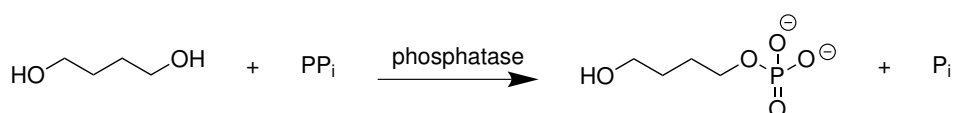
Figure 44: Phosphorylation of 14OH with PP$_i$ as donor

Time studies were performed with 4 U mL^{-1} of the acid phosphatases PiACP, PhoN-Sf, PhoC-Mm-2, NSAP-Eb-11, Lw and 1 U mL^{-1} of PhoN-Se, as the reaction was too quick to track with a larger amount of enzyme (data not shown). 500 mM 14OH substrate

and a donor concentration of 100 mM were chosen, following the general procedure in Section 3.3.2. The pH was selected to be 4.2 according to earlier observations in the project. As Figure 45 indicates, all enzymes except PhoC-Mm-2 and NSAP-Eb-11 reached the highest levels of 4-hydroxybutyl phosphate after 20–30 minutes, which was almost completely hydrolyzed by the enzyme again after 24 h. Reduced hydrolytic activity of inosine 5'-monophosphate (5'-IMP) has been reported with PhoC-Mm-2 and NSAP-Eb-11 [28, 29]. The phospho*transferase* activity of these two mutants also appears to apply to 14OH as substrate. Table 5 lists the maximal product amount, the time elapsed until it was reached and the amount of phosphate (P_i) at this time point.

Figure 45: Product formation in phosphorylation of 500 mM 14OH with 100 mM PP$_i$ at pH 4.2, 30 °C, 600 rpm shaking, 1 % DMSO as IS, 1 mL reaction volume and 4 U mL^{-1} PiACP, PhoN-Sf, PhoC-Mm-2, NSAP-Eb-11, Lw or 1 U mL^{-1} PhoN-Se

Table 5: Maximum product levels from Figure 45

enzyme	t [min]	prod. [mM]	P_i [mM]	prod./P_i
PiACP	20	53	147	0.36
PhoN-Sf	30	67	139	0.48
PhoN-Se	30	65	145	0.45
PhoC-Mm-2	240	63	150	0.42
NSAP-Eb-11	240	56	155	0.36
Lw	20	67	145	0.46

47

It is worth mentioning, that at every time point there was more P_i present in the reaction mixture than product, indicating loss of donor through PP_i hydrolysis. In an ideal case, with PP_i as donor, the ratio product/P_i is 1 (max. phosphorylation efficiency).

As an attempt to overcome the chelating effects of pyrophosphate and recover enzyme activity, different amounts of salt supplementation in the form of $MgCl_2$ were assayed with metal-dependent enzymes: AphA-St, $4\,U\,mL^{-1}$, and YniC-Ec, $50\,\mu g\,mL^{-1}$ due to its low specific activity (A_{spec}, see Section 3.3.2.a). Additionally, two different pH values, 4.2 and 5.5, were tested. The substrate (14OH) and donor concentrations, as well as all other parameters did not differ from the general protocol in Section 3.3.2. With AphA-St, which is known to perform well with pNPP as donor and glycols with alcohol groups separated by several carbon atoms as acceptor [149], only about 5 mM product at the maximum were observed with $100\,mM\ MgCl_2$ at pH 4.2. Screenings at pH 5.5 gave even smaller amounts (Figure 46, Table 6). The specific hydrolytic activity of YniC-Ec was very low compared to other phosphatases (see Table 34), transphosphorylation reactions proceeded slowly as well. Also here pH 4.2 yielded higher product levels and after 22 h with $10\,mM\ MgCl_2$ considerable amounts of 4-hydroxybutyl phosphate could be detected (Figure 47, Table 7). Interestingly, in contrast to AphA-St, increased salt concentration led to deactivation of YniC-Ec instead of (partially) recovering its activity. Importantly, in the course of the reaction, no hydrolysis of the product was observed.
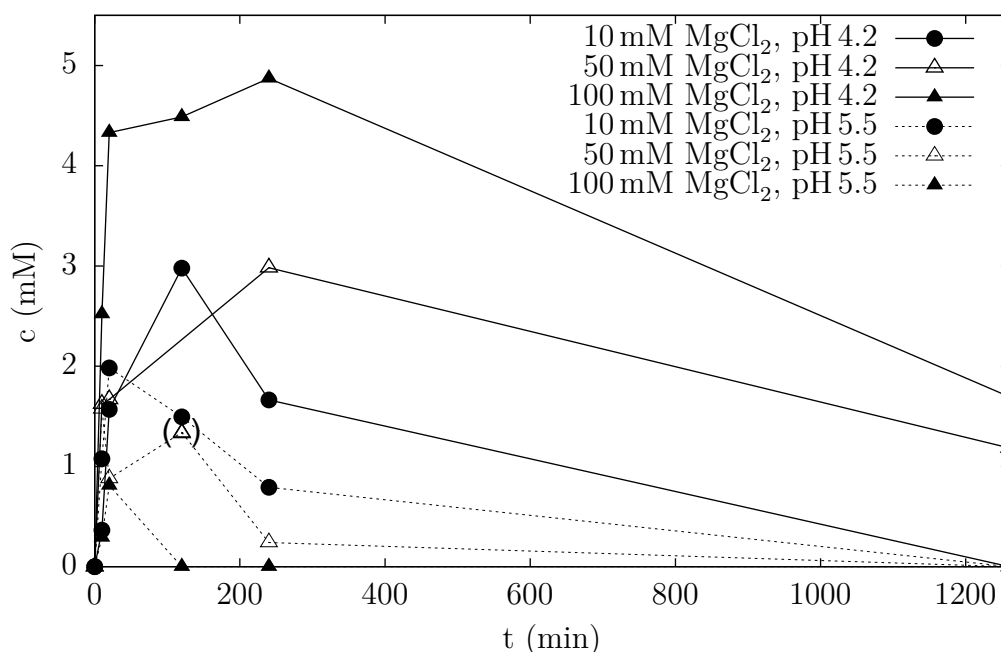
Figure 46: Product formation in phosphorylation of $500\,mM$ 14OH with $100\,mM\ PP_i$ in the presence of various amounts $MgCl_2$ at pH 4.2 and 5.5, 30 °C, 600 rpm shaking, 1 % DMSO as IS, 1 mL reaction volume and $4\,U\,mL^{-1}$ AphA-St

48

Table 6: Maximum product levels from Figure 46

AphA-St	t [min]	prod. [mM]	P_i [mM]	prod./P_i
10 mM $MgCl_2$, pH 4.2	120	3.0	21	0.14
50 mM $MgCl_2$, pH 4.2	240	3.0	42	7.1×10^{-2}
100 mM $MgCl_2$, pH 4.2	240	4.9	27	0.18
10 mM $MgCl_2$, pH 5.5	20	2.0	9	0.22
50 mM $MgCl_2$, pH 5.5	10	1.6	14	0.11
100 mM $MgCl_2$, pH 5.5	20	0.8	17	4.7×10^{-2}
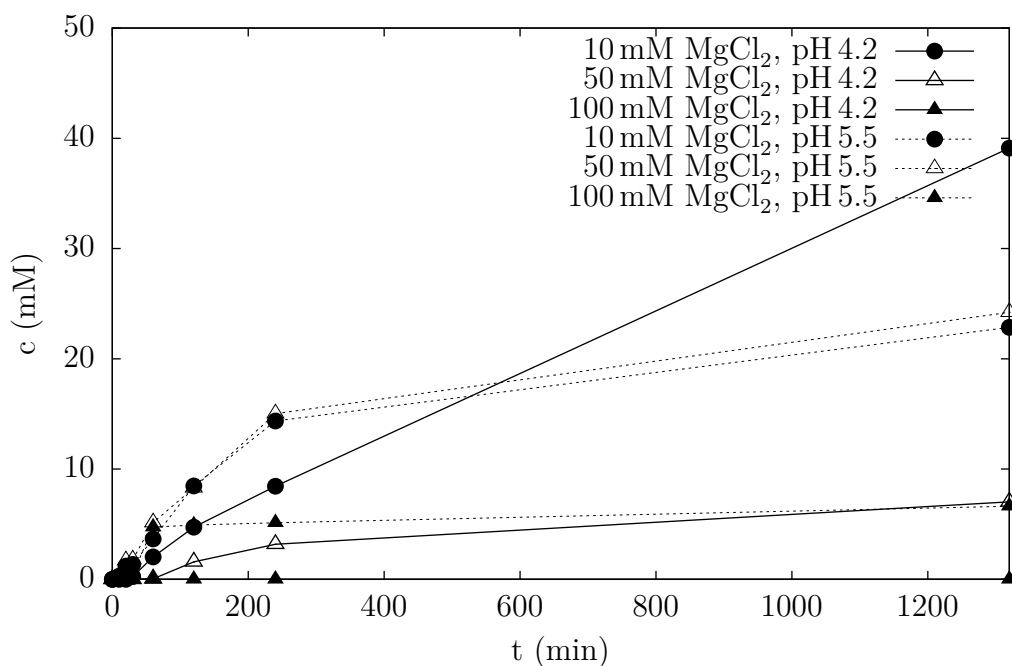
Figure 47: Product formation in phosphorylation of 500 mM 14OH with 100 mM PP_i in the presence of various amounts $MgCl_2$ at pH 4.2 and 5.5, 30 °C, 600 rpm shaking, 1 % DMSO as IS, 1 mL reaction volume and 50 µg mL^{-1} YniC-Ec

Table 7: Maximum product levels from Figure 47

YniC-Ec	t [min]	prod. [mM]	P_i [mM]	prod./P_i
10 mM $MgCl_2$, pH 4.2	1320	39	72	0.54
50 mM $MgCl_2$, pH 4.2	1320	7.0	21	0.33
100 mM $MgCl_2$, pH 4.2		n.c.		
10 mM $MgCl_2$, pH 5.5	1320	23	113	0.20
50 mM $MgCl_2$, pH 5.5	1320	24	104	0.23
100 mM $MgCl_2$, pH 5.5	1320	6.6	66	0.10

2.5.2 Transphosphorylation with AcP as Donor
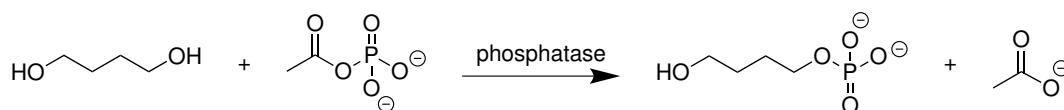
Figure 48: Phosphorylation of 14OH with AcP as donor

All enzymes of the first set (Figure 49 and Table 8) delivered remarkable amounts of 4-hydroxybutyl phosphate utilizing acetyl phosphate (AcP) as donor. For PiACP, PhoN-Sf, PhoN-Se and Lw product levels similar to PP_i could be observed. NSAP-Eb-11 (40 vs. 63 mM) and PhoC-Mm-2 (25 vs. 56 mM) displayed almost no product hydrolysis but did not perform better with AcP than with PP_i. This may be due to a competing and faster hydrolysis reaction of the donor and therefore reduced availability for transphosphorylation.

As already indicated in Section 2.3, the initial concentration of AcP is uncertain, however, at the maximum level of 4-hydroxybutyl phosphate 100 % phosphate donor consumption can be assumed. At this point in some cases good product to phosphate ratios (with AcP, the ideal ratio is not measurable, because all the phosphate would be transferred on the alcohol) were obtained (above 1 for PhoN-Sf and Lw, see Table 8, indicating > 50 % phosphate transfer efficiency).
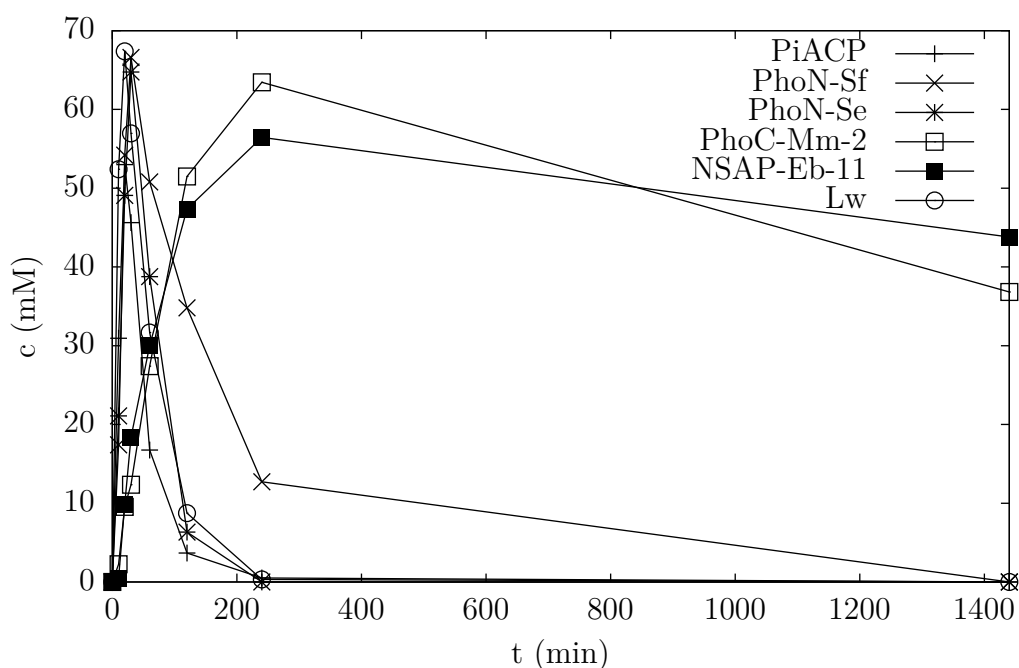

Figure 49: First set of enzymes: Product formation in phosphorylation of 500 mM 14OH with 100 mM AcP at pH 4.2, 30 °C, 600 rpm shaking, 1 % DMSO as IS, 1 mL reaction volume and $4\,U\,mL^{-1}$ enzyme

Figure 50: Second set of enzymes: Product formation in phosphorylation of 500 mM 14OH with 100 mM AcP at pH 4.2 except for SPHSX (pH 9.0), 30 °C, 600 rpm shaking, 1 % DMSO as IS, 1 mL reaction volume, 10 mM $MgCl_2$ for AphA-St and YniC-Ec, 10 mM $ZnCl_2$ and 10 mM $CaCl_2$ for SPHSX, 4 U mL^{-1} enzyme, except for 6 U with phytase pH 4.2 and 50 or 200 µg mL^{-1} YniC-Ec

Table 8: Maximum product levels from Figure 49 and Figure 50 in comparison with PP_i from Table 5, 6 and 7 (10 mM $MgCl_2$); 1 U PhoN-Se was used with PP_i

	AcP				PP_i		
	t [min]	prod. [mM]	P_i [mM]	prod./ P_i	t [min]	prod. [mM]	prod./ P_i
PiACP	10	51	52	0.98	20	53	0.36
PhoN-Sf	20	60	39	1.5	30	67	0.48
PhoN-Se	10	44	60	0.73	30	65	0.45
PhoC-Mm-2	1620	40	50	0.80	240	63	0.42
NSAP-Eb-11	1620	25	69	0.36	240	56	0.36
Lw	20	67	38	1.8	20	67	0.46
AphA-St	10	41	65	0.63	120	3.0	0.14
YniC-Ec 50 µg mL^{-1}	4320	36	65	0.55	1320	39	0.54
YniC-Ec 200 µg mL^{-1}	120	46	50	0.92			
SPHSX	4320	2.3	89	2.6×10^{-2}			
phytase pH 2.5	60	2.6	99	2.6×10^{-2}			
phytase pH 4.2	20	0.9	99	9.1×10^{-3}			

In the second set of enzymes (Figure 50 and Table 8), SPHSX and phytase at both pH values were almost not active on AcP in terms of transphosphorylation. Because of its limited stability (i.e. spontaneous hydrolysis), the amount of hydrolysis of the donor by these enzymes could not be quantified. AphA-St and YniC-Ec $50\,\mu g\,mL^{-1}$ showed similar characteristics with the organic donor as with PP_i but displayed drastically improved levels of 4-hydroxybutyl phosphate. This may be associated with the decreased chelating abilities of AcP towards divalent metal ions and thus availability of sufficient amounts of Mg^{2+} to both enzymes. YniC-Ec $200\,\mu g\,mL^{-1}$ gave around $46\,mM$ product after $60\,min$ and hardly any product hydrolysis took place. Later it was found that because of the different kinetics of hydrolysis and transphosphorylation, the hydrolysis/transphosphorylation ratio could be changed by modification of the enzyme concentration. This tool for enhancing product formation is further described in Section 2.10.

PhoN-Se, PiACP and AphA-St were very active on AcP and the highest product concentration was already reached at the first time point. In order to assure that no hydrolysis had occurred until then and identify the maximum product level, screenings with those phosphatases were repeated with $1\,U$ of enzyme in order to slow down the whole process (Figure 51 and Table 9).
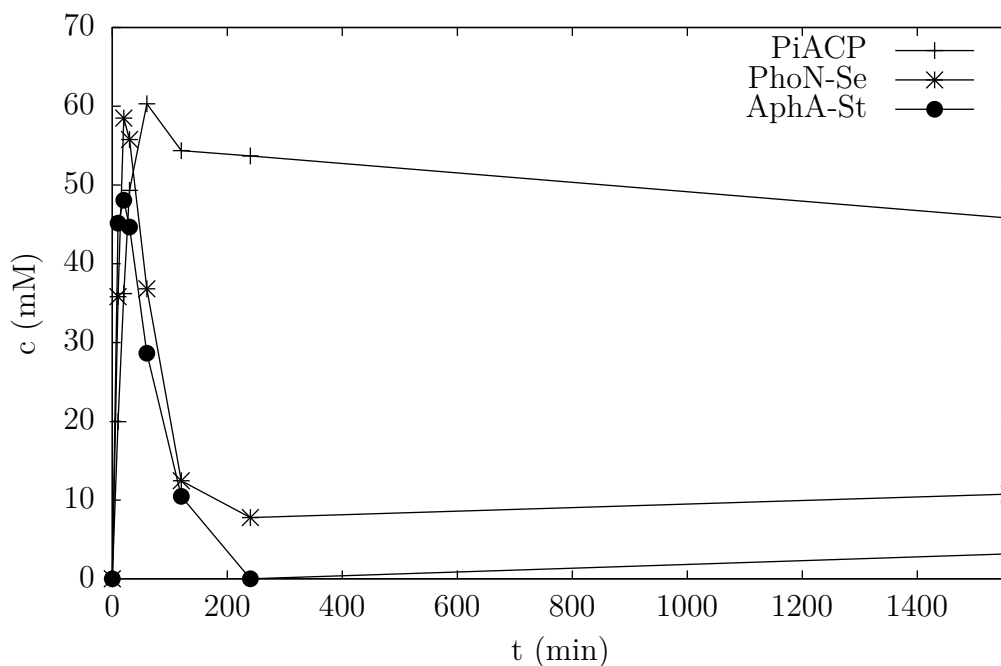
Figure 51: Product formation in phosphorylation of $500\,mM$ 14OH with $100\,mM$ AcP at pH 4.2, $30\,°C$, $600\,rpm$ shaking, $1\,\%$ DMSO as IS, $1\,mL$ reaction volume, $10\,mM$ $MgCl_2$ for AphA-St, $1\,U\,mL^{-1}$ enzyme

Figure 51 also indicates reduced product hydrolysis with PiACP, which, similar to YniC-Ec $200\,\mu g\,mL^{-1}$, likely is due to coincidential proper choice of enzyme concentration.

Table 9: Max. prod. levels from Figure 51 (1 U) with AcP in comparison with use of PP$_i$ as donor from Table 5 (4 U, 1 U for PhoN-Se) & Table 6 (4 U, 10 mM MgCl$_2$)

	AcP				PP$_i$		
	t [min]	prod. [mM]	P$_i$ [mM]	prod./ P$_i$	t [min]	prod. [mM]	prod./ P$_i$
PiACP	60	60	42	1.4	20	53	0.36
PhoN-Se	20	58	44	1.3	30	65	0.45
AphA-St	20	48	42	1.1	120	3.0	0.14

2.5.3 Transphosphorylation with PEP as Donor
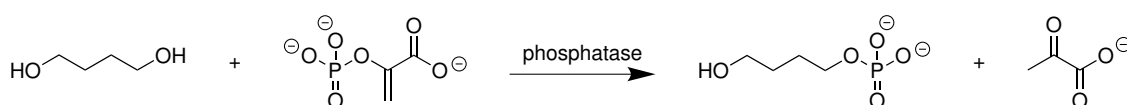
Figure 52: Phosphorylation of 14OH with PEP as donor

Phosphoenolpyruvate (PEP) acted as a very capable phosphate donor with the first set of enzymes (Figure 53 and Table 10) yielding product levels similar to PP$_i$. PhoC-Mm-2 and NSAP-Eb-11 gave results resembling AcP, with NSAP-Eb-11 being slower. Interestingly, no hydrolysis of 4-hydroxybutyl phosphate could be observed in the first set of enzymes. In addition, apart from PhoN-Se and PhoC-Mm-2, PEP was not fully converted after 25 h (amounts of P$_i$ plus product in Table 10 < 100 mM). Hence, possible enzyme deactivation or inhibition was assumed and further studies were carried out with this donor in order to confirm these assumptions in Section 2.6. Second set of enzymes (Figure 54 and Table 10): Similar to reactions with AcP, SPHSX and phytase did not show significant transphosphorylation activity with PEP. As PEP is regarded to be stable under screening conditions for days (Section 2.3), the high amounts of phosphate in the reaction mixture can be attributed to merely hydrolytic activity of these enzymes on the organic donor since the phosphorylated product remained stable. In comparison with AcP, AphA-St produced low levels of 4-hydroxybutyl phosphate (which was almost fully hydrolyzed again after 25 h) in spite of 10 mM MgCl$_2$ supplementation. Variations in salt concentration (10–100 mM) or pH (3.7–6) did not result in increased product levels with AphA-St (data not shown). In contrast, YniC-Ec 50 µg mL^{-1}, which is also Mg^{2+} dependent and was supplemented with 10 mM MgCl$_2$, gave product concentrations almost identical to the reactions with AcP. With YniC-Ec 200 µg mL^{-1}, the reaction proceeded faster and about twice the amount of product was formed. It is furthermore worth mentioning that with PiACP, PhoN-Sf, PhoN-Se, PhoC-Mm-2, NSAP-Eb-11, Lw and YniC-Ec more 4-hydroxybutyl phosphate was present in the reaction mixture than phosphate at the maximum product level.
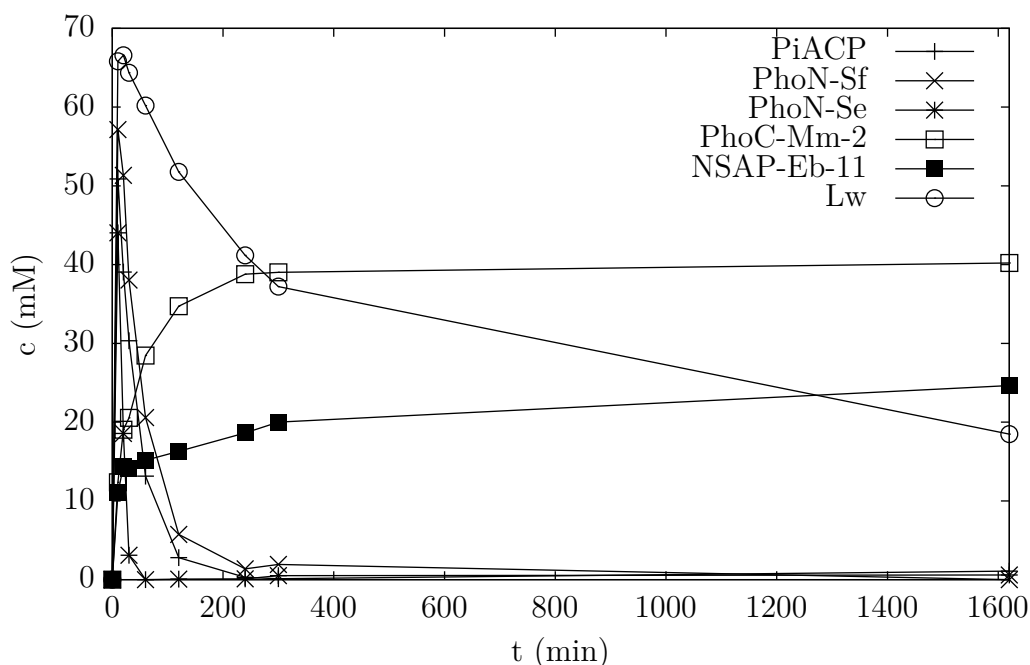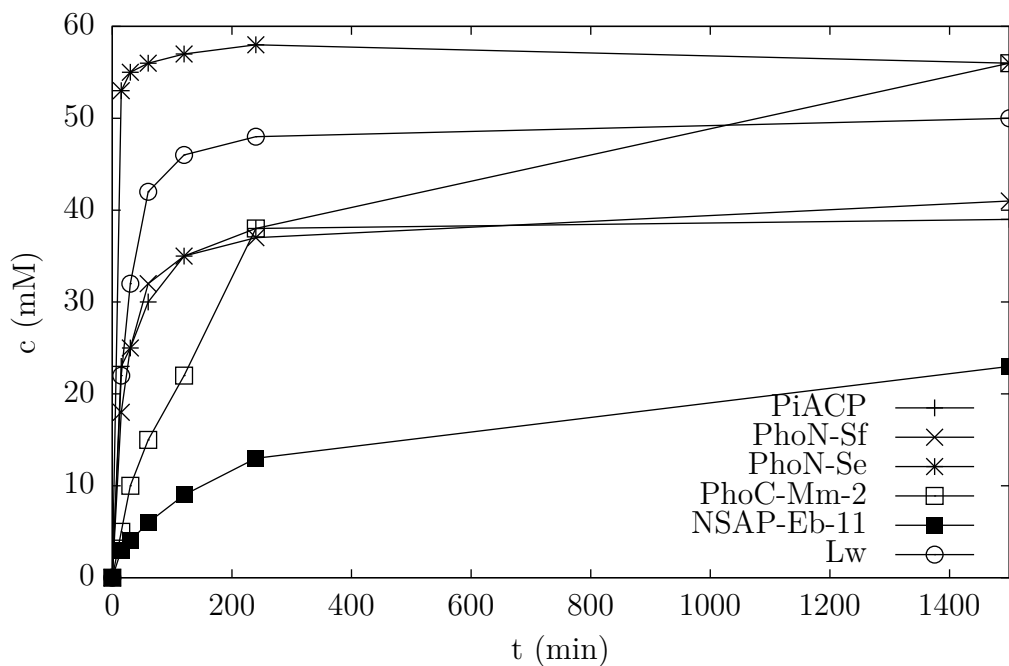
Figure 53: First set of enzymes: Product formation in phosphorylation of 500 mM 14OH with 100 mM PEP at pH 4.2, 30 °C, 600 rpm shaking, 1 % DMSO as IS, 1 mL reaction volume and 4 U mL^{-1} enzyme
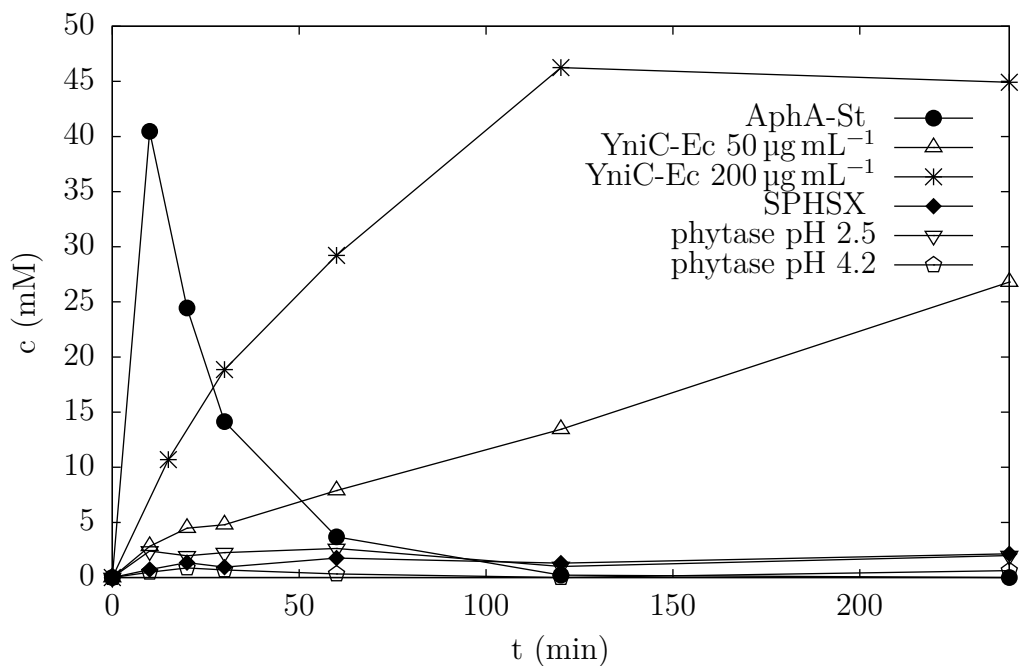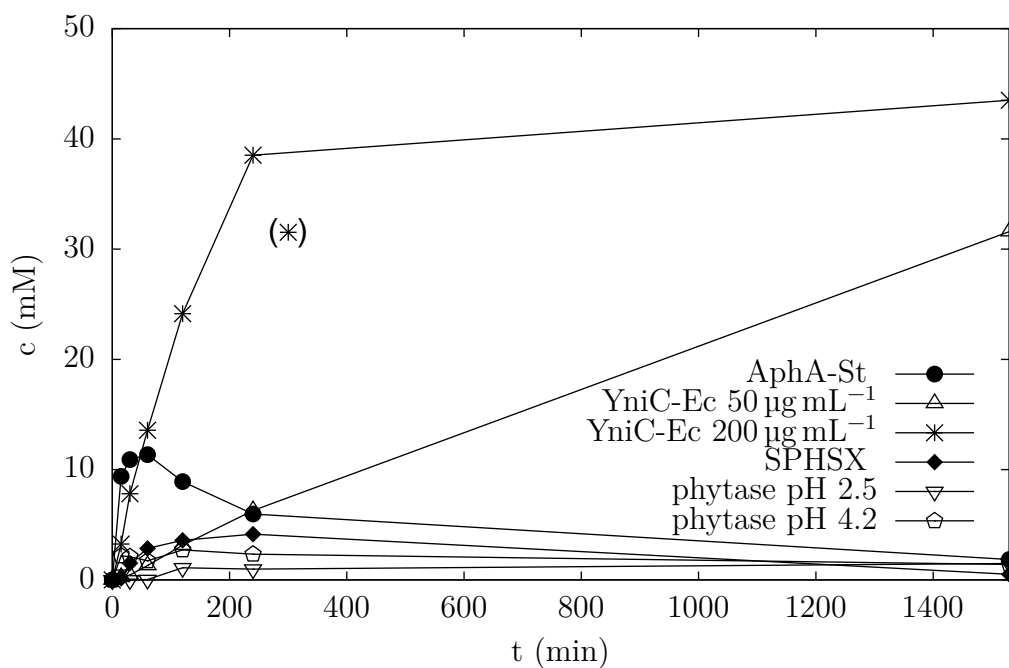

Figure 54: Second set of enzymes: Product formation in phosphorylation of 500 mM 14OH with 100 mM PEP at pH 4.2 except for SPHSX (pH 9.0), 30 °C, 600 rpm shaking, 1 % DMSO as IS, 1 mL reaction volume, 10 mM MgCl$_2$ for AphA-St and YniC-Ec, 10 mM ZnCl$_2$ and 10 mM CaCl$_2$ for SPHSX, 4 U mL^{-1} enzyme, except for 6 U with phytase pH 4.2 and 50 or 200 µg mL^{-1} YniC-Ec

Table 10: Maximum product levels from Figure 53 and Figure 54 in comparison with PP$_i$ from Table 5, 6 and 7 (10 mM MgCl$_2$); 1 U PhoN-Se was used with PP$_i$

	PEP				PP$_i$		
	t [min]	prod. [mM]	P$_i$ [mM]	prod./ P$_i$	t [min]	prod. [mM]	prod./ P$_i$
PiACP	1500	40	23	1.7	20	53	0.36
PhoN-Sf	1500	41	15	2.7	30	67	0.48
PhoN-Se	240	58	39	1.5	30	65	0.45
PhoC-Mm-2	1500	56	43	1.3	240	63	0.42
NSAP-Eb-11	1500	24	22	1.1	240	56	0.36
Lw	1500	50	24	2.1	20	67	0.46
AphA-St	60	11	43	0.26	120	3.0	0.14
YniC-Ec 50 µg mL^{-1}	1530	32	16	2.0	1320	39	0.54
YniC-Ec 200 µg mL^{-1}	3180	60	30	2.0			
SPHSX	240	4.1	89	4.6×10^{-2}			
phytase pH 2.5	1530	1.5	95	1.6×10^{-2}			
phytase pH 4.2	120	2.7	88	3.1×10^{-2}			

2.5.4 Transphosphorylation with CP as Donor
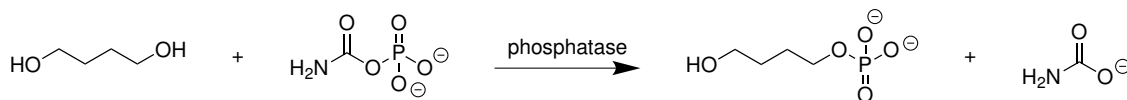
Figure 55: Phosphorylation of 14OH with CP as donor

All phosphatases but SPHSX (Figure 56 and 57 and Table 11) were capable of transphosphorylation with carbamoyl phosphate (CP) as donor and, except for phytase, good to excellent amounts of 4-hydroxybutyl phosphate could be observed. As mentioned in Section 2.3, due to the low stability of CP, its initial concentration at 0 min could not be precisely determined (similar to AcP), yet with PhoC-Mm-2 and NSAP-Eb-11 there was significantly less phosphate observed than product at the maximum product level. PiACP, PhoN-Sf, PhoN-Se and AphA-St were also very active on CP and like with AcP, reactions with those enzymes were repeated with 1 U phosphatase to evaluate the maximum product level (Figure 58 and Table 12). Lw was only available in the screening with 1 U enzyme.

Even with just 1 U of phosphatase reactions with CP proceeded rapidly and good amounts of product were obtained. Most likely this is due to its very low $\Delta G''^\circ$ value for hydrolysis of $-51 \, \text{kJ} \, \text{mol}^{-1}$ [68], which is comparable to PEP ($-61.9 \, \text{kJ} \, \text{mol}^{-1}$) [4].
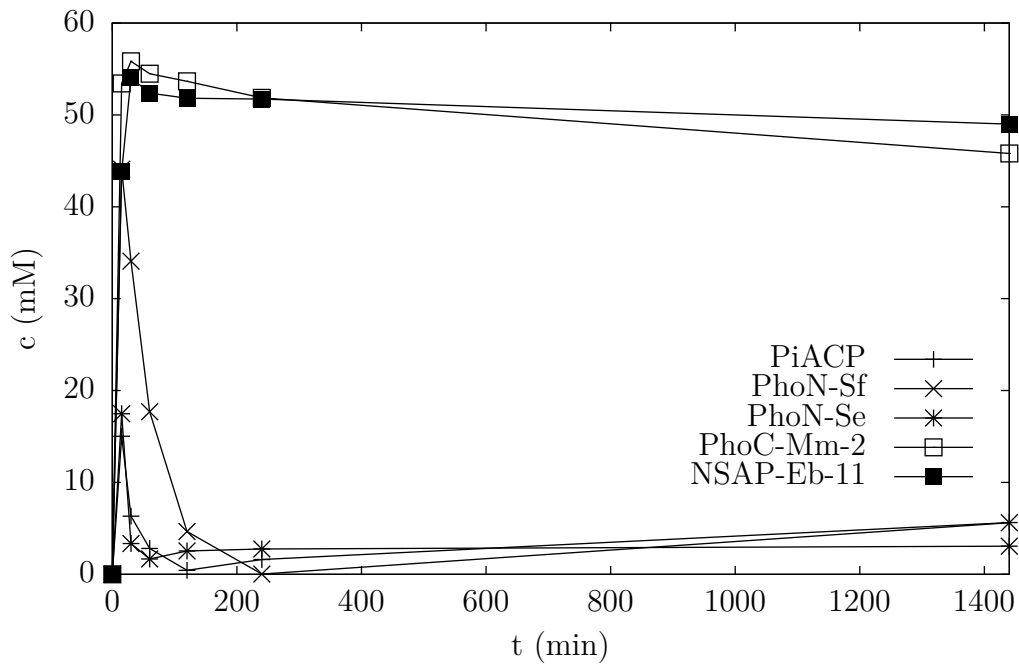
Figure 56: First set of enzymes: Product formation in phosphorylation of $500\,\mathrm{mM}$ 14OH with $100\,\mathrm{mM}$ CP at pH 4.2, $30\,^{\circ}\mathrm{C}$, $600\,\mathrm{rpm}$ shaking, $1\,\%$ DMSO as IS, $1\,\mathrm{mL}$ reaction volume and $4\,\mathrm{U\,mL^{-1}}$ enzyme
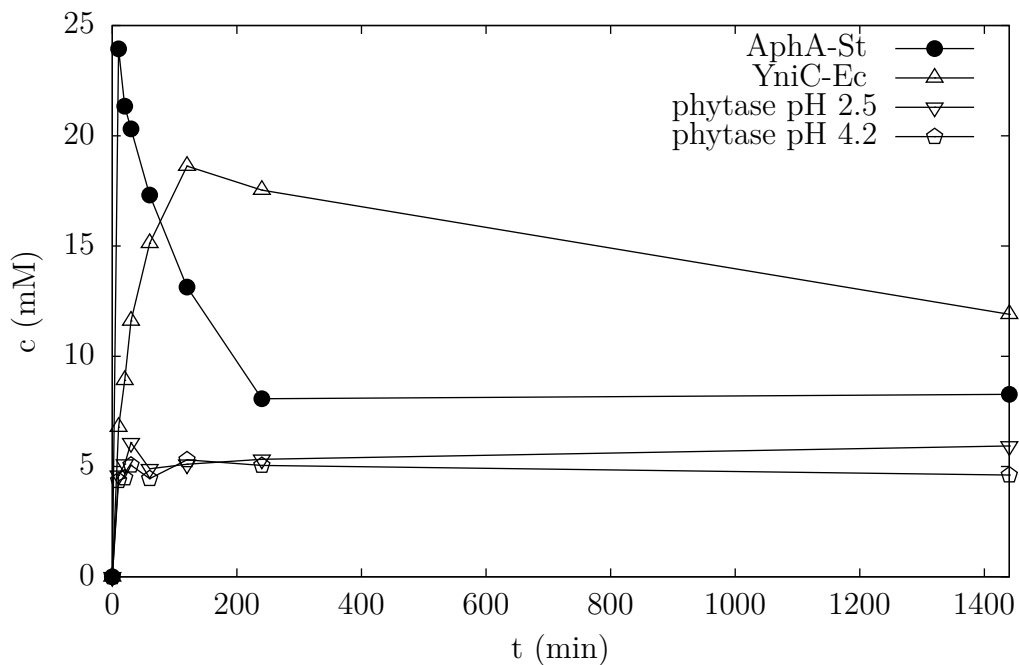
Figure 57: Second set of enzymes: Product formation in phosphorylation of $500\,\mathrm{mM}$ 14OH with $100\,\mathrm{mM}$ CP at pH 4.2, $30\,^{\circ}\mathrm{C}$, $600\,\mathrm{rpm}$ shaking, $1\,\%$ DMSO as IS, $1\,\mathrm{mL}$ reaction volume, $10\,\mathrm{mM}$ $MgCl_2$ for AphA-St and YniC-Ec, $4\,\mathrm{U\,mL^{-1}}$ enzyme, except for $6\,\mathrm{U}$ with phytase pH 4.2 and $50\,\mathrm{\mu g\,mL^{-1}}$ YniC-Ec

Table 11: Maximum product levels from Figure 56 and Figure 57 in comparison with PP_i from Table 5, 6 and 7 (10 mM $MgCl_2$); just 1 U PhoN-Se was used with PP_i

|	CP				PP_i		
	t [min]	prod. [mM]	P_i [mM]	prod./ P_i	t [min]	prod. [mM]	prod./ P_i
PiACP	15	15	70	0.21	20	53	0.36
PhoN-Sf	15	44	37	1.2	30	67	0.48
PhoN-Se	15	17	71	0.24	30	65	0.45
PhoC-Mm-2	30	56	35	1.6	240	63	0.42
NSAP-Eb-11	30	54	38	1.4	240	56	0.36
AphA-St	10	24	55	0.44	120	3.0	0.14
YniC-Ec	120	19	67	0.28	1320	39	0.54
SPHSX		n.c.					
phytase pH 2.5	30	6.1	81	7.5×10^{-2}			
phytase pH 4.2	120	5.3	81	6.5×10^{-2}			
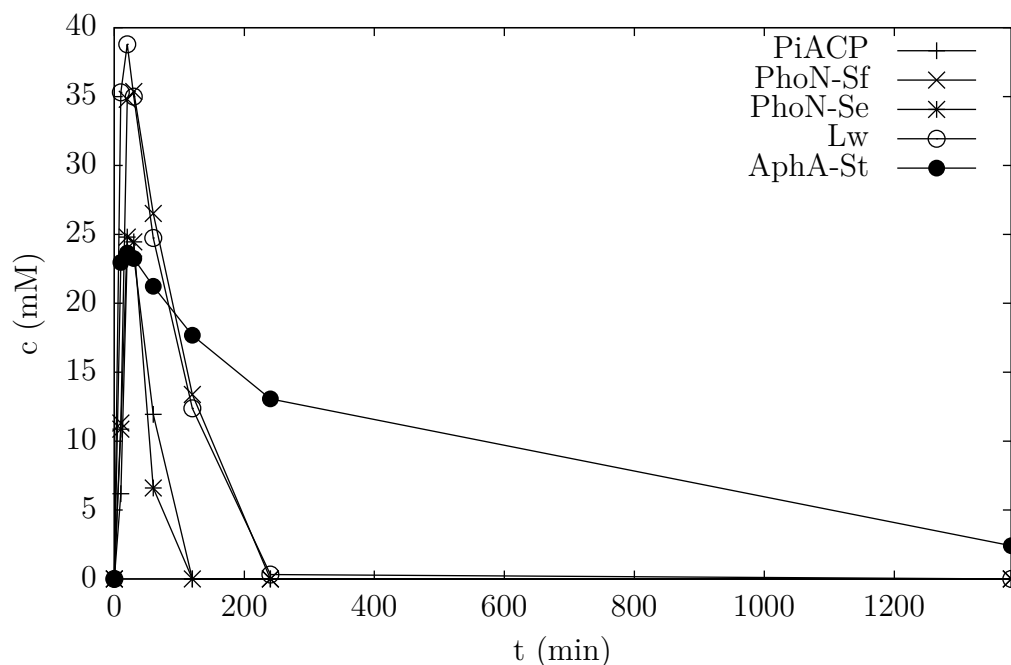
Figure 58: Product formation in phosphorylation of 500 mM 14OH with 100 mM CP at pH 4.2, 30 °C, 600 rpm shaking, 1 % DMSO as IS, 1 mL reaction volume, 10 mM $MgCl_2$ for AphA-St, 1 U mL^{-1} enzyme

57

Table 12: Maximum product levels from Figure 58 (1 U) in comparison with PP_i from Table 5 (4 U, except for 1 U PhoN-Se) and Table 6 (4 U, 10 mM $MgCl_2$)

	CP				PP_i		
	t [min]	prod. [mM]	P_i [mM]	prod./ P_i	t [min]	prod. [mM]	prod./ P_i
PiACP	20	24	42	0.57	20	53	0.36
PhoN-Sf	30	35	34	1.0	30	67	0.48
PhoN-Se	20	25	43	0.58	30	65	0.45
Lw	20	39	32	1.2	20	67	0.46
AphA-St	20	24	60	0.40	120	3.0	0.14

2.5.5 Transphosphorylation with PC as Donor
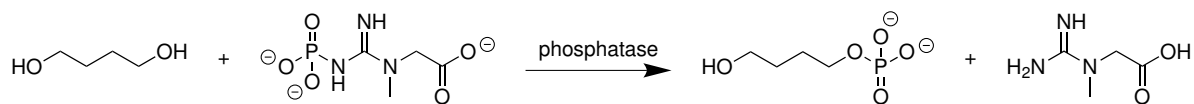
Figure 59: Phosphorylation of 14OH with PC as donor

In order to further broaden the spectrum of organic donors, the phosphoamide phosphocreatine (PC) was assayed with a selection of the most promising enzyme candidates from the preceding studies (PiACP, PhoN-Sf, PhoN-Se, PhoC-Mm-2, NSAP-Eb-11). Unfortunately it was hardly accepted as a donor for transphosphorylation by any phosphatase and its hydrolysis was dominant (Figure 60 and Table 13).

Table 13: Maximum product levels from Figure 60 in comparison with PP_i from Table 5; just 1 U PhoN-Se was used with PP_i

	PC				PP_i		
	t [min]	prod. [mM]	P_i [mM]	prod./ P_i	t [min]	prod. [mM]	prod./ P_i
PiACP	10	3.6	81	4.4×10^{-2}	20	53	0.36
PhoN-Sf	30	4.0	83	4.8×10^{-2}	30	67	0.48
PhoN-Se	20	4.1	83	4.9×10^{-2}	30	65	0.45
PhoC-Mm-2	30	5.7	83	6.9×10^{-2}	240	63	0.42
NSAP-Eb-11	10	5.6	83	6.7×10^{-2}	240	56	0.36
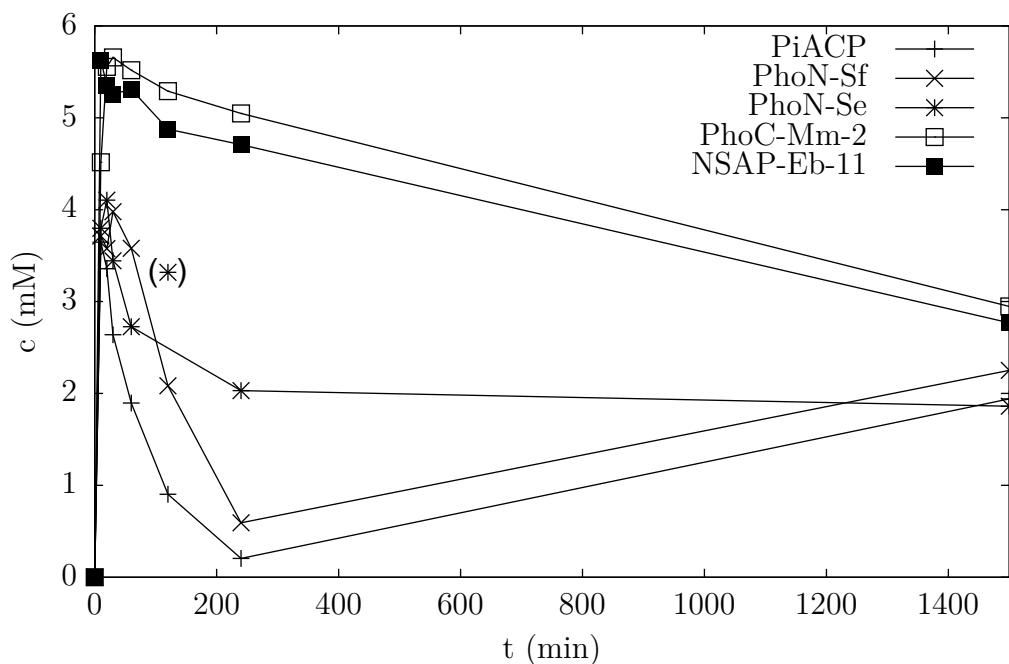
Figure 60: Product formation in phosphorylation of $500\,\text{mM}$ 14OH with $100\,\text{mM}$ PC at pH 4.2, $30\,°\text{C}$, $600\,\text{rpm}$ shaking, $1\,\%$ DMSO as IS, $1\,\text{mL}$ reaction volume and $4\,\text{U}\,\text{mL}^{-1}$ enzyme

2.6 Reduced Product Hydrolysis with PEP

During the initial studies with phosphoenolpyruvate (PEP) as donor in Section 2.5.3, it was found that hydrolysis of the product 4-hydroxybutyl phosphate was suppressed with several phosphatases. In the first set of enzymes, except with PhoN-Se and PhoC-Mm-2 (Figure 53 and Table 10), there was in addition still unused donor left in the reaction mixture at the maximum product level, suggesting inhibition or deactivation of the enzymes. The following chapter is dedicated to studies investigating the rationale behind this behavior.

2.6.1 Hydrolysis of PEP by various Enzymes without Acceptor

The hydrolysis of PEP by PhoN-Se, PhoN-Sf, PiACP, Lw, AphA-St and SPHSX was investigated via HPLC-RI according to the procedure described in Section 3.3.3. Table 14 depicts that PhoN-Se was by far the fastest phosphatase, being able to break down $50\,\%$ of the total amount of PEP in about $20\,\text{min}$. Even when just $1\,\text{U}$ phosphatase was employed, the half-life of the donor did not exceed $240\,\text{min}$. Hence, very likely, PhoN-Se, in contrast to PhoN-Sf, PiACP and Lw, was fast enough to drive phosphate transfer reactions to completion before any deactivation or inhibition could occur.

Table 14: Half-life of PEP being hydrolyzed by various phosphatases, determined via HPLC-RI following the general procedure mentioned in in Section 3.3.3

enzyme	amount [U]	$t_{1/2}$ of PEP [min]
PhoN-Se	4	20
PhoN-Se	1	240
PhoN-Sf	4	240
PiACP	4	50
Lw	4	120
AphA-St	4	120
SPHSX	4	> 1320

2.6.2 Reactions in the Presence of Pyruvate

In order to exclude inhibition of the enzymes by a side product formed during transphosphorylation, the hydrolytic performance of PhoN-Se and AphA-St was assayed spectrophotometrically in the pNPP assay (Figure 61) in the presence of various amounts of pyruvate, which is released upon hydrolysis of PEP (Figure 52).
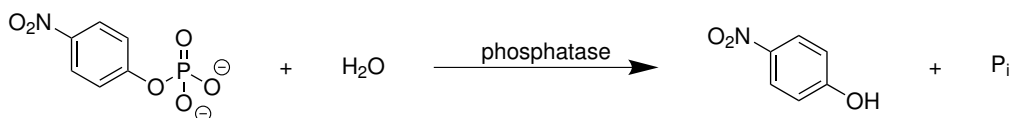
Figure 61: Hydrolysis of *p*-nitrophenyl phosphate (pNPP)

Reactions were performed as delineated in Section 3.1.3, except for an extended incubation time of 1 h at 30 °C and 450 rpm, with 100 µg mL^{-1} AphA-St or PhoN-Se at pH 6.0 in the presence of 0, 10, 50 and 100 mM sodium pyruvate. To reactions with AphA-St another 2 mM MgCl$_2$ were added. Conversion of pNPP was obtained via the spectrophotometric determination of released *p*-nitrophenol (see Section 3.1.3, Table 15). Even 100 mM pyruvate had almost no effect on the hydrolytic activity of any enzyme at pH 6.

Therefore, transphosphorylation of 500 mM 14OH was tested at pH 4.2 with 1 U PhoN-Se and 100 mM PP$_i$ as donor with 10, 50 and 100 mM sodium pyruvate being present in the reaction mixture. In line with the observations before, Figure 62 clearly shows that neither product formation nor hydrolysis were influenced by any amount of pyruvate. In all three screenings the maximum of 63 mM 4-hydroxybuyl phosphate was reached after 30 min.

Table 15: Hydrolytic activity of AphA-St and PhoN-Se in the pNPP assay in the presence of various amounts of pyruvate after 1 h pre-incubation at 30 °C.

|	sodium pyruvate			
	0 mM	10 mM	50 mM	100 mM
PhoN-Se A_{spec} [µmol min^{-1} mg^{-1}]	31	34	33	42
AphA-St A_{spec} [µmol min^{-1} mg^{-1}]	41	51	55	60

Figure 62: Product formation in phosphorylation of 500 mM 14OH with 100 mM PP$_i$ at pH 4.2, 30 °C, 600 rpm shaking, 1 % DMSO as IS, 1 mL reaction volume and 1 U mL^{-1} PhoN-Se in the presence of 10, 50 and 100 mM sodium pyruvate

2.6.3 Effects of Substrate and Donor Concentration with PhoN-Se

Since pyruvate could be excluded as being responsible for displaying inhibitory properties, further experiments were carried out to gain insight into phosphate transfer reactions with PEP and PhoN-Se, the fastest enzyme. Different substrate and donor concentrations were tested.
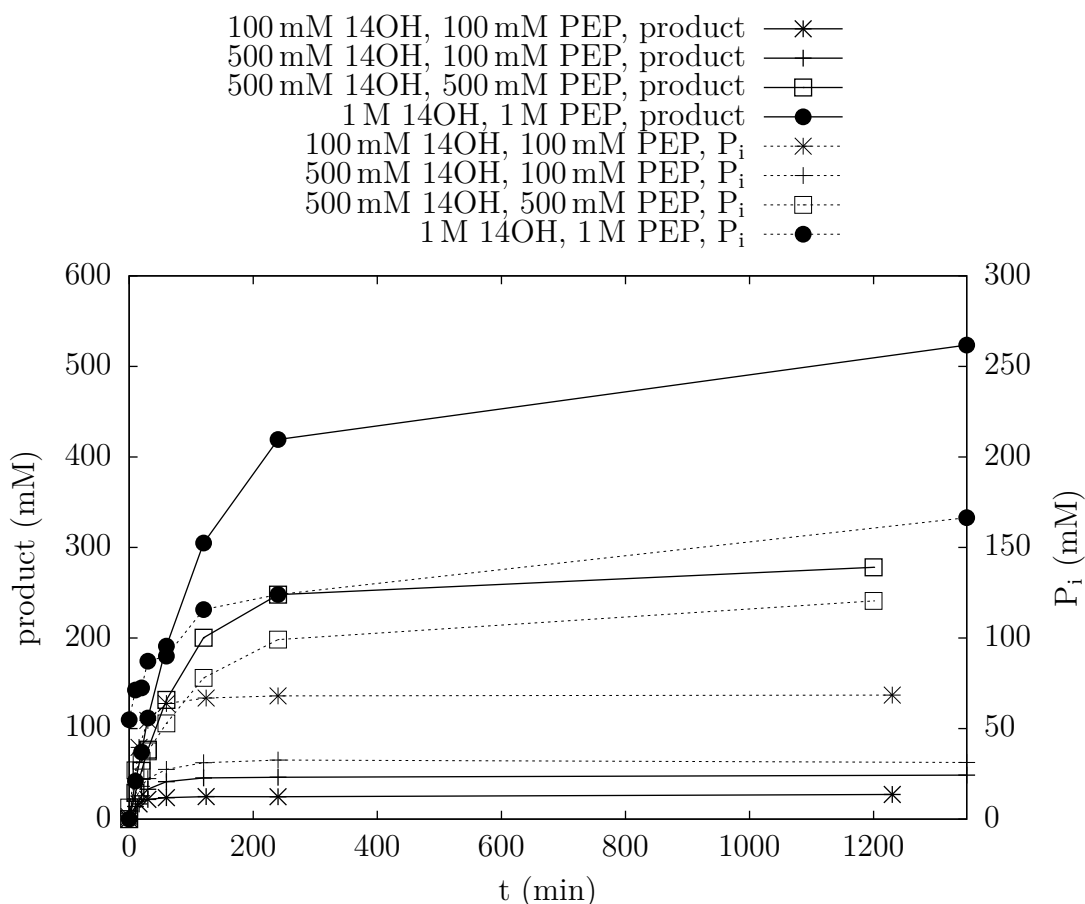
Figure 63: Product and P_i formation in phosphorylation of 100–1000 mM 14OH with 100–1000 mM PEP at pH 4.2, 30 °C, 600 rpm shaking, 1 % DMSO as IS, 1 mL reaction volume and $1\,U\,mL^{-1}$ PhoN-Se

With 100 mM 14OH only about 30 mM product were furnished (compared to ~ 60 mM 4-hydroxybutyl phosphate with 500 mM 14OH and the same concentration of PEP, see Table 10), which is most probably due to the educt concentration falling below the K_M of PhoN-Se (Figure 63). Hence, increasing the concentration of the donor while maintaining a constant 500 mM 14OH (except for 1 M 14OH with 1 M PEP) was attempted. Apparently, deactivation or inhibition of the enzyme occurred at any donor concentration, but not equally fast. An explanation for this behavior is given in Section 2.6.4.

Table 16: Maximum product levels from Figure 63

| | PhoN-Se | | | |
	t [min]	prod. [mM]	P_i [mM]	prod./P_i
100 mM 14OH, 100 mM PEP	1230	27	69	0.39
500 mM 14OH, 100 mM PEP	1350	49	31	1.6
500 mM 14OH, 500 mM PEP	1200	278	120	2.3
1 M 14OH, 1 M PEP	1350	523	166	3.2

2.6.4 pH Studies

The effect of pH on the system 14OH, PEP, PhoN-Se was investigated (Figure 64 and Table 17). Interestingly, hydrolytic activity of the enzyme on the product could be detected at high pH values after reaching a maximum concentration of 65 mM at pH 5.0, which is equal to the amount obtained with PP_i as donor (Table 5), whereas at pH 3.5 and 3.8, product formation rate was reduced and no 4-hydroxybutyl phosphate degradation took place.

Figure 64: Product formation in phosphorylation of 500 mM 14OH with 100 mM PEP at pH 3.5–6.0, 30 °C, 600 rpm shaking, 1 % DMSO as IS, 1 mL reaction volume and 1 U mL^{-1} PhoN-Se

Clearly, these results indicated a slowdown of the reaction at reduced pH. Yet they did not clarify, why PhoN-Se performed well with other donors at pH 4.2, while at the same pH displaying signs of deactivation with PEP. It was estimated that in reactions with PEP, the initial pH of 4.2 was shifted towards more acidic levels during the course

Table 17: Maximum product levels from Figure 64

	PEP		
	t [min]	prod. [mM]	P_i [mM]
pH 3.5	1200	4.0	8.7
pH 3.8	1200	33	23
pH 4.2	1350	49	31
pH 5.0	30	65	33
pH 6.0	30	42	30

of the reaction, rendering the enzyme inactive. This assumption could be confirmed by carefully monitoring the pH with a pH electrode during transphosphorylation of 500 mM 14OH with 100 mM PEP and 1 U PhoN-Se (Figure 65). The enzyme was found to be inactive, once a pH threshold of ~ 3.3 was undercut (proven by absence of product formation upon addition of fresh donor, data not shown). Most likely, the drop in pH was due to the release of pyruvate, which has a pKa of 2.49 [168].
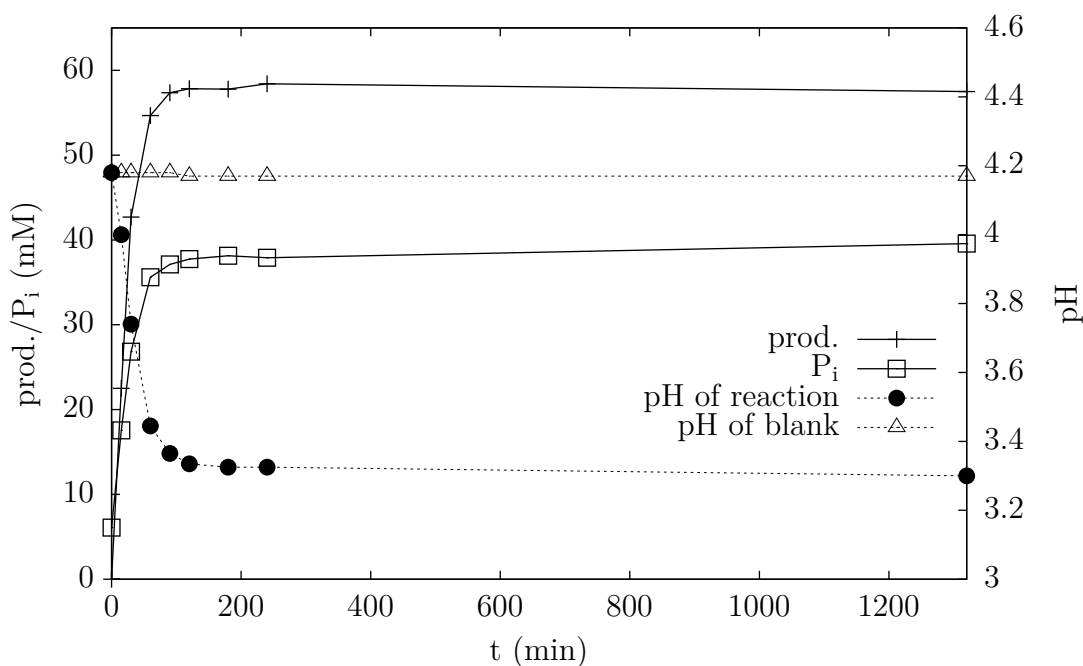
Figure 65: Product, P_i formation and development of pH in phosphorylation of 500 mM 14OH with 100 mM PEP at pH 4.2, 30 °C, 600 rpm shaking, 1 % DMSO as IS, 1 mL reaction volume and 1 U mL^{-1} PhoN-Se

To probe the reversibility of this deactivation and demonstrate the generality of pH associated deactivation, PiACP, PhoN-Sf, PhoN-Se and Lw were assayed with 500 mM 14OH and 100 mM PEP and after 2 h reaction time, where approximately the plateau was reached in Figure 53, the pH was readjusted to 5.0 (Figure 66 and Table 18).

Immediately after, transphosphorylation as well as P_i formation (data not shown) could be detected again in every case and remarkable product levels were reached. In addition, adjusting the pH in the reverse direction, from 6.0 to 4.2 after 30 min led to deactivation of PhoN-Se in about 100 min (Figure 67). Most probably PiACP, PhoN-Sf and Lw, which also exhibited reduced product hydrolysis with PEP as donor in Section 2.5.3, were shut off in a similar fashion. In contrast, they did not perform as fast as PhoN-Se and thus the donor was not used up entirely.
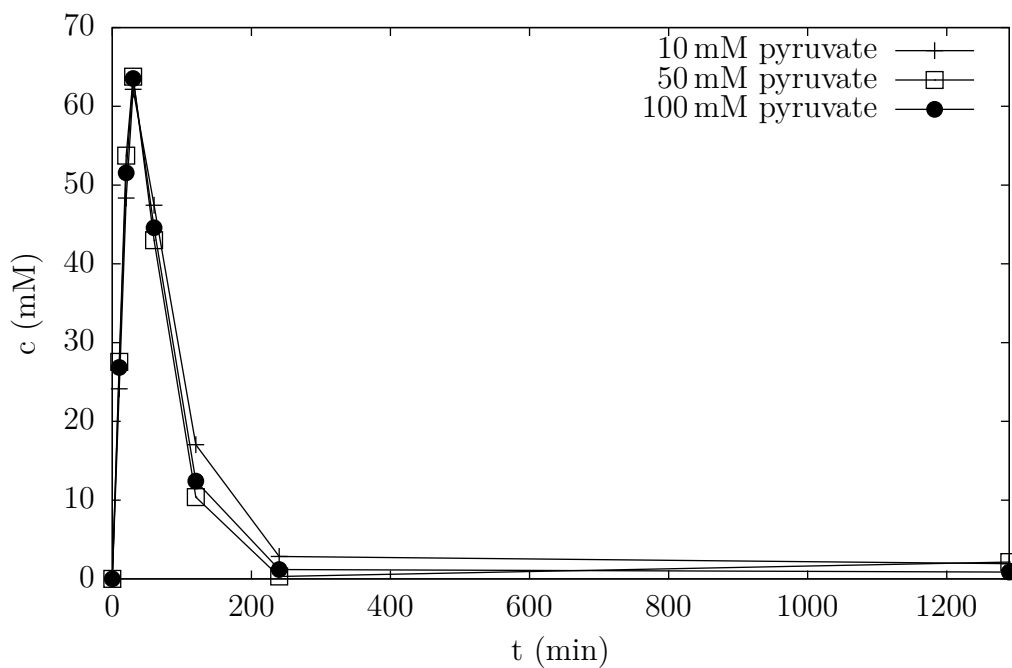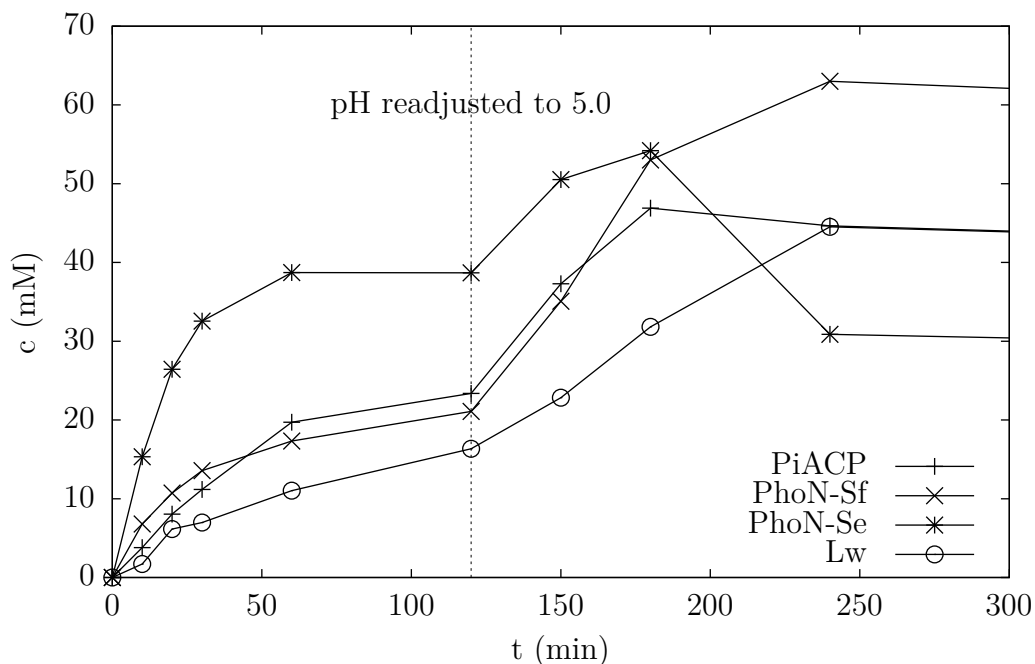

Figure 66: Product formation in phosphorylation of 500 mM 14OH with 100 mM PEP at pH 4.2, 30 °C, 600 rpm shaking, 1 % DMSO as IS, 1 mL reaction volume and 1 U mL^{-1} enzyme, pH readjusted to 5.0 after 2 h reaction time

Table 18: Maximum product levels from Figure 66

|	PEP		
	t [min]	prod. [mM]	P_i [mM]
PiACP	180	47	37
PhoN-Sf	240	63	37
PhoN-Se	180	54	47
Lw	240	45	31
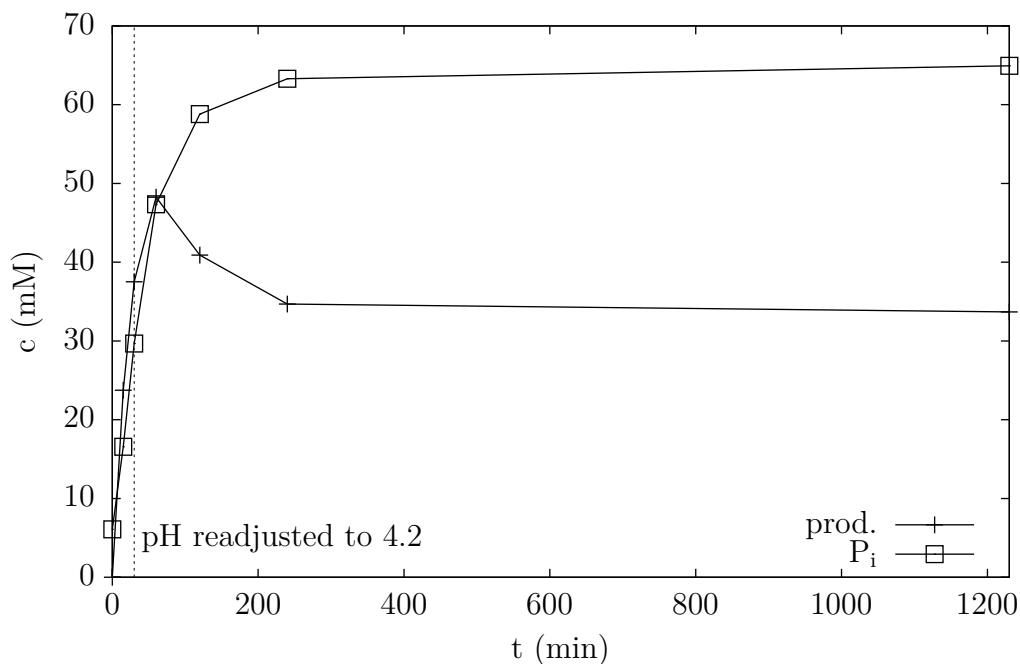
Figure 67: Product and P_i formation in phosphorylation of 500 mM 14OH with 100 mM PEP at pH 6.0, 30 °C, 600 rpm shaking, 1 % DMSO as IS, 1 mL reaction volume and 1 U mL^{-1} PhoN-Se, pH readjusted to 4.2 after 30 min reaction time

2.7 Correlation between pH and the Hydrolytic Side Reaction

It was assumed that for every enzyme, a distinct pH threshold similar to the one observed with PhoN-Se in the previous section existed. In order to determine this value, pH studies were conducted following the general procedure (Section 3.3.2.a) with 500 mM 14OH and 100 mM AcP. During these studies, an "optimum" pH of ~ 3.3, close to the pH of complete deactivation was found for PhoN-Se, where the product was not depleted, but still produced in good amounts (Table 19 and Figure 68). Also the pH was monitored at start values of 3.3, 3.45, 3.5, 3.8 and 4.2 and was found to be stable during the course of the reaction (Figure 69). AphA-St, PiACP, PhoN-Sf and Lw were also subjected to pH studies with AcP (Figure 70) and showed similar characteristics to PhoN-Se: Below a certain threshold, hydrolysis could be prevented while still obtaining decent product levels. This pH was found to be 2.9 for AphA-St, 3.5 for PiACP, 3.8 for PhoN-Sf and 3.5 for Lw.
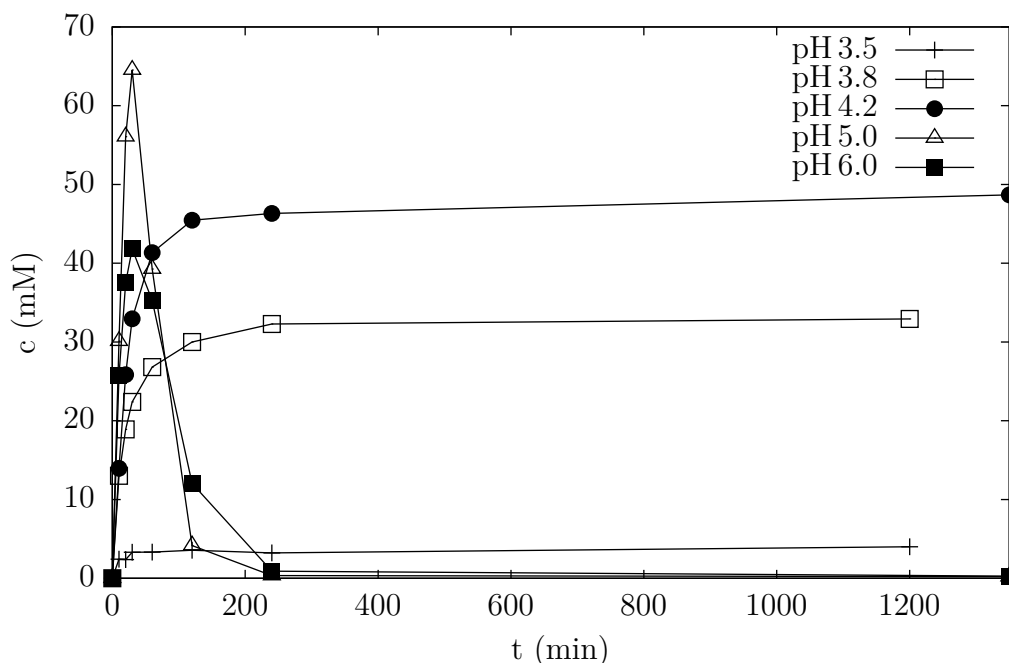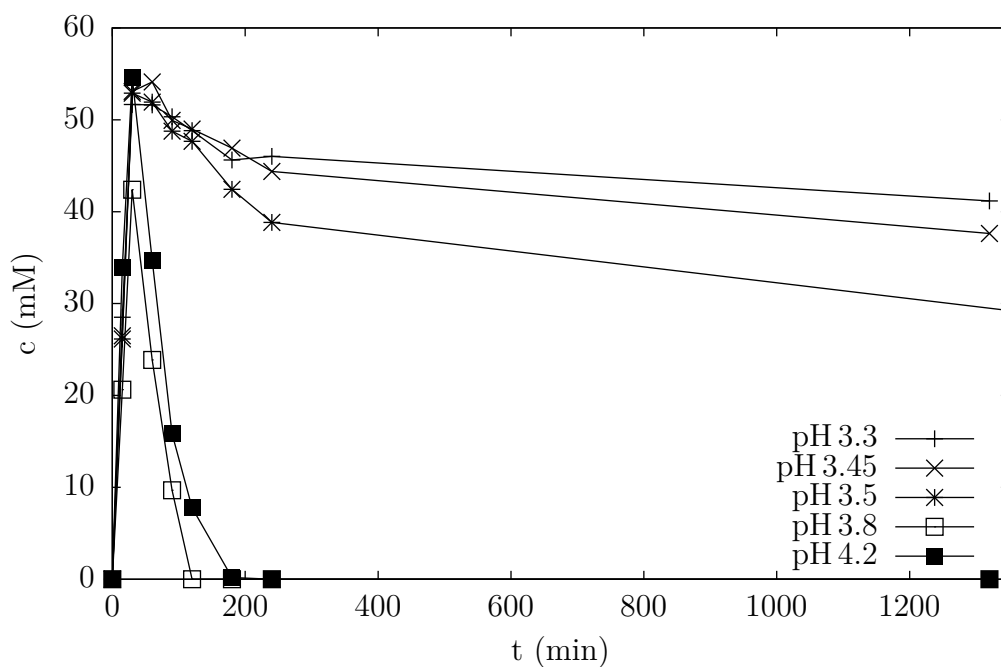
Figure 68: Product formation in phosphorylation of 500 mM 14OH with 100 mM AcP at pH 3.3–4.2, 30 °C, 600 rpm shaking, 1 % DMSO as IS, 1 mL reaction volume and $1\,U\,mL^{-1}$ PhoN-Se

Table 19: Maximum product levels from Figure 68

	AcP		
	t [min]	prod. [mM]	P_i [mM]
pH 3.3	30	52	47
pH 3.45	60	54	46
pH 3.5	30	53	48
pH 3.8	30	42	44
pH 4.2	30	55	46

Figure 69: pH development in phosphorylation of 500 mM 14OH with 100 mM AcP at pH 3.3–4.2, 30 °C, 600 rpm shaking, 1 % DMSO as IS, 1 mL reaction volume and $1\,U\,mL^{-1}$ PhoN-Se

To assure that at the "optimum" pH, determined individually for each enzyme in Figure 70 and Figure 68, no slow deactivation of the enzymes – including phosphotransferase activity – had occurred, a control experiment with 500 mM 14OH and 100 mM AcP was set up. As soon as a steady product level was reached according to Figure 70 (2 h for PiACP and Lw, 3 h for PhoN-Se or 4 h for AphA-St and PhoN-Sf) another 100 mM AcP was added (Figure 71). To our delight, all tested enzyme candidates were found to be active at their "optimum" pH as product formation took place as soon as a new batch of AcP was added.

It is worth mentioning that, as can be seen in Table 20, the observed product concentrations after the first plateau that were reached in reactions at the "optimum" pH (first row for each enzyme) are in the same range as the results from screenings at pH 4.2. Overall, the enzymes have a narrow pH range where transphosphorylation is still intact while hydrolysis is diminished. Inspired by the almost completely suppressed product degradation at the "optimum" pH, several reactions were conducted under these optimized conditions.
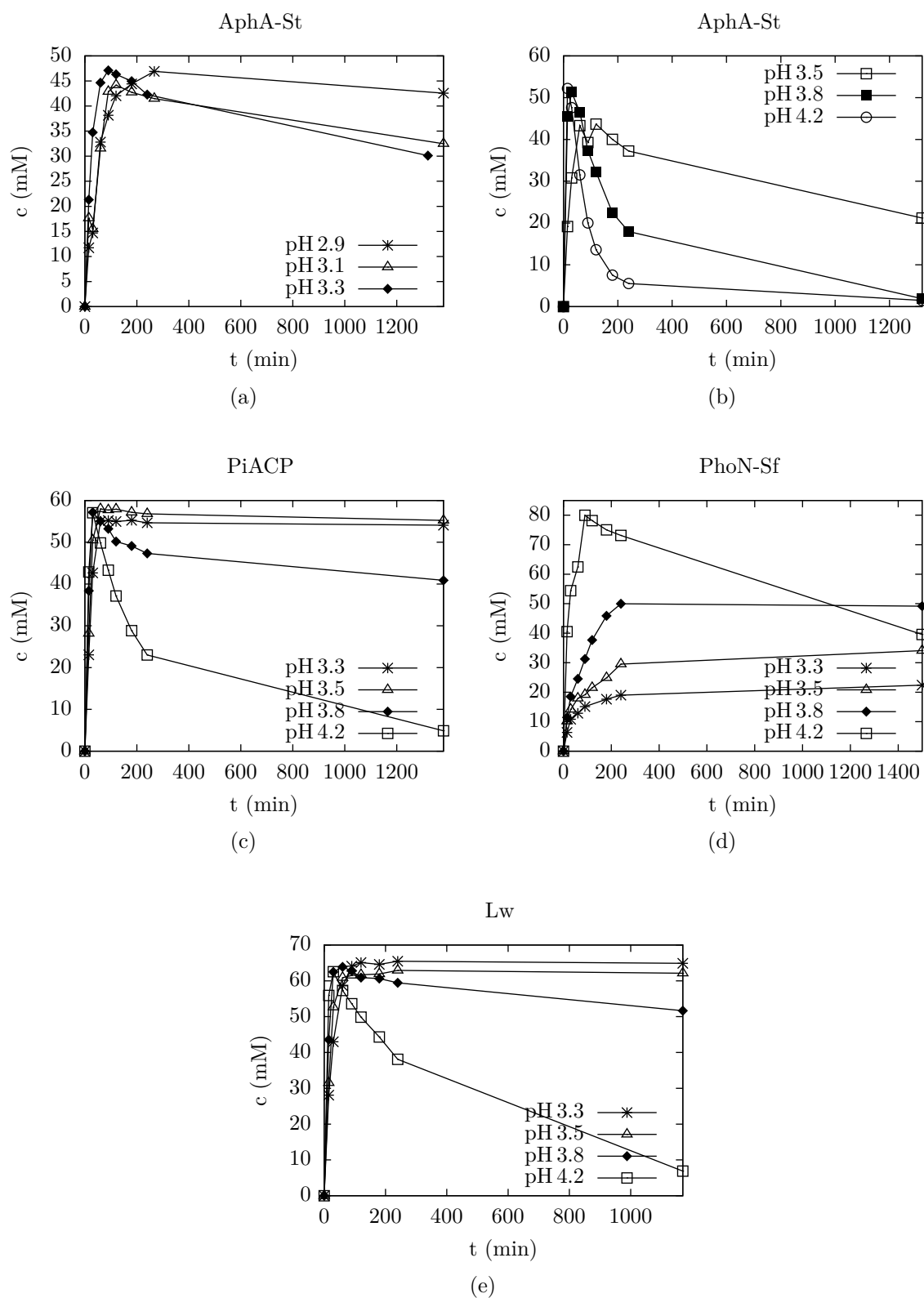
Figure 70: Product formation in the pH study with AphA-St, PiACP, PhoN-Sf, Lw: phosphorylation of 500 mM 14OH with 100 mM AcP, 30 °C, 600 rpm shaking, 1 % DMSO as IS, 1 mL reaction volume, 10 mM $MgCl_2$ for AphA-St and 1 U mL^{-1} enzyme

Figure 71: Phosphorylation of 500 mM 14OH with 100 mM AcP at "optimum" pH, 30 °C, 600 rpm shaking, 1 % DMSO as IS, 1 mL reaction volume, 10 mM MgCl$_2$ for AphA-St and 1 U mL^{-1} enzyme; dashed lines: addition of fresh donor (2 h: PiACP and Lw, 3 h: PhoN-Se, 4 h: AphA-St and PhoN-Sf)

Table 20: Product levels at "optimum" pH and 1 U enzyme from Figure 71 in comparison with the maximum levels at pH 4.2 from Table 8 (a, 4 U enzyme) and Table 9 (b, 1 U enzyme)

	"optimum" pH				pH 4.2		
	t [min]	prod. [mM]	P$_i$ [mM]	prod./ P$_i$	t [min]	prod. [mM]	prod./ P$_i$
PiACP	120	57	42	1.4	60	60[b]	1.4[b]
	360	98	91	1.1			
PhoN-Sf	240	54	47	1.1	10	57[a]	1.5[a]
	480	100	93	1.1			
PhoN-Se	180	50	50	1.0	20	58[b]	1.3[b]
	360	91	107	0.85			
Lw	120	63	37	1.7	20	67[a]	1.8[a]
	480	114	85	1.3			
AphA-St	240	40	51	0.78	20	48[b]	1.1[b]
	480	66	106	0.62			

2.8 Reactions at optimum pH

To demonstrate that pH is a universal tool to control product hydrolysis, reactions at the "optimum" pH, determined for PiACP, PhoN-Sf, PhoN-Se, Lw and AphA-St in Section 2.7 (AphA-St was operated at pH 3.3 instead of the more suitable pH 2.9 identified later) were performed with a broader range of donors, including PP_i for comparison: CP, 2,2,2-trifluoroethyl phosphate (TFEP, synthesis: Section 3.2.3), isopropenyl phosphate (IPP, synthesis: Section 3.2.1) and 1-(2,4-difluorophenyl)vinyl phosphate (DFPVP, synthesis: Section 3.2.2) were assayed. Following the general procedure from Section 3.3.2, 1 U enzyme was employed in conjunction with 500 mM 14OH and 100 mM donor (except for only 50 mM in case of IPP and DFPVP). Furthermore the stability of the product 4-hydroxybutyl phosphate over time was monitored at the "optimum" pH in the presence of 100 mM phosphate and 1 U phosphatase.

2.8.1 Carbamoyl Phosphate

In Screenings with CP (Figure 72 and Table 21), with every tested phosphatase, almost complete product hydrolysis along with slightly lower maximum concentrations than at pH 4.2 were observed in spite of starting the reactions at the "optimum" pH. pH measurements after 240 min reaction time indicated a stark increase to about 7.0–7.5. As mentioned in Section 2.3, this can be attributed to the release of carbamate upon breakdown of CP and its further decomposition into ammonia and carbon dioxide and may be prevented by the employment of a pH stat.

Table 21: Maximum product levels from Figure 72 in comparison with the maximum levels at pH 4.2 from Table 12 (1 U enzyme)

|	"optimum" pH				pH 4.2		
	t [min]	prod. [mM]	P_i [mM]	prod./ P_i	t [min]	prod. [mM]	prod./ P_i
PiACP	15	38	41	0.93	20	24	0.57
PhoN-Sf	30	59	35	1.7	30	35	1.0
PhoN-Se	15	35	50	0.70	20	25	0.58
Lw	15	52	31	1.7	20	39	1.2
AphA-St	15	26	59	0.44	20	24	0.40
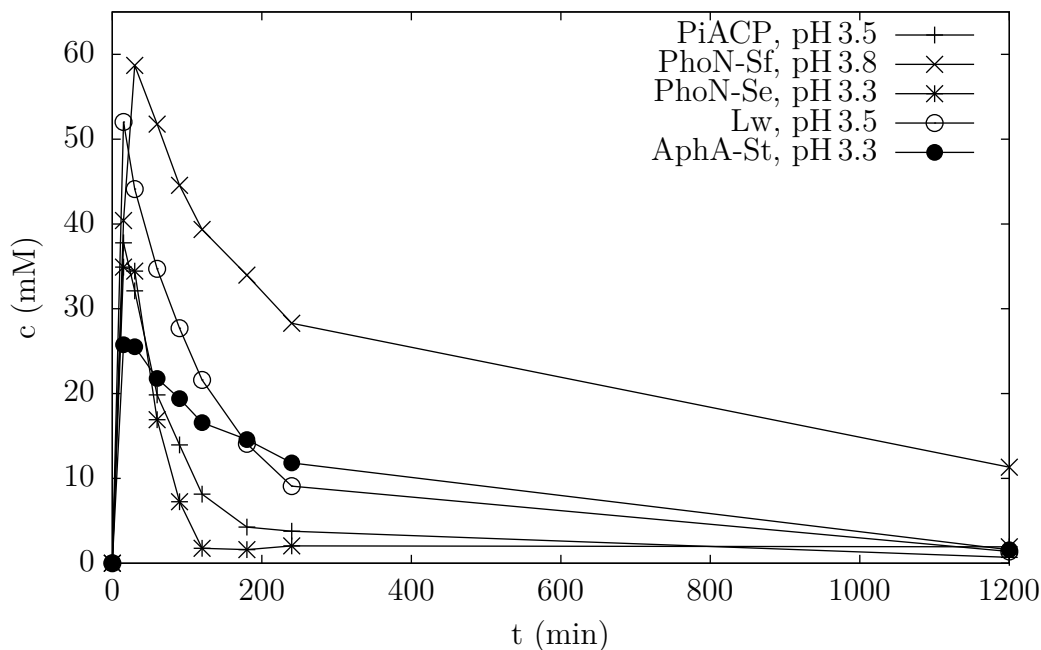
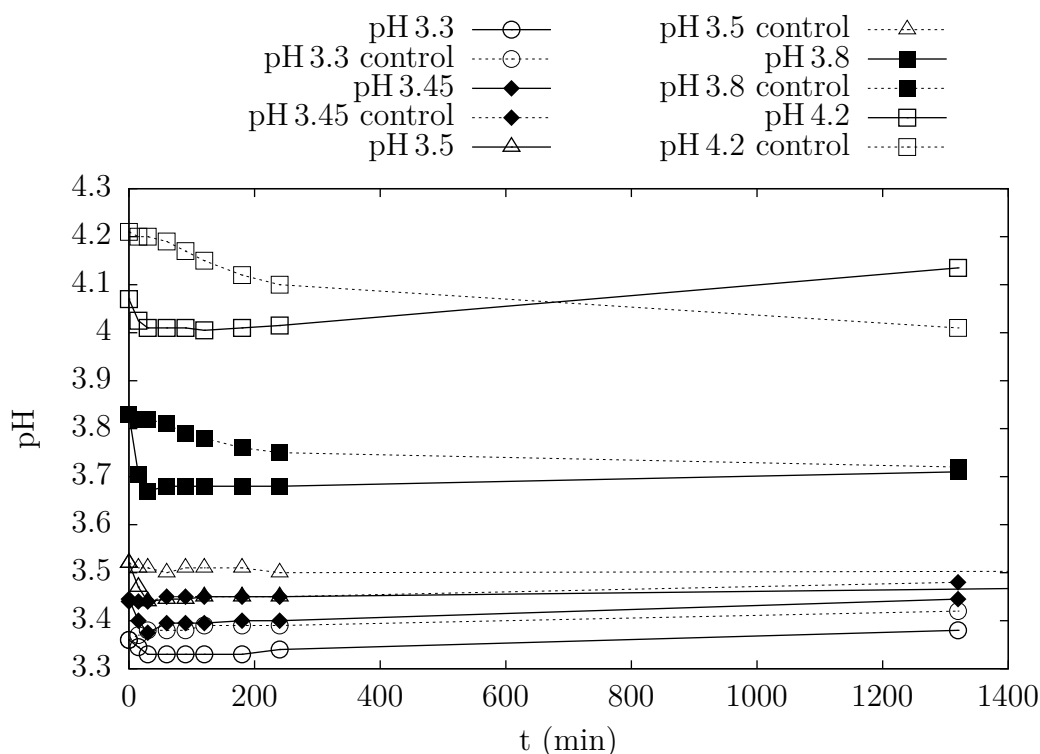Figure 72: Product formation in phosphorylation of 500 mM 14OH with 100 mM CP at "optimum" pH, 30 °C, 600 rpm shaking, 1 % DMSO as IS, 1 mL reaction volume, 10 mM $MgCl_2$ for AphA-St and $1\,U\,mL^{-1}$ enzyme

2.8.2 Pyrophosphate

In assays with PP_i, excellent product levels were observed with all metal-independent enzymes (Figure 73 and Table 22). Reduced product degradation took place with PiACP, PhoN-Sf and Lw, whereas with PhoN-Se only traces of 4-hydroxybutyl phosphate could be detected after 22 h. The greater hydrolytic activity of all phosphatases compared to experiments with AcP can be associated with a marginal increase in pH of ∼0.5 units in 4 h, which again may be impeded by using a pH-stat.

Table 22: Maximum product levels from Figure 73 (1 U) in comparison with the maximum levels at pH 4.2 (4 U) Table 5

	"optimum" pH				pH 4.2		
	t [min]	prod. [mM]	P_i [mM]	prod./ P_i	t [min]	prod. [mM]	prod./ P_i
PiACP	240	70	127	0.55	20	53	0.36
PhoN-Sf	180	76	124	0.61	30	67	0.48
PhoN-Se	60	62	136	0.46	30	65	0.45
Lw	180	80	122	0.66	20	67	0.46

Figure 73: Product formation in phosphorylation of 500 mM 14OH with 100 mM PP_i at "optimum" pH, 30 °C, 600 rpm shaking, 1 % DMSO as IS, 1 mL reaction volume and $1\,U\,mL^{-1}$ enzyme

2.8.3 2,2,2-Trifluoroethyl phosphate
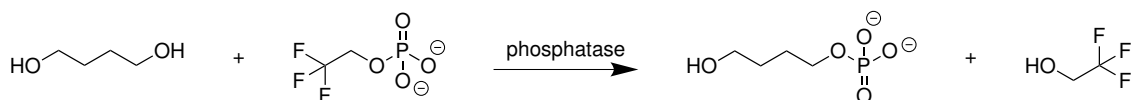
Figure 74: Phosphorylation of 14OH with TFEP as donor

2,2,2-Trifluoroethyl phosphate (TFEP), provided by BASF as cyclohexylammonium salt, was tested as a donor with 14OH as substrate, PhoN-Sf, PhoN-Se and AphA-St and 1 h reaction time using NMR (Section 3.3.2.e, Figure 111). Since product formation was confirmed, a time-study with subsequent analysis on HPLC-RI was set up with PiACP, PhoN-Sf, PhoN-Se, Lw and AphA-St 500 mM 14OH and 100 mM donor to identify the maximum product levels (Figure 75 and Table 23).

Due to the strong electron withdrawing character of the F atoms, trifluoroethanol represents a fairly good leaving group in the formation of the phosphoenzyme intermediate, which makes it a well working phosphate donor. Although the transphosphorylation system was not optimized and hydrolysis took place due to an increase in pH of about one unit with every enzyme (data not shown), the maximum product concentrations were in the same range as in reactions with PP_i as the donor. At the same time, significantly less phosphate by-product was produced. The shift in pH could have been prevented
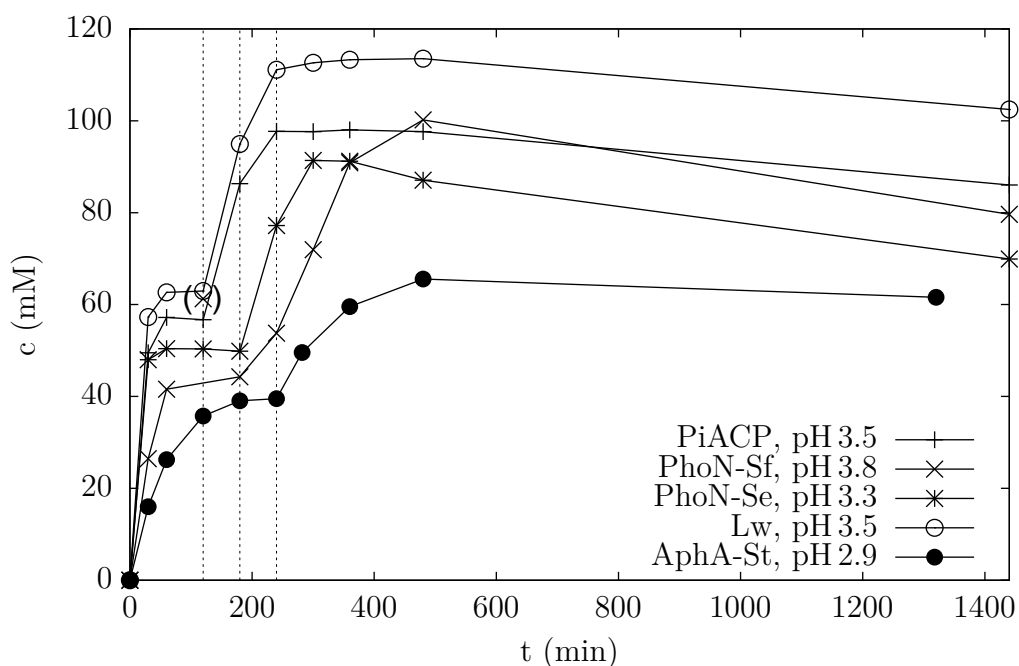
73
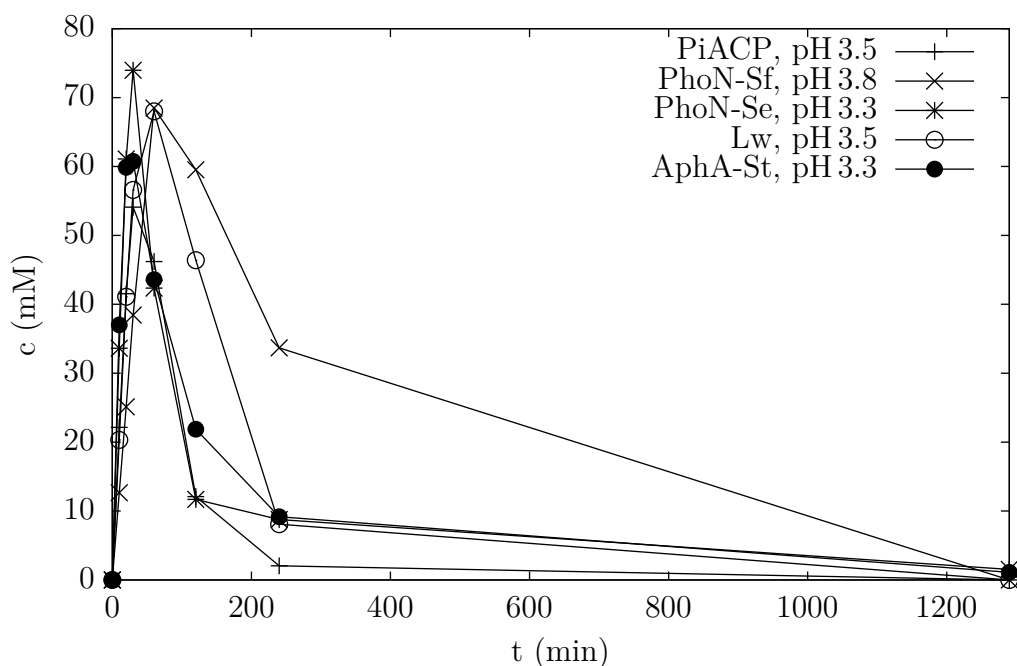
Figure 75: Product formation in phosphorylation of 500 mM 14OH with 100 mM TFEP at "optimum" pH, 30 °C, 600 rpm shaking, 1 % DMSO as IS, 1 mL reaction volume, 10 mM MgCl$_2$ for AphA-St and 1 U mL^{-1} enzyme

Table 23: Maximum product levels from Figure 75 (1 U) in comparison with the maximum levels at pH 4.2 (4 U) Table 5 and Table 6 (10 mM MgCl$_2$)

| | TFEP, "optimum" pH | | | | PP$_i$, pH 4.2 | | |
	t [min]	prod. [mM]	P$_i$ [mM]	prod./ P$_i$	t [min]	prod. [mM]	prod./ P$_i$
PiACP	30	54	29	1.9	20	53	0.36
PhoN-Sf	60	68	24	2.8	30	67	0.48
PhoN-Se	30	74	40	1.9	30	65	0.45
Lw	60	68	35	1.9	20	67	0.46
AphA-St	30	61	43	1.4	120	3.0	0.14

by using a pH-stat. Alternatively, a different salt of the donor may be employed. Finally, TFEP was found to be fairly stable under screening conditions with only 1–3 mM P_i produced within 22 h in control reactions without enzyme, which is comparable to PEP.

2.8.4 Isopropenyl phosphate
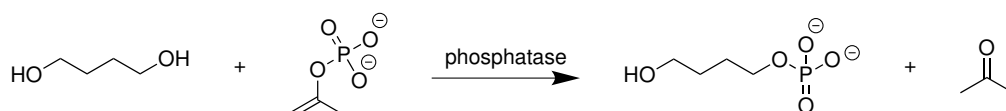
Figure 76: Phosphorylation of 14OH with IPP as donor

Isopropenyl phosphate (IPP) was selected due to its structural similarity to PEP. In reactions with IPP as donor, resembling PEP, an unstable enol is released as by-product, which tautomerizes to give the ketone, rendering the reaction completely irreversible. As isopropenyl phosphate rapidly hydrolyzes in water [167], a buffer solution containing 200 mM citrate, 500 mM 14OH, 1 % DMSO and 1 U of the corresponding enzyme was set up and adjusted to pH 3.3. At 0 min, 50 mM IPP were added to each reaction (V = 1 mL), which increased the pH to ∼3.8 despite the presence of citrate and the reaction was followed in time (Section 3.3.2). PhoN-Se, Lw and AphA-St gave only traces of product (1–2 mM), while PiACP and PhoN-Sf were not active at all (Figure 77 and Table 24). Due to the very low levels of 4-hydroxybutyl phosphate detected as well as analytical challenges (overlap of citrate and P_i & substrate and acetone in HPLC-RI chromatograms, see A.3) and the severe instability of IPP, no further experiments were conducted with this donor.

Table 24: Maximum product levels from Figure 77

	IPP, pH 3.8	
	t [min]	prod. [mM]
PhoN-Se	60	1.7
Lw	1170	< 1.0
AphA-St	120	1.2

Figure 77: Product formation in phosphorylation of $500\,\text{mM}$ 14OH with $50\,\text{mM}$ IPP at pH ~ 3.8, $30\,°\text{C}$, $600\,\text{rpm}$ shaking, $1\,\%$ DMSO as IS, $1\,\text{mL}$ reaction volume, $10\,\text{mM}$ $MgCl_2$ for AphA-St and $1\,\text{U}\,\text{mL}^{-1}$ enzyme

2.8.5 1-(2,4-Difluorophenyl)vinyl phosphate
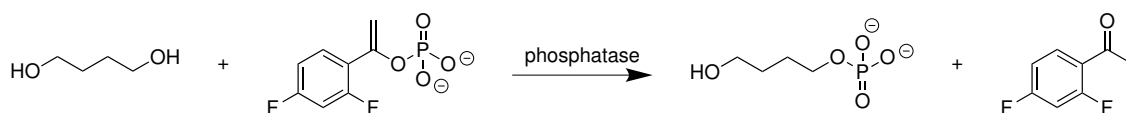
Figure 78: Phosphorylation of 14OH with DFPVP as donor

1-(2,4-Difluorophenyl)vinyl phosphate (DFPVP) was chosen as a compound resembling IPP, but being considerably more stable [167]. However, because of the presence of an aromatic ring, heat was required for at least partial solubilisation, which may have also caused spontaneous hydrolysis and lowered its availability for transphosphorylation. Still, DFPVP was shown to be capable of acting as a non-natural donor and moderate product yields were obtained with all tested phosphatases. Again as with TFEP, because of an increase in pH of about 1 to 1.2 units over time (data not shown), hydrolysis of 4-hydroxybutyl phosphate took place. Due to analytical obstacles on HPLC-RI, the amount of phosphate produced could not be quantified (overlap with DFPVP in chromatogram, see A.3).
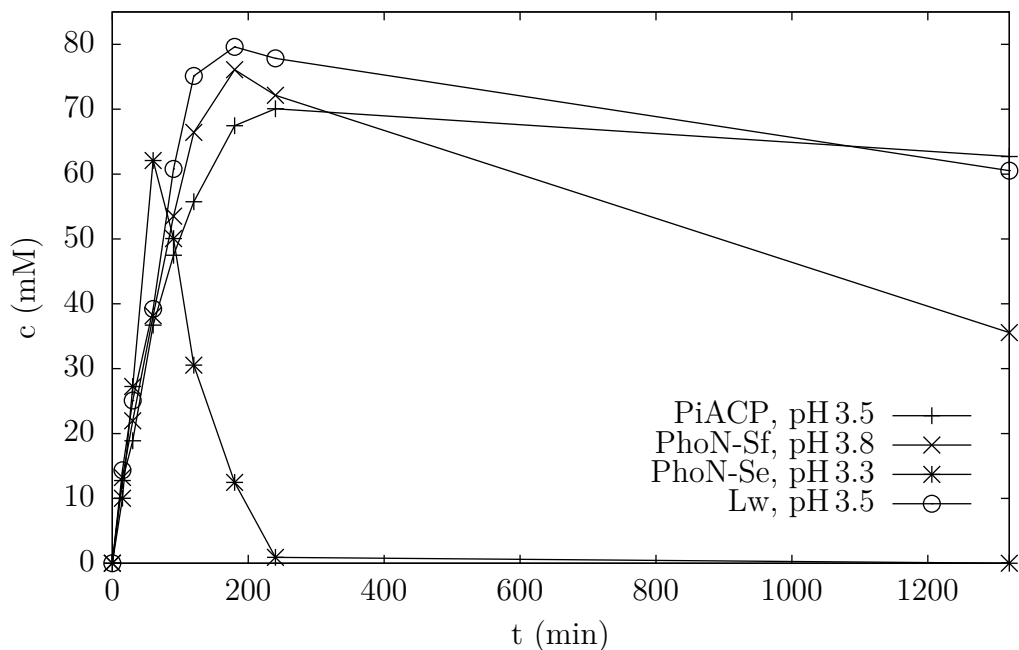
76

Figure 79: Product formation in phosphorylation of 500 mM 14OH with 50 mM DFPVP at "optimum" pH, 30 °C, 600 rpm shaking, 1 % DMSO as IS, 1 mL reaction volume, 10 mM $MgCl_2$ for AphA-St and $1\,U\,mL^{-1}$ enzyme

Table 25: Maximum product levels from Figure 79

	DFPVP, "optimum" pH	
	t [min]	prod. [mM]
PiACP	20	25
PhoN-Sf	60	27
PhoN-Se	20	17
Lw	20	30
AphA-St	60	15

2.8.6 Hydrolysis of 4-Hydroxybutyl phosphate
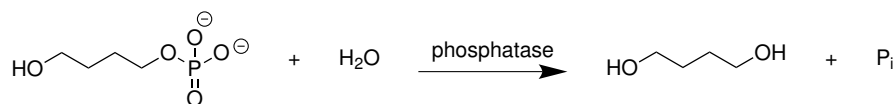
Figure 80: Hydrolysis of 4-hydroxybutyl phosphate

The results from the previous sections clearly demonstrated the narrow pH range for every enzyme, at which reduced product hydrolysis can be observed and transphosphorylation activity was preserved. All new donors tested in these sections were accepted by the phosphatases of choice, however the pH changed during the course of the reaction, leading to product hydrolysis. As carrying out phosphate transfer reactions in buffered media is inconvenient due to more elaborate product isolation, the employment of a pH-stat may help to impede the increase in pH or alternatively a different salt of the donor may be used.

To demonstrate that at a constant "optimum" pH in fact the level of product remains unchanged, 1 U PiACP, PhoN-Sf, PhoN-Se and Lw were incubated with $\sim 60\,\text{mM}$ 4-hydroxybutyl phosphate disodium salt in the presence of $100\,\text{mM}$ phosphate (Figure 81). Although hydrolysis could be detected, it remained minor ($< 4\,\%$) and constant product concentration was finally obtained.
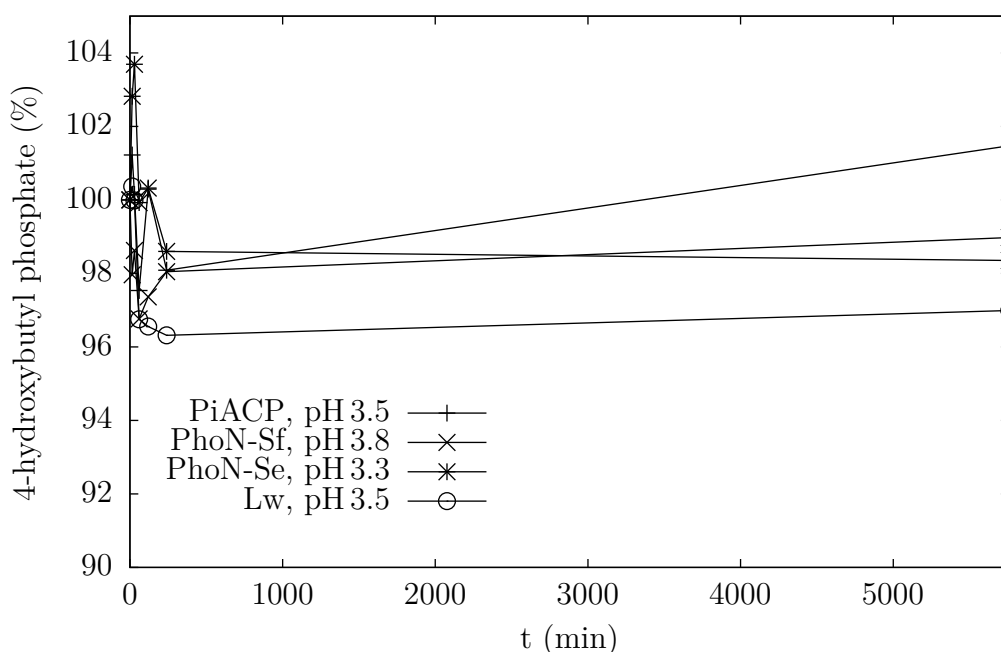
Figure 81: Hydrolysis of $\sim 60\,\text{mM}$ 4-hydroxybutyl phosphate ($100\,\%$ equal to starting value) by 1 U enzyme in the presence of $100\,\text{mM}$ phosphate at "optimum" pH, $30\,°\text{C}$, $600\,\text{rpm}$ shaking, $1\,\%$ DMSO as IS, $1\,\text{mL}$ reaction volume

78

2.9 Reactions with immobilized PhoN-Se

PhoN-Se was the only enzyme in the preliminary studies with PEP and 14OH (Section 2.5.3) that was found to be fast enough to consume the donor entirely before being deactivated by the drop in pH. Because the shutoff was shown to be reversible (Figure 67), reusing PhoN-Se immobilized on various polymer beads (Section 3.3.4.a) and reactivation by addition of fresh reaction solution was envisaged. Unfortunately on both carriers, ReliZyme™ EP403 (RZ) and Immobead 150 (IB), PhoN-Se performed very different to its free form: At an initial pH of 4.2 using PEP, rapid hydrolysis of the product took place. Only at pH 3.3 and 3.5, deactivation with both resins could be detected. The optimum pH appeared to be notably different form the "free" form of PhoN-Se.
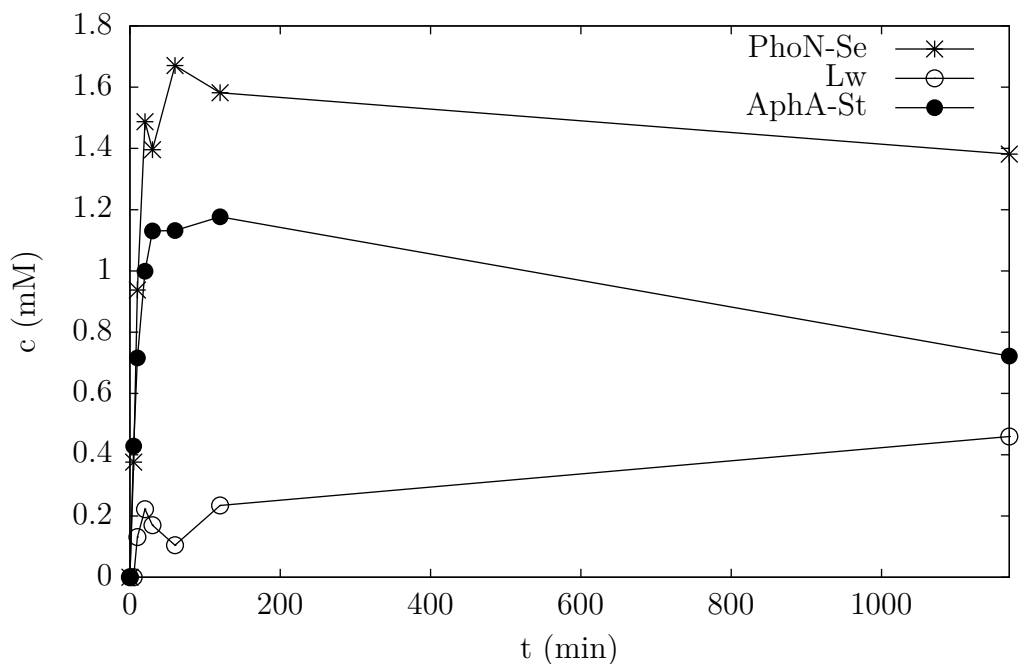

Figure 82: Product formation in phosphorylation of 500 mM 14OH with 100 mM PEP at pH 3.3–4.2, 30 °C, 600 rpm shaking, 1 % DMSO as IS, 1 mL reaction volume, ∼1.9 U immobilized PhoN-Se on ReliZyme™ EP403 (RZ) and ∼0.5 U immobilized on Immobead 150 (IB) beads

79

Table 26: Maximum product levels from Figure 82

	Figure	t [min]	prod. [mM]	P_i [mM]	prod./P_i
PEP, RZ, pH 4.2	82a	30	37	45	0.82
PEP, IB, pH 4.2	82a	15	59	40	1.5
PEP, RZ, pH 3.3	82b	1752	66	40	1.7
PEP, RZ, pH 3.5	82b	1752	59	45	1.3
PEP, IB, pH 3.3	82b	1752	61	44	1.4
PEP, IB, pH 3.5	82b	240	60	42	1.2

2.10 Enzyme Concentration and Product Hydrolysis

In Section 2.5.2 in Figure 51, reduced product hydrolysis with PiACP and AcP as donor was observed when lowering the amount of the phosphatase from 4 U to 1 U. Consequently, 0.5–4 U of enzyme were assayed to further optimize the system and suppress product hydrolysis (Figure 83). Table 27 shows that already 1 U PiACP gave the most desirable results. Nonetheless, these data demonstrate that deliberate choice of the enzyme concentration represents an important parameter in the optimization of phosphatase catalyzed transphosphorylation reactions. This is most likely due to the differences in the kinetics of hydrolysis and transphosphorylation.
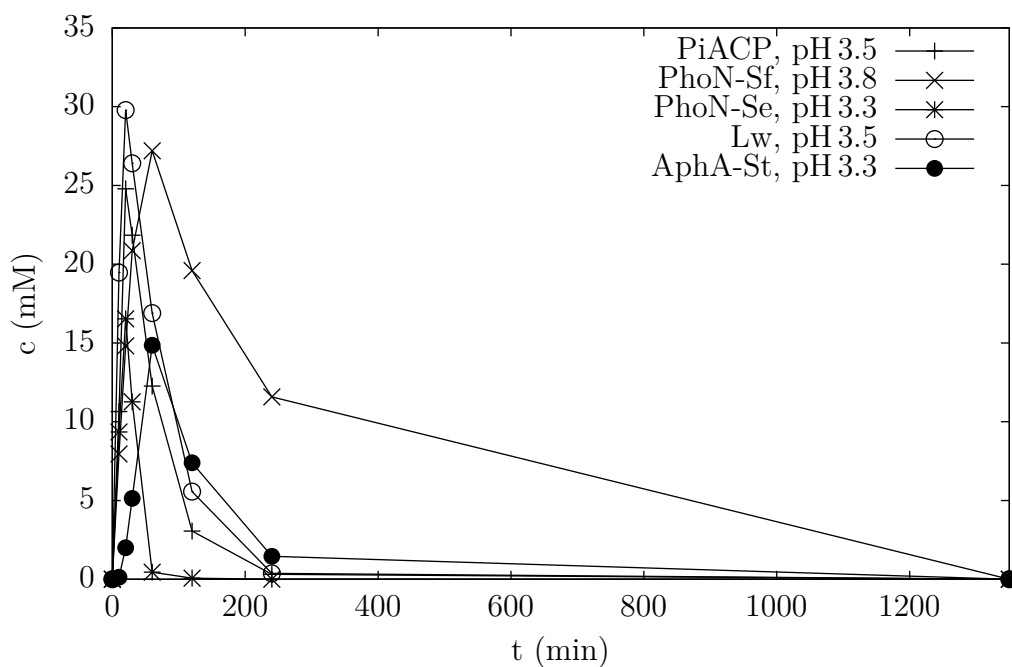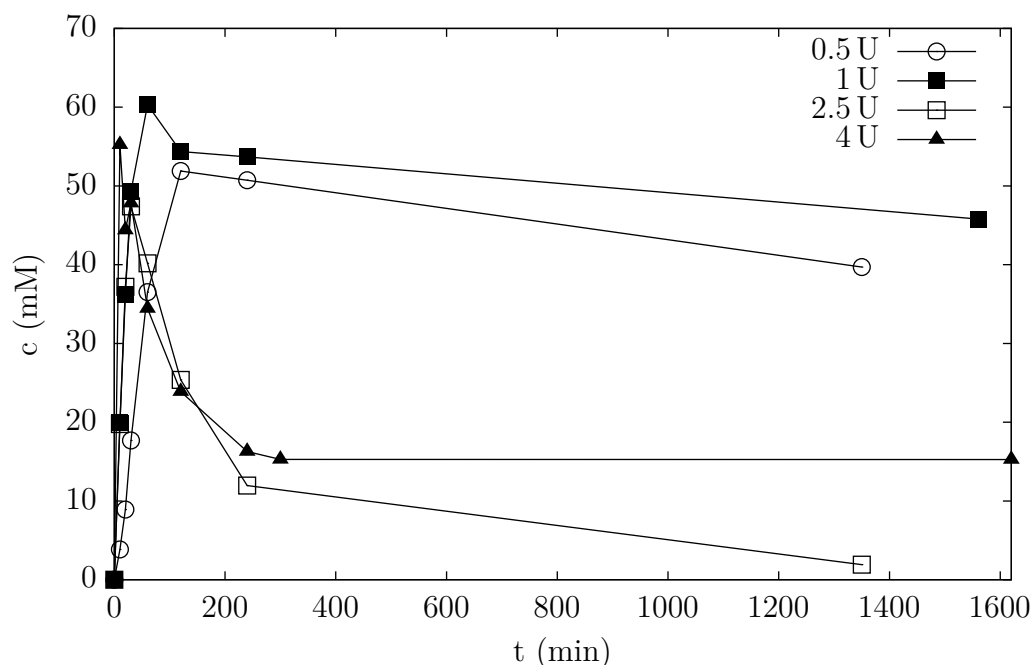

Figure 83: Product formation in phosphorylation of 500 mM 14OH with 100 mM AcP at pH 4.2, 30 °C, 600 rpm shaking, 1 % DMSO as IS, 1 mL reaction volume, 0.5–1 U PiACP

Table 27: Maximum product levels from Figure 83

	AcP, PiACP			
	t [min]	prod. [mM]	P_i [mM]	prod./P_i
0.5 U	120	52	43	1.2
1 U	60	60	42	1.4
2.5 U	30	47	48	0.98
4 U	10	55	47	1.2

2.11 Probing further Substrates with PEP

In the preliminary reactions with PEP at pH 4.2 (Section 2.5.3), an "automatic shutoff", reversible deactivation of the enzymes by the concomitant drop in pH, was discovered with 14OH as the substrate. This section will dwell on experiments with other acceptors, namely 2-hydroxyethyl acrylate (HEA) and methyl α-D-glucopyranoside (MADG), to demonstrate the generality of this phenomenon. For reasons of comparison, these screenings were performed with 500 mM substrate, 100 mM donor and 4 U enzyme, as with 14OH.

2.11.1 2-Hydroxyethyl acrylate (HEA)
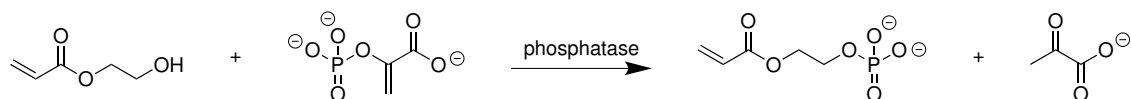
Figure 84: Phosphorylation of HEA with PEP as donor

All tested phosphatases were able to phosphorylate HEA with PEP as donor in moderate yields (Figure 85 and Table 28). Similar to the observations with 14OH as substrate, only PhoN-Se could consume the full amount of donor, before deactivation by a decrease in pH of more than 1 unit (data not shown) occurred. Likewise, AphA-St was almost not active.

Figure 85: Product formation in phosphorylation of 500 mM HEA with 100 mM PEP at pH 4.2, 30 °C, 600 rpm shaking, 1 % DMSO as IS, 1 mL reaction volume, 10 mM $MgCl_2$ for AphA-St and 4 U enzyme

Table 28: Maximum product levels from Figure 85 in comparison with the maximum product levels in the phosphorylation of 14OH from Table 10 (4 U enzyme)

| | HEA | | | | 14OH | | |
	t [min]	prod. [mM]	P_i [mM]	prod./ P_i	t [min]	prod. [mM]	prod./ P_i
PiACP	1380	17	63	0.27	1500	40	1.7
PhoN-Sf	1380	32	26	1.2	1500	41	2.7
PhoN-Se	1380	33	78	0.42	240	58	1.5
Lw	1380	20	56	0.35	1500	50	2.1
AphA-St	30	11	35	0.31	60	11	0.26

2.11.2 Methyl α-D-glucopyranoside
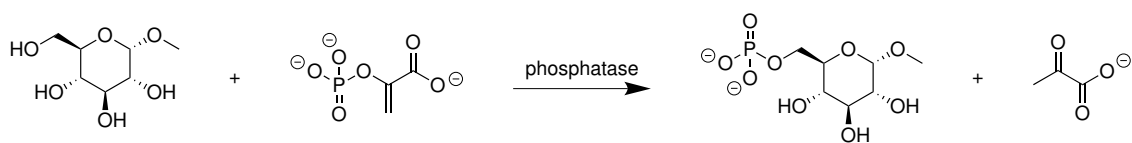
Figure 86: Phosphorylation of MADG with PEP as donor

Methyl α-D-glucopyranoside (MADG) was tested at pH 4.2. PiACP, PhoN-Sf, Lw and AphA-St were not capable of transferring a phosphate group onto the alcohol moiety at position 6 of the hexose, only PhoN-Se displayed some activity (data not shown). The reactions were repeated at a higher pH (pH 4.8), at which all enzymes showed various levels of activity.
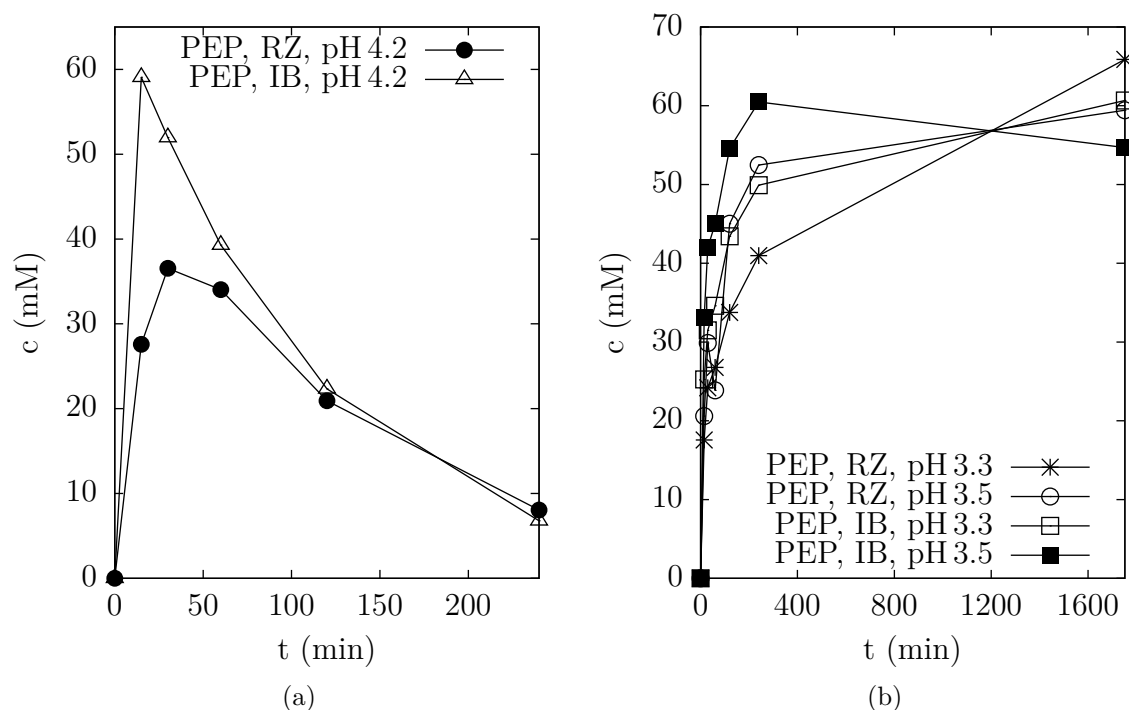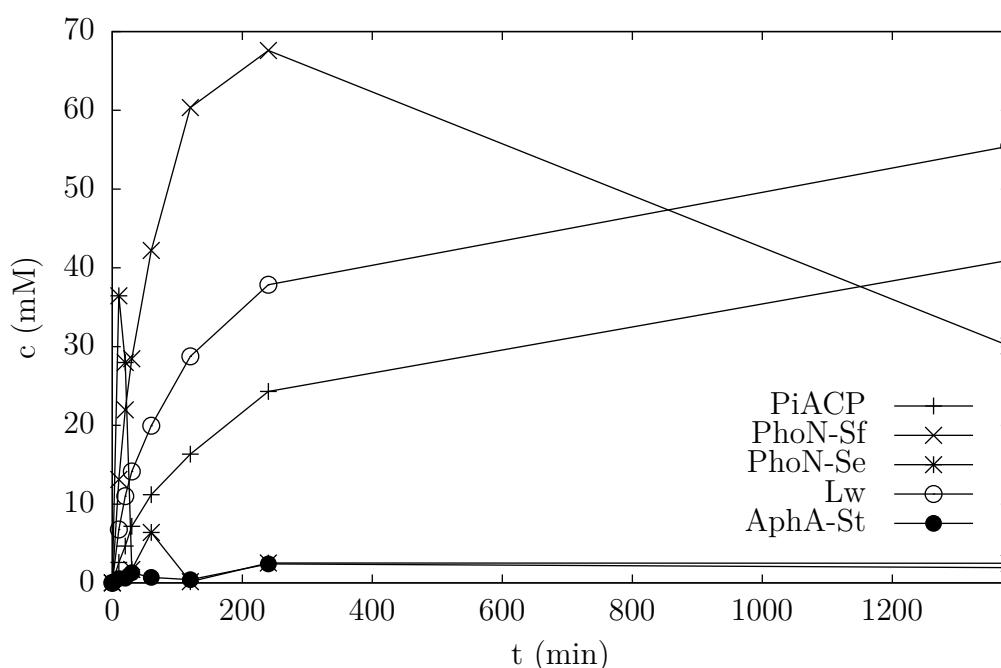

Figure 87: Product formation in phosphorylation of 500 mM MADG with 100 mM PEP at pH 4.8, 30 °C, 600 rpm shaking, 1 % DMSO as IS, 1 mL reaction volume, 10 mM MgCl$_2$ for AphA-St and 4 U enzyme

The product levels in Table 29 are in the same range as with 14OH as the acceptor. Reactions with PhoN-Se most likely were too fast, since already after 10 min the highest product concentration was detected. The observed rapid hydrolysis with PhoN-Se could be attributed to the higher initial pH: More time passed until the system fell below the critical pH threshold. Again, AphA-St performed not very well in terms of transphosphorylation, but notably, the enzyme did hydrolyze the donor to a large extent.

Table 29: Maximum product levels from Figure 87 in comparison with the maximum product levels in the phosphorylation of 14OH from Table 10 (4 U enzyme)

	MADG				14OH		
	t [min]	prod. [mM]	P_i [mM]	prod./ P_i	t [min]	prod. [mM]	prod./ P_i
PiACP	1380	41	22	1.9	1500	40	1.7
PhoN-Sf	240	68	17	4.0	1500	41	2.7
PhoN-Se	10	36	40	0.90	240	58	1.5
Lw	1380	55	34	1.6	1500	50	2.1
AphA-St	240	2.4	78	3.5×10^{-2}	60	11	0.26

2.12 YniC-Ec

The haloacid dehalogenase-like phosphatase YniC-Ec from *E. coli* turned out to be an active enzyme using PP_i, PEP, AcP and CP as donors (Section 2.5). However, the reactions proceeded slowly, which is in good accordance with the low A_{spec} ($2\,\mu mol\,min^{-1}\,mg^{-1}$). Despite several efforts have been made to express YniC-Ec again in various vectors, the activity of the purified protein always remained even lower, around $0.2\,\mu mol\,min^{-1}\,mg^{-1}$. In the following sections, the results of protein expression and further screenings with YniC-Ec are discussed.

2.12.1 Expression

The YniC-Ec gene had been cloned in several vectors in work predating the project [169]. Initially, expression was attempted in pASK-IBA4 as described in Section 3.1.6.a, which adds an N-terminal Strep-tag to the target protein and transcription is controlled by the tetracycline operator/promoter (*tet*). *E. coli* BL21(DE3) cells were selected for expression. Although a good amount of protein was obtained after the Strep-tag purification, the enzyme showed very low A_{spec} (Figure 88).

Therefore expression was attempted with the YniC-Ec gene cloned into the pET28a vector (Section 3.1.6.b) while leaving the type of expression strain unchanged. Transcription now was under control of the T7 promoter, and a N-terminal His-Tag was added to the target protein. Unfortunately, expression in TB medium (Section 3.1.6.b) again yielded almost inactive enzyme ($A_{spec} = 0.2\,\mu mol\,min^{-1}\,mg^{-1}$, Figure 89).

The batch of YniC-Ec expressed in pET28a in TB medium was subjected to a transphosphorylation assay with $500\,mM$ 14OH, $100\,mM$ PEP and $10\,mM$ $MgCl_2$ at pH 4.2 following the general procedure mentioned in Section 3.3.2. Also here the performance of the new batch was less than $25\,\%$ of the original one ($< 10\,mM$ versus $39\,mM$, Figure 90).
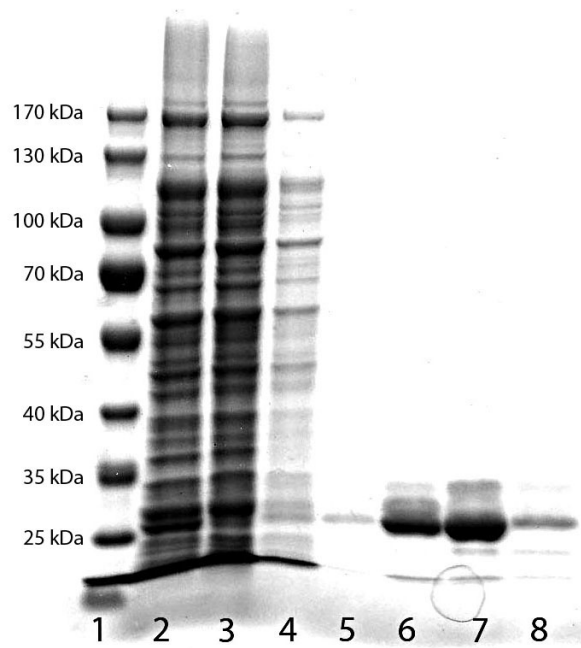
Figure 88: SDS-PAGE: Expression of YniC-Ec in pASK-IBA4. 1: standard, 2: lysate, 3: loading eluate, 4: wash eluate, 5–8: fractions 1–4 from purification via gravity flow column
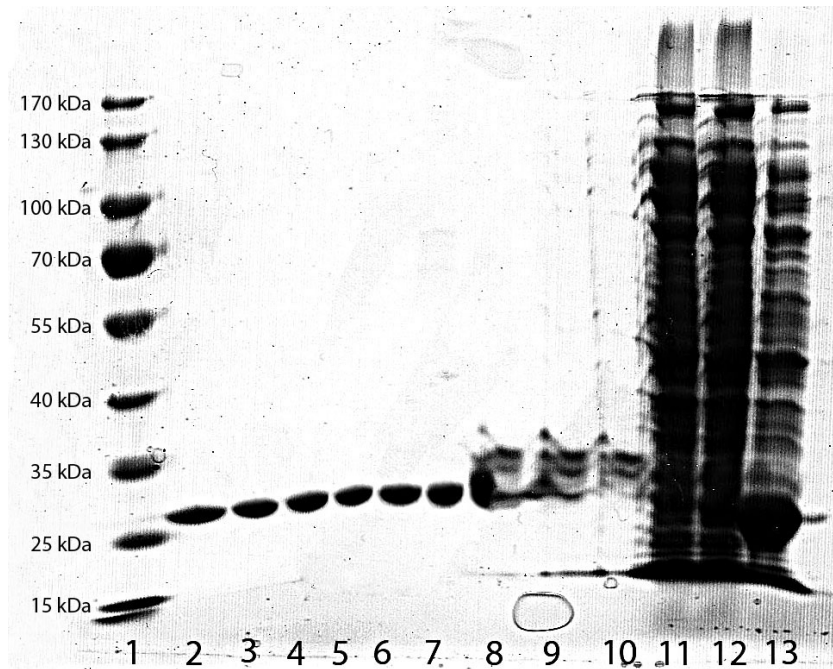
Figure 89: SDS-PAGE: Expression of YniC-Ec in pET28a in TB culture medium. 1: standard, 2–7: fractions 3–8 from purification via FPLC, 8–10: fractions 23–25, 11–12: loading eluate 1+2, 13: wash eluate
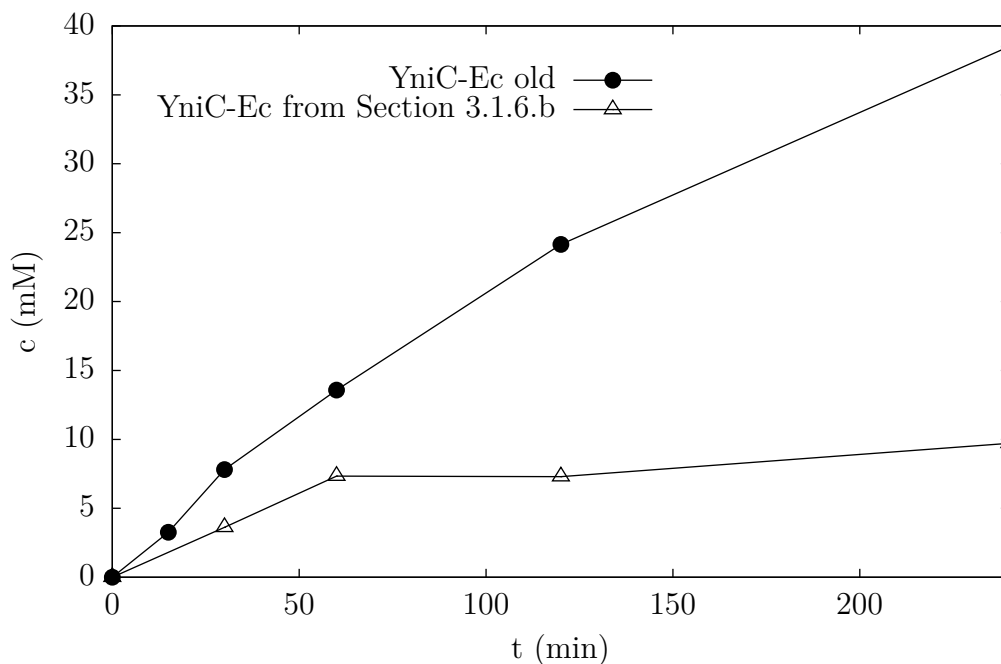
Figure 90: Comparison of the original batch "YniC-Ec old" with the batch expressed in pET28a/*E. coli* BL21(DE3) in TB m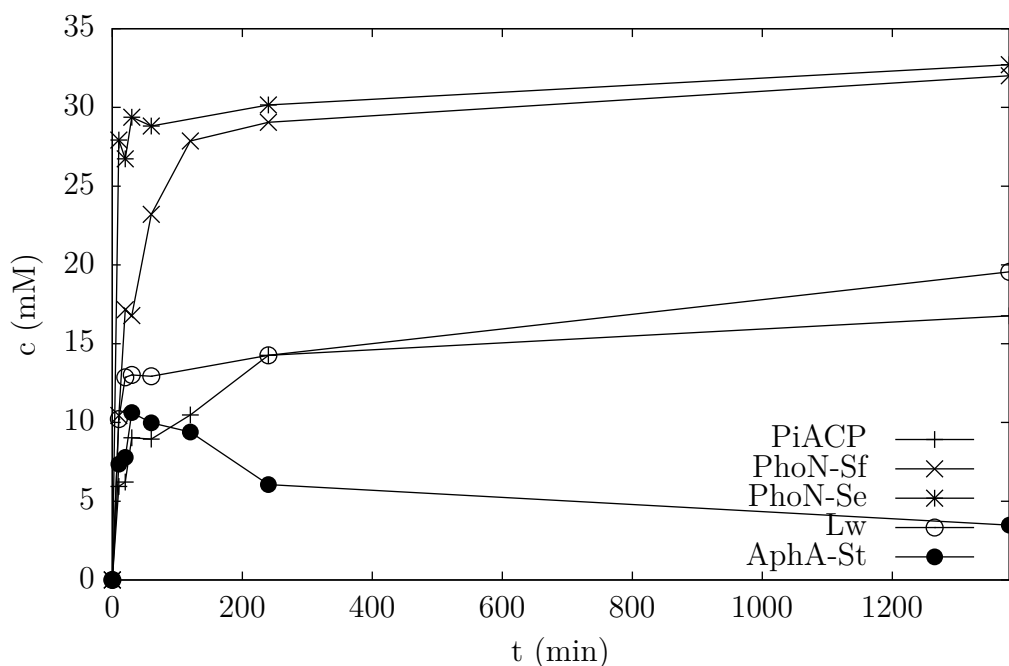edium in the phosphorylation of 500 mM 14OH with 100 mM PEP at pH 4.2, 30 °C, 600 rpm shaking, 1 % DMSO as IS, 1 mL reaction volume, 10 mM $MgCl_2$ and 200 µg mL^{-1} enzyme

The expression was repeated in pET28a in LB medium to slow down expression (Figure 91). In addition, a more conventional method was chosen for dialysis (Section 3.1.6.b) as it was assumed that employing a protein concentrator under the pressure of 4 bar damaged the enzyme. However the activity of the target protein was unchanged ($A_{spec} = 0.13$ µmol min^{-1} mg^{-1}).

Finally expression in pET28a in *E. coli* BL21(DE3) was attempted via autoinduction (Section 3.1.6.c). This technique was first described by Studier et al. [170] and has several advantages over IPTG induction: There is no need to monitor cell density, the final OD_{600} usually is much higher and protein yields are increased [171]. Expression of the target protein is triggered automatically upon depletion of glucose in the culture medium, which is concomitant with a switch to lactose as the energy source and expression of the T7 polymerase, required for transcription.

Still, the activity of YniC-Ec was only 0.17 µmol min^{-1} mg^{-1}. An SDS-PAGE was set up in order to compare the mass of all enzyme batches expressed in pET28a with the original preparation of YniC-Ec produced in work predating the project. Figure 92 shows that regardless of the expression strategy used, protein of identical mass of ~ 25 kDa and very likely the same identity was obtained. Therefore, in order to yield a protein solution with reasonable activity per volume, the enzyme batch from the expression in pET28a
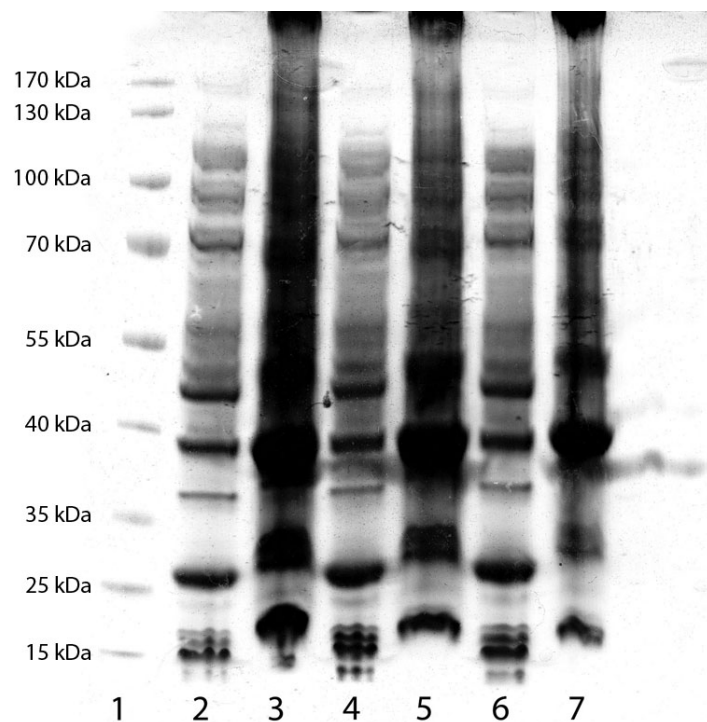
Figure 91: SDS-PAGE: Expression of YniC-Ec in pET28a in LB culture medium. 1: standard, 2/4/6: lysate, 3/5/7: pellet
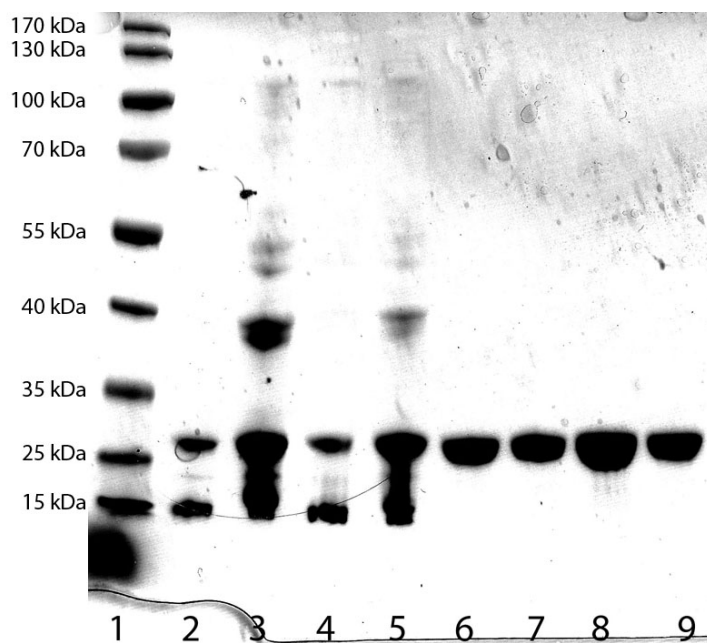
Figure 92: SDS-PAGE: Comparison of the different expression strategies of YniC-Ec in pET28a. 1: standard, 2/4: lysate [autoinduction], 3/5: pellet [autoinduction], 6: pure enzyme via autoinduction, 7: pure enzyme in TB medium, 8: pure enzyme in LB medium, 9: pure original batch "YniC-Ec old"

and TB medium was further concentrated to $53.4\,\mathrm{mg\,mL^{-1}}$ while retaining its activity. This preparation is also listed in Table 34 and was used in 10-fold amount compared to "YniC-Ec old" in further screenings.

2.12.2 Transphosphorylation

The new batch of YniC-Ec (pET28a/TB medium) was also tested in transphosphorylation with $100\,\mathrm{mM}$ AcP, PEP, CP and PP_i with $500\,\mathrm{mM}$ 14OH as acceptor and $1000\,\mathrm{\mu g\,mL^{-1}}$ enzyme at pH 4.2 (Figure 93 and Table 30).
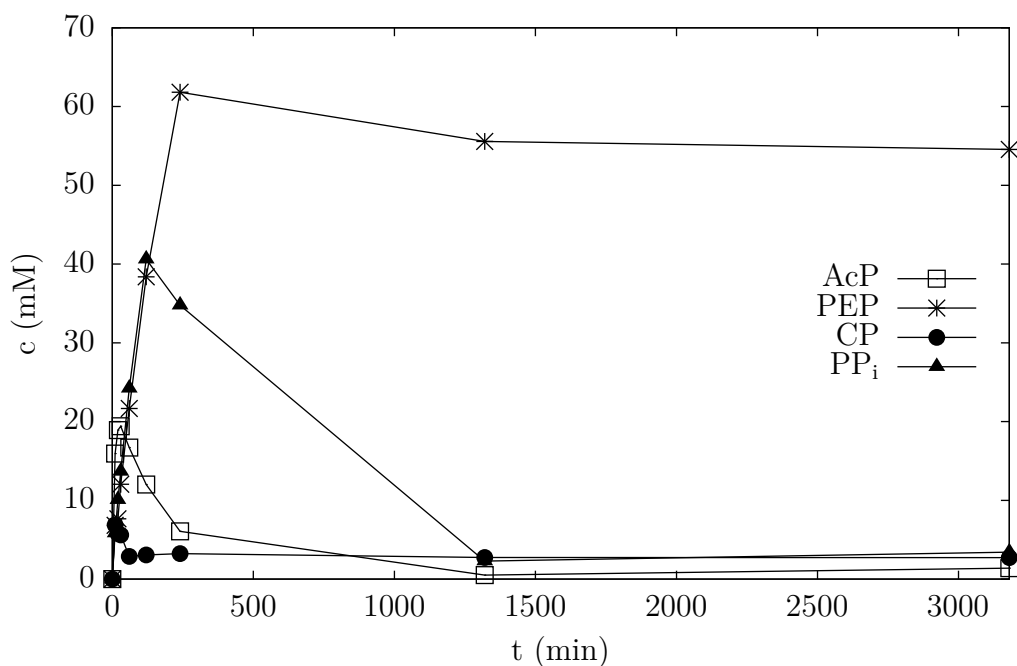
Figure 93: Phosphorylation of $500\,\mathrm{mM}$ 14OH with $100\,\mathrm{mM}$ donor at pH 4.2, $30\,\mathrm{°C}$, $600\,\mathrm{rpm}$ shaking, $1\,\%$ DMSO as IS, $1\,\mathrm{mL}$ reaction volume, $10\,\mathrm{mM}$ $MgCl_2$ and $1000\,\mathrm{\mu g\,mL^{-1}}$ enzyme

Table 30: Maximum product levels from Figure 93

	t [min]	prod. [mM]	P_i [mM]	prod./P_i
AcP	30	19	75	0.25
PEP	240	62	38	1.6
CP	10	6.9	76	9.1×10^{-2}
PP_i	120	41	88	0.47

Similar to earlier results, inhibition of the enzyme could be observed with PEP due to a significant drop in pH to about 3.5. With PP_i as donor the results matched the findings in Section 2.5.1 in spite of the different enzyme amount ($0.2\,\mathrm{U}$ versus $0.1\,\mathrm{U}$). With CP,

the reaction was very fast, as the highest product concentration already was observed after the first time point.

Due to challenges in the expression of YniC-Ec, no further screenings were performed with this enzyme. Nonetheless, YniC-Ec possesses interesting properties for its application in phosphate transfer reactions: Inhibition by chelating agents does not appear to be as drastic as with AphA-St also being Mg^{2+} dependent (Section 2.5.1) and taking into consideration that only 0.1 U of enzyme were employed in the preliminary studies, very satisfying amounts of product were obtained with every donor.

2.13 Conclusion and Outlook

During the course of practical work, eight organic phosphate donors have been characterized in transphosphorylation reactions employing ten different phosphatases and three acceptors of diverse nature (highest product levels with 14OH as acceptor summarized in Table 31). All of them were proven to be not only suitable for the phosphorylation of primary alcohol moieties, but also significantly less P_i by-product was generated compared to inorganic donors like PP_i or polyphosphate, which potentially can simplify product isolation. Moreover, product concentrations in the phosphorylation of 1,4-butanediol were very similar to reactions with pyrophosphate. In this regard 2,2,2-trifluoroethyl phosphate and AcP in particular were shown to be a very promising donor and further investigations may be worth to tackle.

Experiments with PiACP revealed that proper choice of enzyme concentration was a useful tool for suppression of product depletion over time. Thorough investigation of reduced product hydrolysis in reactions with PEP ultimately led to the discovery of another tool for maintaining constant product levels: pH control. For that, AcP was proven to be the most suitable donor, since acetate as the by-product hardly changes the pH in the reaction mixture. Tight pH control, for instance via a pH-stat, might be an option to circumvent the drop in pH brought about by the leaving groups of other donors, such as PEP, rendering their utilization even more feasible.

Insights obtained from the results of this work may support further studies, which might include protein engineering for obtaining a broader range of phosphatases that display reduced product hydrolysis by default like PhoC-Mm-2 and NSAP-Eb-11 to design a capable system for the phosphorylation of a broad range of substrates.

Table 31: Highest product levels in phosphorylation of 500 mM 14OH with various donors (100 mM except for DFPVP/IPP 50 mM) and phosphatases. First row: maximum concentration of 4-hydroxybutyl phosphate [mM]/enzyme-concentration [U mL^{-1} or for YniC-Ec µg mL^{-1}]/pH, second row: product/P_i ratio. AphA-St/PP$_i$: 100 mM MgCl$_2$ or 10 mM with other donors, YniC-Ec: 10 mM MgCl$_2$, SPHSX: 10 mM ZnCl$_2$ and 10 mM CaCl$_2$, underlined: best result per donor

donor	PiACP	PhoN-Sf	PhoN-Se	PhoC-Mm-2	NSAP-Eb-11	AphA-St	SPHSX	phytase	YniC-Ec	Lw
AcP	60/1/4.2 1.4	60/4/4.2 1.5	58/1/4.2 1.3	40/4/4.2 0.80	25/4/4.2 0.36	48/1/4.2 1.1	2.3/4/9.0 <0.1	2.6/4/2.5 <0.1	46/200/4.2 0.92	67/4/4.2 _1.8_
PEP	40/4/4.2 1.7	41/4/4.2 2.7	58/4/4.2 1.5	56/4/4.2 1.3	24/4/4.2 1.1	11/4/4.2 0.26	4.1/4/9.0 <0.1	2.7/6/4.2 <0.1	60/200/4.2 _2.0_	50/4/4.2 2.1
CP	38/1/3.5 0.93	59/1/3.8 _1.7_	35/1/3.3 0.70	56/4/4.2 1.6	54/4/4.2 1.4	26/1/3.3 0.44	n.c.	6.1/4/2.5 <0.1	19/4/4.2 0.28	52/1/3.5 1.7
PC	3.6/4/4.2 <0.1	4.0/4/4.2 <0.1	4.1/4/4.2 <0.1	5.7/4/4.2 _<0.1_	5.6/4/4.2 <0.1					
PP$_i$	70/1/3.5 0.55	76/1/3.8 0.61	65/1/4.2 0.46	63/4/4.2 0.42	56/4/4.2 0.36	4.9/4/4.2 0.18			39/50/4.2 0.54	80/1/3.5 _0.66_
IPP			1.7/1/3.8 _ _			1.2/1/3.8				
DFPVP	25/1/3.5	27/1/3.8	17/1/3.3			15/1/3.3				30/1/3.5
TFEP	54/1/3.5 1.9	68/1/3.8 2.8	74/1/3.3 _1.9_			61/1/3.3 1.4				68/1/3.5 1.9

3 Experimental

All chemicals were from commercial suppliers and used without further purification. Immobead 150, disodium pyrophosphate (PP$_i$), lithium potassium acetyl phosphate (AcP), lithium carbamoylphosphate dibasic hydrate (CP), phosphocreatine disodium salt hydrate (PC) and 4-nitrophenyl phosphate disodium salt hexahydrate (pNPP) were purchased from Sigma, phosphoenolpyruvate monopotassium salt (PEP) was from Alfa Aesar, Relizyme™ EP403 beads were from Resindion. The protein assay dye and the Laemmli sample buffer were from BioRad. Isopropenyl phosphate (di)cyclohexylammonium salt (IPP) and 1-(2,4-difluorophenyl)vinyl phosphate (di)cyclohexylammonium salt (DFPVP) were synthesized in Section 3.2. 4-Hydroxybutyl phosphate disodium salt was prepared in-house in work predating the project. Phytase from *A. niger* and 2,2,2-trifluoroethyl phosphate monocyclohexylammonium salt (TFEP) were kind gifts from BASF (synthesis: Section 3.2.3). PiACP, AphA-St, PhoN-Sf, PhoN-Se, PhoK, PhoC-Mm-2 and NSAP-Eb-11 were expressed in *E. coli* in earlier work on the project and carried either His- or Strep-Tags for purification by means of affinity chromatography [169]. The expression of Lw and YniC-Ec is described in Sections 3.1.6 and 3.1.5. The Ni-NTA column for His-tag purification and the IBA gravity flow column (*Strep*-Tactin® Superflow®) were from GE Healthcare Life Sciences. PAGE gels (Express-Plus, 10 % Bis-tris) were from GenScript, the prestained protein ladder (PageRuler™) was from Fermentas. NMR spectra were recorded on a Bruker Avance III 300 MHz NMR spectrometer. Chemical shifts (δ) are given in parts per million (ppm) relative to tetramethylsilane (TMS, ^{1}H and ^{13}C) or H$_3$PO$_4$ (^{31}P) as a reference. HPLC analysis was performed on a Dionex Ultimate 3000 system equipped with a Shodex RI-101 refractory index detector (HPLC-RI) and on an Agilent 1260 Infinity system equipped with an Agilent Q6120 quadrupole mass spectrometer using electrospray ionization (HPLC-MS).

3.1 Protein Expression and Characterization

3.1.1 Transformation of In-house Competent Cells

After fully thawing the in-house *E. coli* BL21(DE3) cells on ice, 100 µL were transferred into an Eppendorf tube and plasmid (Lw: pASK-IBA4, YniC-Ec: pASK-IBA4 or pET28a) was added. Next, the cells were incubated for 30 minutes on ice, before a 30 second heat shock at 42 °C was applied in an Eppendorf shaker. 900 µL LB medium (10 g L^{-1} tryptone, 5 g L^{-1} yeast extract, 10 g L^{-1} NaCl) were added and the cells were allowed to grow for 1 h at 37 °C. 200 µL were plated on LB plates containing suitable antibiotics and incubated at 37 °C overnight.

3.1.2 Determination of Protein Concentration

The protein content was specified in triplicates using the Bradford assay: The BioRad assay dye was diluted 1+4 with DI H_2O. The protein solution needed to be within a concentration range of 0.1 and $0.5\,mg\,mL^{-1}$ to match the calibration range of the photometer and was diluted if necessary. For the sample, $20\,\mu L$ of diluted protein solution and $980\,\mu L$ diluted Bradford dye were combined. For the control sample, $20\,\mu L$ DI H_2O were used. Before measuring the samples against the control sample at $\lambda = 595\,nm$, they were incubated for 10 minutes at room temperature.

3.1.3 Hydrolytic Activity of Phosphatases

Determination of specific hydrolytic activity (A_{spec}), expressed in $\mu mol\,min^{-1}\,mg^{-1}$ ($\equiv$ $U\,mg^{-1}$), of both lysates and purified enzymes was conducted by spectrophotometrically measuring the dephosphorylation of p-nitrophenyl phosphate (pNPP) via the release of p-nitrophenol (Figure 61).

$50\,\mu g\,mL^{-1}$ enzyme or $100\,\mu g\,mL^{-1}$ lysate were added to maleate buffer (pH 6.0, final concentration: $100\,mM$) to a final volume of $480\,\mu L$, followed by incubation at $30\,°C$ for five minutes at $450\,rpm$ and addition of $20\,\mu L$ $250\,mM$ pNPP (final concentration: $10\,mM$ in H_2O). After 60 seconds of mixing at $30\,°C$ and $450\,rpm$, the reaction was quenched with $500\,\mu L$ 1 M NaOH and the absorbance of p-nitrophenol at $\lambda = 405\,nm$ was measured. Each reaction was done in triplicates. The concentration of p-nitrophenol was calculated by considering the molar attenuation coefficient of $\epsilon = 18\,500\,L\,mol^{-1}\,cm^{-1}$ [172] and the absorption E:

$$c\,[\mu mol\,L^{-1}] = \frac{E}{\epsilon\,[L\,\mu mol^{-1}\,cm^{-1}] * d\,[cm]} \tag{1}$$

E absorption
ϵ molar attenuation coefficient of p-nitrophenol
d length of cuvette ($1\,cm$)
c concentration of p-nitrophenol

The specific hydrolytic activity, which represents the phosphatase activity (U) of $1\,mg$ protein, was calculated according to Equation 2. One unit (U) of phosphatase activity equates to the amount of p-nitrophenol (μmol) released within one minute under assay conditions.

$$A_{spec} \, [\mathrm{U\,mg^{-1}}] = \frac{pNP \, [\text{µmol}]}{t \, [\text{min}] * P_a \, [\text{mg}]} \tag{2}$$

pNP amount of p-nitrophenol released
t reaction time (1 min)
P_a amount of protein in assay
A_{spec} specific hydrolytic activity
        $(\mathrm{U\,mg^{-1}} \equiv \text{µmol}\,\mathrm{min^{-1}\,mg^{-1}})$

3.1.4 SDS-PAGE

PAGE gels were run in a BioRad MiniProtean system. 5 µL of prestained protein ladder, were used in all cases. Samples for each lane were prepared by adding 10 µL of 2x Laemmli sample buffer [125 mM Tris-HCl, 20 % glycerol, 4 % (w/v) SDS, 0.02 % (w/v) bromophenol blue, 10 % (v/v) β-mercaptoethanol, pH 6.8] to 10 µL of properly diluted protein sample, denaturing the protein for 5 minutes at 95 °C and loading 15 µL per slot. If not otherwise stated, a protein amount of 15 µg per well was intended. In case of cell debris, where an exact amount could not be loaded, a few milligrams were added to 10 µL of DI H_2O and 10 µL of 2x Laemmli sample buffer before denaturation.

Gels were run at 100 V in 1x MOPS running buffer (from 20x buffer: 50 mM MOPS, 50 mM Tris Base, 0.1 % SDS, 1 mM EDTA, pH 7.7) and stained and destained by standard Coomassie protocol.

3.1.5 Expression and Purification of *L. wadei* Phosphatase in pASK-IBA4

The expression of the phosphatase from *L. wadei* (Lw) was performed in *E. coli* BL21 (DE3), "BL21", strains.

In a 50 mL Sarstedt tube holding 10 mL LB medium (10 g L^{-1} tryptone, 5 g L^{-1} yeast extract, 10 g L^{-1} NaCl) an overnight culture (ONC) from an in-house glycerol stock was set up using 10 µL stock. 100 µg mL^{-1} ampicillin (AMP) were added. The ONC was allowed to grow at 37 °C and 130 rpm overnight.

Three cell cultures (BL21-1–3) were grown in 1 L baffled culture flasks in TB media (24 g L^{-1} yeast extract, 12 g L^{-1} tryptone, 4 mL L^{-1} glycerol, 2.3 g L^{-1} KH$_2$PO$_4$ and 12.5 g L^{-1} K$_2$HPO$_4$) in the presence of 100 µg mL^{-1} AMP. The potassium phosphate buffer required separate autoclaving.

For inoculation, 2 % (v/v) of ONC, which had an OD$_{600}$ of ~ 4, were added and the cultures were grown at 37 °C and 130 rpm. The development of the cell density was monitored by measuring the OD$_{600}$. After 105 min an OD$_{600}$ of ~ 0.9 was reached and

the culture flasks were shifted to the expression temperature of $20\,°C$. 30 minutes later, the cultures were induced by addition of $35\,µL$ of a $2\,g\,L^{-1}$ anhydrotetracycline (AHTC) stock in ethanol to obtain a concentration of $200\,µg\,L^{-1}$ AHTC in the cultures.

After $3\,h$ expression at $130\,rpm$ the cell cultures were pelleted at $4\,°C$ and $5000\,rpm$ for 20 minutes, the supernatants were discarded, the pellets were resuspended in $40\,mL$ $0.9\,\%$ NaCl solution, transferred into a $50\,mL$ Sarstedt tube and centrifuged again at $4\,°C$ and $4000\,rpm$ for 20 minutes. After removing the supernatant, the yield of wet cells was $1.84\,g$ for BL21-1, $1.27\,g$ for BL21-2 and $1.22\,g$ for BL21-3.

After shock freezing with liquid N_2, the cells were stored at $-20\,°C$ overnight. The cells were then fully thawn on ice and resuspended in $4\,mL$ per gram wet cells lysis buffer ($50\,mM$ Tris-HCl, $150\,mM$ NaCl, $0.1\,\%$ Triton X-100, $1\,mM$ EDTA, pH 8.0). The suspensions were subsequently sonicated for 25 minutes on ice using the settings depicted in Table 32.

Table 32: Settings for ultrasound disruption of cells

parameter	value
amplitude	$40\,\%$
pulse on	$1\,s$
pulse off	$4\,s$
run time	$5\,min$

The resulting solutions were pelleted at $4\,°C$ and $15\,000\,rpm$ for 20 minutes. After transferring the supernatant into $15\,mL$ Sarstedt tubes, the pellets were washed with $\sim 10\,mL$ $0.9\,\%$ NaCl solution and centrifuged at $4\,°C$ and $4000\,rpm$ for 20 minutes for reference. In Figure 94 an SDS-PAGE is given, on which lysates and pellets are compared. Soluble protein with a mass of about $25\,kDa$ was detected.

The activity and the concentration of the lysates was determined according to the standard protocol (Sections 3.1.3 and 3.1.2). $A_{spec} = 3.85\,µmol\,min^{-1}\,mg^{-1}$, $20.0\,mg\,mL^{-1}$ protein content for BL21-1, $A_{spec} = 3.85\,µmol\,min^{-1}\,mg^{-1}$, $17.9\,mg\,mL^{-1}$ protein content for BL21-2, $A_{spec} = 3.75\,µmol\,min^{-1}\,mg^{-1}$, $17.0\,mg\,mL^{-1}$ protein content for BL21-3.

The lysates were combined and purified after filtration through a $0.22\,µm$ syringe filter. Following conditioning of the IBA gravity flow column with lysis buffer (see above), the cell-free extracts were loaded at atmospheric pressure and room temperature and washed 2x with lysis buffer. Then, the protein was eluted with elution buffer ($150\,mM$ NaCl, $50\,mM$ Tris-HCl, $0.1\,\%$ Triton X-100, $2.5\,mM$ desthiobiotin, pH 8.0). Five fractions of $\sim 30\,mL$ in total were collected.
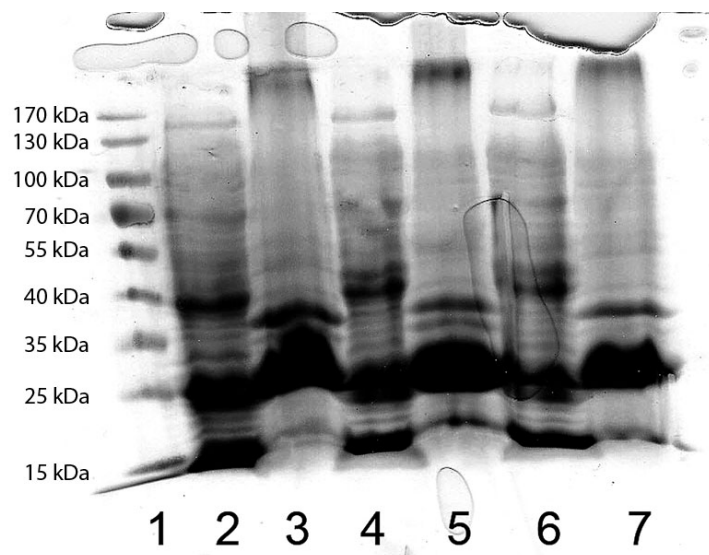
Figure 94: SDS-PAGE: Expression of Lw in pASK-IBA4. 1: standard, 2/4/6: lysate, 3,5,7: pellet

According to SDS-PAGE, fractions 1–4 contained the desired enzyme. The fractions were concentrated to a volume of $\sim 1\,\text{mL}$ in a $20\,\text{mL}$ Sartorius VivaSpin protein concentrator with a $10\,\text{kDa}$ cutoff and dialyzed against sodium acetate buffer ($20\,\text{mM}$, pH 5.0) yielding $750\,\mu\text{L}$ of target enzyme solution.

Activity and concentration of the pure enzyme was determined according to the standard protocol (Sections 3.1.3 and 3.1.2). $A_{spec} = 60.9\,\mu\text{mol}\,\text{min}^{-1}\,\text{mg}^{-1}$, $15.4\,\text{mg}\,\text{mL}^{-1}$ protein content, expressed protein: $11\,\text{mg}\,\text{L}^{-1}$ culture.

3.1.6 Expression and Purification of *E. Coli* Phosphatase YniC-Ec

3.1.6.a Expression in pASK-IBA4

E. coli BL21(DE3), "BL21", competent cells were transformed according to the standard protocol (Section 3.1.1) and plated on LB plates with $100\,\mu\text{g}\,\text{mL}^{-1}$ AMP. The plasmid DNA was prepared by work predating the project [169].

An ONC was prepared in a $50\,\text{mL}$ Sarstedt tube: $15\,\text{mL}$ LB medium ($10\,\text{g}\,\text{L}^{-1}$ tryptone, $5\,\text{g}\,\text{L}^{-1}$ yeast extract, $10\,\text{g}\,\text{L}^{-1}$ NaCl), $100\,\mu\text{g}\,\text{mL}^{-1}$ AMP, one colony from LB plate. The ONC was allowed to grow at $37\,°\text{C}$ and $130\,\text{rpm}$ overnight. OD_{600} on the following day was ~ 3.

Three main cultures (BL21-1–3) from the ONC, $1\,\%$ (v/v), were grown at $37\,°\text{C}$ and $130\,\text{rpm}$ in $1\,\text{L}$ baffled culture flasks in the presence of $100\,\mu\text{g}\,\text{mL}^{-1}$ AMP in TB media ($24\,\text{g}\,\text{L}^{-1}$ yeast extract, $12\,\text{g}\,\text{L}^{-1}$ tryptone, $4\,\text{mL}\,\text{L}^{-1}$ glycerol, $2.3\,\text{g}\,\text{L}^{-1}$ KH_2PO_4 and

$12.5\,\mathrm{g\,L^{-1}}$ K_2HPO_4). The potassium phosphate buffer required separate autoclaving. The development of cell density was monitored by measuring the OD_{600}.

After 2 h, 30 min before induction with $35\,\mu L$ of a $2\,\mathrm{g\,L^{-1}}$ AHTC stock in ethanol at an OD_{600} of ~ 1.0, the cultures were shifted to the expression temperature of $20\,°C$. Expression was done overnight at 140 rpm.

All three cell cultures were harvested via centrifugation according to the same protocol as in Section 3.1.5 yielding 3.28 g wet cells for BL21-1, 3.30 g for BL21-2 and 2.82 g for BL21-3. Upon resuspension of the pellets in 2 mL per gram wet cells lysis buffer (50 mM Tris-HCl, 150 mM NaCl, 0.1 % Triton X-100, pH 8.0), they were subjected to the same ultrasound treatment as depicted in Table 32. The cell debris was washed with 0.9 % NaCl and kept for later reference on a SDS-PAGE.

The protein content of the lysates was determined according to the standard protocol (Section 3.1.2) to be $3.23\,\mathrm{mg\,mL^{-1}}$ for BL21-1, $3.55\,\mathrm{mg\,mL^{-1}}$ for BL21-2 and $2.48\,\mathrm{mg\,mL^{-1}}$ for BL21-3.

The activity was measured according to the general procedure described in Section 3.1.3, however with $100\,\mu\mathrm{g\,mL^{-1}}$ protein in the assay A_{405} was below the detection limit in all cases. Further extraction of protein from the cell debris was attempted by addition of 2 mL per gram pellet lysis buffer (see above) as well as $1\,\mathrm{mg\,mL^{-1}}$ lysozyme and lysis for 60 min at room temperature before sonication (Table 32) and pelleting at $4\,°C$ and 15 000 rpm for 20 minutes. The supernatant was almost not active in the pNPP assay (data not shown).

Purification of the lysate obtained first was attempted in the same manner as in Section 3.1.5. The protein containing fractions, determined by SDS-PAGE, were concentrated to a volume of $\sim 2\,\mathrm{mL}$ in a 20 mL Satorius VivaSpin protein concentrator with a 10 kDa cutoff and dialysed against a sodium acetate buffer (20 mM, pH 5.0) yielding $\sim 1.8\,\mathrm{mL}$ of enzyme solution.

The target protein solution had a concentration of $0.98\,\mathrm{mg\,mL^{-1}}$ (expressed protein: $1.7\,\mathrm{mg\,L^{-1}}$ culture), but its activity was only $0.12\,\mu\mathrm{mol\,min^{-1}\,mg^{-1}}$. Therefore, the pNPP hydrolysis protocol was modified slightly by supplementation of the maleate stock with 1 mM $MgCl_2$ in the first attempt and 2 mM $MgCl_2$ in the second. Yet no increase in activity could be discovered. Also supplementation of the enzyme solution with 1 mM $MgCl_2$ directly and incubation for seven days had no influence on activity.

3.1.6.b Expression in pET28a

TB Medium

E. coli BL21(DE3), "BL21", competent cells were transformed according to the standard protocol (Section 3.1.1) and plated on petri plates with $30\,\mu g\,mL^{-1}$ kanamycin (KAN). The plasmid DNA was prepared by work predating the project [169].

An ONC was prepared in a $50\,mL$ Sarstedt tube: $15\,mL$ LB medium ($10\,g\,L^{-1}$ tryptone, $5\,g\,L^{-1}$ yeast extract, $10\,g\,L^{-1}$ NaCl), $30\,\mu g\,mL^{-1}$ KAN, one colony from LB plate. The ONCs were allowed to grow at $37\,°C$ and $130\,rpm$ overnight. OD_{600} on the following day was ~ 2.6.

Three main cultures (BL21-1–3) from the ONC, $1\,\%$ (v/v), were grown at $37\,°C$ and $130\,rpm$ in $1\,L$ baffled culture flasks in the presence of $30\,\mu g\,mL^{-1}$ KAN in TB media ($24\,g\,L^{-1}$ yeast extract, $12\,g\,L^{-1}$ tryptone, $4\,mL\,L^{-1}$ glycerol, $2.3\,g\,L^{-1}$ KH_2PO_4 and $12.5\,g\,L^{-1}$ K_2HPO_4). The potassium phosphate buffer required separate autoclaving. The development of cell density was monitored by measuring the OD_{600}.

After about $2.5\,h$, $20\,min$ before induction with $175\,\mu L$ of a $1\,M$ IPTG stock in water at an OD_{600} of ~ 0.9, the cultures were shifted to the expression temperature of $20\,°C$. Expression was done overnight at $140\,rpm$.

All three cell cultures were harvested via centrifugation according to the same protocol as in Section 3.1.5 yielding $3.53\,g$ wet cells for BL21-1, $5.07\,g$ for BL21-2 and $7.30\,g$ for BL21-3. Upon resuspension of the pellets in $2\,mL$ per gram wet cells lysis buffer ($50\,mM$ KH_2PO_4, $10\,mM$ imidazole, $300\,mM$ NaCl, pH 7.5), they were subjected to the same ultrasound treatment as depicted in Table 32. The cell debris was washed with $0.9\,\%$ NaCl and kept for later reference on a SDS-PAGE.

The protein content of the lysates was determined according to the standard protocol (Section 3.1.2) to be $16.4\,mg\,mL^{-1}$ for BL21-1, $23.5\,mg\,mL^{-1}$ for BL21-2 and $30.5\,mg\,mL^{-1}$ for BL21-3.

For purification, the combined lysates were loaded onto a FPLC system equipped with a $5\,mL$ Ni-NTA affinity column. The system was equilibrated with binding buffer ($50\,mM$ KH_2PO_4, $300\,mM$ NaCl, $10\,mM$ imidazole, pH 7.5 at $4\,°C$, degassed) for $10\,min$ at a flow of $2\,mL\,min^{-1}$, followed by loading of the lysate at $2\,mL\,min^{-1}$ and washing with $\sim 100\,mL$ wash buffer ($50\,mM$ KH_2PO_4, $300\,mM$ NaCl, $50\,mM$ imidazole, pH 7.5 at $4\,°C$, degassed) at $2\,mL\,min^{-1}$ until the UV detector indicated ceased protein elution off the column. For elution of the target protein, a gradient from $100\,\%$ wash buffer A to $100\,\%$ elution buffer B ($50\,mM$ KH_2PO_4, $300\,mM$ NaCl, $300\,mM$ imidazole, pH 7.5 at $4\,°C$,

degassed) was run at a constant flow of $2\,\mathrm{mL\,min^{-1}}$: Linear gradient elution from A, $0\,\mathrm{mL}$, to B, $44\,\mathrm{mL}$, then isocratic elution of B until the final volume of $134\,\mathrm{mL}$. Fractions with a volume of $2\,\mathrm{mL}$ were collected for the first $44\,\mathrm{mL}$, then their size was increased to $5\,\mathrm{mL}$.

The protein containing fractions, determined by UV signal, were concentrated to a volume of $\sim 30\,\mathrm{mL}$ in a $250\,\mathrm{mL}$ Satorius Vivacell 250 protein concentrator with a $10\,\mathrm{kDa}$ cutoff at a pressure of $4\,\mathrm{bar}$. Subsequently, $200\,\mathrm{mL}$ dialysis buffer ($50\,\mathrm{mM}$ Tris-HCl, $2\,\mathrm{mM}$ $MgCl_2$, pH 7.0 at $4\,^\circ\mathrm{C}$) were added and the solution was concentrated to a final volume of $15\,\mathrm{mL}$.

The target protein solution had a concentration of $9.09\,\mathrm{mg\,mL^{-1}}$ (expressed protein: $130\,\mathrm{mg\,L^{-1}}$ culture), but again A_{405} was below the detection limit when determining the activity following the protocol in Section 3.1.3 with $50\,\mathrm{\mu g\,mL^{-1}}$ protein in presence of additional $2\,\mathrm{mM}$ $MgCl_2$ in the maleate buffer. Hence, a protein concentration of $200\,\mathrm{\mu g\,mL^{-1}}$ was chosen, which translated into an A_{spec} as low as $0.2\,\mathrm{\mu mol\,min^{-1}\,mg^{-1}}$.

In order to obtain reasonable activity per volume, the enzyme solution was further concentrated in a $20\,\mathrm{mL}$ Sartorius VivaSpin protein concentrator with a $10\,\mathrm{kDa}$ cutoff to $53.4\,\mathrm{mg\,mL^{-1}}$. The activity remained unchanged.

LB Medium

The expression was repeated, following the same procedure as before, but in LB medium ($4.95\,\mathrm{g}$ yeast, $4.95\,\mathrm{g}$ NaCl and $9.9\,\mathrm{g}$ tryptone for 3x $330\,\mathrm{mL}$ main culture) utilizing $20\,\mathrm{\mu L}$ of the glycerol stock from BL21 for $15\,\mathrm{mL}$ of ONC.

The expression was done at $20\,^\circ\mathrm{C}$, $120\,\mathrm{rpm}$, yielding $1.99\,\mathrm{g}$ wet cells for BL21-1, $1.98\,\mathrm{g}$ for BL21-2 and $2.05\,\mathrm{g}$ for BL21-3. After shock freezing with liquid N_2, the cells were stored at $-20\,^\circ\mathrm{C}$ overnight. The cell disruption was performed according to the general protocol. The cell debris was washed with $0.9\,\%$ NaCl and kept for later reference on a SDS-PAGE.

The concentration (Section 3.1.2) of the three lysates was $25.8\,\mathrm{mg\,mL^{-1}}$ for BL21-1, $26.0\,\mathrm{mg\,mL^{-1}}$ for BL21-2 and $25.6\,\mathrm{mg\,mL^{-1}}$ for BL21-3. The pNPP hydrolysis activity test was conducted according to the procedure depicted in Section 3.1.3, albeit with an additional $2\,\mathrm{mM}$ $MgCl_2$ in the maleate stock and a protein concentration of $1\,\mathrm{mg\,mL^{-1}}$ to obtain a value above LOD for A_{405}: $A_{spec} = 0.014\,\mathrm{\mu mol\,min^{-1}\,mg^{-1}}$ for BL21-1, $0.017\,\mathrm{\mu mol\,min^{-1}\,mg^{-1}}$ for BL21-2 and $0.018\,\mathrm{\mu mol\,min^{-1}\,mg^{-1}}$ for BL21-3.

Purification of the combined lysates was done as before, except after the loading step for another $5\,\mathrm{min}$ binding buffer at a flow of $2\,\mathrm{mL\,min^{-1}}$ was run through the system. In

order to prevent damage to the enzyme, another method for dialysis and concentration was chosen: The fractions from the FPLC, which contained protein according to UV signal, were collected and put in a dialysis tube, which was immersed in 7 L of dialysis buffer (50 mM Tris-HCl, 2 mM $MgCl_2$, pH 7.0 at 4 °C). After dialysis overnight, the protein solution was concentrated to a final volume of ~2 mL in a 20 mL Sartorius VivaSpin protein concentrator with a 10 kDa cutoff.

The concentration of the target protein was 16.7 mg mL^{-1} (expressed protein: 32 mg L^{-1} culture), but the activity was minute: $A_{spec} = 0.13$ µmol min^{-1} mg^{-1}. For the pNPP hydrolysis test a protein concentration of 500 µg mL^{-1}, was chosen to stay within the linear range of the photometer.

3.1.6.c Expression in pET28a with Autoinduction

E. coli BL21(DE3), "BL21", competent cells were transformed according to the standard protocol (Section 3.1.1) and plated on a petri plate with 30 µg mL^{-1} KAN. The plasmid DNA was prepared by work predating the project [169].

In a 50 mL Sarstedt tube an ONC with one culture from LB plate and 30 µg mL^{-1} KAN in 20 mL LB medium (10 g L^{-1} tryptone, 5 g L^{-1} yeast extract, 10 g L^{-1} NaCl) was set up and allowed to grow at 37 °C and 130 rpm overnight. OD$_{600}$ was ~2.0.

For autoinduction, all solutions listed in Table 33 were prepared. For 670 mL main culture, 620 mL "Medium", 13.4 mL "50x LAC", 33.5 mL "20x NPSC", 2 mL "FeCl$_3$ · 6 H$_2$O", 2 mL "1000x Trace Elements", 1.34 mL "MgSO$_4$·7 H$_2$O", 20 mL ONC and 670 µL KAN stock with a concentration of 30 mg mL^{-1} were combined.

After three days at 20 °C and 120 rpm, the cells were harvested according to the same protocol as in Section 3.1.5 yielding 7.34 g wet cells, which were shock frozen with liquid N$_2$ and stored at −20 °C overnight.

Cell disruption was performed as in Section 3.1.6.b. The cell debris was washed with 0.9 % NaCl and kept for later reference on a SDS-PAGE.

The protein content of the lysate was determined according to the standard protocol (Section 3.1.2) to be 11.0 mg mL^{-1}, A_{spec} was 0.22 µmol min^{-1} mg^{-1} following the procedure in Section 3.1.3 with 2 mM MgCl$_2$ in the maleate stock.

Purification of the combined lysates was done on FPLC in the same manner as in Section 3.1.6.b, except after loading, for another 5 min binding buffer at a flow of 2 mL min^{-1} was run through the system. In order to prevent damage to the enzyme, the following method for dialysis and concentration was chosen: The fractions from the FPLC, which

Table 33: Solutions for autoinduction medium [173]

Medium	conc.	per 620 mL DI H_2O
yeast extract	$40\,g\,L^{-1}$	11.04 g
tryptone	$80\,g\,L^{-1}$	22.08 g
20x NPSC	conc.	per 200 mL DI H_2O
NH_4Cl	1 M	10.7 g
Na_2SO_4	0.1 M	2.84 g
KH_2PO_4	0.5 M	13.6 g
Na_2HPO_4	0.5 M	14.2 g
50x LAC	conc.	per 100 mL DI H_2O
glycerol	25 % (w/v)	25 g
glucose (add. after autoclaving)	2.5 % (w/v)	2.5 g
lactose (add. after autoclaving)	10 % (w/v)	10 g
$MgSO_4 \cdot 7\,H_2O$	conc.	per 10 mL DI H_2O
$MgSO_4 \cdot 7\,H_2O$	1 M	2.46 g
$FeCl_3 \cdot 6\,H_2O$	conc.	per 10 mL 60 mM HCl (filtered)
$FeCl_3 \cdot 6\,H_2O$	50 mM	0.135 g
1000x Trace Elements	conc.	per 20 mL 60 mM HCl (filtered)
$CaCl_2$	20 mM	44 mg
$MnCl_2 \cdot 4\,H_2O$	10 mM	39.6 mg
$ZnSO_4 \cdot 7\,H_2O$	10 mM	57.5 mg
$CoSO_4 \cdot 7\,H_2O$	2 mM	11.2 mg
$CuCl_2 \cdot H_2O$	2 mM	6.8 mg
$Na_2MoO_4 \cdot 2\,H_2O$	2 mM	9.7 mg
H_3BO_3	2 mM	2.5 mg
$Na_2SeO_3 \cdot 5\,H_2O$	2 mM	10.5 mg
$NiCl_2 \cdot 8\,H_2O$	2 mM	9.5 mg

contained protein according to UV signal, were collected and put in a dialysis tube, which was immersed in 7 L of dialysis buffer (50 mM Tris-HCl, 2 mM $MgCl_2$, pH 7.0 at 4 °C). After dialysis overnight, the protein solution was concentrated to a final volume of ∼ 2 mL in a 20 mL Sartorius VivaSpin protein concentrator with a 10 kDa cutoff.

The concentration of the target protein was determined to be 19.7 mg mL^{-1} (expressed protein: 38 mg L^{-1} culture), however the activity was still too low in spite of 1 mM $MgCl_2$ supplementation in in the reaction: $A_{spec} = 0.17$ µmol min^{-1} mg^{-1}. The protein concentration in the assay was 100 µg mL^{-1}.

3.2 Synthesis of Organic Donors

3.2.1 Isopropenyl phosphate

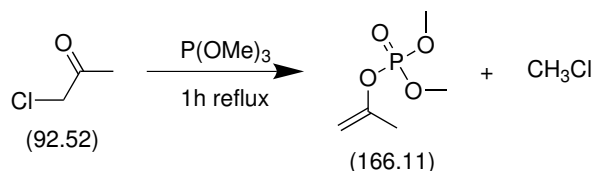*3.2.1.a Step 1: Dimethyl isopropenyl phosphate*

Figure 95: Synthesis of dimethyl isopropenyl phosphate: Perkow reaction

Literature: modified from Moriguchi et al. [167, p. 144]

1276 µL (1 eq.; 10.8 mmol) trimethyl phosphite were put in a 5 mL two-necked flask, immersed in an ice bath, and 870 µL (1 eq.; 10.8 mmol) chloroacetone were added dropwise. Upon completion, the ice bath was removed and the mixture was refluxed for one hour.[2] The residue was distilled under reduced pressure to obtain a brown liquid (1.73 g, 96 %).

Characterisation of the crude product via TLC (silica, petroleum ether/ethyl acetate 2:3; potassium permanganate solution): R_f [P(OMe)$_3$, faint]: 0.3; R_f [crude product]: 0.5 and R_f [chloroacetone, faint]: 0.95

The crude product was purified via flash chromatography (petroleum ether/ethyl acetate 2:3; potassium permanganate solution) to yield 1.46 g (81 %) of pure product (slightly yellow liquid).

^{1}H, ^{13}C and ^{31}P NMR spectra of the compound in CDCl$_3$ were recorded. (see A.2.1)

300 MHz ^{1}H-NMR: δ 1.96 (3H, s, Me), 3.82 (6H, d, J = 9.0 Hz, Me of ester), 4.49–4.56 (1H, m, C**H** of vinyl), 4.74–4.80 (1H, m, C**H** of vinyl)
121 MHz ^{31}P-NMR: δ -4.54, sept, J = 10.9 Hz
75 MHz ^{13}C-NMR: δ 20.59, 54.70, 98.27, 152.0

---

[2] Stirring at room temperature overnight instead produced a mixture between the desired product and its constitutional isomer, dimethyl 2-oxopropylphosphonate, obtained from a competing Michaelis-Arbuzov reaction. (confirmed by NMR, data not shown)

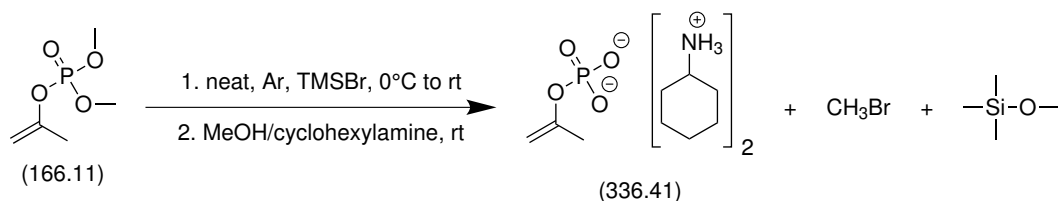### 3.2.1.b Step 2: Isopropenyl phosphate (di)cyclohexylammonium salt

Figure 96: Hydrolysis via bis(trimethylsilyl) ester and precipitation as (di)cyclohexyl-
ammonium salt

Literature: modified from García-Alles et al. [174, p. 3228]

In a microwave tube, kept under argon and immersed in an ice bath, 202 mg (1 eq.; 1.22 mmol) of dimethyl isopropenyl phosphate (synthesis: Section 3.2.1.a) were placed. Through a syringe 321 µL (2 eq.; 2.44 mmol) bromotrimethylsilane were slowly added. The reaction was stirred for 1 h at 0–4 °C and another hour at room temperature. Then, the excess of bromotrimethylsilane was removed at high vacuum (10^{-3} Torr).

The residue was added dropwise to 281 µL (2 eq.; 2.44 mmol) cyclohexylamine in 15 mL MeOH/ether 1:5 (v/v). The white precipitate was filtered, washed three times with 8 mL ether and stored under argon. Yield: 247 mg (60 %)

An ^{1}H NMR spectrum of the compound in D_2O containing 0.1 N NaOH was recorded. (see A.2.2)

300 MHz ^{1}H-NMR: δ 1.1–1.8 (20H, m, cyclohexylamine: aliphatic H), 2.07 (s, Me), 2.64–2.81 (2H, m, cyclohexylamine: **H**-C(-C)(-C)-NH$_2$), 4.09–4.15 (m, C**H** of vinyl), 4.33–4.40 (m, C**H** of vinyl)

Due to the very short half-life of the product even under basic conditions (30 minutes, according to Moriguchi et al. [167, p. 141]) the molar ratio of cyclohexylamine to the product could not be determined properly via NMR. The characteristic peaks of vinyl protons confirmed the presence of product (δ 4.1 and 4.4). For yield calculations and all enzymatic reactions a di(cyclohexylammonium) salt was assumed, which is in good accordance with the findings by García-Alles et al. [174].

3.2.2 1-(2,4-Difluorophenyl)vinyl phosphate

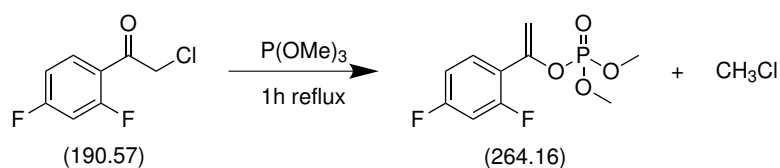*3.2.2.a Step 1: 1-(2,4-Difluorophenyl)vinyl dimethyl phosphate*

Figure 97: Synthesis of 1-(2,4-difluorophenyl)vinyl dimethyl phosphate: Perkow reaction

Literature: modified from Moriguchi et al. [167, p. 144]

2.00 g (1 eq.; 10.5 mmol) 2-chloro-2',4'-difluoroacetophenone were put in a 5 mL two-necked flask, immersed in an ice bath, and 1238 μL (1 eq.; 10.5 mmol) trimethyl phosphite were added slowly. Upon completion, the ice bath was removed, the mixture was refluxed for one hour and the residue was distilled under reduced pressure to obtain a yellow liquid (2.42 g, 87 %).

Characterisation of the crude product via TLC (silica, petroleum ether/ethyl acetate 2:3; potassium permanganate solution): R_f [P(OMe)$_3$, faint]: 0.3; R_f [crude product]: 0.5 and R_f [2-chloro-2',4'-difluoroacetophenone, faint]: 0.95

The crude product was purified via flash chromatography (petroleum ether/ethyl acetate 2:3; potassium permanganate solution) to yield 2.06 g (74 %) of pure product (slightly yellow liquid).

^{1}H, ^{13}C and ^{31}P NMR spectra of the compound in DMSO-d$_6$ were recorded. (see A.2.3)

300 MHz ^{1}H-NMR: δ 3.77 (6H, d, J = 9.0 Hz, Me), 5.30–5.39 (2H, m, C**H$_2$**), 7.14–7.23 (1H, m, Ar), 7.32–7.44 (1H, m, Ar), 7.56–7.68 (1H, m, Ar)
121 MHz ^{31}P-NMR: δ -4.29 – -4.41, m
75 MHz ^{13}C-NMR: δ 55.33, 103.8, 105.4, 112.4, 130.5, 146.3, 158.2, 161.6, 164.5

3.2.2.b Step 2: 1-(2,4-Difluorophenyl)vinyl phosphate (di)cyclohexylammonium salt

Figure 98: Hydrolysis via bis(trimethylsilyl) ester and precipitation as (di)cyclohexyl-
ammonium salt

Literature: modified from García-Alles et al. [174, p. 3228] and Moriguchi et al. [167, p. 144]

In a microwave tube, kept under argon and immersed in an ice bath, 265 mg (1 eq.; 1.00 mmol) of 1-(2,4-difluorophenyl)vinyl dimethyl phosphate (synthesis: Section 3.2.2.a) were placed. Through a syringe slowly 291 µL (2.2 eq.; 2.20 mmol) bromotrimethylsilane were added. The reaction was stirred for 1 h at 0–4 °C and another hour at room temperature. After, the excess of bromotrimethylsilane was removed at high vacuum (10^{-3} Torr).

The residue was added dropwise to 231 µL (2 eq.; 2.00 mmol) cyclohexylamine in 60 mL MeOH/ether 1:5 (v/v). The white precipitate was filtered under reduced pressure, washed three times with 8 mL ether and stored under argon. Yield: 305 mg (70 %)

^{1}H, ^{13}C and ^{31}P NMR spectra of the compound in D_2O were recorded (upon heating, see A.2.4).

300 MHz ^{1}H-NMR: δ 1.0–1.8 (20H, m, cyclohexylamine: aliphatic H), 2.09 (s, acetone [cont.]), 2.91–3.05 (2H, m, cyclohexylamine: **H**-C(-C)(-C)-NH$_3$$^+$), 5.02–5.08 (1H, m, C**H** of vinyl), 5.09–5.14 (1H, m, C**H** of vinyl), 6.80–6.93 (2H, m, Ar), 7.54–7.65 (1H, m, Ar)
121 MHz ^{31}P-NMR: δ 0 (s, inorganic phosphate), -1.77 – -1.97 (m, product P)
75 MHz ^{13}C-NMR: δ 23.73, 24.21, 30.26, 50.24, 103.7, 104.3, 111.0, 130.1, 148.0, 158.1, 161.6, 163.7

The ratio of phosphate to cyclohexylamine was determined to be ~ 1.8 by comparing the integral of the vinyl proton at 5.05 ppm to the area of the peak at 3.0 ppm (**H**-C(-C)(-C)-NH$_3$$^+$) of cyclohexylamine. Nonetheless, for yield calculations and all enzymatic reactions the molar mass of a (di)cyclohexylammonium salt was used.

3.2.3 2,2,2-Trifluoroethyl phosphate monocyclohexylammonium salt (Synthesis performed at BASF)
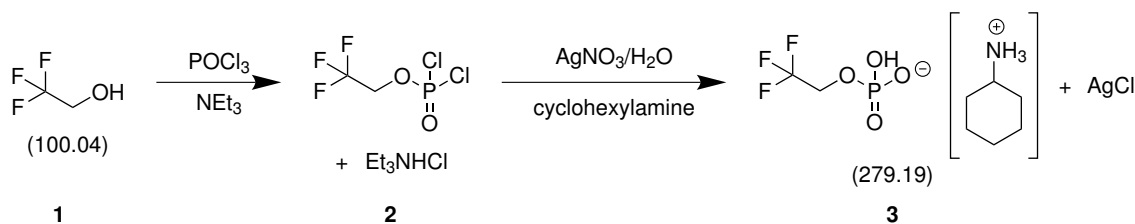

Figure 99: Synthesis of 2,2,2-trifluoroethyl phosphate monocyclohexylammonium salt

Literature: Modro et al. [175]

76.7 g (0.5 mol) of phosphoric acid trichloride in diethyl ether (500 mL) was cooled to 0 °C. With stirring a mixture of 100 g (0.5 mol) 2,2,2-trifluoroethanol (**1**) and 50.6 g (0.5 mol) triethylamine was added dropwise while keeping the temperature at 0 °C. Upon complete addition the mixture was allowed to warm up to room temperature and then it was heated to reflux for 3 h. Stirring was continued at room temperature overnight.

Precipitated salt was removed by filtration, the solids were washed with diethyl ether (2x 200 mL) and the combined filtrates were concentrated in vacuum (100 mbar, rt). The remainder was subjected to a distillation at 31 mbar. Pure ester **2** was collected at a boiling point of 64–66 °C/31 mbar. Yield: 71 g (72 %) phosphoric acid ester dichloride **2** as a colorless oil.

^{1}H-NMR (400 MHz, CDCl$_3$): δ 4.60 (2H, quint, J = 8.3 Hz)

Hydrolysis step:

67.45 g (0.4 mol) AgNO$_3$ were dissolved in a mixture of water (50.5 mL) and acetonitrile (50.5 mL). The solution was cooled to 0 °C and 39 g (0.18 mol) of the ester **2** was added dropwise with stirring while keeping the temperature at 0–5 °C. Upon complete addition, stirring was continued for another hour. The mixture was allowed to stand overnight at 5 °C, then precipitated AgCl was removed by filtration. As the filtrate was turbid, it was allowed to stand for another 24 h at 5 °C, followed by removal of precipitated salts. The filtrate was concentrated in vacuum and the remaining oil was dissolved in isopropanol (280 mL).

After cooling to 0 °C the solution was treated with 17 g (0.17 mol) cyclohexylamine. The resulting suspension was heated to reflux and water was added dropwise until the salts were dissolved. Upon standing and cooling to room temperature the cyclohexylammonium salt **3** precipitated. Filtration and drying in vacuum yielded 6.9 g (16 %) of a white powder, melting point: 180 °C (decomp.).

^{1}H, ^{13}C and ^{31}P NMR spectra of the compound in D_2O were recorded. (see A.2.5)

300 MHz ^{1}H-NMR: δ 0.9–2.0 (10H, m, cyclohexylamine: aliphatic H), 2.91–3.13 (1H, m, cyclohexylamine: **H**-C(-C)(-C)-NH_3^+), 4.16 (2H, quint, J = 6.0 Hz)
121 MHz ^{31}P-NMR: δ -0.43, t, J = 8.5 Hz
75 MHz ^{13}C-NMR: 23.74, 24.22, 30.26, 50.30, 61.86, 62.34, 121.5, 125.3

3.3 Enzymatic Reactions

3.3.1 Half-Life of Donors for Transphosphorylation

The half-life of AcP, CP and PC was determined under conditions typical for transphosphorylation, described more thoroughly in Section 3.3.2, via NMR as follows:

In a Sarstedt tube, 5 mL of a stock solution of 500 mM 14OH, 100 mM donor and 1 % (v/v) DMSO in DI H_2O were prepared, adjusted to a pH of 4.2 (± 0.05) with a pH meter with 1 M or 10 M NaOH or 2 M and 12 M HCl and kept on ice. In an NMR tube, 600 µL of the solution were then mixed with 100 µL 350 mM dimethyl methylphosphonate (internal standard) in D_2O.

Immediately after preparation of the sample, ^{31}P-NMR spectra were recorded employing inverse gated decoupling with 32 scans and 20 s relaxation time. Total run time was 8 h with four samples per hour for the first 2 h and two samples per hour for the last 6 h.

Spectra were integrated manually with MestReNova 6.0.2-5475. For quantification of P_i, a calibration curve, obtained from average values of two identical sets, was set up (Figure 100). All peaks were referenced to the internal standard. To ascertain the stability of the analyte, the time was plotted against the percent of donor as well as against the percent of P_i in the same graph. The x-value of the intercept of both curves gave the half-life.
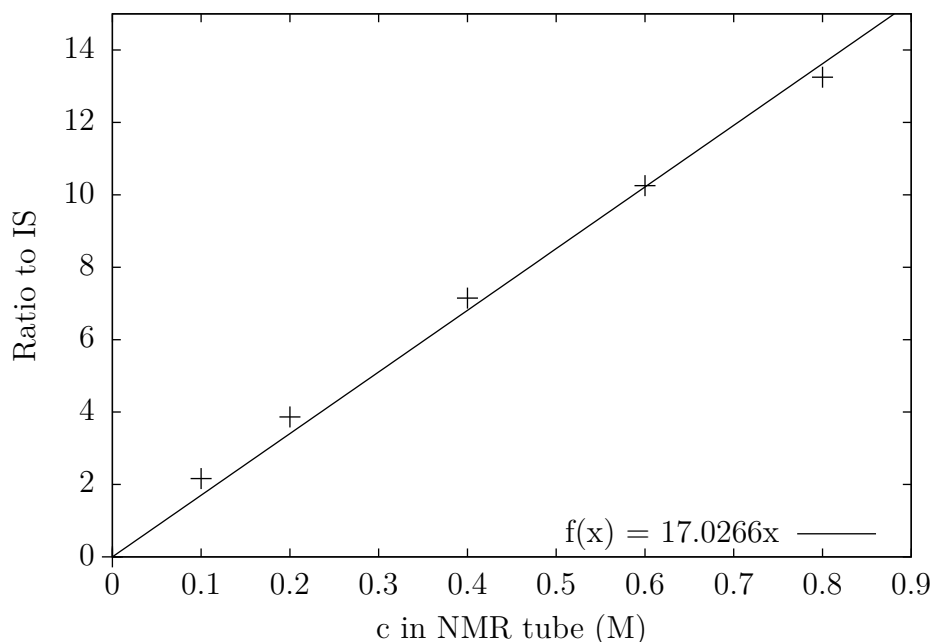

Figure 100: Calibration curve for P_i, $R^2 = 0.992$

3.3.2 Transphosphorylation

3.3.2.a Typical Setup

The reactions were performed in 1.5 mL glass screw-cap vials. Stock solutions were prepared in Sarstedt tubes in DI H_2O or 200 mM citrate buffer with IPP as donor, containing 500 mM substrate, 100 mM AcP, PEP, CP, PC, TFEP or PP_i or 50 mM IPP or DFPVP, 1 % (v/v) DMSO as internal standard and salt supplementation for the metal dependent enzymes AphA-St, YniC-Ec (10 mM $MgCl_2$) and SPHSX (10 mM $ZnCl_2$ plus 10 mM $CaCl_2$).

Subsequently, the solutions were set to the desired pH (± 0.05) with a pH meter with 1 M or 10 M NaOH or 2 M and 12 M HCl. Reactions with PiACP, PhoN-Sf, PhoN-Se, Lw, NSAP-Eb-11, PhoC-Mm-2 and AphA-St were run at pH 4.2, SPHSX at pH of 9.0 and phytase was tested at both pH 4.2 and pH 2.5.

For each reaction, 1 mL of the stock solution was combined with an aliquot of protein to reach a certain enzymatic activity (Equation 3). In case of immobilized enzyme, the stock solutions were added directly to the wet beads. Specific activity, A_{spec}, of the enzymes was determined in the hydrolytic direction in the pNPP assay (Section 3.1.3) and is listed in Table 34.

$$V \ [\text{µL}] = \frac{U_{reaction} \ [\text{U}]}{A_{spec} \ [\text{U mg}^{-1}] * c \ [\text{mg µL}^{-1}]} \tag{3}$$

V	volume of purified protein
$U_{reaction}$	enzymatic activity (units) desired in reaction
A_{spec}	specific hydrolytic activity of purified protein
c	concentration of purified protein

Because of the low A_{spec} of YniC-Ec compared to other phosphatases, 50 µg mL^{-1} and 200 µg mL^{-1} were used in reactions with "YniC-Ec old" while in screenings with "YniC-Ec from Section 3.1.6.b" (pET28a/TB medium) 1000 µg mL^{-1} were employed due to its minute activity.

During the course of the screening, the glass vials were shaken at 600 rpm and 30 °C in an Eppendorf shaker.

All reactions were done in duplicates to assure proper accuracy. Moreover control samples were prepared, containing all substances, except the phosphatase.

Table 34: Specific Activity and Concentration of Phosphatases

	A_{spec} [µmol min^{-1} mg^{-1}]	conc. [mg mL^{-1}]
PiACP	93.5	7.2
AphA-St	87.1	1.8
PhoN-Sf	55.6	13.8
PhoN-Se	36.3	2.1
PhoK/SPHSX	1300	0.25
PhoC-Mm-2	6.9	17.2
NSAP-Eb-11	30.5	12.8
Lw old	59.5	3.3
Lw from Section 3.1.5	60.9	15.4
phytase	150	3.9
YniC-Ec old	2.1	2.8
YniC-Ec from Section 3.1.6.b	0.2	53.4

3.3.2.b Sampling and Analytics on HPLC-RI

To keep track of the transphosphorylation reaction, 25 µL samples were taken from the reaction mixture at given time points and diluted with 475 µL 5 mM H_2SO_4 in HPLC grade H_2O in an HPLC vial. The accompanying drop to a pH ~ 2.0 was sufficient to quench the reaction. To prevent damage to the HPLC column by cyclohexylamine, in screenings with IPP, DFPVP and TFEP samples were diluted 40x with 5 mM H_2SO_4 instead of 20x.

Method on HPLC-RI: 40 µL injection volume, 0.4 mL min^{-1} flow, 50 °C column temperature, 16 min per run, eluent: 5 mM H_2SO_4 in HPLC grade H_2O. Column: Alltech IOA-2000 Organic Acids (length: 150 mm, diameter: 6.5 mm, particle size: 8 µm).

All chromatograms were integrated manually. Peaks were identified by comparison of the retention time with reference compounds (see A.3). Concentrations in mM were calculated from calibration curves, shown in Section 3.3.2.c, for 14OH, HEA, MADG, pyruvate and phosphate (P_i).

The amount of product in mM was calculated via the loss of substrate during the course of the reaction in comparison with a control sample, where 100 % of the substrate remained. For reactions with 14OH, in which the amount of substrate could not be quantified due to an overlap with another compound, a "pseudo" calibration curve (Figure 106) was set up from another screening, plotting the concentration of the product, determined by the consumption of 14OH in distinct reactions, against the area ratio of the product peak to the internal standard. This method was used for IPP for instance, where acetone was produced as an interfering by-product.

A calibration curve for pyruvate (Figure 104) was necessary to quantify the consumption of PEP, because of an overlap of the donor with chloride, deriving from HCl, used to set the pH of the stocks.
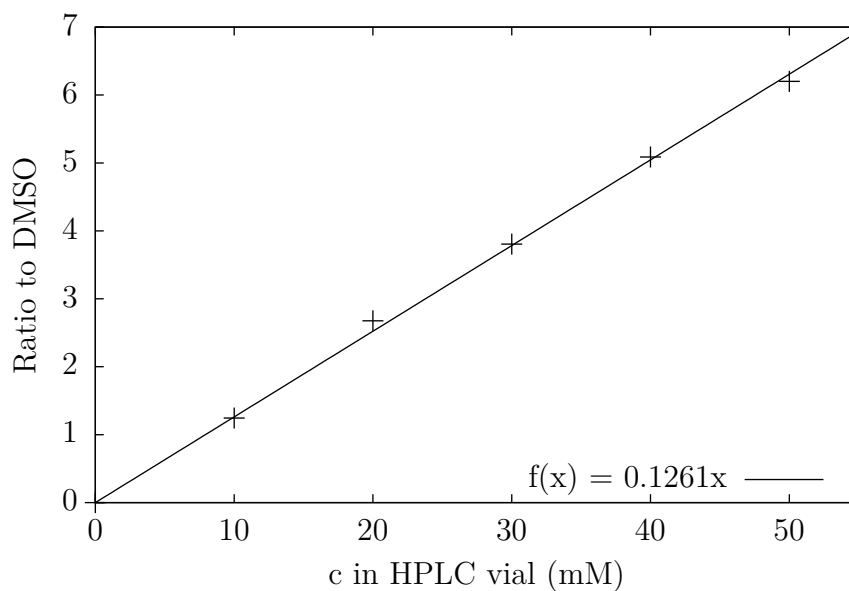
3.3.2.c Calibration for HPLC-RI

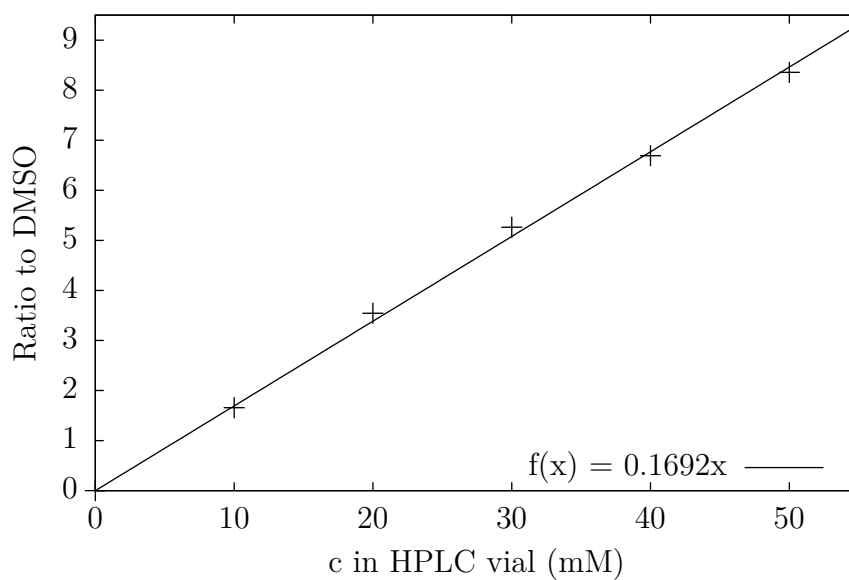Figure 101: Calibration curve for 14OH, $R^2 = 0.998$
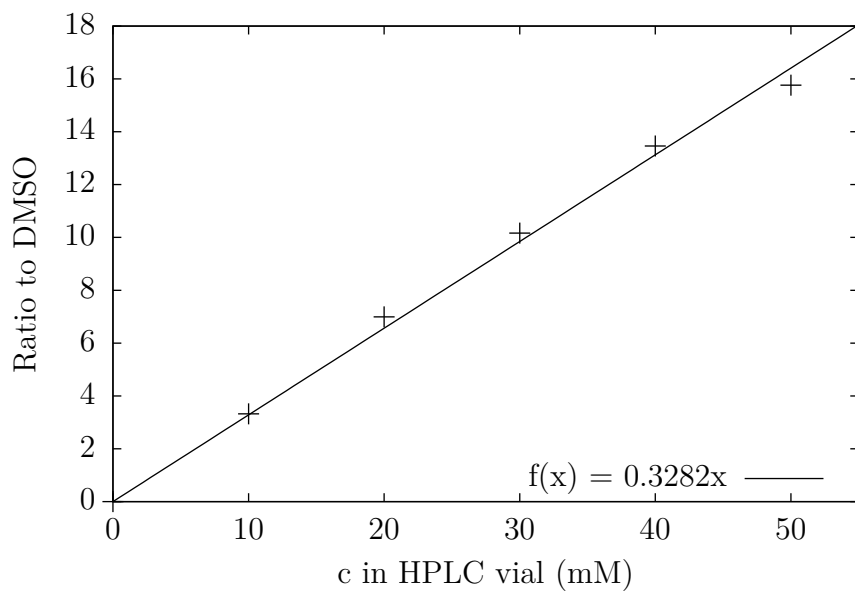

Figure 102: Calibration curve for HEA, $R^2 = 0.997$
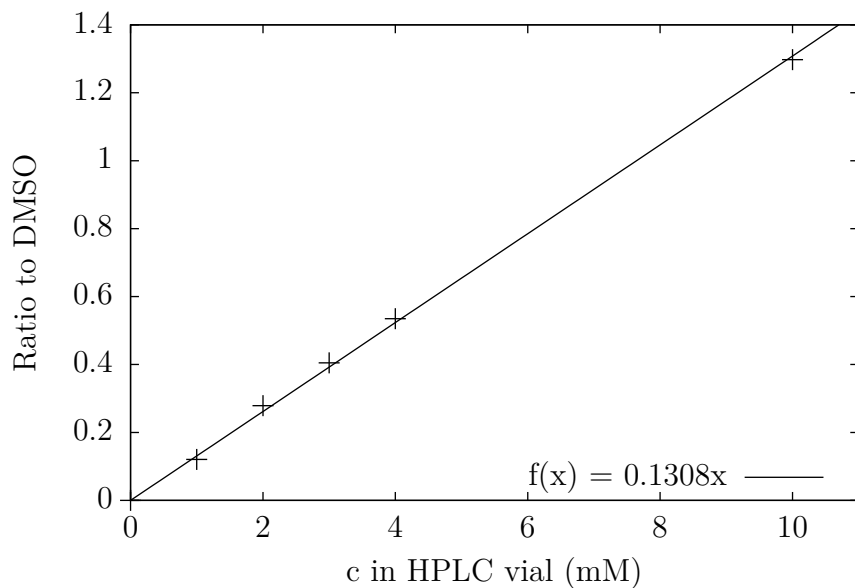
Figure 103: Calibration curve for MADG, $R^2 = 0.992$

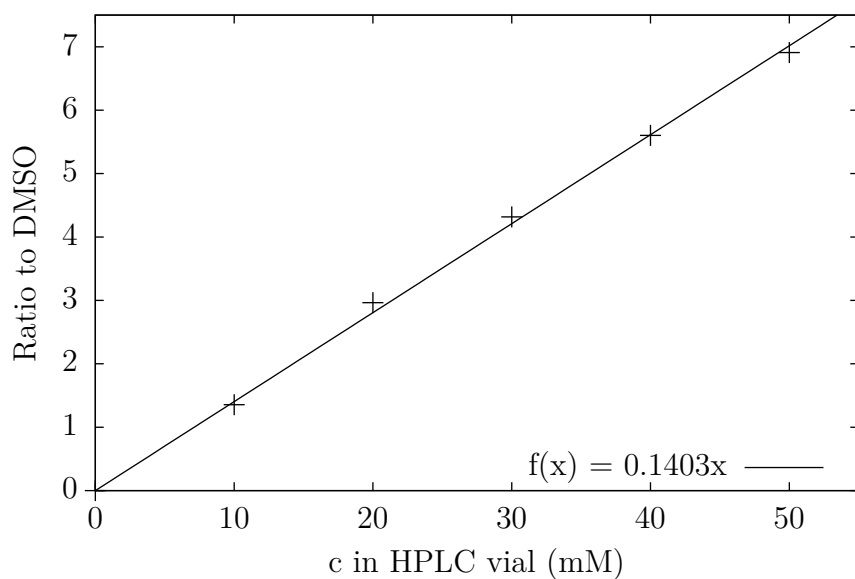Figure 104: Calibration curve for pyruvate, $R^2 = 0.999$
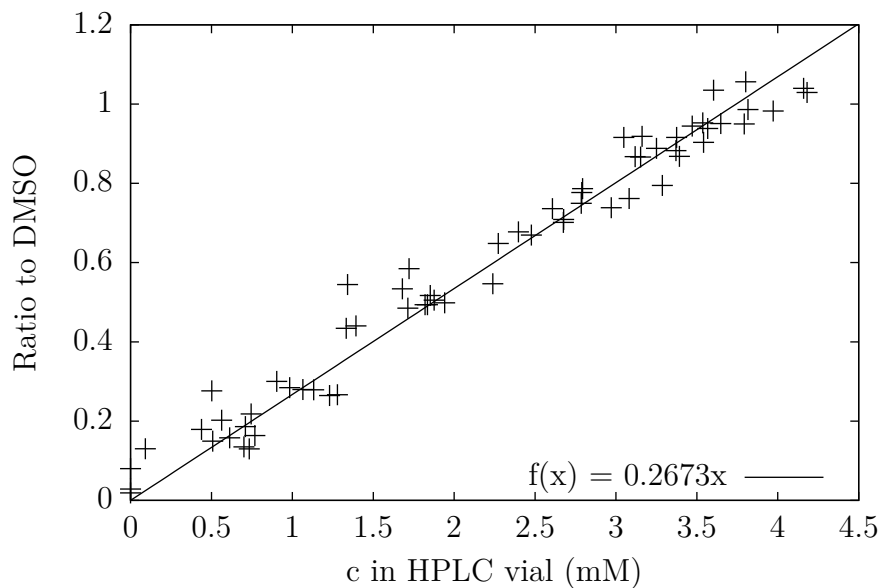
Figure 105: Calibration curve for P_i, $R^2 = 0.997$

Figure 106: "Pseudo" calibration curve for 14OP, $R^2 = 0.966$

113

3.3.2.d Sample Preparation and Analytics on HPLC-MS

HPLC-MS was used for product identification. Samples were prepared by dilution of 10 µL HPLC-RI sample with 990 µL 0.1 % formic acid in HPLC grade H_2O.

Method for HPLC-MS: 5 µL injection volume, $1\,mL\,min^{-1}$ flow, eluent: 0.1 % formic acid in HPLC grade H_2O, 40 °C column temperature, 13 min per run. Column: Agilent Zorbax 300-SCX. MS settings for 14OH: negative mode, SIM: set to m/z = 169 (monophosphorylated product minus 1), 249 (diphosphorylated product minus 1) and 124 (diphosphorylated product minus 2 divided by 2), then SCAN: m/z range from 90–300.

3.3.2.e Sampling and Analytics on NMR

NMR was also used for product identification. In contrast to analysis on HPLC-RI, where multiple samples at various time points could be prepared from a single batch, analysis via NMR required one reaction per sample: After the desired time, the reactions were quenched by addition of 30 µL 12 M HCl. In an NMR tube, 600 µL reaction mixture were subsequently combined with 100 µL 350 mM dimethyl methylphosphonate (internal standard) in D_2O.

Method for ^{31}P-NMR: Inverse gated decoupling, 32 scans and 20 s relaxation time (except for A.2.1 and A.2.5). Analysis of the spectra with MestReNova 6.0.2-5475.

3.3.2.f Identity of 4-hydroxybutyl phosphate

The identity of the product 4-hydroxybutyl phosphate was confirmed via HPLC-MS and NMR according to Sections 3.3.2.d and 3.3.2.e with PP_i, PEP, AcP, CP, DFPVP, TFEP as donors and PhoN-Sf, PhoN-Se and AphA-St at the "optimum" pH, determined in Section 2.7. On no account di- or oligophosphate esters were detected.

3.3.3 Hydrolysis of Donors and Products

Hydrolysis of the phosphate donor PEP in the presence of a phosphatase was determined by setting up stock solutions like in Section 3.3.2.a, but without substrate. To simulate reaction conditions with different enzymes, various stocks were prepared with pH values of 4.2 and 9.0 as well as 10 mM $MgCl_2$ or 10 mM $ZnCl_2$ and 10 mM $CaCl_2$ supplementation. $4\,U\,mL^{-1}$ of enzyme were employed, with the exception of $1\,U\,mL^{-1}$ in case of PhoN-Se. Sampling and analytics on HPLC-RI did not differ from Section 3.3.2.b.

The hydrolysis of the product 4-hydroxybutyl phosphate, provided as a disodium salt, at a concentration of 100 mM by PiACP, PhoN-Sf, PhoN-Se, Lw and AphA-St was tested following the same protocol, in the presence of 100 mM phosphate or PEP at various pH values.

3.3.4 Reactions with immobilized PhoN-Se

3.3.4.a General Procedure for immobilizing PhoN-Se

ReliZyme™ EP403 and Immobead 150 beads, both being epoxy-functionalized, were used. 10 mg (± 0.2 mg) of resin were weighed into 1.5 mL glass screw-cap vials. In total, ten vials per bead type were prepared. To each, 500 μL of 1.25 M "K-P_i" buffer, pH 8.0, and 10 U of PhoN-Se were added. Then the beads were shaken and the activity of 10 μL supernatant was monitored via the pNPP assay (Section 3.1.3). The absorption at $\lambda = 405$ nm is given in the table below.

Table 35: A_{405} values

resin	A_{405}		
	0 h	4 h	overnight
ReliZyme™ EP403	3.42	1.46	0.71
Immobead 150	3.46	0.04	

After 4 h (Immobead) or overnight (ReliZyme), the supernatant was removed with a Pasteur pipette and the beads were endcapped overnight by adding 500 μL 2 M glycine pH 8.5. Then the beads were washed two times with 500 μL DI H_2O. For testing the activity of the resin, 230 μL DI H_2O and 250 μL 200 mM maleate stock, pH 6.0, were added to one of the ten glass vials prepared per bead type. After incubation at 30 °C and 450 rpm for 5 min, 20 μL of a 250 mM pNPP solution in DI H_2O were added directly to the vials. The reactions were quenched after 1 min at 20 °C with 500 μL 1 M NaOH and the supernatant was diluted with H_2O 50x in case of Immobead 150 and 20x in

case of ReliZyme in a 1 mL cuvette. Finally, the samples were measured at the spectrophotometer as described in Section 3.1.3. All resin preparations were stored at 4 °C in 500 µL 100 mM "K-P$_i$" buffer at pH 7.

The immobilization yield was calculated from the loss of at A$_{405}$ given in Table 35. The amount of protein in the pNPP assay gave rise to further parameters, which are depicted in Table 36.

Table 36: Immobilization of PhoN-Se

resin	immobilization yield [%]	A_{spec} [µmol min^{-1} mg^{-1}] protein	A_{spec} [µmol min^{-1} g^{-1}] beads
ReliZyme™ EP403	79	6.81	187.3
Immobead 150	> 99	2.49	54.42

4 References

[1] F. H. Westheimer, Why nature chose phosphates, Science 235 (1987) 1173–1178.

[2] M. J. Berridge, R. F. Irvine, Inositol trisphosphate, a novel second messenger in cellular signal transduction, Nature 312 (1984) 315–321.

[3] L. Stryer, J. M. Berg, J. L. Tymoczko, Biochemistry, 4th Edition, W. H. Freeman, New York, 1995.

[4] J. N. Andexer, M. Richter, Emerging enzymes for ATP regeneration in biocatalytic processes, ChemBioChem 16 (2015) 380–386.

[5] W. Kroutil, H. Mang, K. Edegger, K. Faber, Biocatalytic oxidation of primary and secondary alcohols, Adv. Synth. Catal. 346 (2004) 125–142.

[6] G. P. Moss, Recommendations of the nomenclature committee of the international union of biochemistry and molecular biology on the nomenclature and classification of enzymes by the reactions they catalyse, `http://www.chem.qmul.ac.uk/iubmb/enzyme/`, [Online; accessed 2015-10-09] (1992).

[7] A. Pollak, R. L. Baughn, G. M. Whitesides, Large-scale enzymic synthesis with cofactor regeneration: glucose 6-phosphate, J. Am. Chem. Soc. 99 (1977) 2366–2367.

[8] V. M. Rios-Mercadillo, G. M. Whitesides, Enzymic synthesis of *sn*-glycerol 3-phosphate, J. Am. Chem. Soc. 101 (1979) 5828–5829.

[9] C. Goedl, T. Sawangwan, P. Wildberger, B. Nidetzky, Sucrose phosphorylase: a powerful transglucosylation catalyst for synthesis of α-D-glucosides as industrial fine chemicals, Biocatal. Biotransform. 28 (2010) 10–21.

[10] L. N. Johnson, S. H. Hu, D. Barford, Catalytic mechanism of glycogen phosphorylase, Faraday Discuss. 93 (1992) 131–142.

[11] J. R. Knowles, Enzyme-catalyzed phosphoryl transfer reactions, Ann. Rev. Biochem. 49 (1980) 877–919.

[12] O.-A. Neumüller, Phosphorsäure. In: Römpps Chemie-Lexikon, 8th Edition, Vol. 4: M–Pk, Franckh'sche Verlagshandlung, Stuttgart, 1985, pp. 3168–3169.

[13] R. Appel, Tertiary phosphane/tetrachloromethane, a versatile reagent for chlorination, dehydration, and P-N linkage, Angew. Chem. Int. Ed. 14 (1975) 801–811.

[14] O. Mitsunobu, M. Yamada, Preparation of esters of carboxylic and phosphoric acid via quaternary phosphonium salts, Bull. Chem. Soc. Jpn. 40 (1967) 2380–2382.

[15] H. A. van Kalkeren, F. L. van Delft, F. P. J. T. Rutjes, Organophosphorus catalysis to bypass phosphine oxide waste, ChemSusChem 6 (2013) 1615–1624.

[16] D. Guijarro, B. Manchefio, M. Yus, Direct transformation of trialkyl phosphates into organolithium compounds by a DTBB-catalysed lithiation, Tetrahedron 50 (1994) 8551–8558.

[17] H. Quast, T. Dietz, Dehydration of secondary alcohols via thermolysis of in situ generated alkyl diphenyl phosphates: An inexpensive and environmentally compatible method for the preparation of alkenes, Synthesis (1995) 1300–1304.

[18] A. Yanagisawa, N. Nomura, H. Yamamoto, Transition metal-catalyzed substitution reaction of allylic phosphates with grignard reagents, Tetrahedron 50 (1994) 6017–6028.

[19] M. Terada, Chiral phosphoric acids as versatile catalysts for enantioselective transformations, Synthesis (2010) 1929–1982.

[20] K. Faber, Biotransformations in Organic Chemistry, 6th Edition, Springer-Verlag, Berlin, Heidelberg, 2011.

[21] M. Brovetto, D. Gamenara, P. Saenz Mendez, G. A. Seoane, C-C bond-forming lyases in organic synthesis, Chem. Rev. 111 (2011) 4346–4403.

[22] L. Gómez, E. Molinar-Toribio, M. Á. Calvo-Torras, C. Adelantado, M. E. Juan, J. M. Planas, X. Cañas, C. Lozano, S. Pumarola, P. Clapés, J. L. Torres, D-Fagomine lowers postprandial blood glucose and modulates bacterial adhesion, Br. J. Nutr. 107 (2012) 1739–1746.

[23] Y. Asano, Sugar-mimicking glycosidase inhibitors: bioactivity and application, Cell. Mol. Life Sci. 66 (2009) 1479–1492.

[24] J. Calveras, M. Egido-Gabás, L. Gómez, J. Casas, T. Parella, J. Joglar, J. Bujons, P. Clapés, Dihydroxyacetone phosphate aldolase catalyzed synthesis of structurally diverse polyhydroxylated pyrrolidine derivatives and evaluation of their glycosidase inhibitory properties, Chem. Eur. J. 15 (2009) 7310–7328.

[25] T. van Herk, A. F. Hartog, L. Babich, H. E. Schoemaker, R. Wever, Improvement of an acid phosphatase/DHAP-dependent aldolase cascade reaction by using directed evolution, ChemBioChem 10 (2009) 2230–2235.

[26] E. ichiro Suzuki, K. Ishikawa, Y. Mihara, N. Shimba, Y. Asano, Structural-based engineering for transferases to improve the industrial production of 5'-nucleotides, Bull. Chem. Soc. Jpn. 80 (2007) 276–286.

[27] Y. Asano, Y. Mihara, H. Yamada, A new enzymatic method of selective phosphorylation of nucleosides, J. Mol. Catal. B: Enzym. 6 (1999) 271–277.

[28] Y. Mihara, K. Ishikawa, E.-i. Suzuki, Y. Asano, Improving the pyrophosphate-inosine phosphotransferase activity of *Escherichia blattae* acid phosphatase by sequential site-directed mutagenesis, Biosci., Biotechnol., Biochem. 68 (2004) 1046–1050.

[29] Y. Mihara, T. Utagawa, H. Yamada, Y. Asano, Phosphorylation of nucleosides by the mutated acid phosphatase from *Morganella morganii*, Appl. Environ. Microbiol. 66 (2000) 2811–2816.

[30] Y. Mihara, T. Utagawa, H. Yamada, Y. Asano, Acid phosphatase/phosphotransferases from enteric bacteria, J. Biosci. Bioeng. 92 (2001) 50–54.

[31] K. Ishikawa, Y. Mihara, N. Shimba, N. Ohtsu, H. Kawasaki, E.-i. Suzuki, Y. Asano, Enhancement of nucleoside phosphorylation activity in an acid phosphatase, Protein Eng. 15 (2002) 539–543.

[32] Y. Asano, Y. Mihara, H. Yamada, A novel selective nucleoside phosphorylating enzyme from *Morganella morganii*, J. Biosci. Bioeng. 87 (1999) 732–738.

[33] D. Auriol, R. Nalin, F. Lefevre, A. Ginolhac, D. de Guembecker, C. Zago, EP 1 995 323 A1, Chem. Abstr. 2008:1419327 (2008-11-26).

[34] K. M. Huttunen, H. Raunio, J. Rautio, Prodrugs—from serendipity to rational design, Pharmacol. Rev. 63 (2011) 750–771.

[35] P. R. Scudder, R. A. Dwek, T. W. Rademacher, G. S. Jacob, EP 0 413 674 A2, Chem. Abstr. 1991:472143 (1991-02-20).

[36] M. G. Nicolaou, C.-S. Yuan, R. T. Borchardt, Phosphate prodrugs for amines utilizing a fast intramolecular hydroxy amide lactonization, J. Org. Chem. 61 (1996) 8636–8641.

[37] T. M. Chapman, G. L. Plosker, C. M. Perry, Fosamprenavir: a review of its use in the management of antiretroviral therapy-naive patients with HIV infection, Drugs 64 (2004) 2101–2124.

[38] B. A. Boucher, Fosphenytoin: a novel phenytoin prodrug, Pharmacother. 16 (1996) 777–791.

[39] T. R. Browne, A. R. Kugler, M. A. Eldon, Pharmacology and pharmacokinetics of fosphenytoin, Neurology 46 (1996) 53–57.

[40] C. Schultz, Prodrugs of biologically active phosphate esters, Bioorg. Med. Chem. 11 (2003) 885–898.

[41] S. J. Hecker, M. D. Erion, Prodrugs of phosphates and phosphonates, J. Med. Chem. 51 (2008) 2328–2345.

[42] M. D. Erion, K. R. Reddy, S. H. Boyer, M. C. Matelich, J. Gomez-Galeno, R. H. Lemus, B. G. Ugarkar, T. J. Colby, J. Schanzer, P. P. D. Van, Design, synthesis, and characterization of a series of cytochrome P(450) 3A-activated prodrugs (HepDirect prodrugs) useful for targeting phosph(on)ate-based drugs to the liver, J. Am. Chem. Soc. 126 (2004) 5154–5163.

[43] P. G. M. Wuts, T. W. Greene, Protection for the Phosphate Group. In: Greene's Protective Groups in Organic Synthesis, 4th Edition, John Wiley & Sons, Inc., Hoboken, New Jersey, 2007, Ch. 9, pp. 934–985.

[44] R. A. Aitken, C. J. Collett, S. T. E. Mesher, Convenient preparation of long-chain dialkyl phosphates: synthesis of dialkyl phosphates, Synthesis (2012) 2515–2518.

[45] A. Sakakura, M. Katsukawa, K. Ishihara, Selective synthesis of phosphate monoesters by dehydrative condensation of phosphoric acid and alcohols promoted by nucleophilic bases, Org. Lett. 7 (2005) 1999–2002.

[46] M. Yoshikawa, T. Kato, T. Takenishi, Phosphorylation. III. selective phosphorylation of unprotected nucleosides, Bull. Chem. Soc. Jpn. 42 (1969) 3505–3508.

[47] T. Sowa, S. Ouchi, The facile synthesis of 5'-nucleotides by the selective phosphorylation of a primary hydroxyl group of nucleosides with phosphoryl chloride, Bull. Chem. Soc. Jpn. 48 (1975) 2084–2090.

[48] T. A. Khawaja, C. B. Reese, o-phenylene phosphorochloridate. a convenient phosphorylating agent, J. Am. Chem. Soc. 88 (1966) 3446–3447.

[49] T. A. Khwaja, C. B. Reese, J. C. M. Stewart, A convenient general procedure for the conversion of alcohols into their monophosphate esters, J. Chem. Soc. C (1970) 2092–2100.

[50] H. A. Kellner, R. G. K. Schneiderwind, H. Eckert, I. K. Ugi, Bis(2,2,2-trichloro-1,1-dimethylethyl) monochlorophosphate, a selective reagent for the phosphorylation and protection of the 5'-OH group of nucleoside derivatives, Angew. Chemie Int. Ed. 20 (1981) 577–578.

[51] H. Tolkmith, Aromatic phosphorodichloridites and phosphorodichloridothiates. I. aryl phosphorodichloridites, J. Org. Chem. 23 (1958) 1682–1684.

[52] A. Maderna, R. Huertas, M. F. Hawthorne, R. Luguya, M. G. H. Vicente, Synthesis of a porphyrin-labelled carboranyl phosphate diester: a potential new drug for boron neutron capture therapy of cancer, Chem. Commun. (2002) 1784–1785.

[53] T. Carell, Synthesis of nucleotides and oligo-nucleotides. Course chemical biology I nucleic acids, `http://online-media.uni-marburg.de/chemie/bioorganic/vorlesung1/kapitel2e.html?/chemie/bioorganic/vorlesung1/k2e-16.html`, [Online; accessed 2015-11-01] (2004).

[54] S. Jones, C. Smanmoo, N-phosphoryl oxazolidinones as effective phosphorylating agents, Tetrahedron Lett. 45 (2004) 1585–1588.

[55] H. Ohkawa, M. Eto, Alkylation of mercaptans and inhibition of "SH enzyme" by saligenin cyclic phosphate and phosphorothiolate esters, Agric. Biol. Chem. 33 (1969) 443–451.

[56] M. Eto, H. Ohkawa, K. Kobayashi, T. Hosoi, Saligenin cyclic phosphorus esters as biological alkylating agents and fungicides, Agric. Biol. Chem. 32 (1968) 1056–1058.

[57] M. Eto, M. Sasaki, M. Iio, M. Eto, H. Ohkawa, Synthesis of 2-(methylthio)-4H-1,3,2-benzodioxaphosphorine 2-oxide by thiono-thiol conversion and its use as a phosphorylating agent, Tetrahedron Lett. 12 (1971) 4263–4266.

[58] L. A. Slotin, Current methods of phosphorylation of biological molecules, Synthesis (1977) 737–752.

[59] J. W. Perich, R. B. Johns, A new, convenient and efficient general procedure for the conversion of alcohols into their dibenzyl phosphorotriesters using N,N-dibenzyl phosphoramidite, Tetrahedron Lett. 28 (1987) 101–102.

[60] M. Hoffmann, A convenient synthesis of alkyl hydrogen 1-(benzyloxycarbonyl-amino)alkanephosphonates, Synthesis (1986) 557–559.

[61] N. Galeotti, J. Coste, P. Bedos, P. Jouin, A straightforward synthesis of α-amino phosphate monoesters using BroP or TPyClU, Tetrahedron Lett. 37 (1996) 3997–3998.

[62] C. Dueymes, C. Pirat, R. Pascal, Facile synthesis of simple mono-alkyl phosphates from phosphoric acid and alcohols, Tetrahedron Lett. 49 (2008) 5300–5301.

[63] L. M. Lira, D. Vasilev, R. A. Pilli, L. A. Wessjohann, One-pot synthesis of organophosphate monoesters from alcohols, Tetrahedron Lett. 54 (2013) 1690–1692.

[64] A. Sakakura, M. Katsukawa, K. Ishihara, The oxorhenium(VII)-catalyzed direct condensation of phosphoric acid with an alcohol, Angew. Chem., Int. Ed. 46 (2007) 1423–1426.

[65] T. Hata, K.-J. Chong, p-Nitrophenyl phosphate as a phosphorylating reagent in nucleotide synthesis, Bull. Chem. Soc. Jpn. 45 (1972) 654.

[66] G. M. Tener, 2-Cyanoethyl phosphate and its use in the synthesis of phosphate esters, J. Am. Chem. Soc. 83 (1961) 159–168.

[67] H. Takaku, Y. Shimada, Phosphorylation of alcohols with diethyl phosphorochloridodithioite, Tetrahedron Lett. 13 (1972) 411–414.

[68] R. Wever, T. van Herk, Hydrolysis and Formation of P-O Bonds. In: Enzyme Catalysis in Organic Synthesis, 3rd Edition, Vol. 2, K. Drauz, H. Gröger, O. May (Eds.), Wiley-VCH Verlag GmbH, Weinheim, 2012, Ch. 25, pp. 1001–1033.

[69] J. Zhang, B. Wu, Y. Zhang, P. Kowal, P. G. Wang, Creatine phosphate—creatine kinase in enzymatic synthesis of glycoconjugates, Org. Lett. 5 (2003) 2583–2586.

[70] G. M. Whitesides, Formation and Cleavage of P-O Bonds. In: Enzyme Catalysis in Organic Synthesis, 2nd Edition, Vol. 2, K. Drauz, H. Waldmann (Eds.), Wiley-VCH Verlag GmbH, Weinheim, 2002, Ch. 13, pp. 895–929.

[71] R. K. Thauer, K. Jungermann, K. Decker, Energy conservation in chemotrophic anaerobic bacteria, Bacteriol. Rev. 41 (1977) 100–180.

[72] D. C. Crans, G. M. Whitesides, A convenient synthesis of disodium acetyl phosphate for use in in situ ATP cofactor regeneration, J. Org. Chem. 48 (1983) 3130–3132.

[73] B. L. Hirschbein, F. P. Mazenod, G. M. Whitesides, Synthesis of phosphoenolypyruvate and its use in ATP cofactor regeneration, J. Org. Chem. 47 (1982) 3765–3766.

[74] H. K. Chenault, R. F. Mandes, K. R. Hornberger, Synthetic utility of yeast hexokinase. substrate specificity, cofactor regeneration, and product isolation, J. Org. Chem. 62 (1997) 331–336.

[75] D. C. Crans, G. M. Whitesides, Glycerol kinase: substrate specificity, J. Am. Chem. Soc. 107 (1985) 7008–7018.

[76] A. Gross, O. Abril, J. M. Lewis, S. Geresh, G. M. Whitesides, Practical synthesis of 5-phospho-D-ribosyl α-1-pyrophosphate (PRPP): enzymatic routes from ribose 5-phosphate or ribose, J. Am. Chem. Soc. 105 (1983) 7428–7435.

[77] T. Soderberg, Phosphoryl transfer reactions. In: Organic Chemistry with a Biological Emphasis, Vol. 2, Chemistry Faculty. Paper 2, 2010, Ch. 10, pp. 1–39.

[78] H. K. Chenault, E. S. Simon, G. M. Whitesides, Cofactor regeneration for enzyme-catalyzed synthesis, Biotechnol. Genet. Eng. Rev. 6 (1988) 221–270.

[79] R. J. Kazlauskas, G. M. Whitesides, Synthesis of methoxycarbonyl phosphate, new reagent having high phosphoryl donor potential for use in ATP cofactor regeneration, J. Org. Chem. 50 (1985) 1069–1076.

[80] R. Wever, L. Babich, A. F. Hartog, Transphosphorylation. In: Biocatalysis in Organic Synthesis, 1st Edition, Vol. 1, K. Faber, W.-D. Fessner, N. J. Turner (Eds.), Georg Thieme Verlag KG, Stuttgart, 2015, Ch. 1.3.3, pp. 223–254.

[81] C. A. Janson, W. W. Cleland, Inhibition of acetate, pyruvate, and 3-phosphoglycerate kinases by chromium adenosine triphosphate, J. Biol. Chem. 249 (1974) 2567–2571.

[82] C.-H. Wong, G. M. Whitesides, Enzyme-catalyzed organic synthesis: NAD(P)H cofactor regeneration by using glucose-6-phosphate and the glucose-5-phosphate dehydrogenase from *Leuconostoc mesenteroides*, J. Am. Chem. Soc. 103 (1981) 4890–4899.

[83] D. G. Drueckhammer, C. H. Wong, Chemoenzymic syntheses of fluoro sugar phosphates and analogs, J. Org. Chem. 50 (1985) 5912–5913.

[84] H. K. Chenault, L. F. Chafin, S. Liehr, Kinetic chiral resolutions of 1,2-diols and desymmetrization of glycerol catalyzed by glycerol kinase, J. Org. Chem. 63 (1998) 4039–4045.

[85] C. H. Wong, G. M. Whitesides, Synthesis of sugars by aldolase-catalyzed condensation reactions, J. Org. Chem. 48 (1983) 3199–3205.

[86] T. van Herk, A. F. Hartog, H. E. Schoemaker, R. Wever, Simple enzymatic in situ generation of dihydroxyacetone phosphate and its use in a cascade reaction for the production of carbohydrates: Increased efficiency by phosphate cycling, J. Org. Chem. 71 (2006) 6244–6247.

[87] D. R. Walt, M. A. Findeis, V. M. Rios-Mercadillo, J. Auge, G. M. Whitesides, An efficient chemical and enzymic synthesis of nicotinamide adenine dinucleotide (NAD$^+$), J. Am. Chem. Soc. 106 (1984) 234–239.

[88] A. Kornberg, N. N. Rao, D. Ault-Riche, Inorganic polyphosphate: a molecule of many functions, Annu. Rev. Biochem. 68 (1999) 89–125.

[89] T. Mukai, S. Kawai, S. Mori, B. Mikami, K. Murata, Crystal structure of bacterial inorganic polyphosphate/ATP-glucomannokinase: Insights into kinase evolution, J. Biol. Chem. 279 (2004) 50591–50600.

[90] E. V. Schaftingen, I. Gerin, The glucose-6-phosphatase system, Biochem. J. 362 (2002) 513–532.

[91] B. G. Neel, N. K. Tonks, Protein tyrosine phosphatases in signal transduction, Curr. Opin. Cell Biol. 9 (1997) 193–204.

[92] W. B. Anderson, R. C. Nordlie, Inorganic pyrophosphate-glucose phosphotransferase activity associated with alkaline phosphatase of *Escherichia coli*, J. Biol. Chem. 242 (1967) 114–119.

[93] W. W. Cleland, A. C. Hengge, Enzymatic mechanisms of phosphate and sulfate transfer, Chem. Rev. 106 (2006) 3252–3278.

[94] M. C. Thaller, S. Schippa, G. M. Rossolini, Conserved sequence motifs among bacterial, eukaryotic, and archaeal phosphatases that define a new phosphohydrolase superfamily, Protein Sci. 7 (1998) 1647–1652.

[95] L. F. Hass, P. D. Boyer, A. M. Reynard, Possible phosphoryl enzyme formation in catalysis by hexokinase, pyruvate kinase, and glucose-6-phosphatase, J. Biol. Chem. 236 (1961) 2284–2291.

[96] E. G. Mueller, M. W. Crowder, B. A. Averill, J. R. Knowles, Purple acid phosphatase: a diiron enzyme that catalyzes a direct phospho group transfer to water, J. Am. Chem. Soc. 115 (1993) 2974–2975.

[97] S. R. Jones, L. A. Kindman, J. R. Knowles, Stereochemistry of phosphoryl group transfer using a chiral [^{16}O, ^{17}O, ^{18}O] stereochemical course of alkaline phosphatase, Nature 275 (1978) 564–565.

[98] G. Lowe, B. V. L. Potter, The stereochemical course of phosphoryl transfer catalyzed by glucose 6-phosphatase, Biochem. J. 201 (1982) 665–668.

[99] G. Schenk, N. Mitic, G. R. Hanson, P. Comba, Purple acid phosphatase: A journey into the function and mechanism of a colorful enzyme, Coord. Chem. Rev. 257 (2013) 473–482.

[100] D. J. Rigden, The histidine phosphatase superfamily: structure and function, Biochem. J. 409 (2008) 333–348.

[101] R. K. Morton, Phosphotransferase activity of phosphatases. III. comparison of enzymic catalysis by acid phosphatase with nonenzymic catalysis at acid pH values, Biochem. J. 70 (1958) 150–155.

[102] D. E. C. S. Rao, K. V. Rao, T. P. Reddy, V. D. Reddy, Molecular characterization, physicochemical properties, known and potential applications of phytases: An overview, Crit. Rev. Biotechnol. 29 (2009) 182–198.

[103] X. G. Lei, C. H. Stahl, Biotechnological development of effective phytases for mineral nutrition and environmental protection, Appl. Microbiol. Biotechnol. 57 (2001) 474–481.

[104] R. Schoevaart, F. van Rantwijk, R. A. Sheldon, A four-step enzymatic cascade for the one-pot synthesis of non-natural carbohydrates from glycerol, J. Org. Chem. 65 (2000) 6940–6943.

[105] K. Kolmodin, J. Aqvist, The catalytic mechanism of protein tyrosine phosphatases revisited, FEBS Lett. 498 (2001) 208–213.

[106] Y. Zhao, Z.-Y. Zhang, Reactivity of alcohols toward the phosphoenzyme intermediate in the protein-tyrosine phosphatase-catalyzed reaction: Probing the transition state of the dephosphorylation step, Biochemistry 35 (1996) 11797–11804.

[107] K. N. Allen, D. Dunaway-Mariano, Markers of fitness in a successful enzyme superfamily, Curr. Opin. Struct. Biol. 19 (2009) 658–665.

[108] A. Seifried, J. Schultz, A. Gohla, Human HAD phosphatases: structure, mechanism, and roles in health and disease, FEBS J. 280 (2013) 549–571.

[109] E. Kuznetsova, M. Proudfoot, C. F. Gonzalez, G. Brown, M. V. Omelchenko, I. Borozan, L. Carmel, Y. I. Wolf, H. Mori, A. V. Savchenko, C. H. Arrowsmith, E. V. Koonin, A. M. Edwards, A. F. Yakunin, Genome-wide analysis of substrate specificities of the *Escherichia coli* haloacid dehalogenase-like phosphatase family, J. Biol. Chem. 281 (2006) 36149–36161.

[110] J. E. Coleman, Structure and mechanism of alkaline phosphatase, Annu. Rev. Biophys. Biomol. Struct. 21 (1992) 441–483.

[111] R. K. Morton, Phosphotransferase activity of phosphatases. II. studies with purified alkaline phosphomonoesterases and some substrate-specific phosphatases, Biochem. J. 70 (1958) 139–150.

[112] J. G. Zalatan, T. D. Fenn, D. Herschlag, Comparative enzymology in the alkaline phosphatase superfamily to determine the catalytic role of an active-site metal ion, J. Mol. Biol. 384 (2008) 1174–1189.

[113] S. C. Bihani, A. Das, K. S. Nilgiriwala, V. Prashar, M. Pirocchi, S. K. Apte, J.-L. Ferrer, M. V. Hosur, X-ray structure reveals a new class and provides insight into evolution of alkaline phosphatases, PLoS One 6 (2011) e22767.

[114] S. Gutteridge, G. S. Reddy, G. Lorimer, The synthesis and purification of 2'-carboxy-D-arabinitol 1-phosphate, a natural inhibitor of ribulose 1,5-bisphosphate carboxylase, investigated by phosphorus-31 NMR, Biochem. J. 260 (1989) 711–716.

[115] R. Breslow, I. Katz, Relative reactivities of p-nitrophenyl phosphate and phosphorothioate toward alkaline phosphatase and in aqueous hydrolysis, J. Am. Chem. Soc. 90 (1968) 7376–7377.

[116] B. Edwards, A. Sparks, J. C. Voyta, R. Strong, O. Murphy, I. Bronstein, Naphthyl dioxetane phosphates: synthesis of novel substrates for enzymic chemiluminescent assays, J. Org. Chem. 55 (1990) 6225–6229.

[117] J. Sambrook, D. W. Russell, Molecular cloning: A laboratory manual, `http://www.molecularcloning.com/index.php?prt=151`, [Online; accessed 2015-10-14] (2015).

[118] A. Pradines, A. Klaebe, J. Perie, F. Paul, P. Monsan, Enzymic synthesis of phosphoric monoesters with alkaline phosphatase in reverse hydrolysis conditions, Tetrahedron 44 (1988) 6373–6386.

[119] A. Pradines, A. Klaebe, J. Perie, F. Paul, P. Monsan, Large-scale enzymic synthesis of glycerol 1-phosphate, Enzyme Microb. Technol. 13 (1991) 19–23.

[120] P. Gettins, M. Metzler, J. E. Coleman, Alkaline phosphatase. phosphorus-31 NMR probes of the mechanism, J. Biol. Chem. 260 (1985) 2875–2883.

[121] G. M. Rossolini, S. Schippa, M. L. Riccio, F. Berlutti, L. E. Macaskie, M. C. Thaller, Bacterial nonspecific acid phosphohydrolases. physiology, evolution, and use as tools in microbial biotechnology, Cell. Mol. Life Sci. 54 (1998) 833–850.

[122] C.-J. Pan, K.-J. Lei, B. Annabi, W. Hemrika, J. Y. Chou, Transmembrane topology of glucose-6-phosphatase, J. Biol. Chem. 273 (1998) 6144–6148.

[123] W. Hemrika, R. Wever, A new model for the membrane topology of glucose-6-phosphatase: the enzyme involved in von gierke disease, FEBS Lett. 409 (1997) 317–319.

[124] A. F. Neuwald, An unexpected structural relationship between integral membrane phosphatases and soluble haloperoxidases, Protein Sci. 6 (1997) 1764–1767.

[125] R. Renirie, W. Hemrika, R. Wever, Peroxidase and phosphatase activity of active-site mutants of vanadium chloroperoxidase from the fungus *Curvularia inaequalis*. implications for the catalytic mechanisms, J. Biol. Chem. 275 (2000) 11650–11657.

[126] N. Tanaka, V. Dumay, Q. Liao, A. J. Lange, R. Wever, Bromoperoxidase activity of vanadate-substituted acid phosphatases from *Shigella flexneri* and *Salmonella enterica ser. typhimurium*, Eur. J. Biochem. 269 (2002) 2162–2167.

[127] K. Ishikawa, Y. Mihara, K. Gondoh, E.-i. Suzuki, Y. Asano, X-ray structures of a novel acid phosphatase from *Escherichia blattae* and its complex with the transition-state analog molybdate, EMBO J. 19 (2000) 2412–2423.

[128] T. van Herk, A. F. Hartog, A. M. van der Burg, R. Wever, Regioselective phosphorylation of carbohydrates and various alcohols by bacterial acid phosphatases; probing the substrate specificity of the enzyme from *Shigella flexneri*, Adv. Synth. Catal. 347 (2005) 1155–1162.

[129] M. M. Babu, S. Kamalakkannan, Y. V. B. K. Subrahmanyam, K. Sankaran, *Shigella* apyrase - a novel variant of bacterial acid phosphatases?, FEBS Lett. 512 (2002) 8–12.

[130] R. D. Makde, V. Kumar, G. D. Gupta, J. Jasti, T. P. Singh, S. K. Mahajan, Expression, purification, crystallization and preliminary X-ray diffraction studies of recombinant class B non-specific acid phosphatase of *Salmonella typhimurium*, Acta Crystallogr. Sect. D-Biol. Crystallogr. 59 (2003) 1849–1852.

[131] R. Wang, K. Ohtani, Y. Wang, Y. Yuan, S. Hassan, T. Shimizu, Genetic and biochemical analysis of a class C non-specific acid phosphatase (NSAP) of *Clostridium perfringens*, Microbiology 156 (2010) 167–173.

[132] R. D. Makde, K. Dikshit, V. Kumar, Protein engineering of class-A non-specific acid phosphatase (PhoN) of *Salmonella typhimurium*: Modulation of the pH-activity profile, Biomol. Eng. 23 (2006) 247–251.

[133] R. D. Makde, S. K. Mahajan, V. Kumar, Structure and mutational analysis of the PhoN protein of *Salmonella typhimurium* provide insight into mechanistic details, Biochemistry 46 (2007) 2079–2090.

[134] N. Tanaka, Z. Hasan, A. F. Hartog, T. van Herk, R. Wever, Phosphorylation and dephosphorylation of polyhydroxy compounds by class A bacterial acid phosphatases, Org. Biomol. Chem. 1 (2003) 2833–2839.

[135] R. D. Makde, G. D. Gupta, S. K. Mahajan, V. Kumar, Structural and mutational analyses reveal the functional role of active-site Lys-154 and Asp-173 of *Salmonella typhimurium* AphA protein, Arch. Biochem. Biophys. 464 (2007) 70–79.

[136] T. Kimura, V. P. Vassilev, G.-J. Shen, C.-H. Wong, Enzymic synthesis of β-hydroxy-α-amino acids based on recombinant D- and L-threonine aldolases, J. Am. Chem. Soc. 119 (1997) 11734–11742.

[137] T. van Herk, A. F. Hartog, H. J. Ruijssenaars, R. Kerkman, H. E. Schoemaker, R. Wever, Optimization of the kinetic resolution of the DL-phosphomonoesters of threonine and serine by random mutagenesis of the acid phosphatase from *Salmonella enterica*, Adv. Synth. Catal. 349 (2007) 1349–1352.

[138] A. Straub, F. Effenberger, P. Fischer, Enzyme-catalyzed reactions. part 4. aldolase-catalyzed carbon-carbon bond formation for stereoselective synthesis of nitrogen containing carbohydrates, J. Org. Chem. 55 (1990) 3926–3932.

[139] B. Axelrod, A new mode of enzymatic phosphate transfer, J. Biol. Chem. 172 (1948) 1–13.

[140] J. Appleyard, Effect of alcohols on the hydrolysis of sodium phenolphthalein diphosphate by prostatic extracts, Biochem. J. 42 (1948) 596–597.

[141] W. Uerkvitz, Periplasmic nonspecific acid phosphatase II from *Salmonella typhimurium* LT2. crystallization, detergent reactivation, and phosphotransferase activity, J. Biol. Chem. 263 (1988) 15823–15830.

[142] E. F. Brunngraber, E. Chargaff, Action of nucleotide phosphotransferase of *Escherichia coli* on nicotinamide riboside and nicotinamide mononucleotide, Proc. Natl. Acad. Sci. U. S. A. 74 (1977) 4160–4162.

[143] E. F. Brunngraber, E. Chargaff, Nucleotide phosphotransferase of *Escherichia coli*: Purification by affinity chromatography, Proc. Natl. Acad. Sci. U. S. A. 74 (1977) 3226–3229.

[144] W. J. Arion, B. K. Wallin, P. W. Carlson, A. J. Lang, Specificity of glucose 6-phosphatase of intact liver microsomes, J. Biol. Chem. 247 (1972) 2558–2565.

[145] H. Mori, A. Iida, T. Fujio, S. Teshiba, A novel process of inosine 5'-monophosphate production using overexpressed guanosine/inosine kinase, Appl. Microbiol. Biotechnol. 48 (1997) 693–698.

[146] A. F. Holleman, E. Wiberg, N. Wiberg, Die Stickstoffgruppe ("Pentele"). In: Lehrbuch der Anorganischen Chemie, 102nd Edition, Walter de Gruyter & Co., Berlin, New York, 2007, Ch. XIV, p. 804.

[147] L. Babich, A. F. Hartog, M. A. van der Horst, R. Wever, Continuous-flow reactor-based enzymatic synthesis of phosphorylated compounds on a large scale, Chem. Eur. J. 18 (2012) 6604–6609.

[148] A. F. Hartog, T. van Herk, R. Wever, Efficient regeneration of NADPH in a 3-enzyme cascade reaction by in situ generation of glucose 6-phosphate from glucose and pyrophosphate, Adv. Synth. Catal. 353 (2011) 2339–2344.

[149] K. Dissing, W. Uerkvitz, Class B nonspecific acid phosphatase from *Salmonella typhimurium* LT2: Phosphotransferase activity, stability and thiol group reactivity, Enzyme Microb. Technol. 38 (2006) 683–688.

[150] I. Sanchez-Moreno, J. Francisco Garcia-Garcia, A. Bastida, E. Garcia-Junceda, Multienzyme system for dihydroxyacetone phosphate-dependent aldolase catalyzed C-C bond formation from dihydroxyacetone, Chem. Commun. (2004) 1634–1635.

[151] D. Franke, T. Machajewski, C.-C. Hsu, C.-H. Wong, One-pot synthesis of L-fructose using coupled multienzyme systems based on rhamnulose-1-phosphate aldolase, J. Org. Chem. 68 (2003) 6828–6831.

[152] L. Babich, L. J. C. van Hemert, A. Bury, A. F. Hartog, P. Falcicchio, J. van der Oost, T. van Herk, R. Wever, F. P. J. T. Rutjes, Synthesis of non-natural carbohydrates from glycerol and aldehydes in a one-pot four-enzyme cascade reaction, Green Chem. 13 (2011) 2895–2900.

[153] L. Babich, A. F. Hartog, L. J. C. van Hemert, F. P. J. T. Rutjes, R. Wever, Synthesis of carbohydrates in a continuous flow reactor by immobilized phosphatase and aldolase, ChemSusChem 5 (2012) 2348–2353.

[154] I. B. Wilson, J. Dayan, K. Cyr, Some properties of alkaline phosphatase from *Escherichia coli*. transphosphorylation, J. Biol. Chem. 239 (1964) 4182–4185.

[155] O. Meyerhof, H. Green, Synthetic action of phosphatase. II. transphosphorylation by alkaline phosphatase in the absence of nucleotides, J. Biol. Chem. 183 (1950) 377–390.

[156] H. Neumann, Phosphoryl transfer from S-substituted monoesters of phosphorothioic acid to various acceptors catalyzed by alkaline phosphatase from *Escherichia coli*, Eur. J. Biochem. 8 (1969) 164–173.

[157] C. Passariello, C. Forleo, V. Micheli, S. Schippa, R. Leone, S. Mangani, M. C. Thaller, G. M. Rossolini, Biochemical characterization of the class B acid phosphatase (AphA) of *Escherichia coli* MG1655, Biochim. Biophys. Acta, Proteins Proteomics 1764 (2006) 13–19.

[158] B. C. Jeong, H. W. Kim, L. E. Macaskie, Phosphotransferase activity of acid phosphatases of a *Citrobacter sp.*, FEMS Microbiol. Lett. 147 (1997) 103–108.

[159] M. Y. Kamel, R. L. Anderson, Enzymatic phosphorylation of D-glucose with acetyl phosphate, J. Biol. Chem. 239 (1964) PC3607–8.

[160] Y. Tani, T. Tochikura, H. Yamada, K. Ogata, Crystalline acid phosphatase having pyridoxine-phosphorylating activity, Biochem. Biophys. Res. Commun. 28 (1967) 769–772.

[161] S. Koizumi, A. Maruyama, T. Fujio, Purification and characterization of ascorbic acid phosphorylating enzyme from *Pseudomonas azotocolligans*, Agric. Biol. Chem. 54 (1990) 3235–3239.

[162] A. Fujimoto, R. A. Smith, Metabolism of phosphoramidates. II. further studies on the *Escherichia coli* phosphoramidate phosphoryl transfer enzyme, Biochim. Biophys. Acta 56 (1962) 501–511.

[163] X. Chen, T. Ansai, S. Awano, T. Iida, S. Barik, T. Takehara, Isolation, cloning, and expression of an acid phosphatase containing phosphotyrosyl phosphatase activity from *Prevotella intermedia*, J. Bacteriol. 181 (1999) 7107–7114.

[164] K. S. Nilgiriwala, A. Alahari, A. S. Rao, S. K. Apte, Cloning and overexpression of alkaline phosphatase PhoK from *Sphingomonas sp.* strain BSAR-1 for bioprecipitation of uranium from alkaline solutions, Appl. Environ. Microbiol. 74 (2008) 5516–5523.

[165] F. Lipmann, L. C. Tuttle, Acetyl phosphate: Chemistry, determination, and synthesis, J. Biol. Chem. 153 (1944) 571–582.

[166] Römpps Chemie-Lexikon, Essigsäure, `https://roempp.thieme.de/roempp4.0/do/data/RD-05-01764`, [Online; accessed 2016-01-24] (2016).

[167] T. Moriguchi, K. Okada, K. Seio, M. Sekine, Synthesis and stability of 1-phenylethenyl phosphate derivatives and their phosphoryl transfer activity, Lett. Org. Chem. 1 (2004) 140–144.

[168] Römpps Chemie-Lexikon, Brenztraubensäure, `https://roempp.thieme.de/roempp4.0/do/data/RD-02-02574`, [Online; accessed 2015-09-16] (2015).

[169] G. Tasnadi, M. Lukesch, M. Zechner, W. Jud, M. Hall, K. Ditrich, K. Baldenius, A. F. Hartog, R. Wever, K. Faber, Exploiting acid phosphatases in the synthesis of phosphorylated monoalcohols and diols, Eur. J. Org. Chem. 2016 (2016) 45–50.

[170] F. W. Studier, Protein production by auto-induction in high-density shaking cultures, Protein Express. Purif. 41 (2005) 207–234.

[171] A. Grabski, M. Mehler, D. Drott, The overnight express autoinduction system: High-density cell growth and protein expression while you sleep, Nat. Methods 2 (2005) 233–235.

[172] J. George N. Bowers, R. B. McComb, R. C. Christensen, R. Schaffer, High-purity 4-nitrophenol: Purification, characterization, and specifications for use as a spectrophotometric reference material, Clin. Chim. 26 (1980) 724–729.

[173] S. E. Deacon, M. J. McPherson, Enhanced expression and purification of fungal galactose oxidase in *Escherichia coli* and use for analysis of a saturation mutagenesis library, ChemBioChem 12 (2011) 593–601.

[174] L. F. García-Alles, B. Erni, Synthesis of phosphoenolpyruvate (PEP) analogues and evaluation as inhibitors of PEP-utilizing enzymes, Eur. J. Biochem. 269 (2002) 3226–3236.

[175] A. M. Modro, T. A. Modro, An improved synthesis of monoesters of phosphoric acid, Org. Prep. Proced. Int. 24 (1992) 57–60.

A Appendix

A.1 Abbreviations

14OH 1,4-butanediol

AcP Acetyl phosphate

AHTC Anhydrotetracycline

AMP Ampicillin

ATP Adenosine triphosphate

CAM Chloramphenicol

CP Carbamoyl phosphate

DFPVP 1-(2,4-difluorophenyl)vinyl phosphate

DI deionized

DMSO Dimethyl sulfoxide

DNA Deoxyribonucleic Acid

EDTA Ethylenediaminetetraacetic acid

FPLC Fast Protein Liquid Chromatography

HEA 2-hydroxyethyl acrylate

HPLC-MS High Performance Liquid Chromatography with Mass Spectrometer Detector

HPLC-RI High Performance Liquid Chromatography with Refractory Index Detector

IPP Isopropenyl phosphate

IPTG Isopropyl β-D-1-thiogalactopyranoside

IS Internal Standard

KAN Kanamycin

LB Lysogeny Broth

LOD Limit of Detection

MADG Methyl α-D-glucopyranoside

MeOH Methanol

MOPS 3-(N-morpholino)propanesulfonic acid

n.c. no conversion

NMR Nuclear Magnetic Resonance

NSAP non-specific acid phosphatase

OD$_{600}$ Optical density, absorption at $600\,\mathrm{nm}$

ONC Overnight Culture

PC Phosphocreatine

PEP Phosphoenolpyruvate

P$_\mathbf{i}$ Phosphate

PP$_\mathbf{i}$ Pyrophosphate

pNPP *para*-Nitrophenylphosphate

rt room temperature

SDS Sodium dodecyl sulfate

SDS-PAGE Polyacrylamide gel electrophoresis of proteins denaturated via SDS

TB Terrific Broth

TFEP Trifluoroethyl phosphate

Tris Tris(hydroxymethyl)aminomethane

A.2 NMR-Spectra

A.2.1 Dimethyl isopropenyl phosphate

13C

20.59
54.70
76.62
77.04
77.47
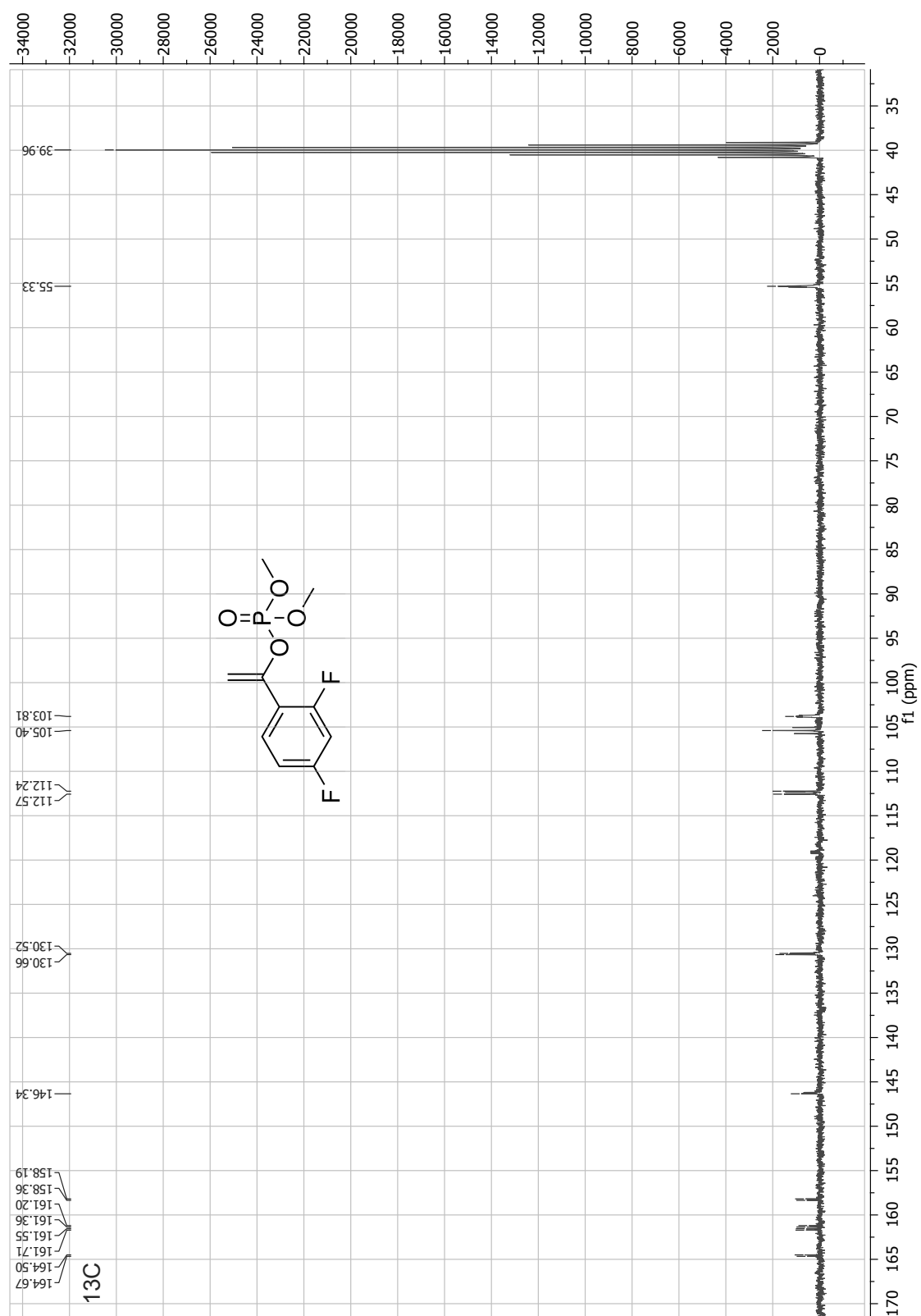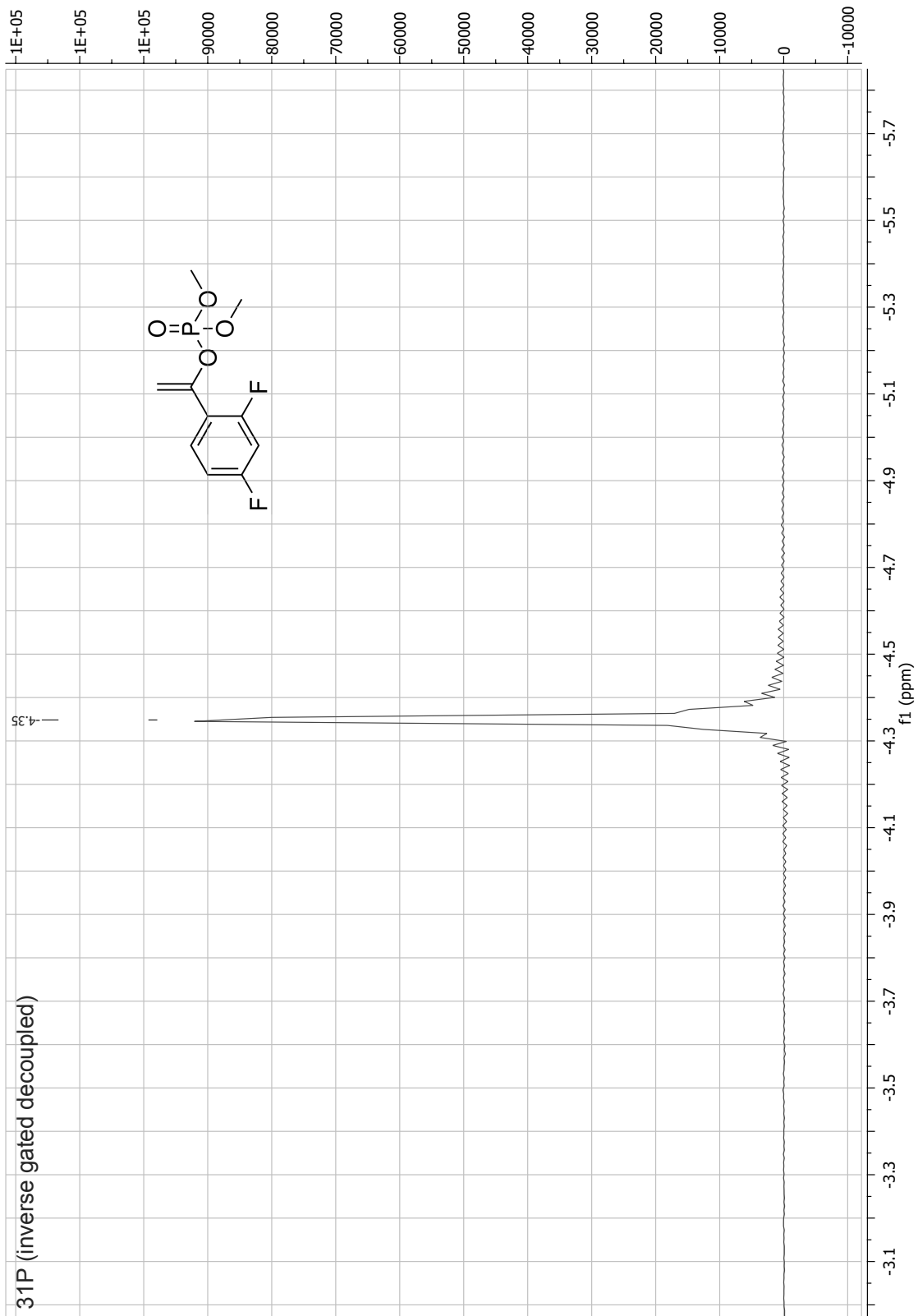98.27
152.03

iii
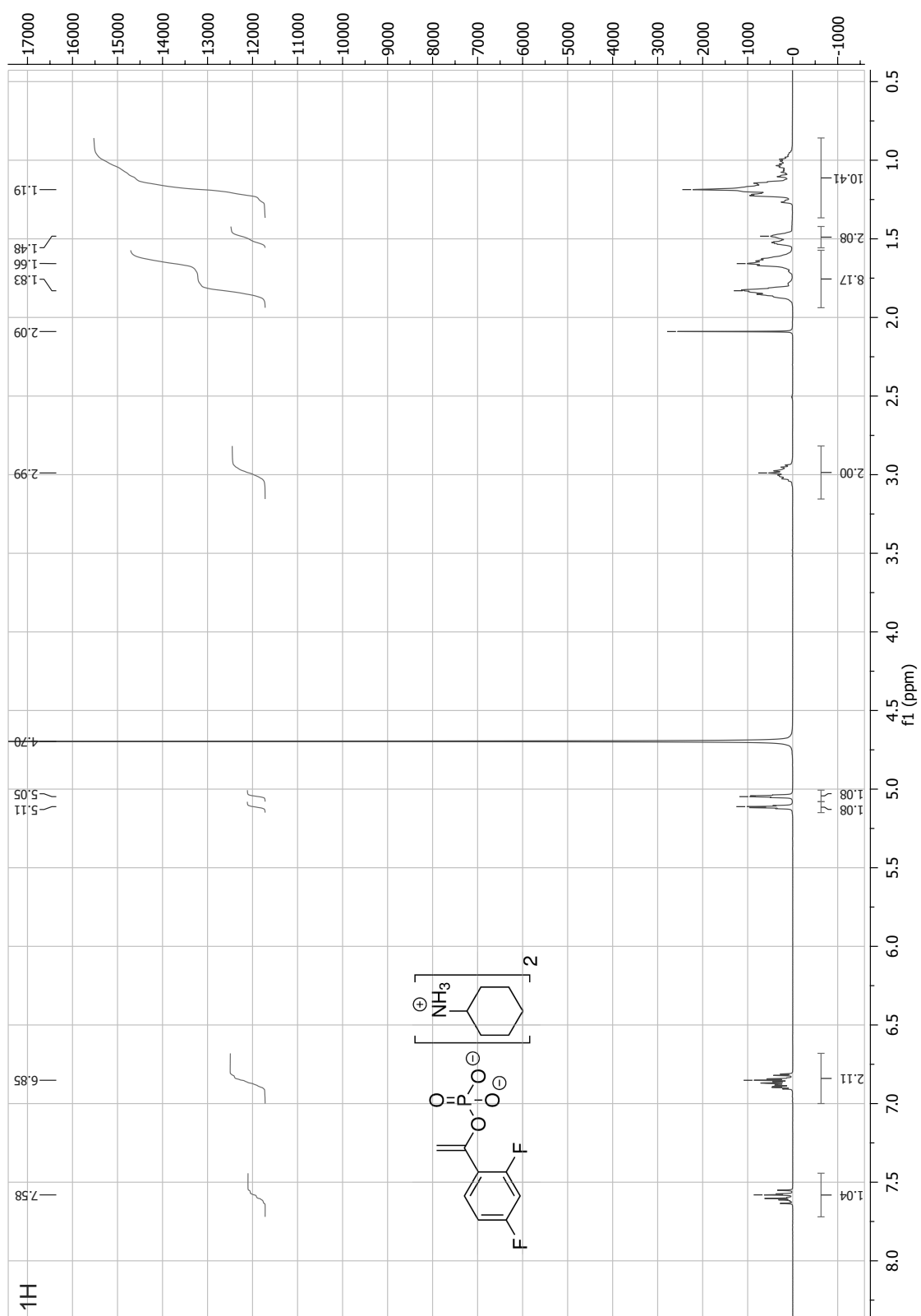
31P (coupled)

iv
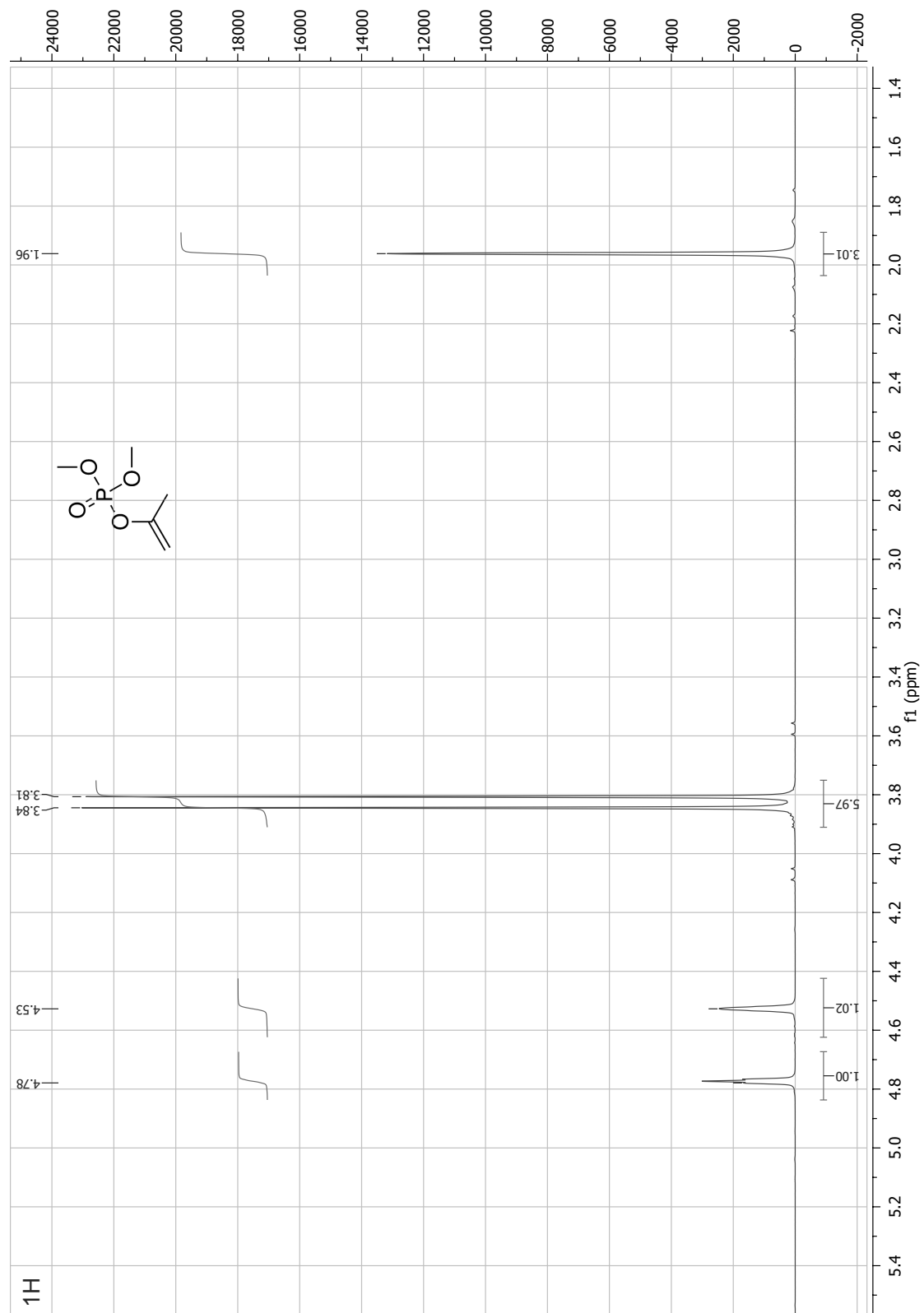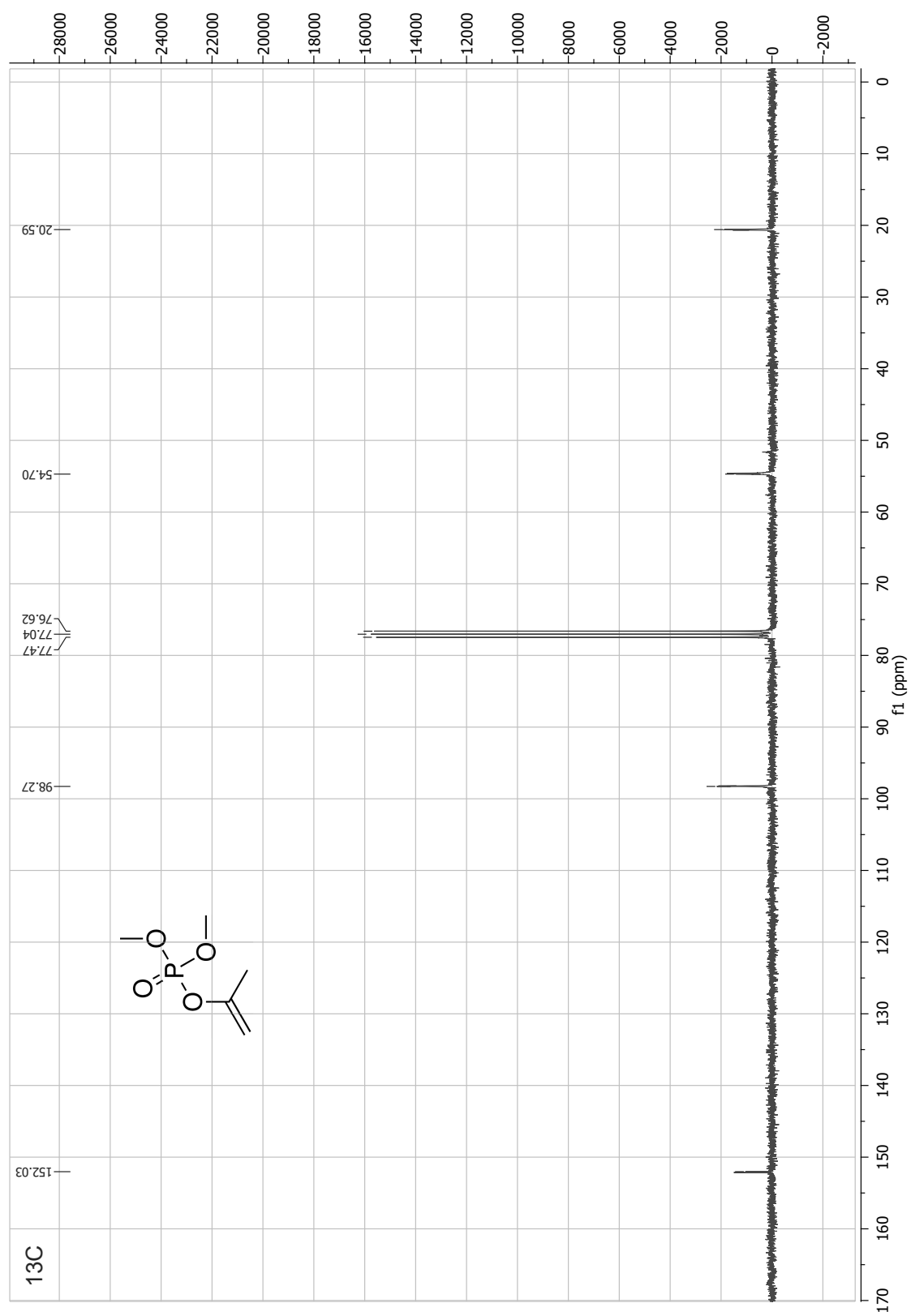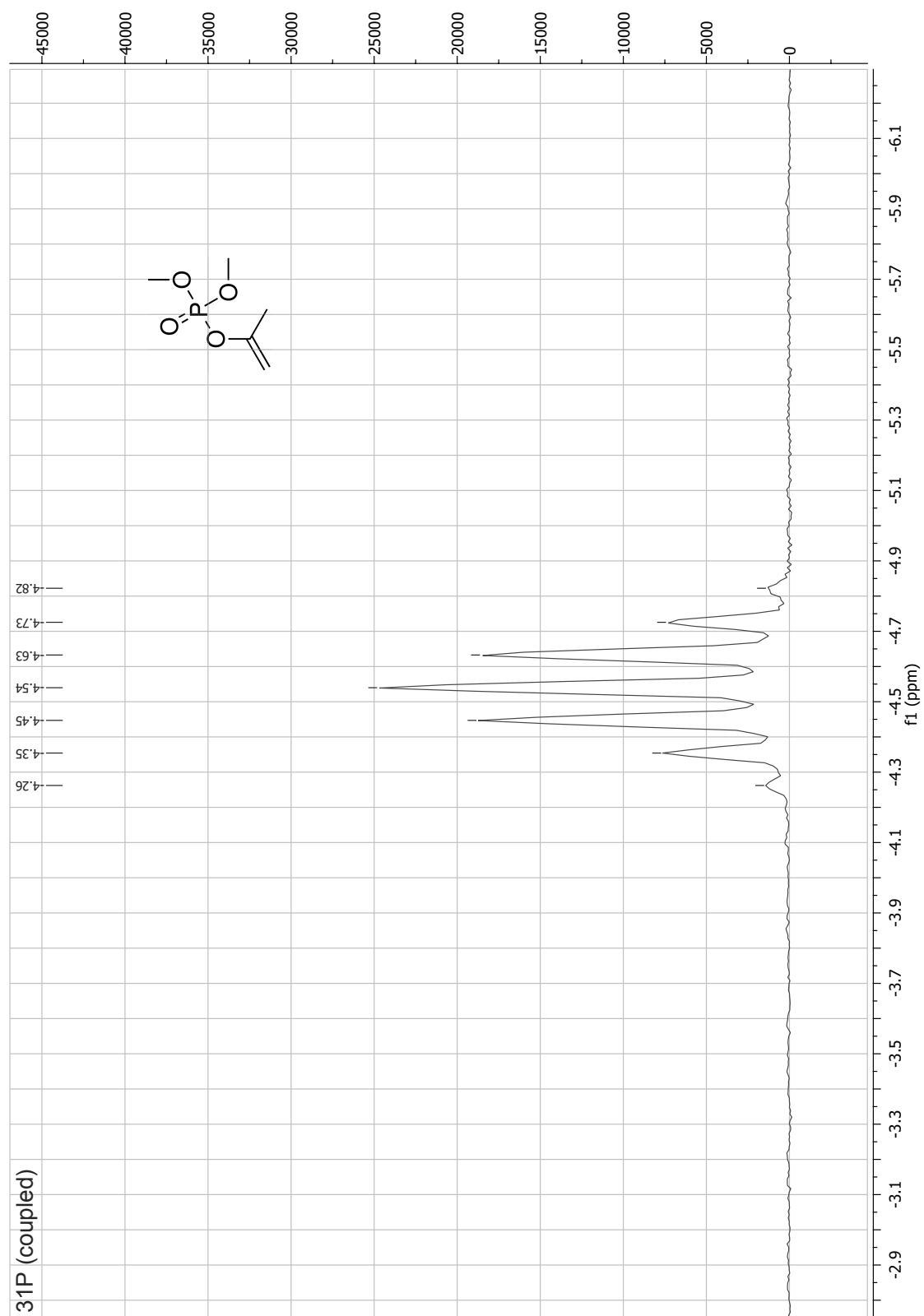
A.2.2 Isopropenyl phosphate (di)cyclohexylammonium salt

A.2.3 1-(2,4-Difluorophenyl)vinyl dimethyl phosphate
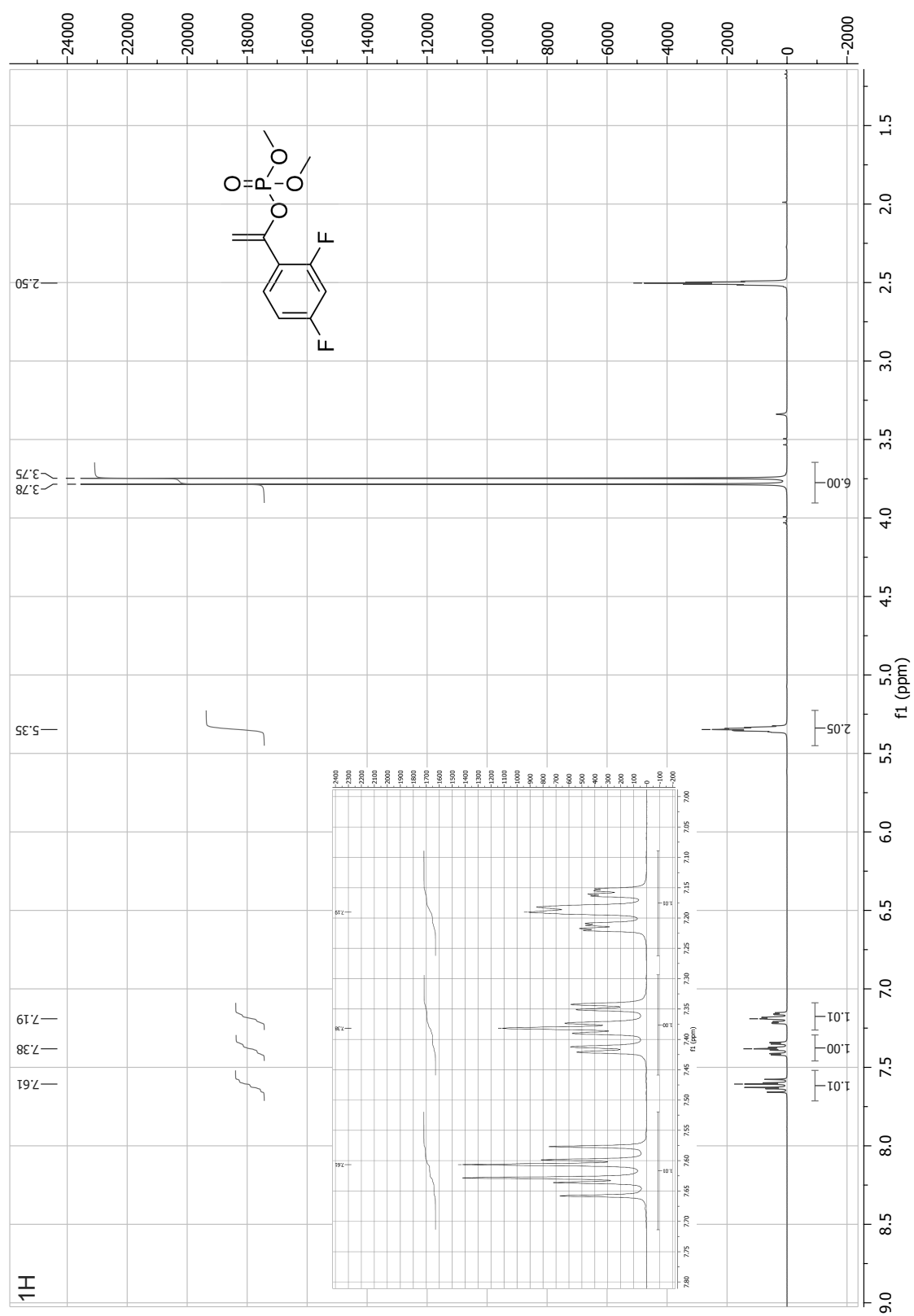
31P (inverse gated decoupled)

—-4.35

f1 (ppm)

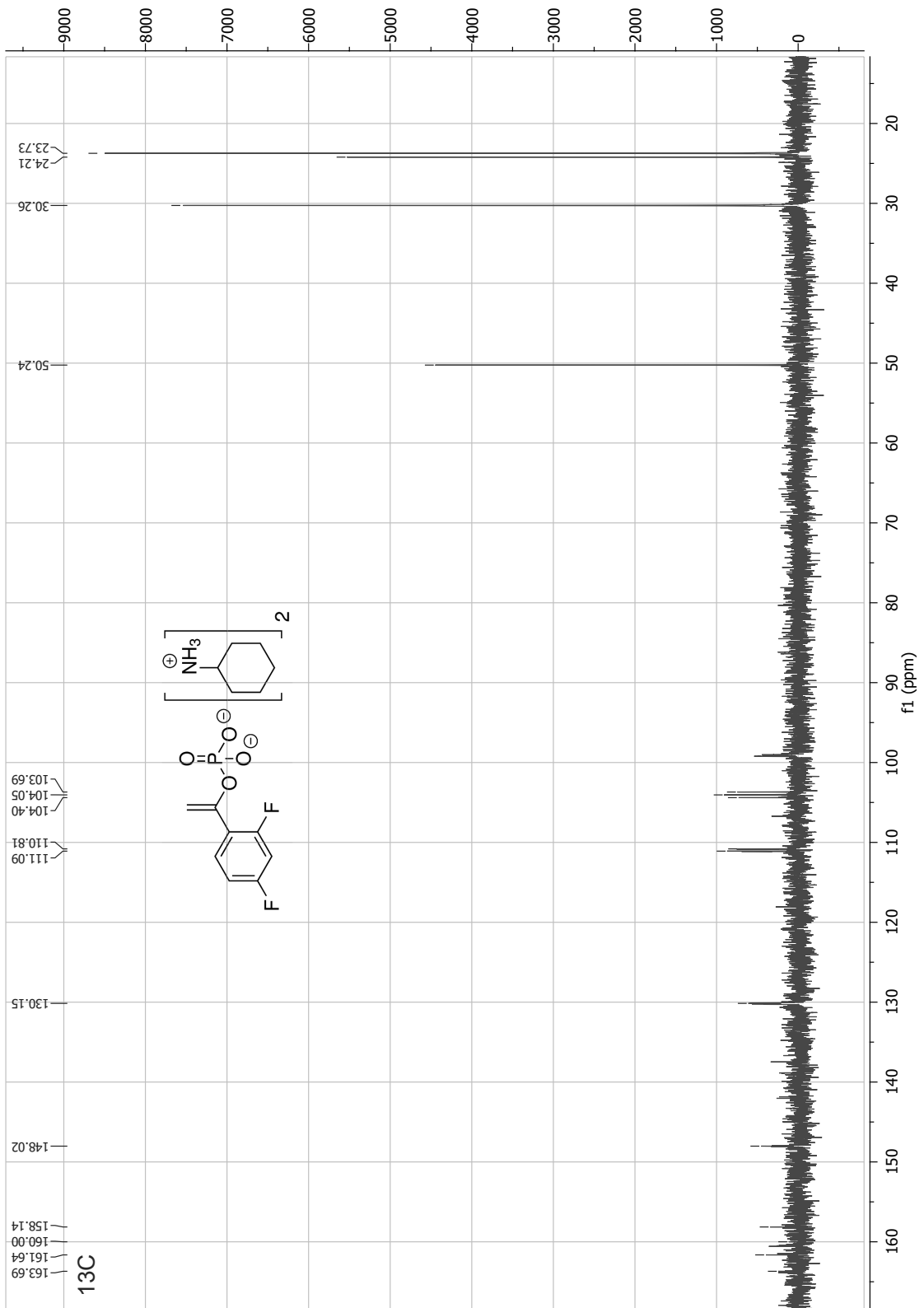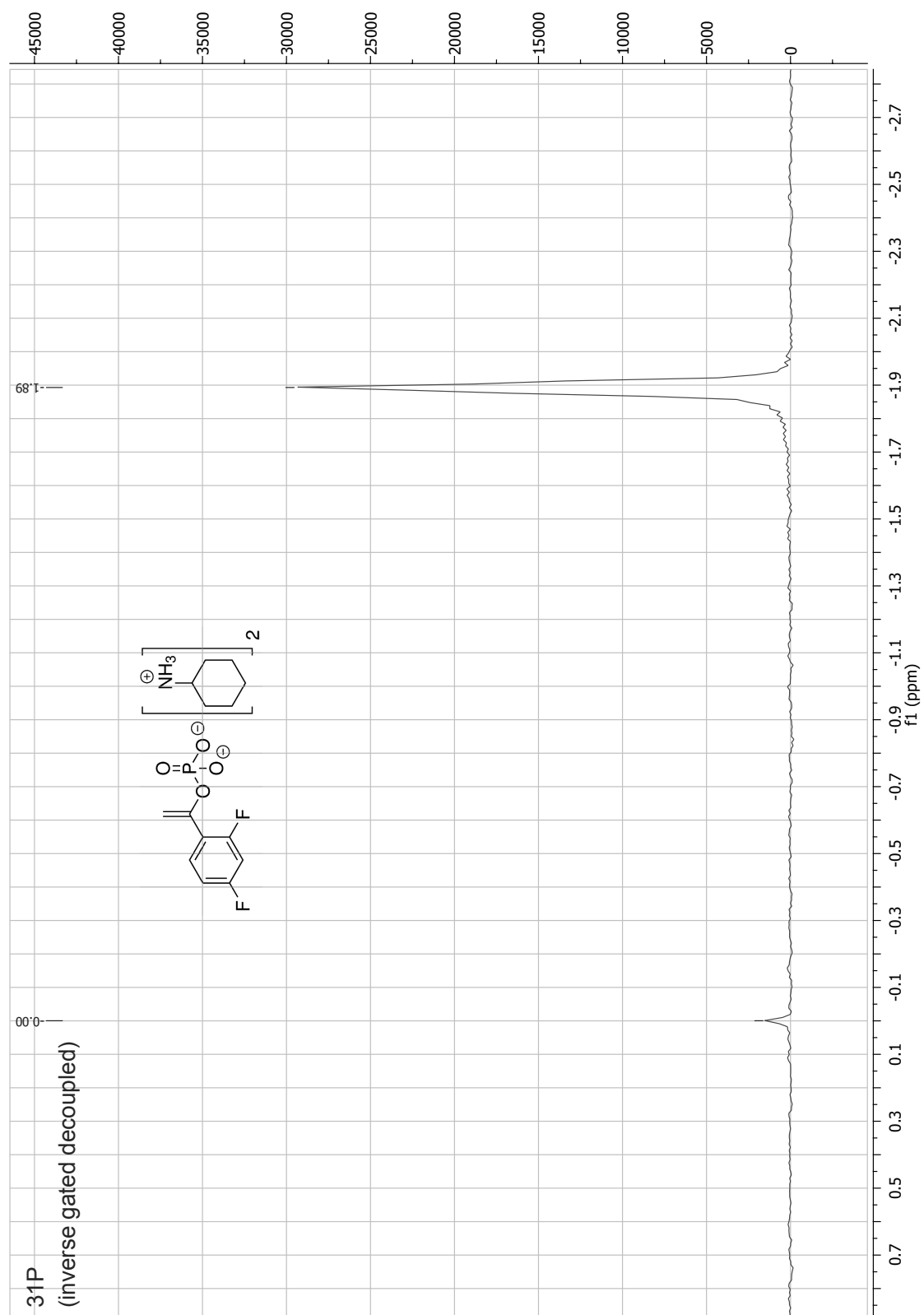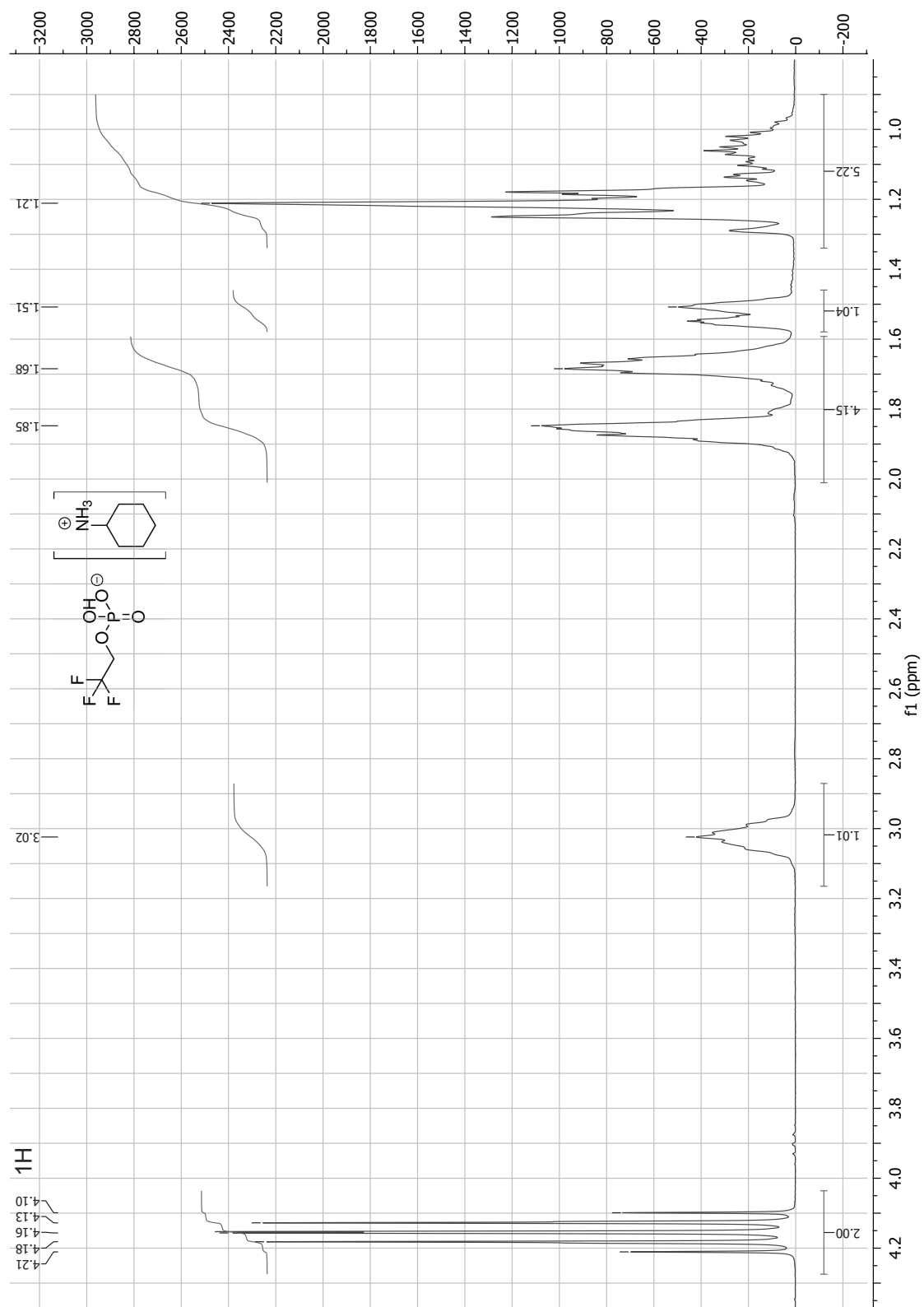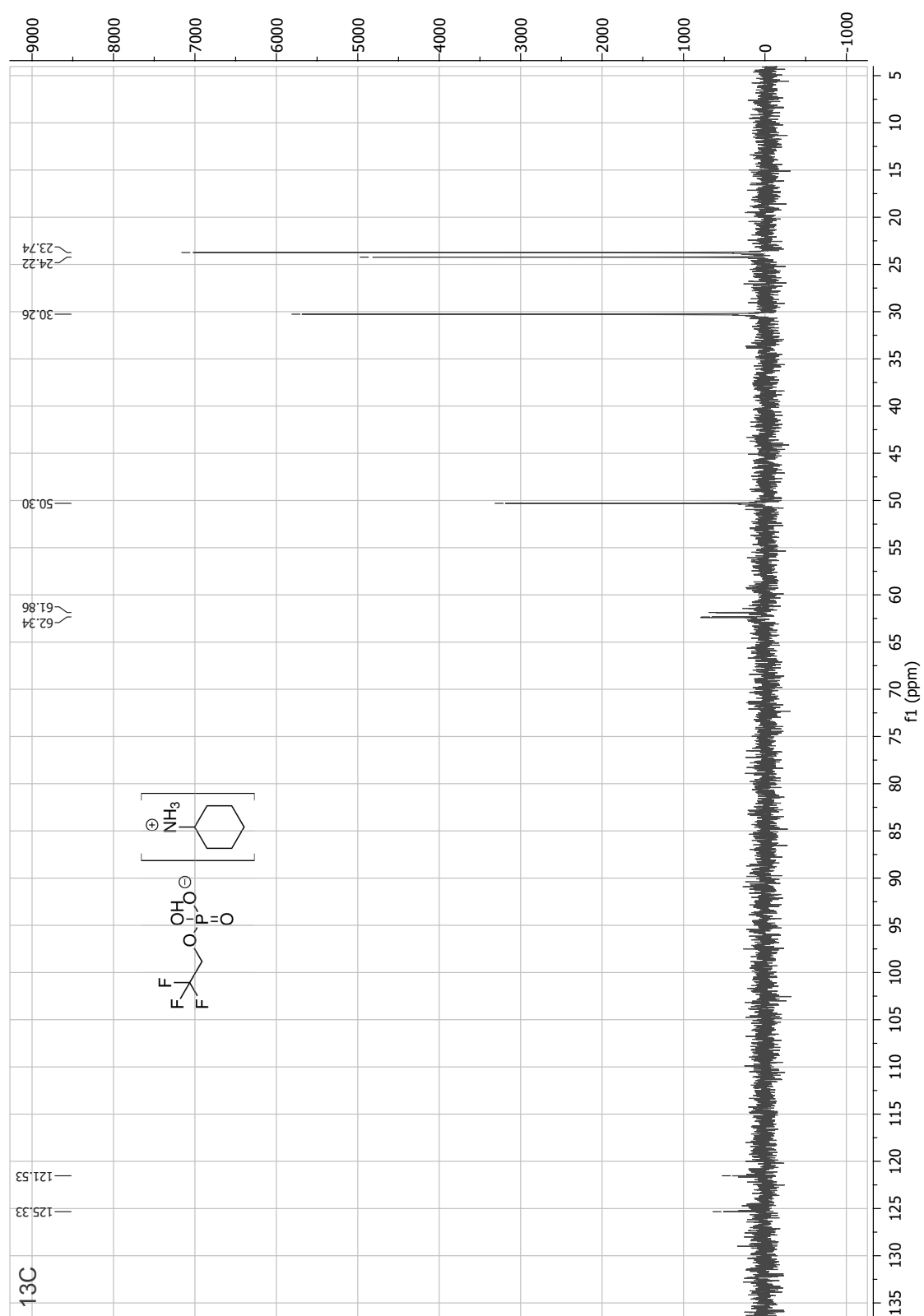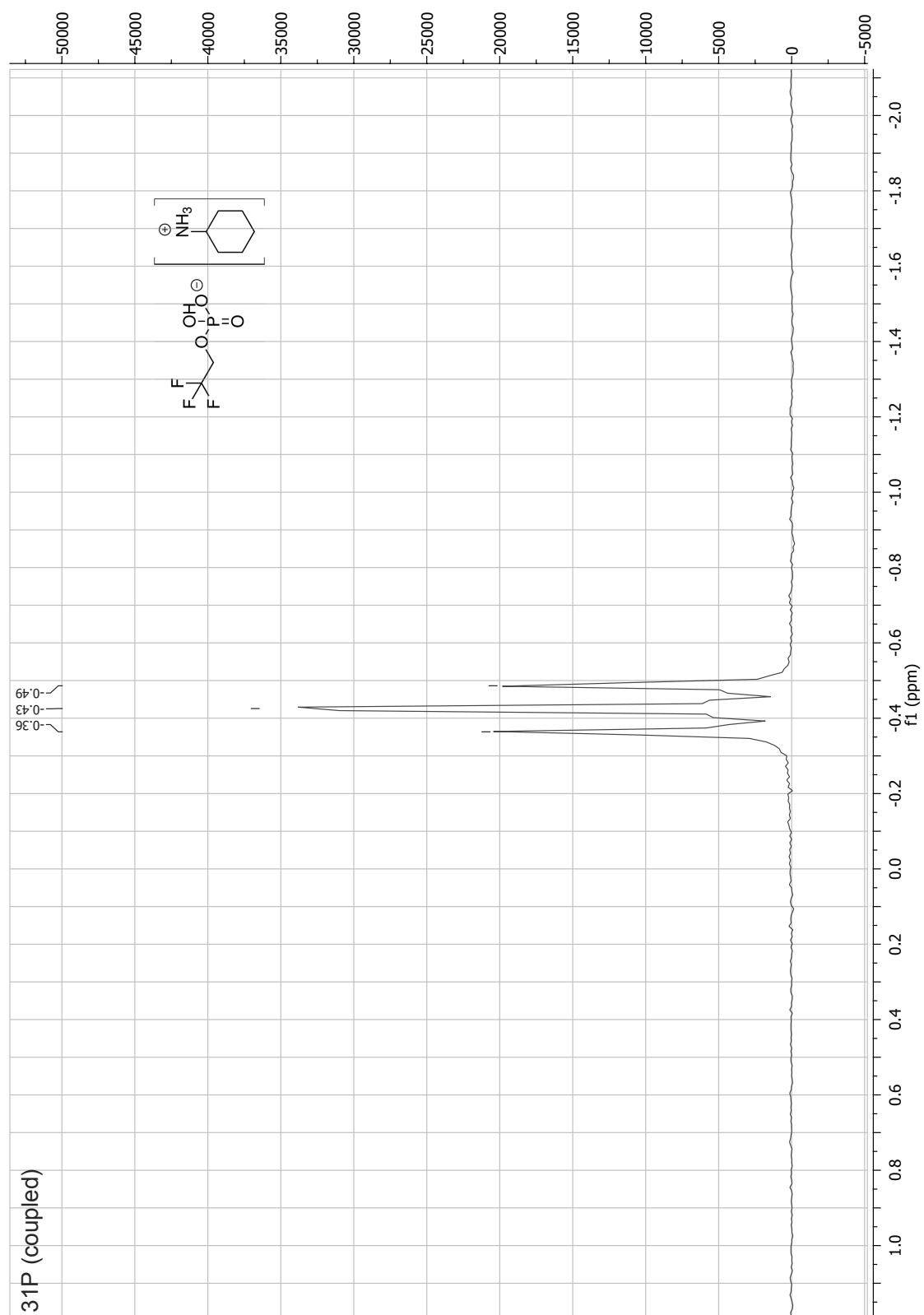## A.2.4 1-(2,4-Difluorophenyl)vinyl phosphate (di)cyclohexylammonium salt

31P
(inverse gated decoupled)

-1.89

0.00

f1 (ppm)

A.2.5 2,2,2-Trifluoroethyl phosphate monocyclohexylammonium salt

13C

23.74
24.22
30.26
50.30
61.86
62.34
121.53
125.33

31P (coupled)

-0.49
-0.43
-0.36

f1 (ppm)

A.2.6 Transphorylation

Figure 107: 121 MHz ^{31}P-NMR, 15 % D$_2$O, phosphorylation of 500 mM 14OH with 100 mM PEP (4), CP (3), PP$_i$ (2) or AcP (1) at pH 2.9 (PP$_i$/AcP) or 4.2 (CP/PEP), 30 °C, 600 rpm shaking, 1 mL reaction vol., 10 mM MgCl$_2$, 1 U mL^{-1} AphA-St (4 U mL^{-1} for PEP), 4 h reaction time for PP$_i$/AcP, 20 min for CP and 60 min for PEP, 14OP = 4-hydroxybutyl phosphate, standard = dimethyl methylphosphonate

Figure 108: 121 MHz ^{31}P-NMR, 15 % D$_2$O, phosphorylation of 500 mM 14OH with 100 mM PEP (4), CP (3), PP$_i$ (2) or AcP (1) at pH 3.3 (PP$_i$/AcP) or 4.2 (CP/PEP), 30 °C, 600 rpm shaking, 1 mL reaction volume, 1 U mL^{-1} PhoN-Se (4 U mL^{-1} for PEP), 3 h reaction time for PP$_i$/AcP, 20 min for CP and 120 min for PEP, 14OP = 4-hydroxybutyl phosphate, standard = dimethyl methylphosphonate

Figure 109: 121 MHz ^{31}P-NMR, 15 % D$_2$O, phosphorylation of 500 mM 14OH with 100 mM PEP (4), CP (3), PP$_i$ (2) or AcP (1) at pH 3.8 (PP$_i$/AcP) or 4.2 (CP/PEP), 30 °C, 600 rpm shaking, 1 mL reaction volume, 1 U mL^{-1} PhoN-Sf (4 U mL^{-1} for PEP), 4 h reaction time for PP$_i$/AcP, 30 min for CP and 240 min for PEP, 14OP = 4-hydroxybutyl phosphate, standard = dimethyl methylphosphonate

Figure 110: 121 MHz ^{31}P-NMR, 15 % D$_2$O, phosphorylation of 500 mM 14OH with 100 mM DFPVP at pH 3.5, 30 °C, 600 rpm shaking, 1 mL reaction volume, 1 U mL^{-1} PhoN-Sf, PhoN-Se or AphA-St, 10 mM MgCl$_2$ for AphA-St, 1 h reaction time, 14OP = 4-hydroxybutyl phosphate, standard = dimethyl methylphosphonate

Figure 111: 121 MHz ^{31}P-NMR, 15 % D$_2$O, phosphorylation of 500 mM 14OH with 100 mM TFEP at pH 3.8 for PhoN-Sf and 3.3 for PhoN-Se and AphA-St, 30 °C, 600 rpm shaking, 1 mL reaction volume, 1 U mL^{-1} PhoN-Sf, PhoN-Se or AphA-St, 10 mM MgCl$_2$ for AphA-St, 1 h reaction time, 14OP = 4-hydroxybutyl phosphate, standard = dimethyl methylphosphonate
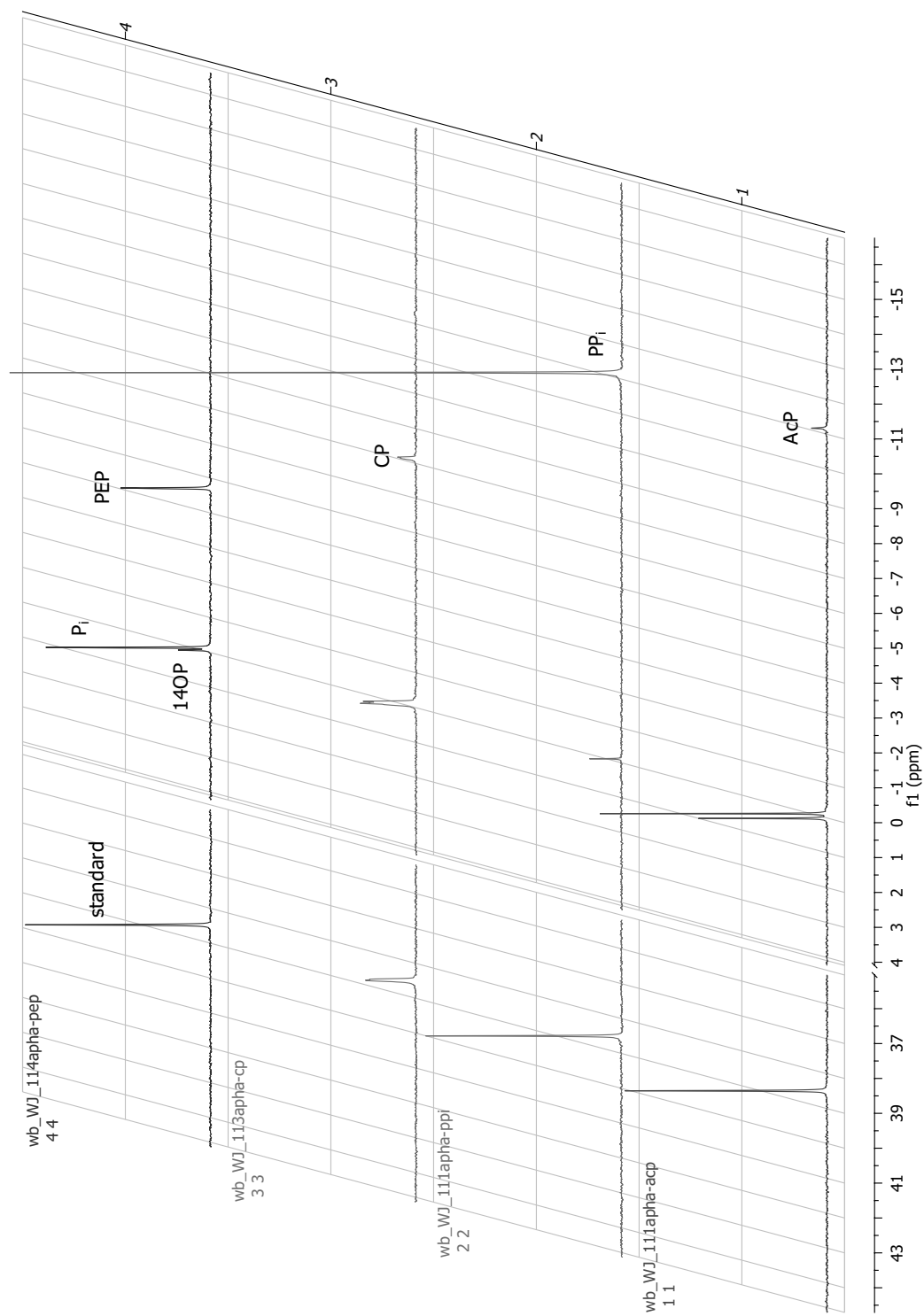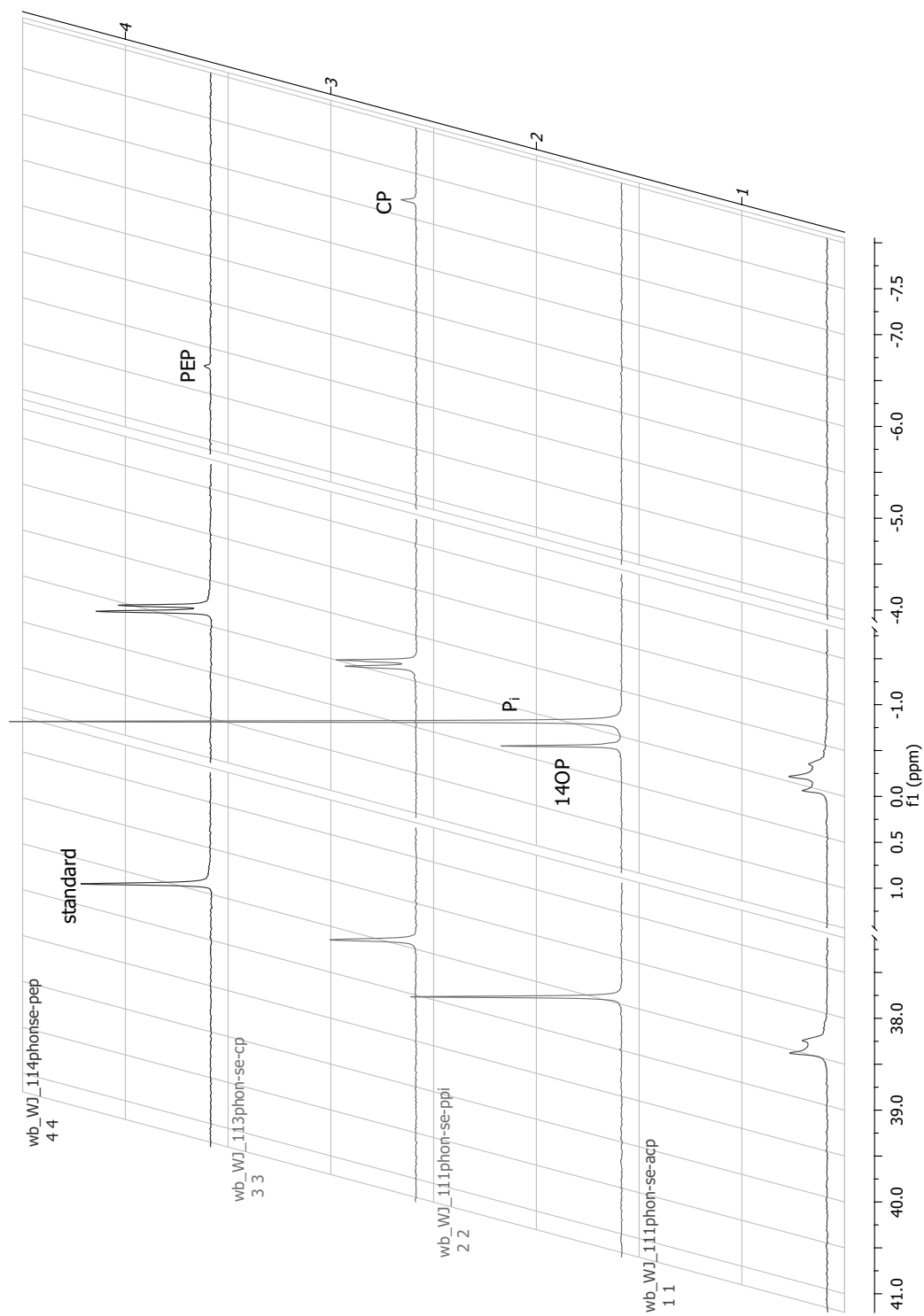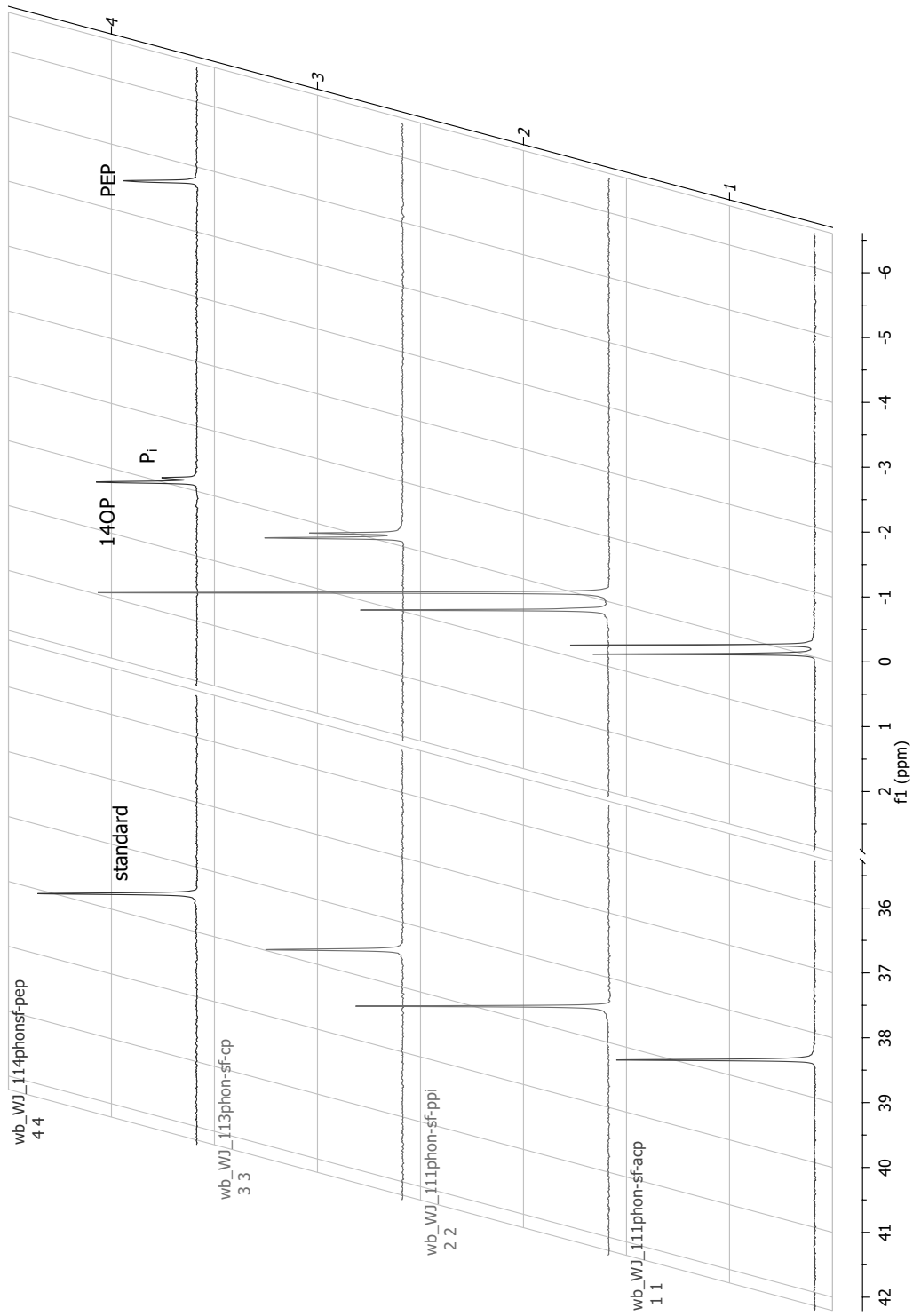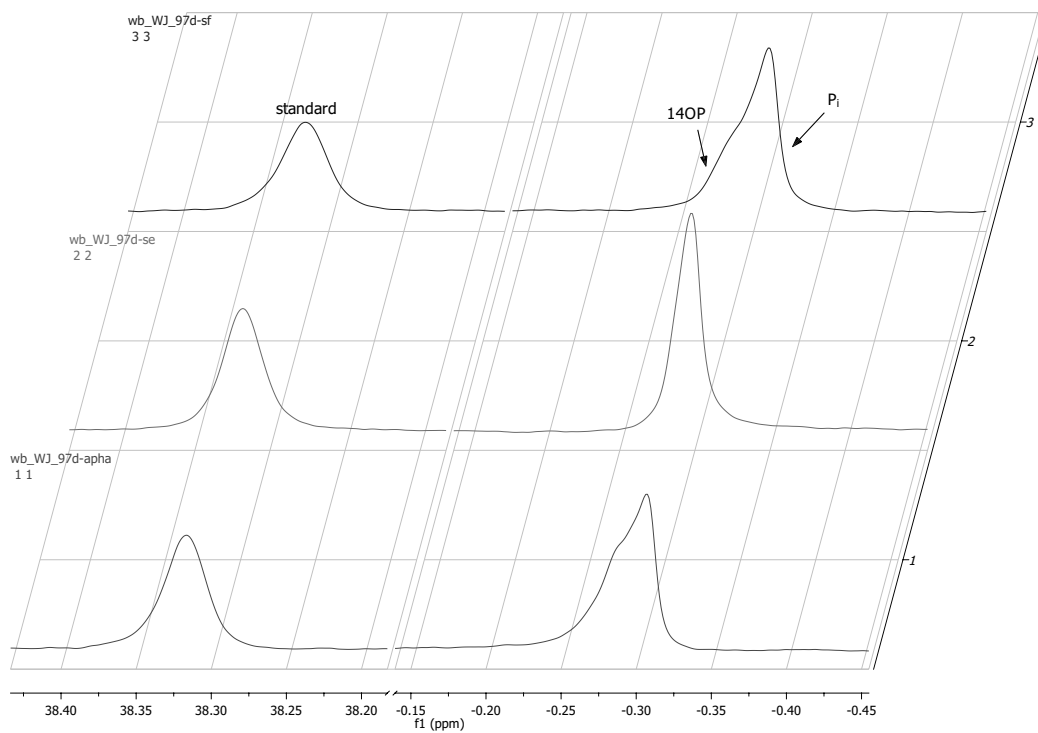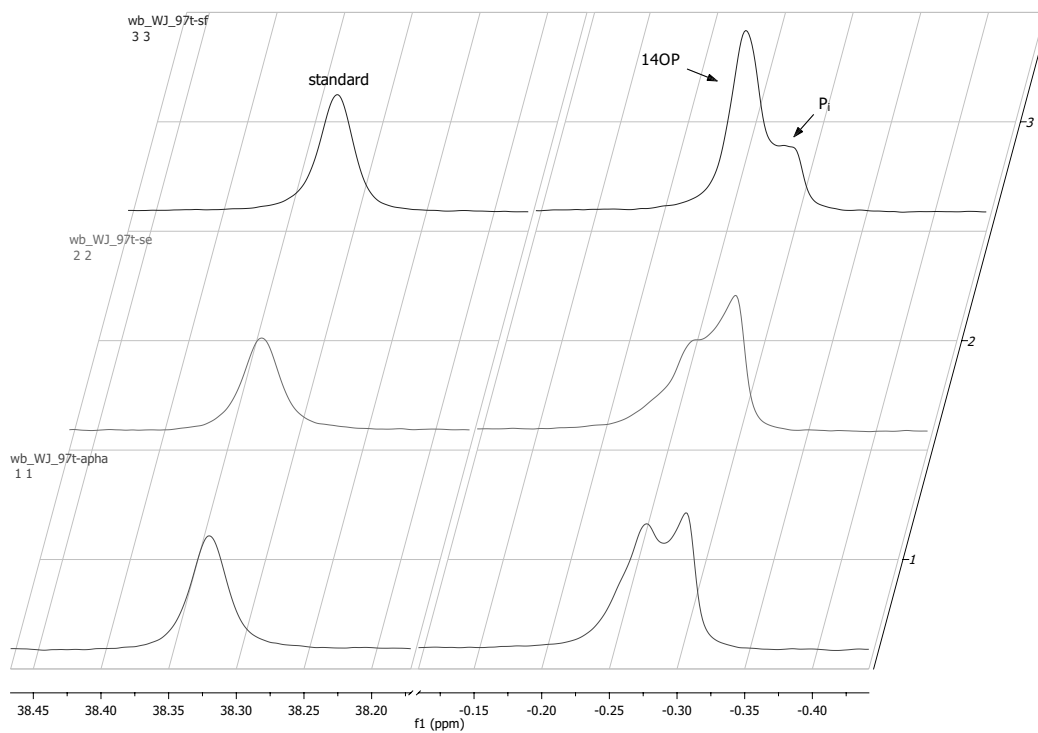
Figure 107

Figure 108

Figure 109

Figure 110

Figure 111

A.3 HPLC-RI Retention Times

Alltech IOA-2000 column (length: 150 mm, diameter: 6.5 mm, particle size: 8 μm), $0.4\,\mathrm{mL\,min^{-1}}$ flow rate, 5 mM H_2SO_4 as eluent, 50 °C column temperature, 40 μL injection volume

DMSO 14.7 min

phosphate (P_i) 4.7 min

1,4-butanediol (14OH) 12.3 min

4-hydroxybutyl phosphate (14OP) 4.2 min

methyl α-D-glucopyranoside (MADG) 6.1 min

methyl α-D-glucopyranoside 6-phosphate (MADGP) 3.2 min

2-hydroxyethyl acrylate (HEA) 13.0 min

2-hydroxyethyl acrylate phosphate (HEAP) 4.0 min

carbamoyl phosphate (CP) 3.2 min

pyrophosphate (PP_i) 3.2 min

acetyl phosphate (AcP) 3.2 min

acetate 8.9 min

phosphoenolpyruvate (PEP) 3.3 min

pyruvate 5.4 min

phosphocreatine (PC) 3.2 min

creatine 4.7 min

2,2,2-trifluoroethyl phosphate (TFEP) 3.2 min

1-(2,4-difluorophenyl)vinyl phosphate (DFPVP) 4.6 min